PROPERTIES OF MIXTURES OF FATTY ACIDS PROPOSED AS LATENT HEAT THERMAL STORAGE FOR SPACE HEATING

© Chaim John Fuks

A Thesis

in

The Centre

for

Building Studies

Faculty

of

Engineering

Presented in Partial Fulfillment of the Requirements
for the degree of Master of Engineering (Building) at
Concordia University
Montréal, Québec, Canada

September 1983

ABSTRACT

An analysis of thermal properties of fatty acids and their binary mixtures has shown that they are attractive candidates for latent heat thermal storage in space heating applications. In this study, the method of differential scanning calorimetry was used to determine the melting point, freezing point, heat of melting and heat of crystallization of the fatty acids and their binary mixtures. These properties are of prime importance in the design of a latent heat thermal storage system.

The melting range of the fatty acids (capric, lauric, palmitic and stearic) was observed to be from approximately 30°C to 65°C. The heat of transition of these acids (melting and crystallization) was observed to have a range from approximately 153J/g to 183J/g.

The eutectic points were determined for the binary mixtures of the fatty acids. The melting points of the eutectics for the binary systems of capric-lauric, lauric-palmitic, lauric-stearic and palmitic-stearic acids were observed to be 18.2°C, 32.7°C, 34.0°C and 51.1°C respectively. The corresponding heats of melting were found to be 120J/g, 147J/g, 152J/g and 159J/g respectively.

The fatty acids and their eutectic mixtures were examined with an X-ray diffractometer and an infrared spectrophotometer to ascertain the polymorphic forms, crystal structures and material purities. The experimental results indicate that the fatty acids are present in the C-polymorphic form.

ACKNOWLEDGEMENTS

I wish to express my gratitude to Professor D. Feldman, who has guided me in my work and has rendered valuable assistance. I am also grateful to Professor M. Shapiro, who has offered thoughtful criticism and provided many worthwhile suggestions. Special thanks are due to Mrs. Dorina Banu, who has aided me on numerous occasions during the experiments.

I also wish to express my thanks to Dr. C. Sandofi of Université de Montréal who has helped me with the interpretation of the infrared spectra and Dr. Bird of Concordia University who has allowed me to use the X-ray diffractometer at Concordia University and later helped me with the interpretation of the X-ray spectra.

To my son

Oren James Fuks

TABLE OF CONTENTS

LIST OF TABLES

LIST OF FIGURES

APPENDIX

List of Tables

APPENDIX

List of Thermograms

APPENDIX

List of X-Ray Diffractometric Spectra

APPENDIX

List of Infrared Spectra

I. INTRODUCTION

Man's requirement for energy is increasing at a rapid rate and, in view of the diminishing supply of the non-renewable sources such as fossil fuels, alternative supplies will need to be developed to meet the demand.

Low temperature heat, particularly in the form of solar energy, is abundantly available and can be utilized in various domestic and industrial applications (i.e., waste heat recovery in plants, space heating, greenhouse heating, domestic hot water generation, solar cooling, etc...). Widespread use of solar energy will depend on many factors. The development of a cost-effective compact thermal energy storage system is one of the most important of these factors.

The phase-change heat storage technique is based on the harnessing of the latent heat energy when a substance undergoes melting and freezing. There are various organic and inorganic materials which can be used for low temperature heat storage. Normally, these materials are classified as paraffins, fatty acids, inorganic salt hydrates and eutectic compounds.

This thesis is confined to the discussion of fatty acids (capric, lauric, palmitic and stearic) and their binary mixtures. These acids have melting points from approximately 30°C to 70°C and, therefore, possess a suitable melting range for solar heat storage, particularly in the space heating application. At the present time, there are a few suitable materials which are available on the market

that can effectively store solar energy for space heating. Several inorganic salt hydrates have been employed but these materials have been shown to be generally unsuitable due to the supercooling effect and the segregation of insoluble compounds.

The supercooling phenomenon is undesirable because it gives rise to instability in crystallization. The inorganic salt hydrates possess poor nucleating properties which result in supercooling of the liquid. The supercooling effect can be reduced by several methods which include (1) the addition of a nucleating agent with a similar crystal structure to that of the mother substance, (2) mechanical agitation and (3) by using rough heat exchanging surfaces to promote heterogeneous nucleation. All of these approaches have been used with a limited success. The other limiting factor of the inorganic salt hydrate is the decomposition of the original salt hydrate. The decomposition process is irreversible. The salt hydrate melts incongruently, producing a saturated aqueous phase and a solid phase containing a lower hydrate of the same salt. Due to the specific gravity difference, the solid settles out at the bottom of the container and does not redissolve by simply increasing the temperature.

Fatty acids meet the thermodynamic and kinetic criteria for low temperature latent heat storage. They have melting points in a low temperature range, possess a high latent heat of fusion per unit mass, have a high density, high specific heat for absorbing sensible heat, high thermal conductivity for maintaining low temperature gradients

during charging and discharging the heat storage material (fatty acid), exhibit small volume changes during the phase transition and have little or no supercooling during freezing. The saturated fatty acids appear to have a good chemical stability and do not decompose after hundreds of phase changes.

The objective of this study is to determine thermal properties of a selected group of fatty acids and their binary mixtures and to demonstrate the potential of using these materials for latent heat thermal storage. The thermal properties which are investigated here include (1) melting point, (2) freezing point, and (3) heats of melting and crystallization. In addition, the temperatures for maximum endothermic heat flow (observed during heating) and maximum exothermic heat flow (observed during cooling) are measured. A differential scanning calorimeter (DSC) was used to generate the thermal data.

The thermal data was, subsequently, used to construct phase diagrams of the binary systems of fatty acids to evaluate the freezing and melting characteristics of the substances. The phase behaviour was found to be characterized by the presence of one eutectic and a region of compound formation. The observations are in general agreement with the previously published data. The published data on melting and freezing points of pure fatty acids and their mixtures were to a large extent developed by the classical capillary tube method. The literature data on the heat of fusion of pure substances were measured by cryoscopic and calorimetric methods.

Little work was done previously in examining the properties of eutectic compounds of fatty acids and there is no experimental data available on the heats of melting and crystallization of these compounds. The heats of melting and crystallization were determined with relative ease and reliability by the differential scanning calorimetry technique. This is in contrast to the classical methods which are laborious and time-consuming. The DSC provides a thermogram on a very small quantity of sample (approximately 1-10 mg.), which can be used to evaluate the melting point, freezing point, degree of supercooling, heats of melting and crystallization and specific heat.

The crystal structure of the pure fatty acids and their eutectic compounds was examined by means of X-ray diffraction and infrared spectroscopy. The experimental data shows that the pure fatty acids and their mixtures are present in the stable C-polymorphic form. This is in agreement with results determined by previous workers.

The text of the thesis has been organized to provide a continuity of ideas in a logical sequence. The subject matter is introduced by giving an overview of the general physical and chemical characteristics of fatty acids with a brief mention of the cost and availability. This is followed by discussion of the DSC technique, apparatus, calibration and precision, and definition of technical terms used in the text. The DSC thermograms are then used in constructing graphs and in tabulating data to facilitate the discussion of thermal properties of the fatty acids and their mixtures. A dis-

cussion is later presented on the phase behaviour of a two-component system of fatty acids. The crystal structure of the fatty acids and their eutectic compounds is examined with the aid of infrared and X-ray diffractometric results. The thermal and structural findings are then used in a general discussion of the theory of melting and crystallization of fatty acids.

The thesis ends with concluding remarks and recommendations for further work. The original thermograms, X-ray and infrared spectra have been included in the appendix.

II. CLASSIFICATION OF FATTY ACIDS

The term "fatty acid" is generally applied to a family of organic compounds containing the carboxyl group. The carboxyl group can be attached to an alkyl group as illustrated below:

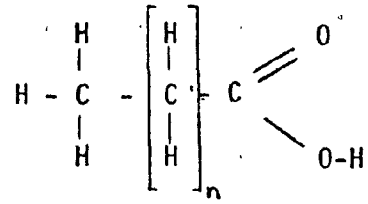

alkyl group carboxyl group

The fatty acid having the above structure is known as a saturated, monobasic, aliphatic acid. The common names and formulas of acids which are considered in this thesis and are part of this group of fatty acids are given below:

$CH_3(CH_2)_8COOH$	$CH_3(CH_2)_{10}COOH$	$CH_3(CH_2)_{14}COOH$	$CH_3(CH_2)_{16}COOH$
capric acid	lauric acid	palmitic acid	stearic acid

The homologous series is characterized by the general formula of $CH_3(CH_2)_{2n}COOH$. The straight-chain acids can have an even number of carbon atoms in the chain, in which case the acid is known as n - or even-chained. When the chain contains an odd number of carbon atoms it is known as iso - or odd-chained. The two different groups of straight-chain acids have different crystalline structures and, therefore, possess different physical properties. The saturated straight-chain acids are chemically stable along the carbon chain

and their reactive properties are mainly determined by the functional carboxyl group.

In the straight-chain structure each carbon atom possesses at least two hydrogen atoms and no carbon atom is bonded to more than two other carbon atoms. In contrast, another group of fatty acids is characterized by double or triple bonds existing between the carbon atoms along the chain. This group is known as unsaturated fatty acids of the ethylenic family and the group consists of three separate series having the composition as shown below:

$C_n H_{2n-2} O_2$ (monoethenoic)

$C_n H_{2n-4} O_2$ (diethenoic)

$C_n H_{2n-6} O_2$ (triethenoic)

Due to the presence of the double bond between the adjacent carbon atoms along the carbon chain, the unsaturated fatty acids are chemically reactive and generally lack stability. These acids have a tendency to react with oxygen, thus making them unsatisfactory candidates for phase-change materials. The reaction generally leads to a branched-chain structure where one carbon atom along the chain can be bonded to three other carbon atoms. The double bond between the carbon atoms along the chain can in some cases alternate with single bonds creating additional groups of fatty acid families; namely, conjugated and nonconjugated. Double bonds can also produce different compounds that have the same formula, the concept known as cis and trans isomerism.

III. SOURCES AND COST OF FATTY ACIDS

Most of the fatty acids are produced commercially by hydrolysis which is a process of splitting the fat. The exception is tall oil, which is not a glyceride. The fat is normally characterized by a 3-pronged glycerol which is connected to the monobasic acids. The hydrolysis of a fat to fatty acids (Ref. 1) is illustrated below:

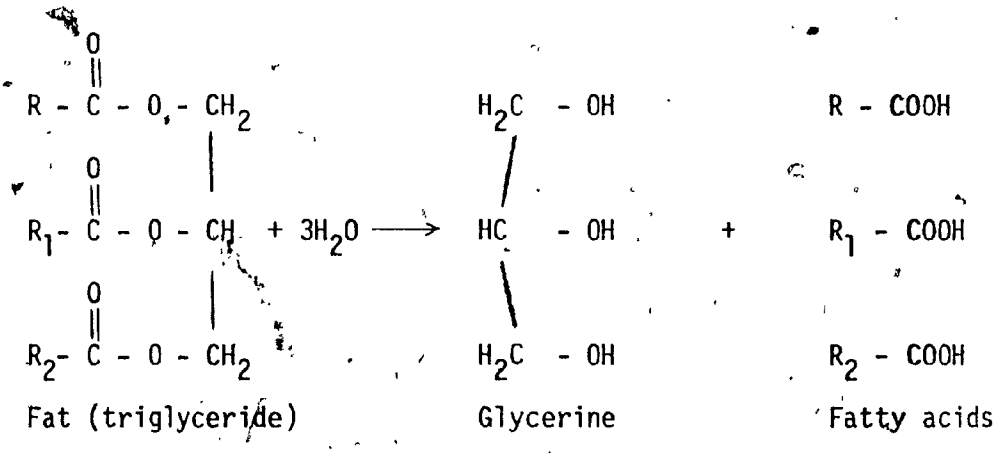

The naturally occurring mixed glycerides provide most of the industrial sources of fatty acids. The glycerides are available in abundant quantities; mostly from animal fat in the form of inedible tallow and vegetable sources. Table I lists the main sources of fatty acids.

TABLE I. Sources of Fatty Acids (Ref. 2)

SATURATED ACIDS	COCONUT OIL	PALM OIL	PALM KERNEL OIL	TALL OIL	BEEF TALLOW
Caproic	0.5%		0.5%		
Caprylic	8%		5%		
Capric	7%		5%		
Lauric	48%		50%		0.1%
Myristic	17%	2%	15%		3%
Palmitic	9%	42%	7%	7%	29%
Stearic	2%	4%	2%		20%

The fatty acids are widely used in the chemical industry. The main uses of fatty acids are listed in Table II.

TABLE II. End-uses of Fatty Acids (Ref. 2)

Fatty Alcohols	12%
Soaps	9%
Emulsion Polymerization	5.5%
Dimer & Trimer	5.5%
Lubricating Grease	5%
Specialty Household Cleaners	5%
Plastic Additives	4%
Food Additives	4%
Cosmetics	4%
Downstream Acids	4%
Ore Flotation	3.5%
Paint & Varnish	3.5%
Other Uses	28%
	100%

The North American production of fatty acids far exceeds the edible and inedible requirements and enjoys an annual growth rate of 2 to 3%. This growth rate is expected to continue for the rest of the decade. The prognosis is that the supply of fatty acids will exceed the demand for many years to come. Therefore, the fatty acid industry appears to be capable of accommodating a higher usage for

the latent heat storage technology.

The cost of fatty acids is generally more expensive than that of inorganic salt hydrates and paraffins. However, with the upsurge in demand and the improved manufacturing economics, the cost of fatty acids is expected to decline. Table III shows the current cost of fatty acids of technical grade in bulk quantities. The prices are on a per kilogram basis prevailing on the Canadian market. The associated latent heats which can be stored per dollar value are also included in the table.

TABLE III. Prices of Fatty Acids

FATTY ACID	PRICE ($/KG)	LATENT HEAT (KJ/$)
Capric	$2.05	76.6
Lauric	$1.52	107.9
Palmitic	$1.41	114.5
Stearic	$0.97	188.7

The cost of material is an important consideration in the selection of materials for latent heat thermal storage applications. The above table illustrates that the latent heat per unit dollar increases with the carbon chain of the fatty acid.

IV. DEFINITION OF TEMPERATURES AND LATENT HEATS EMPLOYED IN DIFFERENTIAL SCANNING CALORIMETERY (DSC)

An interactive DSC Data Analysis Program (V2.0) was used in conjunction with the Dupont 1090 Thermal Analyzer Micro Computer. This program calculates the temperatures and heats associated with transitions in materials.

Fig. 1 shows a typical thermogram depicting the heating and cooling cycles of a sample. Following is a list of parameters which are calculated by the interactive program with their corresponding definitions.

Melting Point: The melting point is defined as the temperature of intersection of the base line with the tangent to the inflection point having the greatest rate of change of heat flow in the heat flow versus the temperature curve for a heating cycle.

Freezing Point: The freezing point is generally affected by the sample behavior since it is not an equilibrium measure. In the absence of supercooling, the freezing point is defined as the temperature of intersection of the base line with the tangent to the inflection point having the greatest rate of change of heat flow in the heat flow versus the temperature curve for a cooling cycle.
If the sample supercools and the temperature rises by more than 0.25°C upon crystallization, then the freezing point is the temperature where the recrystallization started.

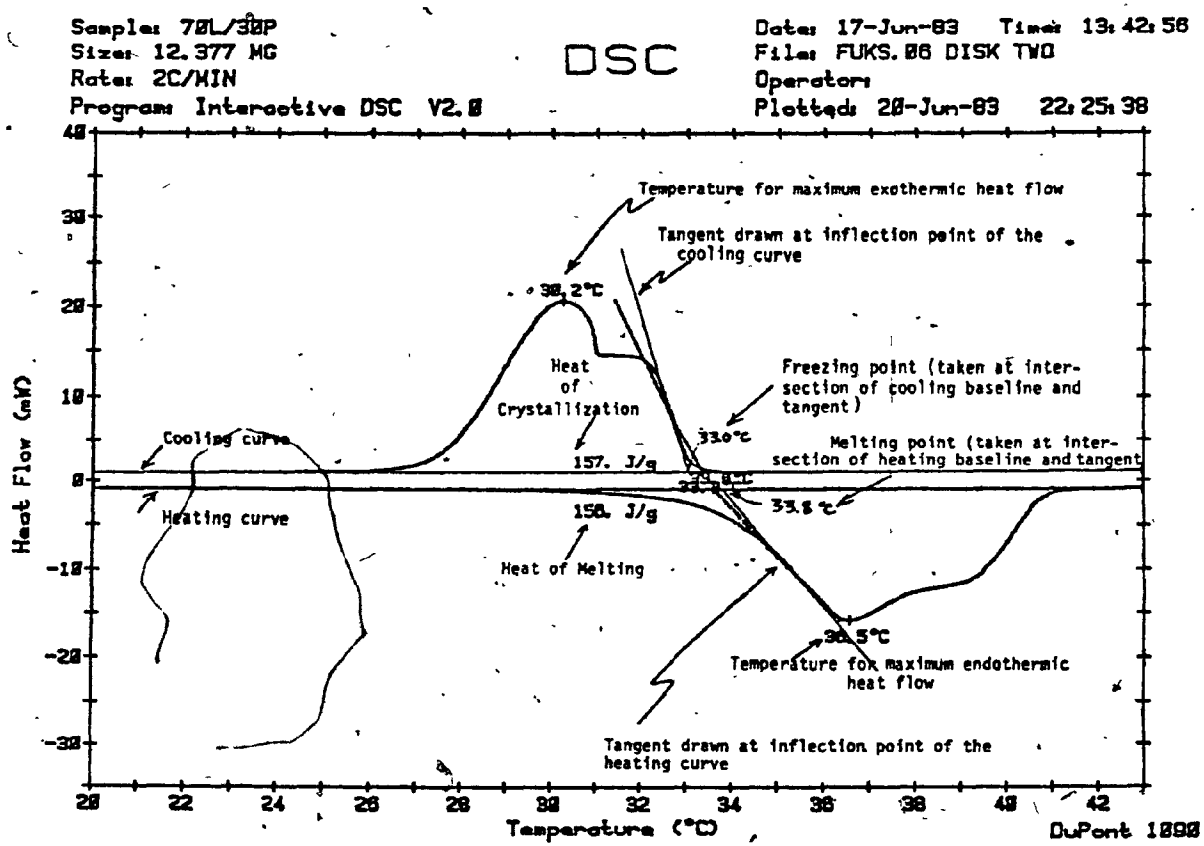

Fig. 1 Typical thermogram showing the parameters computed in DSC.

In both the melting and freezing points calculations, the program uses the least-square fitting method in drawing the tangent line. The program examines the region of the curve of interest and moves along the curve until the inflection point is located. The tangent line is then drawn at the inflection point and is projected to intersect the baseline. To fit the line, the program uses 12.5% of the total number of points between the start and stop limits.

It is apparent from the thermograms that the tangent lines drawn by the computer are skewed and are not true tangents at the inflection points. Consequently, the intersection point of the computer-drawn tangent and the base line does not represent the true transition temperature point. To correct this anomaly, the tangents at the inflection points were drawn by longhand and these points were then used in compiling the data. The fitting of the tangent line is dependent on the data scanning rate, heating or cooling rates and the mass of the sample. The computer program does not appear to be sufficiently responsive to these variables.

When several peaks are present on the thermogram, the tangent is drawn at the peak which has the greatest rate of change of heat flow.

Heat of Melting and Crystallization

The heats of melting and crystallization are calculated from calorimetric measurements of heat flux which are based on the following formula:

$$\Delta H = \frac{K}{m} \int_{t_1}^{t_2} \frac{\Delta \dot{Q}}{f(T)} \, dt$$

where: ΔH = enthalpy

m = sample mass

$\Delta \dot{Q}$ = heat flux

t = time

$f(T)$ = temperature dependent heat transport function

K = calibration constant of DSC cell

The calibration constant, K, is dependent on temperature in a non-linear way. The calibration constant is linearized electronically to a temperature-independent straight line by the thermal analyzer system.

The heat is calculated as the integral of the signal over time from the start to stop points. The limit points are indicated on the thermogram by vertical tick marks which are connected by a straight dashed line. The calculated area represents the heat of transition and is reported in J/g.

Temperature for Maximum Endothermic Heat Flow

This parameter is defined as the temperature of the point that is located furthest from the baseline in a heating cycle.

Temperature for Maximum Exothermic Heat Flow

This parameter is defined as the temperature of the point that is located furthest from the baseline in a cooling cycle.

V. DIFFERENTIAL SCANNING CALORIMETRY TECHNIQUE AND APPARATUS

The pure fatty acids and their binary mixtures were investigated with a Differential Scanning Calorimeter (DSC). Thermograms of each sample were recorded on a Dupont Model 1090 thermal analyzer equipped with a 910 DSC cell. The cell contains a constantan (thermoelectric) disk as a primary heat transfer element that conducts heat to sample and reference pans positioned on the raised portions of the disk. Temperatures of the sample and reference pans are measured by the chromel-constantan area thermocouples. The differential heat flow is calculated using a known sample weight. The cell design is illustrated in Fig. 2. To provide cooling to subambient temperatures, a cooling accessory was improvised and is illustrated in Fig. 3.

The instrument was calibrated using 20 mg of Indium and a heating rate of 10°C/min as recommended by the instrument manufacturer. The observed melting point was 156.6°C with a heat of fusion of 29.1 J/g. This is in agreement with the established values set by the manufacturer. Furthermore, another calibration was performed with Naphtalene ($C_{10}H_8$, pure crystal, Fisher, reagent grade with a melting range of 80-81°C). A sample of 2.144 mg of Naphtalene was heated at 2°C/min and the observed melting point was 80.0°C. The sample and reference pans used in all the experiments were made of aluminum and weighed approximately 13 mg. During the experiments the pans were open (there was no need to hermetically seal the pans, as the substances which were measured are considered

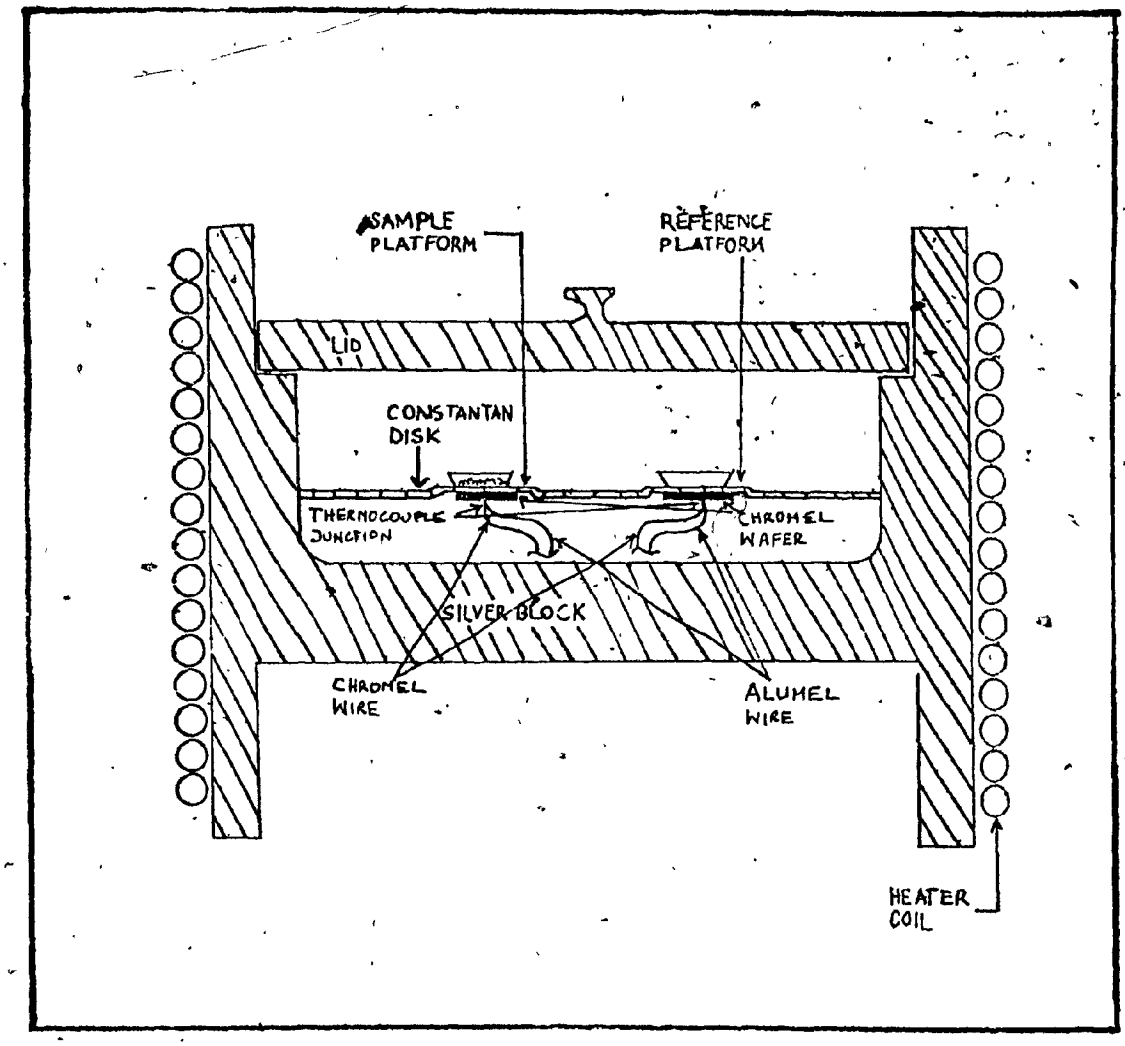

Fig. 2 DSC cell cross section

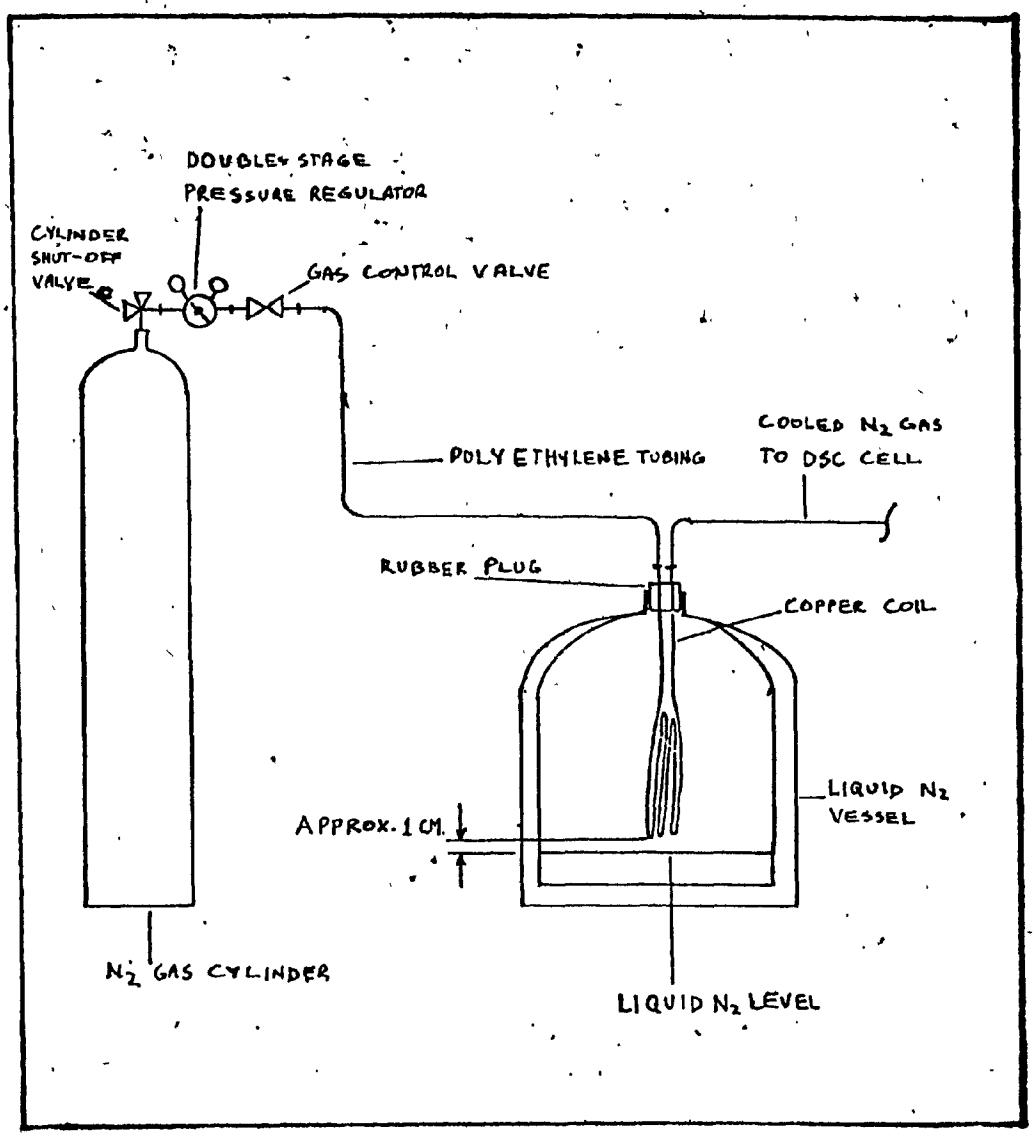

Fig. 3 Cooling accessory for DSC

non-volatile). The samples were weighed after the experiments and no weight loss was observed. The accuracy of the balance was ± 0.005 mg.

The precision of the instrument was determined by performing several melting and freezing runs on palmitic acid. The results are given in Table A-1 of the appendix. Table IV gives the mean and standard deviation of the observed parameters for melting point, temperature for maximum endothermic heat flow, heat of melting, freezing point, temperature for maximum exothermic heat flow and heat of crystallization

PARAMETER	MEAN	STANDARD DEVIATION
Melting Point (°C)	59.0	± 0.6
Temperature for max. endothermic heat flow (°C)	61.5	± 0.1
Heat of Melting (J/g)	175	± 1
Freezing Point (°C)	58.1	± 0.3
Temperature for max. exothermic heat flow (°C)	57.6	± 0.7
Heat of Crystallization (J/g)	173	± 3

TABLE IV. Calculated means and standard deviations of measurements done on palmitic acid (The results were obtained from 4 runs at a data scanning rate of 0.4 seconds per point as listed in table A-1 of the appendix).

The instrument manufacturer claims that the 910 DSC cell constant is linear to within ± 0.3%, the enthalpy coefficient of variation is less than ± 1% and the temperature has a repeatability of 1°C.

The experimental results indicate that the temperature measurements agree with the manufacturer's claim; however, the standard deviation of the enthalpy (heat of crystallization) is 1.7% and, therefore, slightly higher than the level claimed by the manufacturer.

An optimal heating rate for the experiments was determined by using a sample with a composition of 30 mole % capric: 70 mole % lauric at a data scanning rate of 0.4 seconds/point. The sample was subjected to heating rates from 1°C/min to 15°C/min to ascertain the melting point dependence on the heating rate. The results are tabulated in Table V and plotted in Fig. 4. The thermograms appear in Fig. T-1 to T-5 of the appendix.

Heating Rate (°C/min)	Melting Point (°C)
1	21.0
2	21.0
5	21.0
10	21.2
15	21.5

TABLE V. Melting point dependence on heating rate for a 30 mole % capric: 70 mole % lauric mixture.

An optimal heating and cooling rate of 2°C/min and a data scanning rate of 0.4 seconds per point were selected for all the experiments.

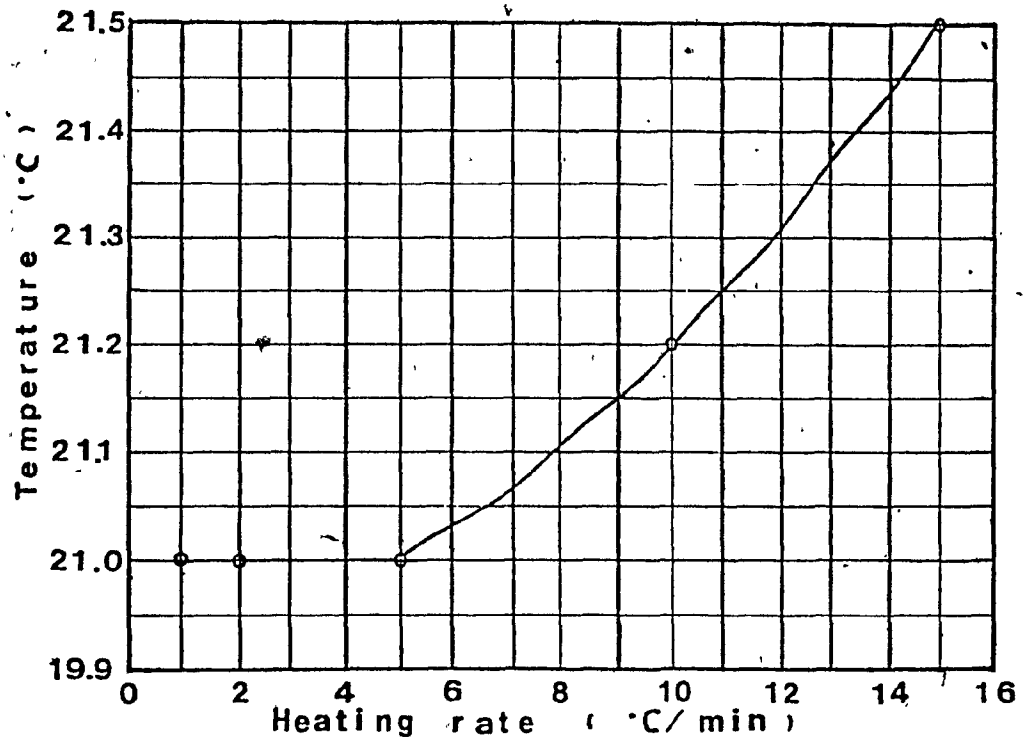

Fig. 4. Melting point dependence on heating rate for 30 mole % capric: 70 mole % lauric mixture.

VI. PHASE BEHAVIOR AND THERMAL PROPERTIES OF BINARY SYSTEMS OF FATTY ACIDS

Binary systems of even straight-chain fatty acids of capric-lauric, lauric-palmitic, lauric-stearic and palmitic-stearic were investigated.

The fatty acids used in the experiments were of reagent grade quality, in a flake form and obtained from commercial sources. The suppliers of the fatty acids and the melting points are listed in Table VI.

The fatty acids were mixed in a solid state in 10 molar ratios from 0 to 100% in multiples of 10% of the low to high molecular weight component. Additional molar ratios were prepared around the eutectic point to clearly establish the thermal data in this region. Subsequently, the samples were melted in an oven before being used on the DSC.

Fig. 5 illustrates the freezing behaviour of a two-component system of even straight-chain fatty acids. The binary systems of fatty acids form a single eutectic and a region with an incongruently melting solid-state compound.

The incongruent compound transforms during melting into two phases; i.e., a higher melting solid phase and a liquid phase in a region containing an excess of the low molecular weight component.

The crystallization process of the system can be explained with the aid of the phase diagram in Fig. 5, which has been developed from freezing point relations (ref. 38 and 39). The liquid solutions, which on cooling, reach the curve line "a u" or "e b" give rise to solids A_s and B_s respectively changing the liquid composition.

TABLE VI. Sources of Saturated Straight-Chain Fatty Acids Used for Experiments

COMMON NAME	FORMULA	MOLECULAR WEIGHT	ACID SOURCE	MELTING POINT (°C)	MELTING POINT RANGE (°C) Ref. 13
Capric	$CH_3(CH_2)_8COOH$	172.27	DX55, P5168 Matheson & Coleman & Bell Reagent	31-32	31-31.35
Lauric	$CH_3(CH_2)_{10}COOH$	200.32	Baker (7-P353) Reagent	43-46	43.92-44.5
Palmitic	$CH_3(CH_2)_{14}COOH$	256.43	Fisher Reagent (A-225)	61-62	62.53-62.82
Stearic	$CG_3(CH_2)_{16}COOH$	284.49	Fisher Reagent (A-293)	67-69	69.2-69.9

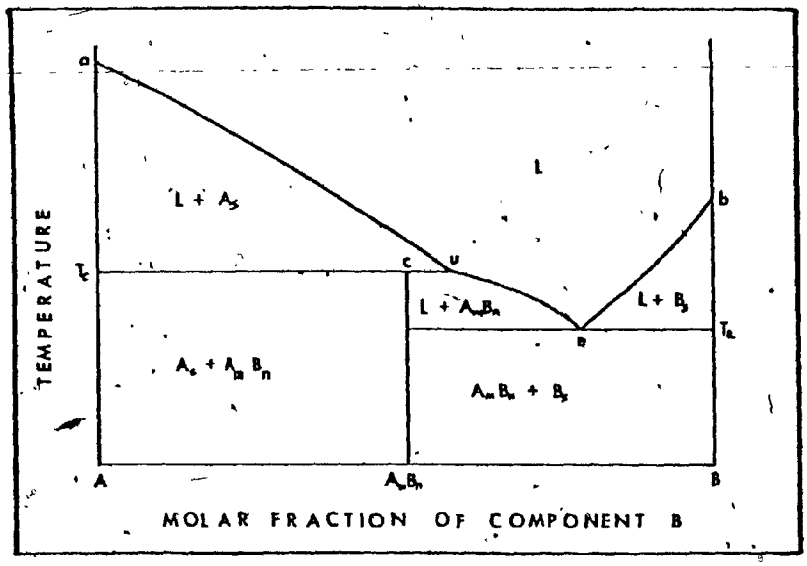

L = liquid mixture of A and B

A_s = solid solution of the shorter-chain fatty acid in the longer-chain fatty acid

B_s = solid solution of the longer-chain fatty acid in the shorter-chain fatty acid

A_mB_n = solid compound of A and B

a = melting point of A

b = melting point of B

c = composition of the solid compound

e = eutectic point

u = transition point

T_c = melting temperature of the compound

T_e = eutectic temperature

Fig. 5. Phase behaviour of a binary system of even straight-chain acids.

Liquid solutions, which on cooling, reach line "a e" give rise to a solid which is a compound containing an equimolar amount of the two components. Crystallization of the liquid solution occurs directly at the eutectic point with no change of composition.

For even straight-chain fatty acids which differ in chain length by two carbon atoms (capric-lauric, palmitic-stearic systems) the eutectic occurs at approximately 73 mole % of the lower-melting component. The hump in the freezing curve, representing the component formation region, occurs at about 50 to 73 mole % of the lower-melting component. These curve characteristics confirm earlier investigations by Francis et al (Ref. 3), Shuette et al (Ref. 4-8), Smith (Ref. 9), Kulka et al (Ref. 10) and Grondal et al (Ref. 11).

Table VII shows the observed eutectics of the binary systems of fatty acids. The eutectic for the capric-lauric system (C_{10}-C_{12}) was found to have a composition of 73 mole % capric: 27 mole % lauric on both the melting and freezing curves. The melting and freezing points of the eutectic are 18.2°C and 16.6°C respectively. The freezing point is slightly lower than the melting point due to the effect of supercooling. Kulka and Sandin (Ref. 10) found the eutectic of the C_{10}-C_{12} system to be 19.6°C at a composition of 72.5 mole % capric 27.5 mole % lauric using the capillary tube method. The small difference in the melting point can be ascribed to the impurities found in the reagent grade substances. Kulka and Sandin used highly purified acids which were repeatedly recrystallized from acetone.

The data for the melting and freezing points, latent heats of transition and temperatures for maximum exothermic and endothermic

heat flow for the C_{10}-C_{12} binary system have been plotted in Fig. 6 to Fig. 11.

TABLE VII. Observed eutectics of binary systems of fatty acids (Taken from phase diagrams).

PARAMETER	LAURIC-CAPRIC SYSTEM	LAURIC-PALMITIC SYSTEM	LAURIC-STEARIC SYSTEM	PALMITIC-STEARIC SYSTEM
Melting Point (°C)	18.2 @ 73C/2/L	32.7 @ 80L/20P	34.0 85L/15S	51.1 @ 72.5P/27.5S
Temperature for max. endothermic flow (°C)	20.8 @ 73C/27L	35.6 @ 80L/20P	36.7 @ 85L/15S	53.8 @ 72.5P/27.5S
Heat of Melting (J/g)	120 @ 72.5C/27.5L	147 @ 80L/20P	152 @ 86L/14S	159 @ 71P/29S
Freezing Point (°C)	16.6 @ 73C/27L	30.3 @ 80L/20P	31.3 @ 86L/14S	50.8@ 72.5P/27.5S
Temperature for max. exothermic heat flow (°C)	16.2 @ 72.5C/27.5L	29.1 @ 80L/20P	30.8 @ 86L/14S	49.7 @ 72.5P/27.5S
Heat of Crystal-lization (J/g)	113 @ 72.5C/27.5L	149 @ 79 L/21P	155 @ 86L/14S	161 @ 72.5P/27.5S

The profiles of the curves for the temperature for maximum exothermic heat flow, heat of melting and heat of crystallization resemble the profile of the curve for freezing points.

This is in agreement with the freezing curve profile developed by Kulka and Sandin. However, the profiles of the curves for melting points and maximum endothermic heat flow points differ in shape from the freezing curve. This occurs in the concentration

range of about 0-40 mole % capric acid and to a lesser degree in the compound formation region of about 40-73 mole % capric acid. In this concentration range, the melting points and the maximum endothermic heat flow points are lower than their corresponding freezing and maximum exothermic heat flow points. This difference in temperature can be explained in terms of the existence of multiple peaks on the thermograms and the method by which these parameters are calculated.

In the DSC calculation, the melting point is located at the peak which possesses the greatest rate change of heat flow. When a mixture contains two components, several peaks are present on the thermogram and the melting point and the maximum endothermic heat flow point can be located at different peaks depending on the concentration of the two components. The shifting of the melting point and the maximum heat flow point between the peaks can result in marked differences in these parameters. For example, for the mixture containing 10 mole % capric: 90 mole % lauric the melting point and the maximum endothermic heat flow point are 35.7°C and 40.1°C respectively and both are located on the second peak of the thermogram. However, for the next higher mixture containing 20 mole % capric: 80 mole % lauric the melting point is 20.9°C, having shifted to the first peak and the maximum endothermic heat flow point is 27.0°C continuing to remain on the second peak. Furthermore, going to the next higher concentration of 30 mole % capric: 70 mole % lauric, the melting point and the maximum endothermic heat flow point of the mixture are 20.4°C and 22.3°C respectively, both of which are found

on the first peak. As can be seen, the shifting between peaks can produce marked temperature differences in adjacent mixtures having different concentrations of the two components. This is also illustrated by the curves of these parameters which show that when shifting occurs between the peaks, the points generally do not fall directly on the curve. The significance of the peaks is discussed in a later section titled "Discussion of Thermograms of Binary Mixtures of Fatty Acids".

The eutectic composition for the palmitic-stearic (C_{16}-C_{18}) system was found to have a concentration of 72.5 mole % palmitic: 27.5 mole % stearic. The melting and freezing points at this concentration are 51.1°C and 49.7°C respectively. Francis et al (Ref. 3) have studied the C_{16}-C_{18} system and found the same composition of the eutectic point havihg a freezing point of 54.5°C. Another study of the C_{16}-C_{18} system was done by Shriner et al (Ref. 12) who also found the eutectic to have the same composition with a freezing point of 53.6°C. Therefore, the eutectic location appears to be in agreement with the published data. The small difference in the freezing point temperature found by the various workers can be attributed to the presence of reagent impurities which can produce a freezing point depression. The C_{16}-C_{18} binary system, similar to the C_{10}-C_{12} system which differs in chain length by two carbon atoms, contains a hump in the freezing curve in the same concentration range of 50-73 mole % palmitic acid demarcating the compound formation region. The data for the freezing and cooling parameters of the C_{16}-C_{18} system is represented graph-

ically in Fig. 12 to Fig. 17.

For even straight-chain fatty acids which differ by more than two carbon atoms in the chain length such as lauric-palmitic (C_{12}-C_{16}) and lauric-stearic (C_{12}-C_{18}) systems, the eutectic location is shifted to a higher molar concentration of the lower-molecular weight component. Also, the compound formation region is displaced to a concentration range containing a higher molar concentration of the lower-molecular weight component.

For the C_{12}-C_{16} binary system, the eutectic occurs at a concentration of 80 mole % lauric: 20 mole % palmitic. The melting and freezing points at this concentration are 32.7°C and 30.3°C respectively. This is in agreement with the results obtained by Waentig and Pescheck (Ref. 13) and Efremov et al (Ref. 13) who observed the eutectic at 80 mole % lauric: 20 mole % palmitic and 77.5 mole % lauric: 22.5 mole % palmitic respectively. The corresponding freezing points were 35.5°C and 31°C respectively. The small difference in freezing temperatures which were determined by the different workers can be explained by the degree of impurities found in the reagent materials. The results of the thermal experiments for the C_{12}-C_{16} binary system are depicted graphically in Fig. 18 to Fig. 23.

For the C_{12}-C_{18} binary system, the melting point of the eutectic was found to be 34°C, having a concentration of 85 mole % lauric: 15 mole % stearic. The freezing point of the eutectic was found to be 31.3°C at a concentration of 86 mole % lauric: 14 mole % stearic. This agrees with the eutectic composition of 82.5 mole % lauric:

12.5 mole % stearic having a freezing point of 36.5°C. The slight difference in the eutectic composition and freezing points are due to impurities in the reagent materials. The thermal data for the C_{12}-C_{18} binary system is shown graphically in Fig. 24 to Fig. 29.

The results of all the DSC runs on C_{10}-C_{12}, C_{12}-C_{16}, C_{12}-C_{18} and C_{16}-C_{18} are tabulated in the appendix tables A-2, A-3, A-4 and A-5 respectively. Thermograms of the samples, T-6 to T-81, also appear in the appendix.

FIG.6 MELTING POINTS OF BINARY SYSTEM CAPRIC-LAURIC ACIDS

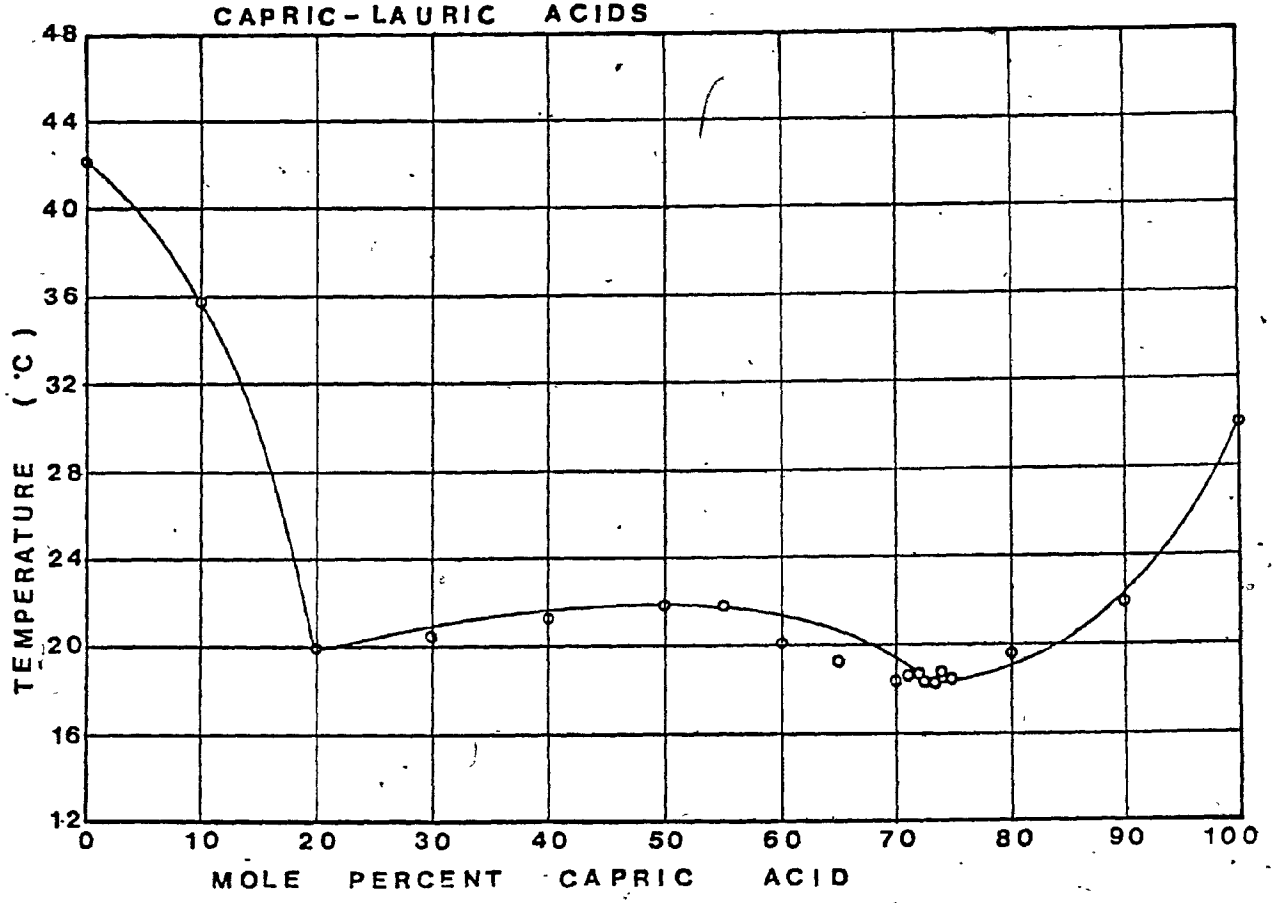

FIG.7 FREEZING POINTS OF BINARY SYSTEM CAPRIC-LAURIC ACIDS

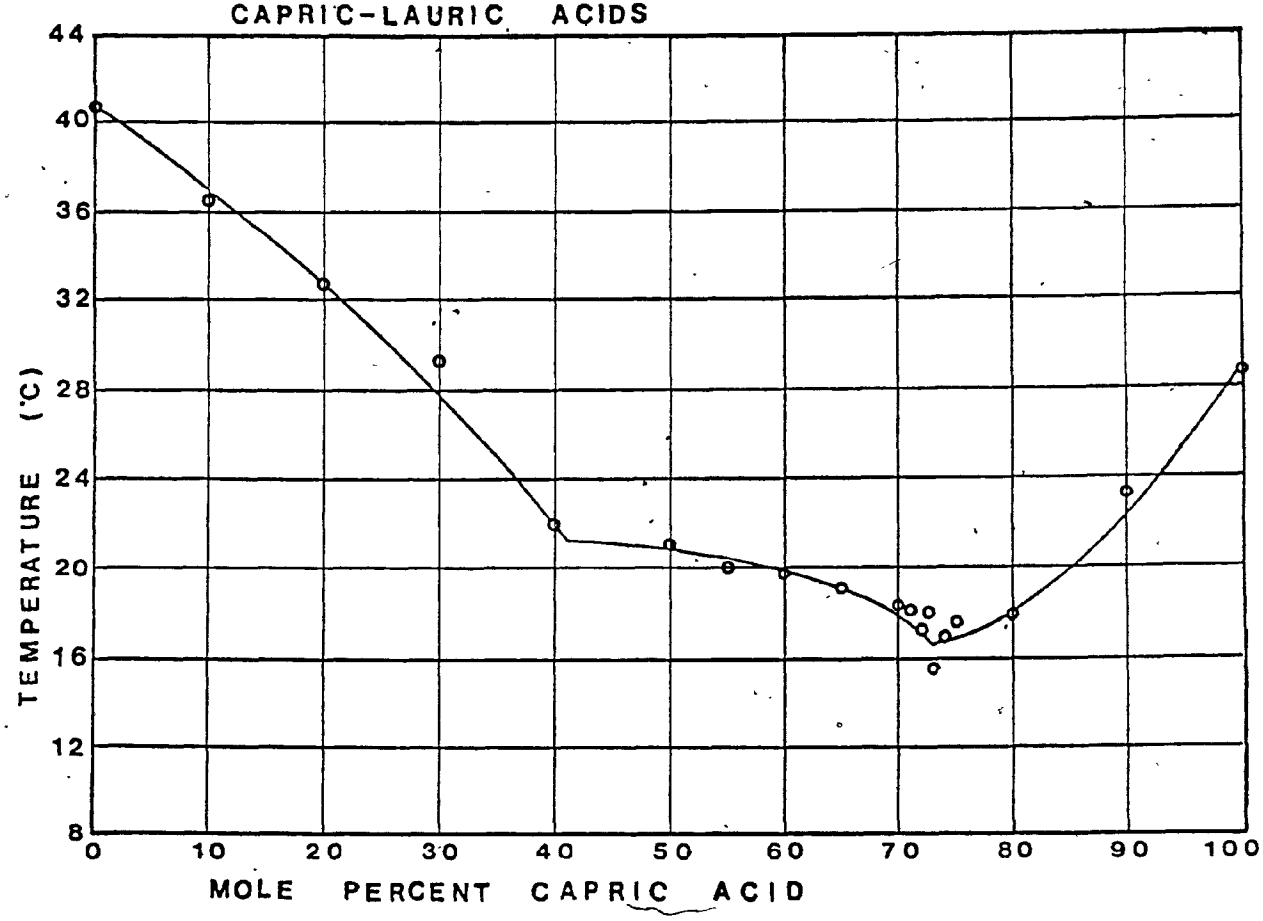

FIG.8 HEAT OF CRYSTALLIZATION OF BINARY SYSTEM. CAPRIC - LAURIC ACIDS

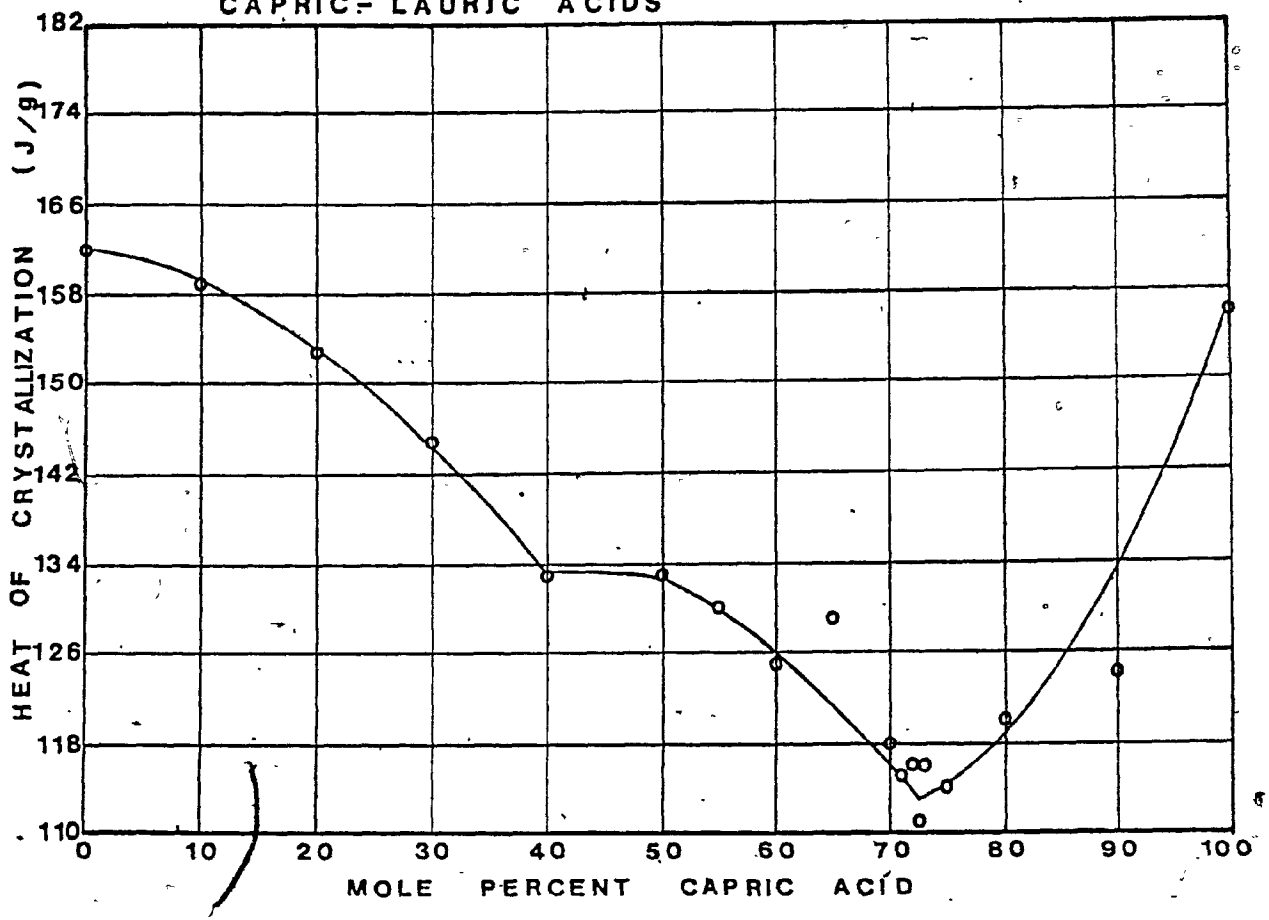

FIG.9 HEAT OF MELTING OF BINARY SYSTEM CAPRIC- LAURIC ACIDS

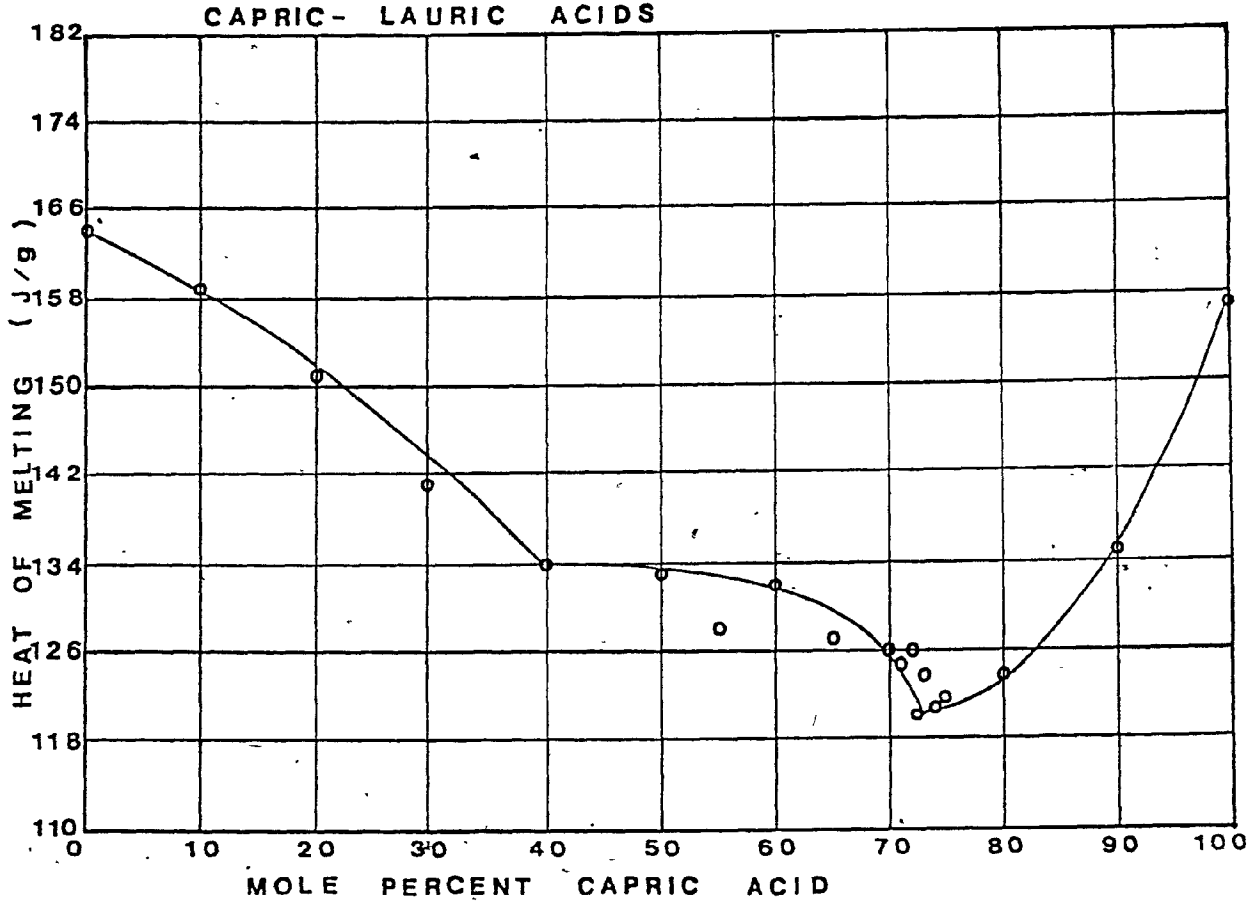

FIG.10 TEMPERATURE FOR MAXIMUM EXOTHERMIC HEAT FLOW OF BINARY SYSTEM CAPRIC-LAURIC ACIDS

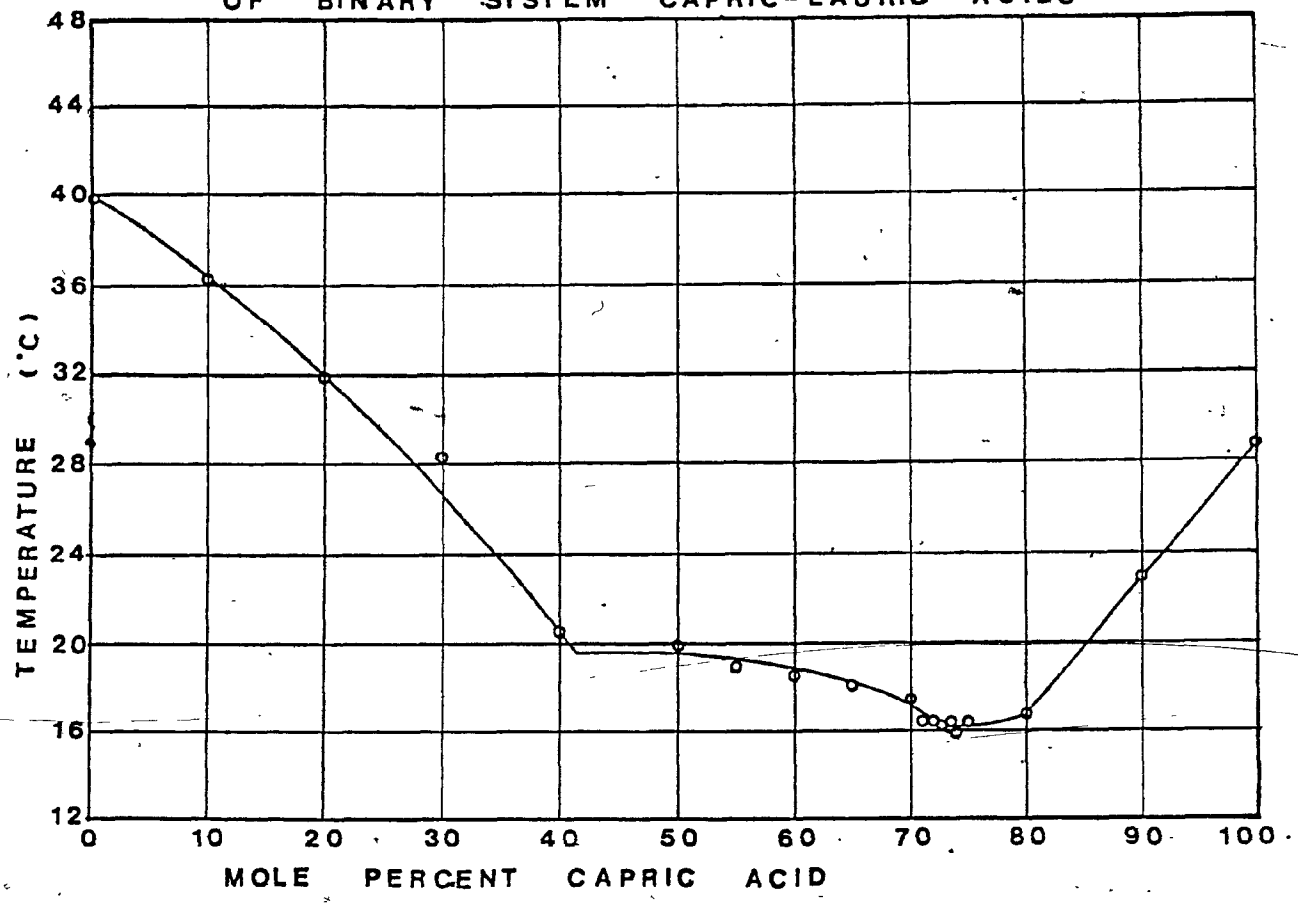

FIG.11 TEMPERATURE FOR MAXIMUM ENDOTHERMIC HEAT FLOW OF BINARY SYSTEM CAPRIC-LAURIC ACIDS

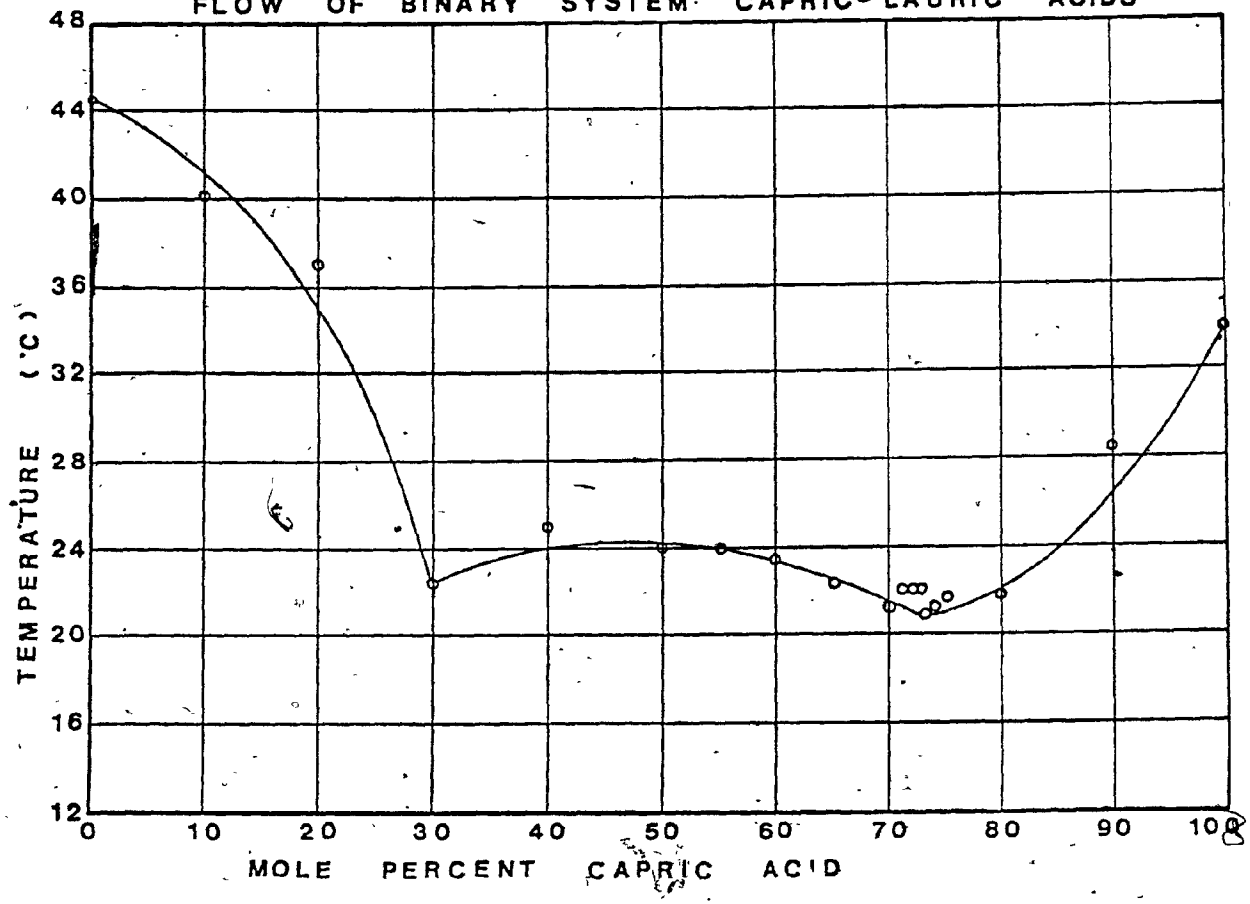

FIG.12 MELTING POINTS OF BINARY SYSTEM PALMITIC - STEARIC ACIDS

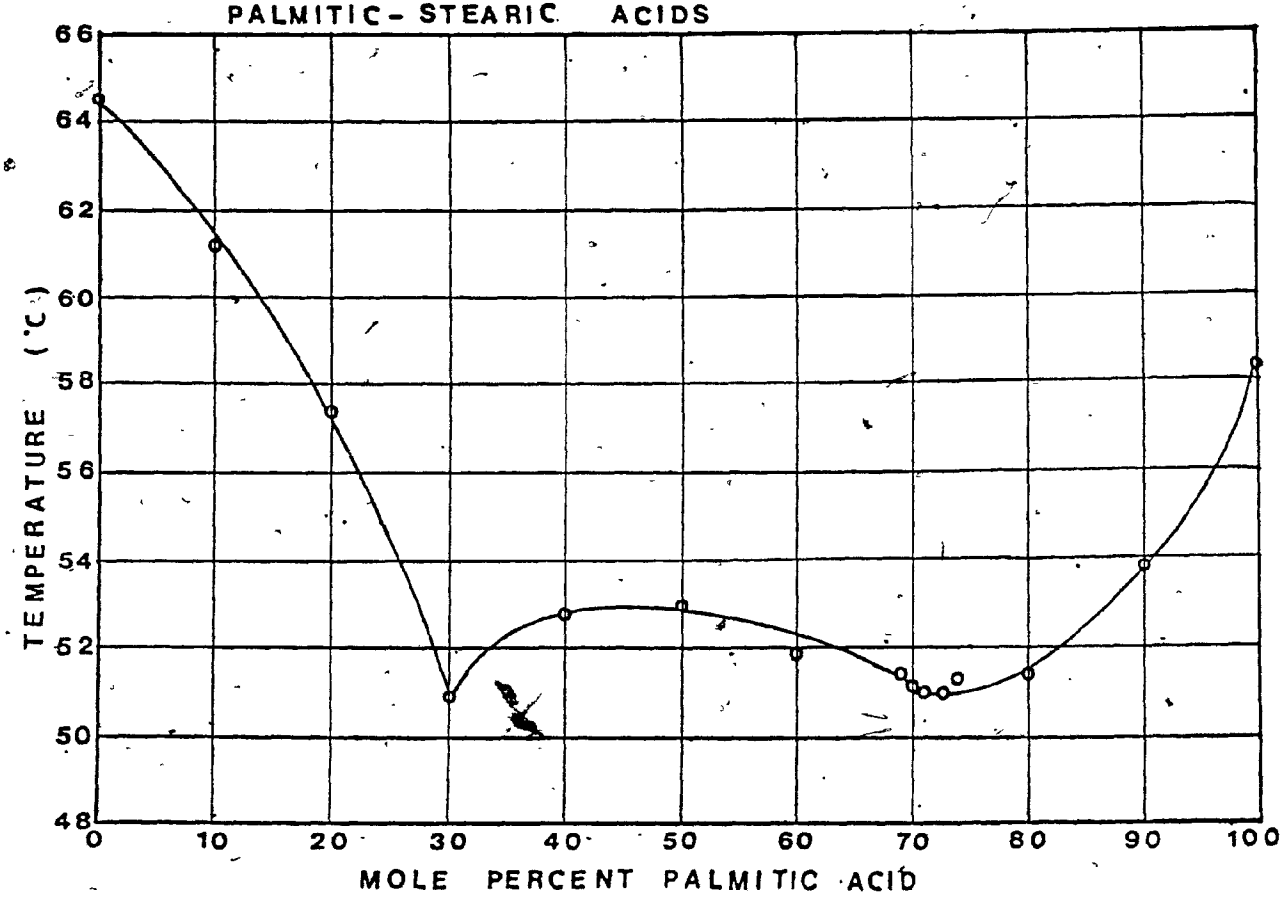

FIG. 13 FREEZING POINTS OF BINARY SYSTEM PAL-ST ACIDS

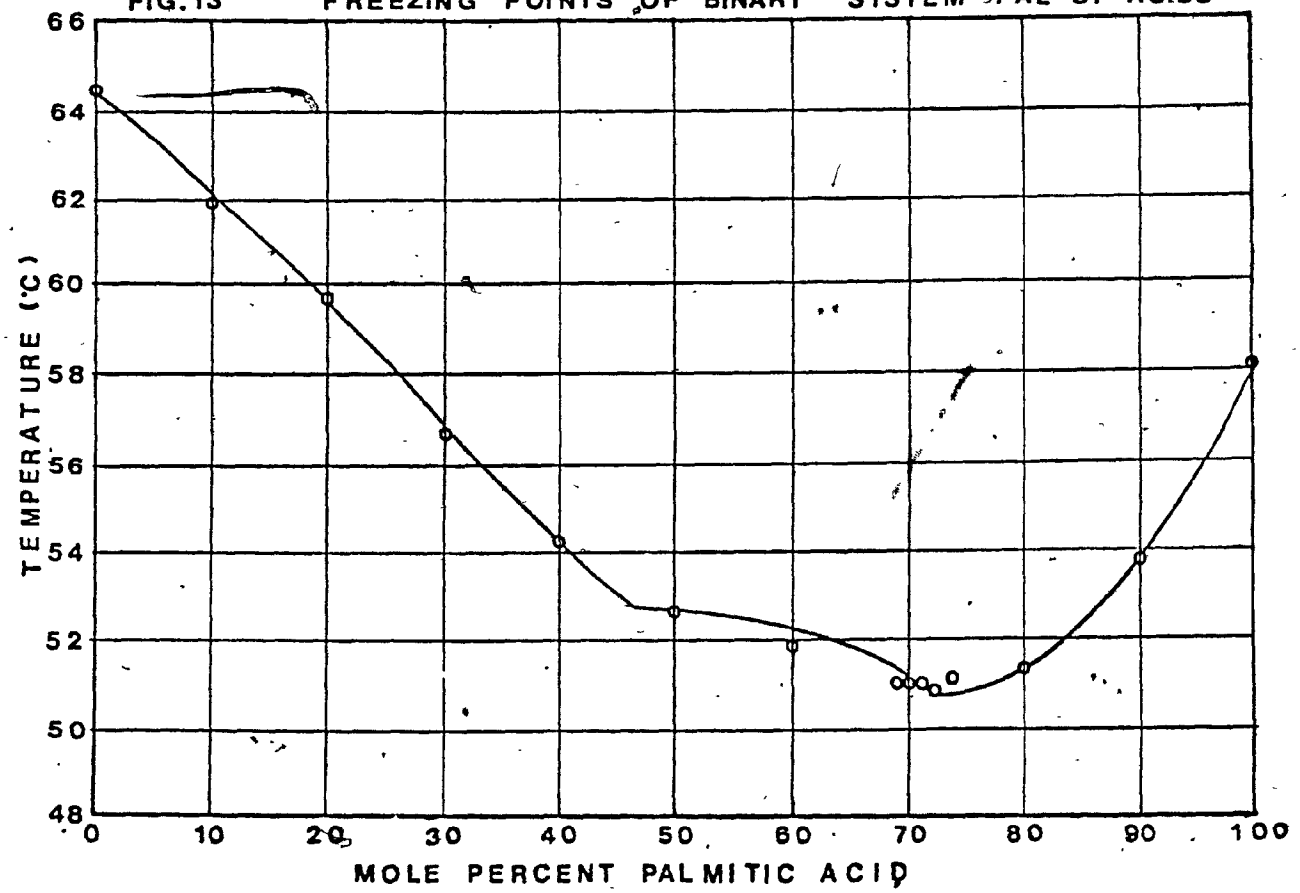

FIG. 14 HEAT OF CRYSTALLIZATION OF BINARY SYSTEM PALMITIC-STEARIC ACIDS

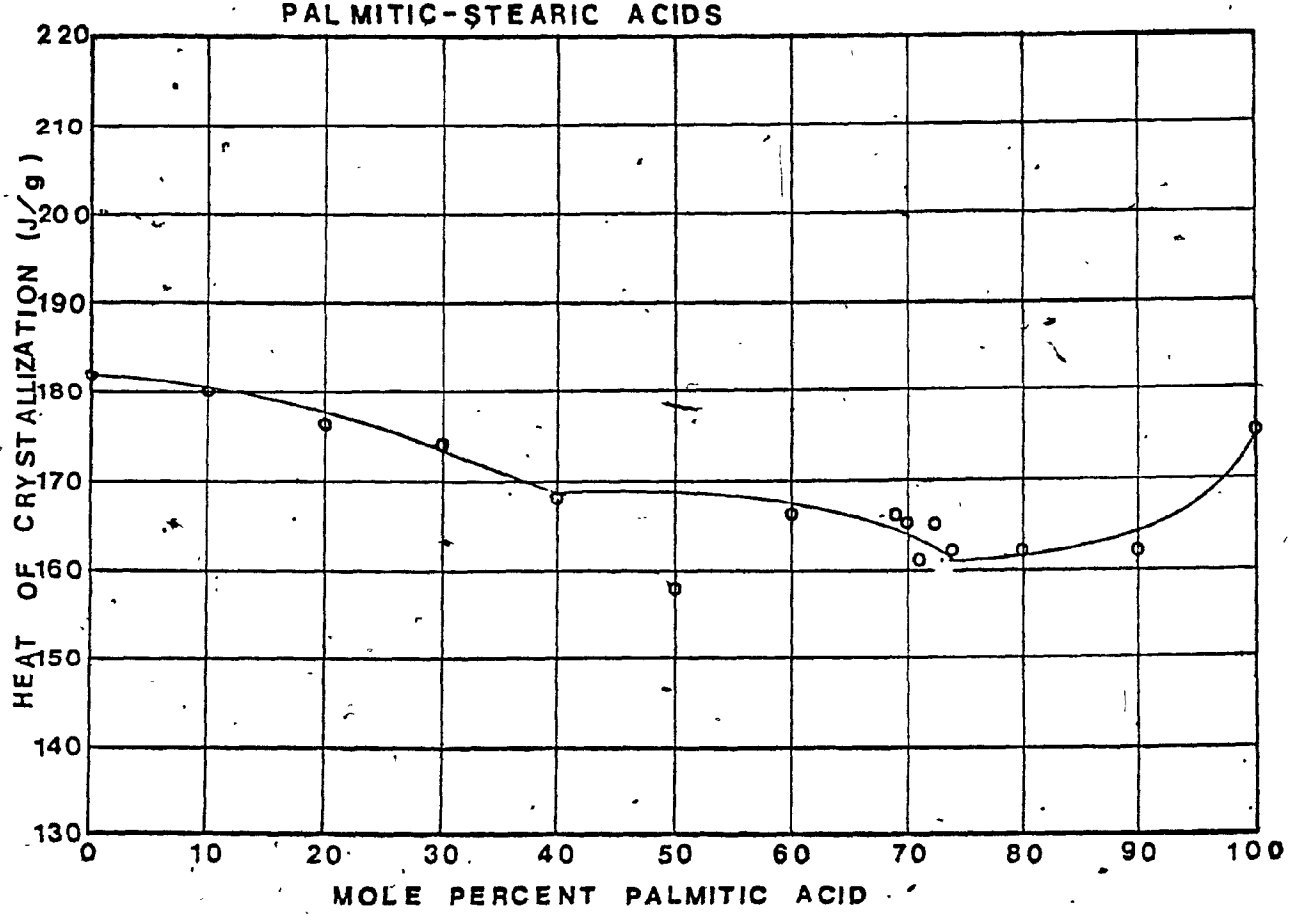

FIG,15 HEAT OF MELTING OF BINARY SYSTEM PALMITIC-STEARIC ACIDS

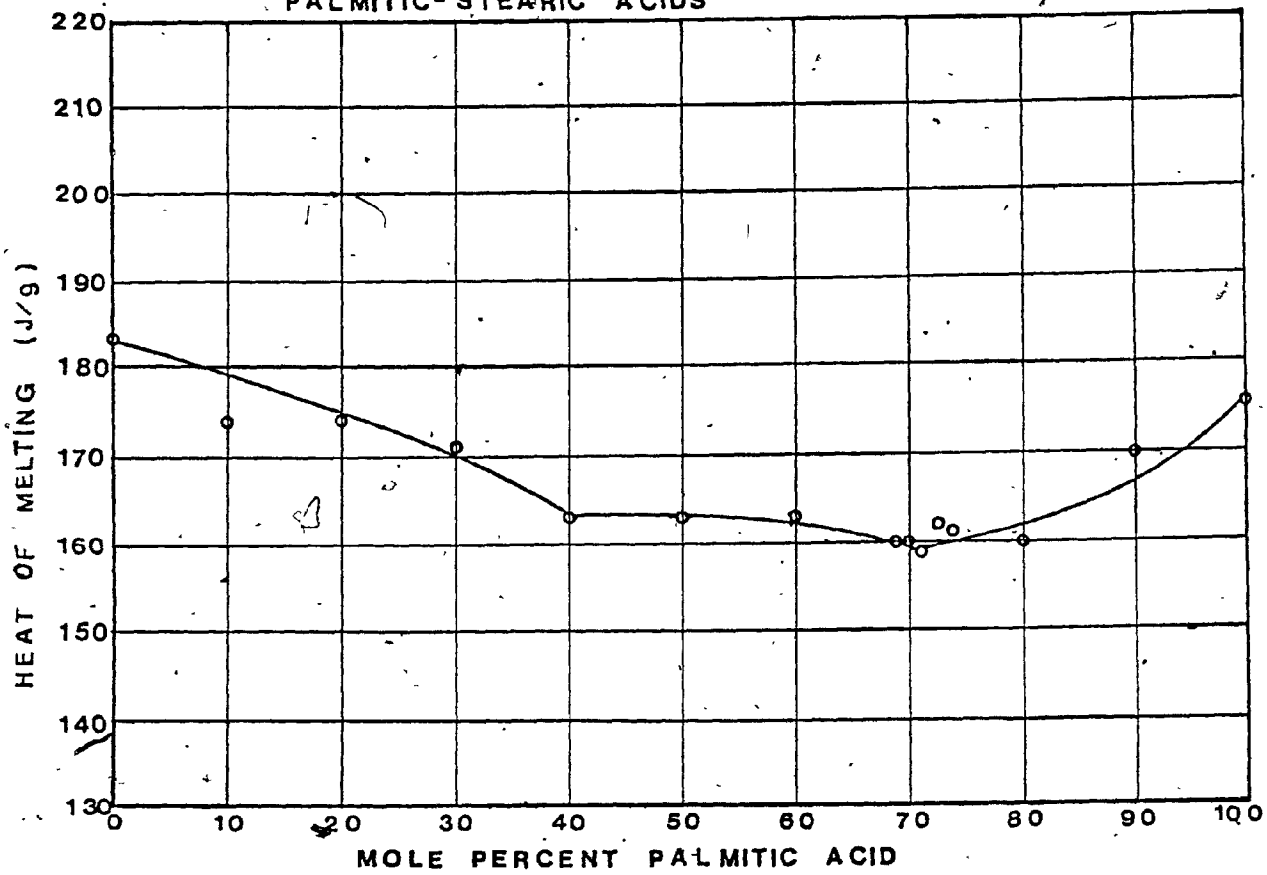

FIG. 16 TEMPERATURE FOR MAXIMUM EXOTHERMIC HEAT FLOW OF BINARY SYSTEM PALMITIC-STEARIC ACIDS

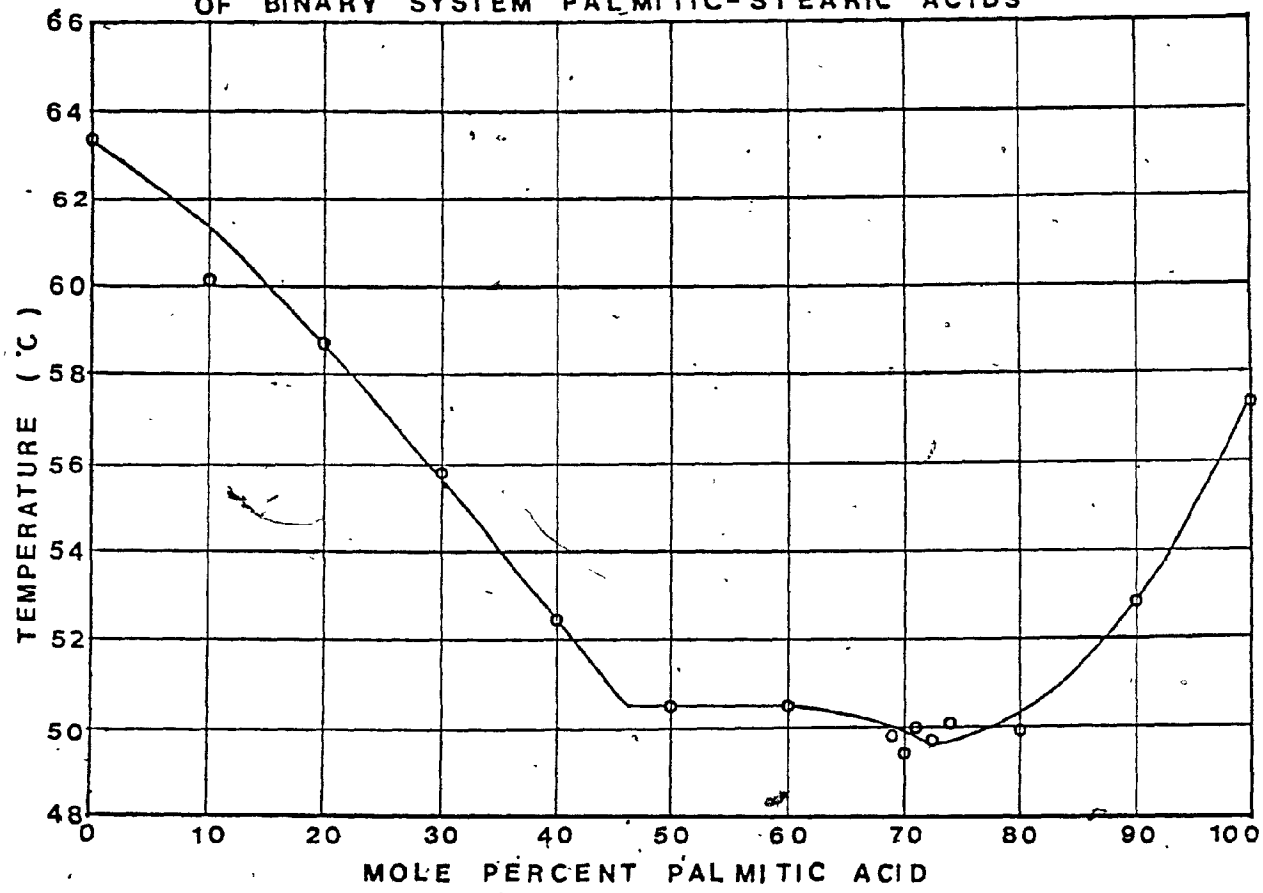

FIG.17 TEMPERATURE FOR MAXIMUM ENDOTHERMIC HEAT FLOW OF BINARY SYSTEM PALMITIC-STEARIC ACIDS

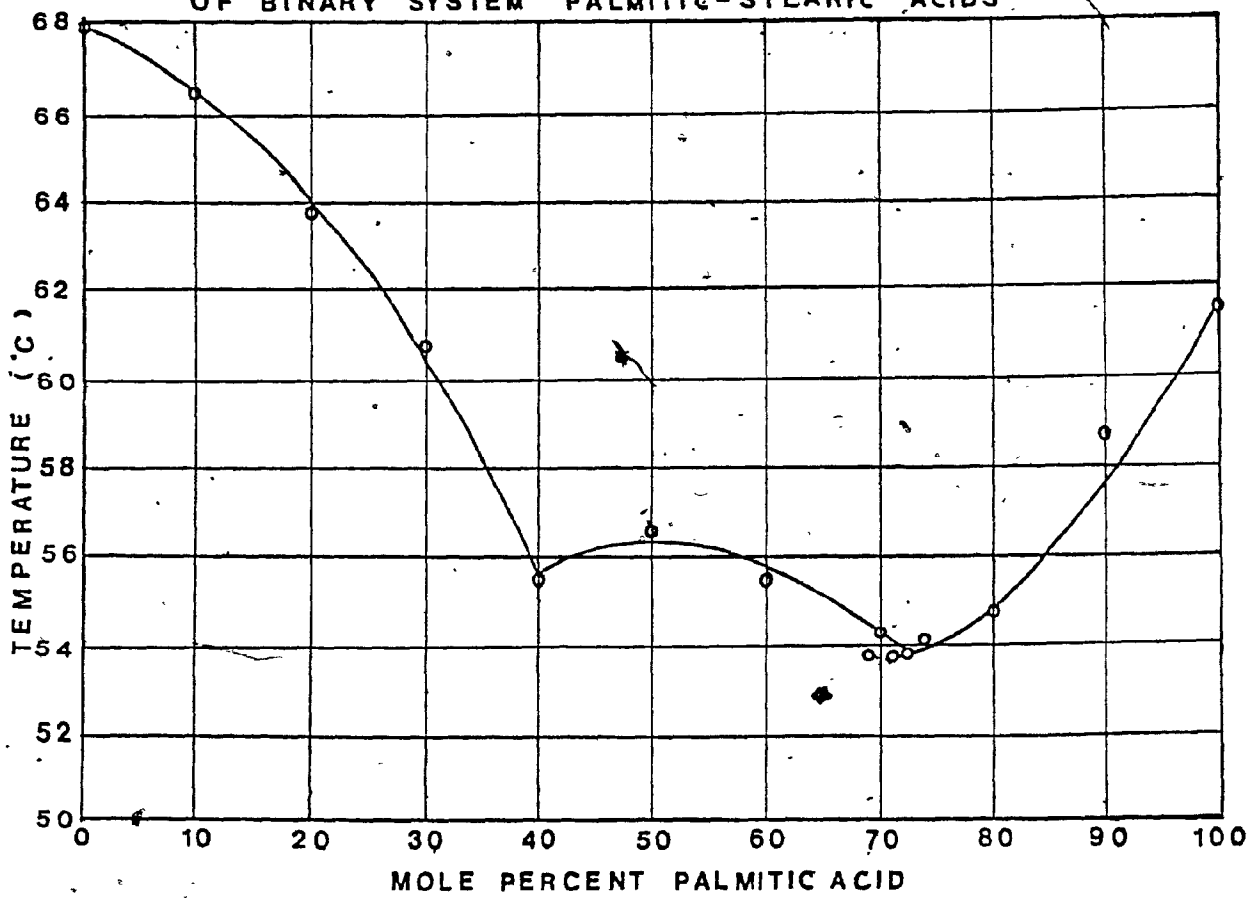

FIG.18 MELTING POINTS OF BINARY SYSTEM LAURIC-PALMITIC ACIDS

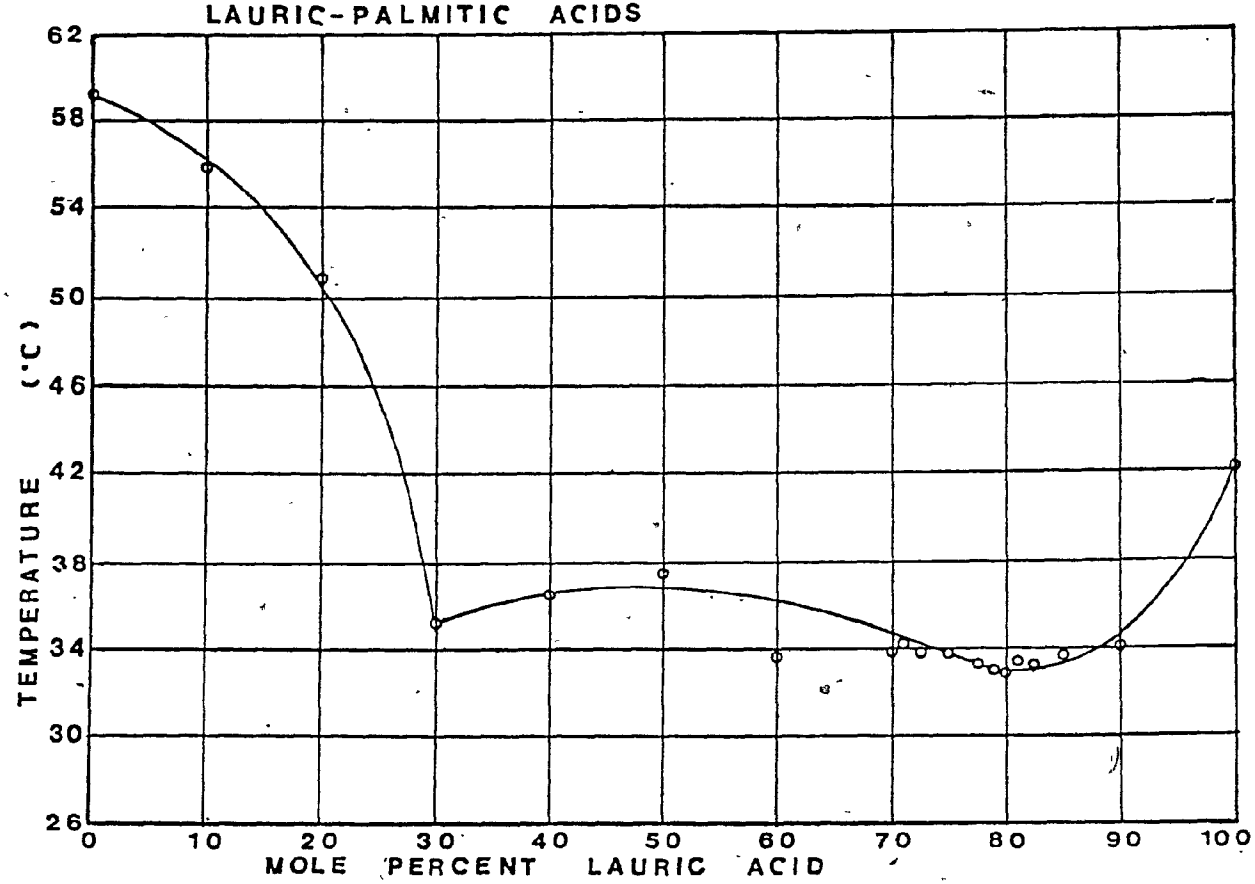

FIG.19 FREEZING POINTS OF BINARY SYSTEM LAURIC-PALMITIC ACIDS

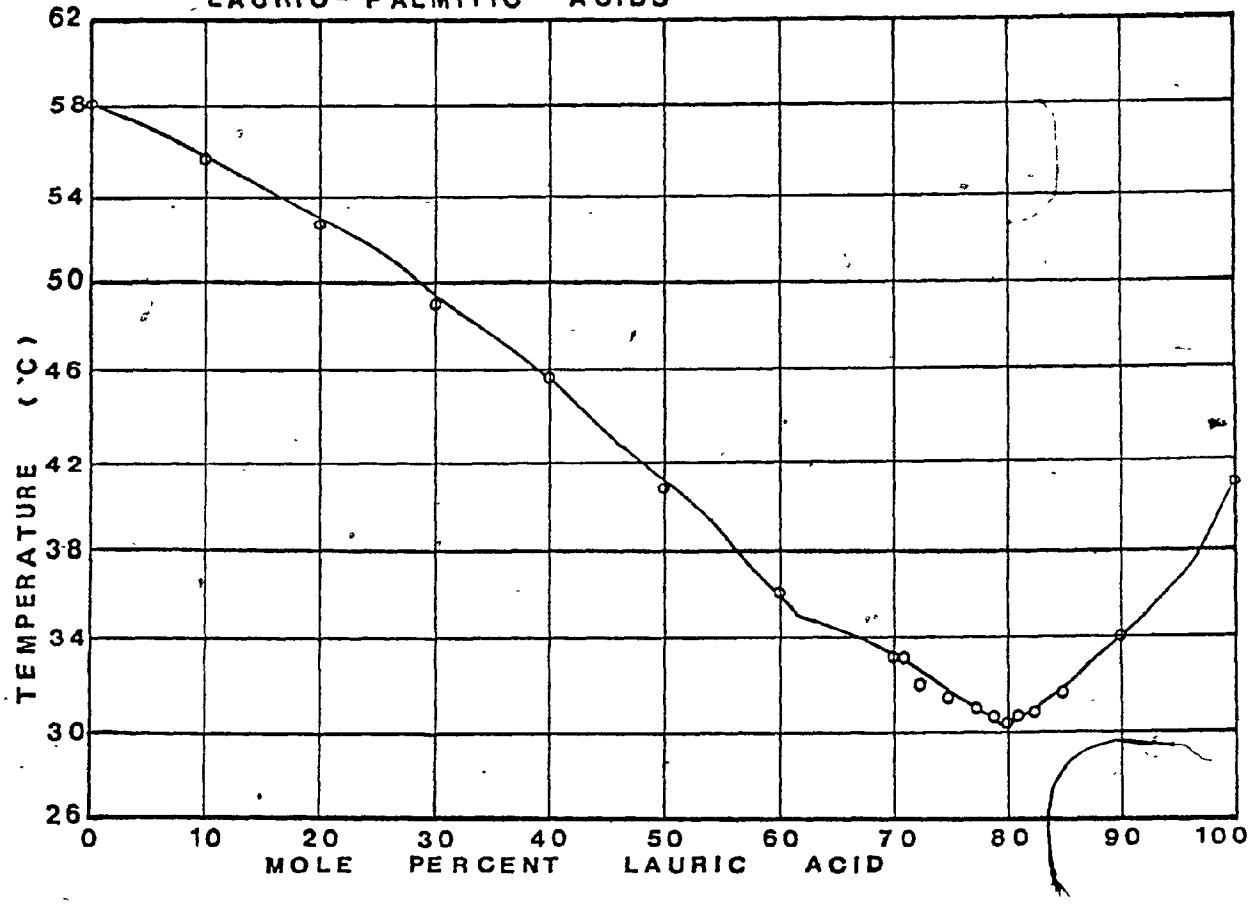

FIG.20 HEAT OF CRYSTALLIZATION OF BINARY SYSTEM LAURIC- PALMITIC ACIDS

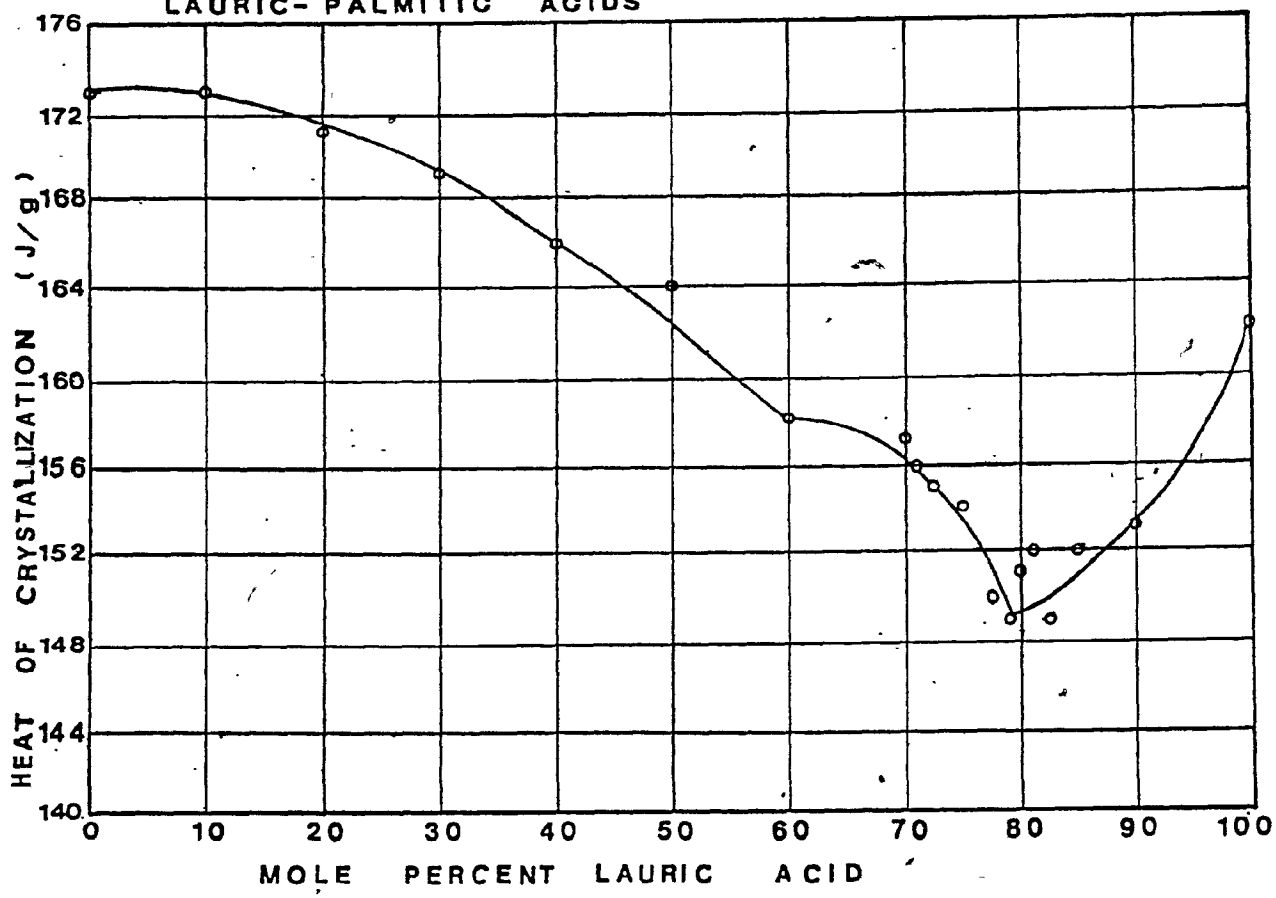

FIG.21 HEAT OF MELTING OF BINARY SYSTEM LAURIC- PALMITIC

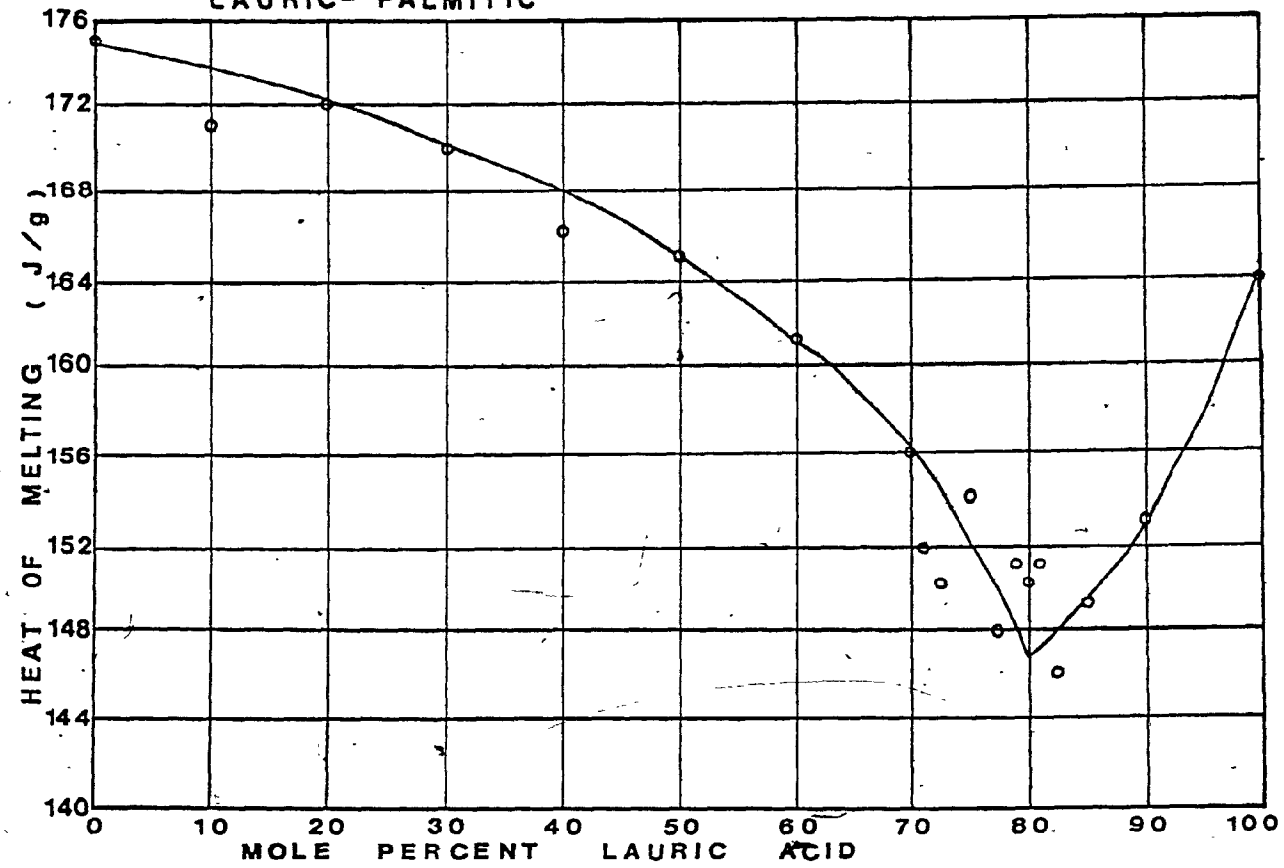

FIG.22 TEMPERATURE FOR MAXIMUM EXOTHERMIC HEAT FLOW OF BINARY SYSTEM LAURIC-PALMITIC ACIDS

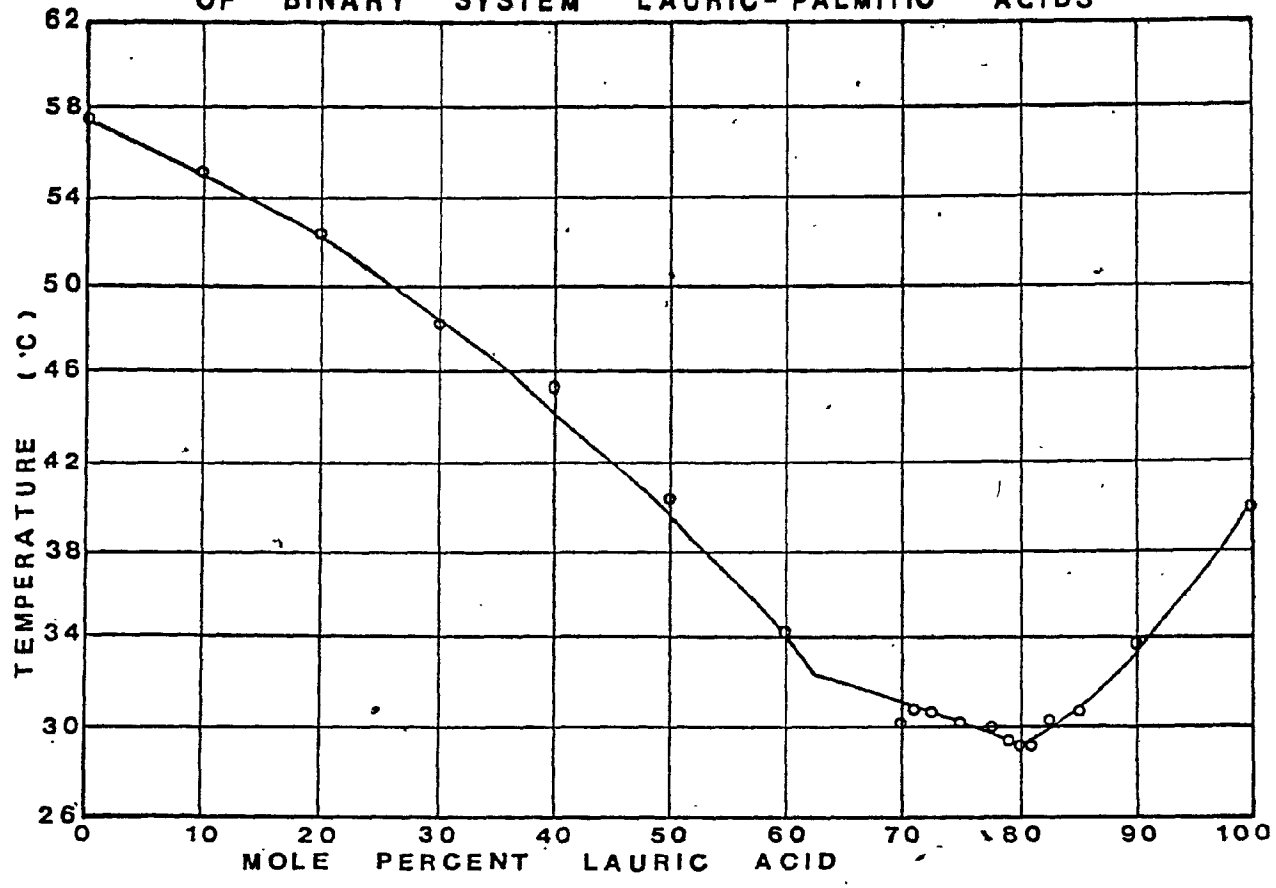

FIG. 23 TEMPERATURE FOR MAXIMUM ENDOTHERMIC HEAT FLOW OF BINARY SYSTEM LAURIC-PALMITIC ACIDS

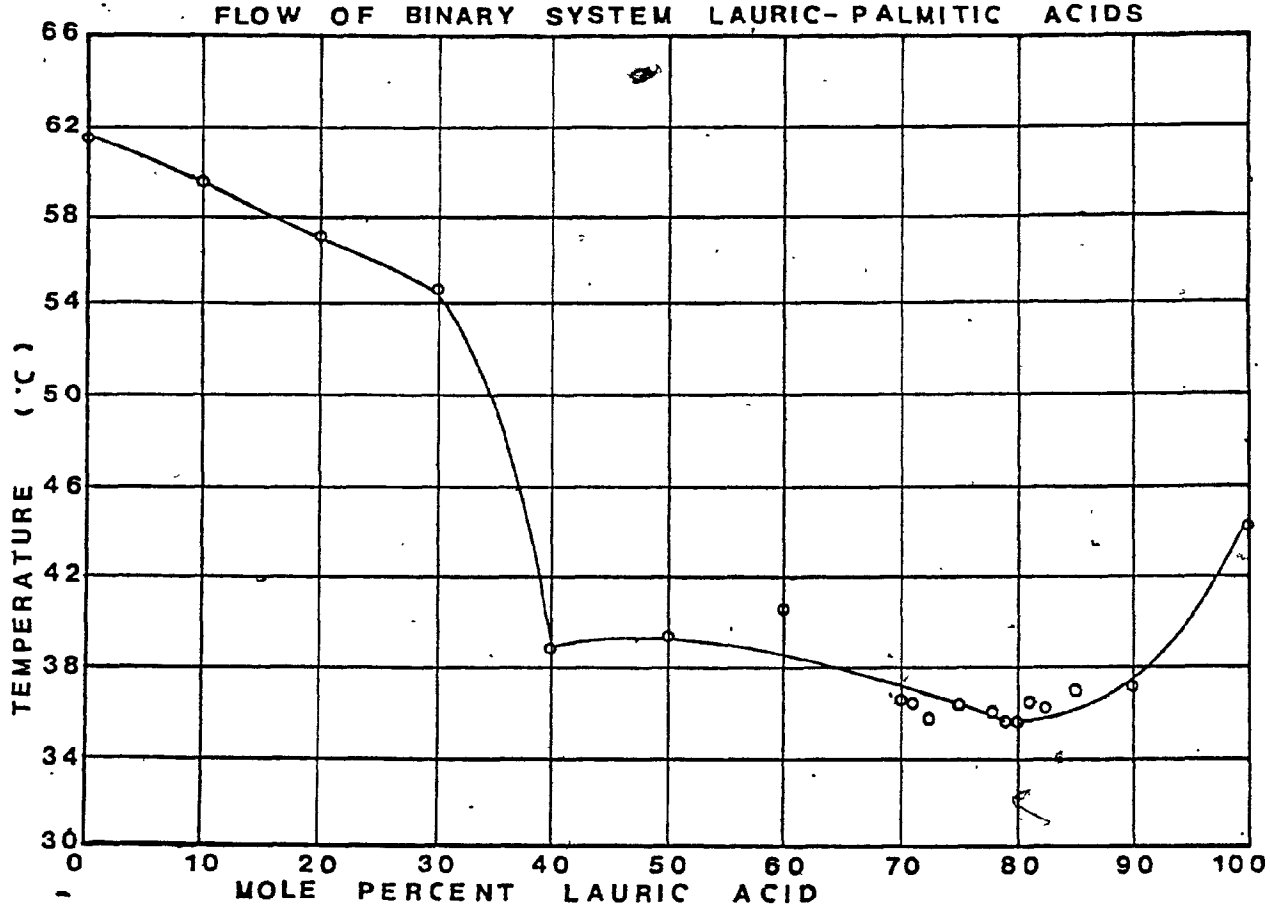

FIG.24 MELTING POINTS OF BINARY SYSTEM LAURIC-STEARIC ACIDS

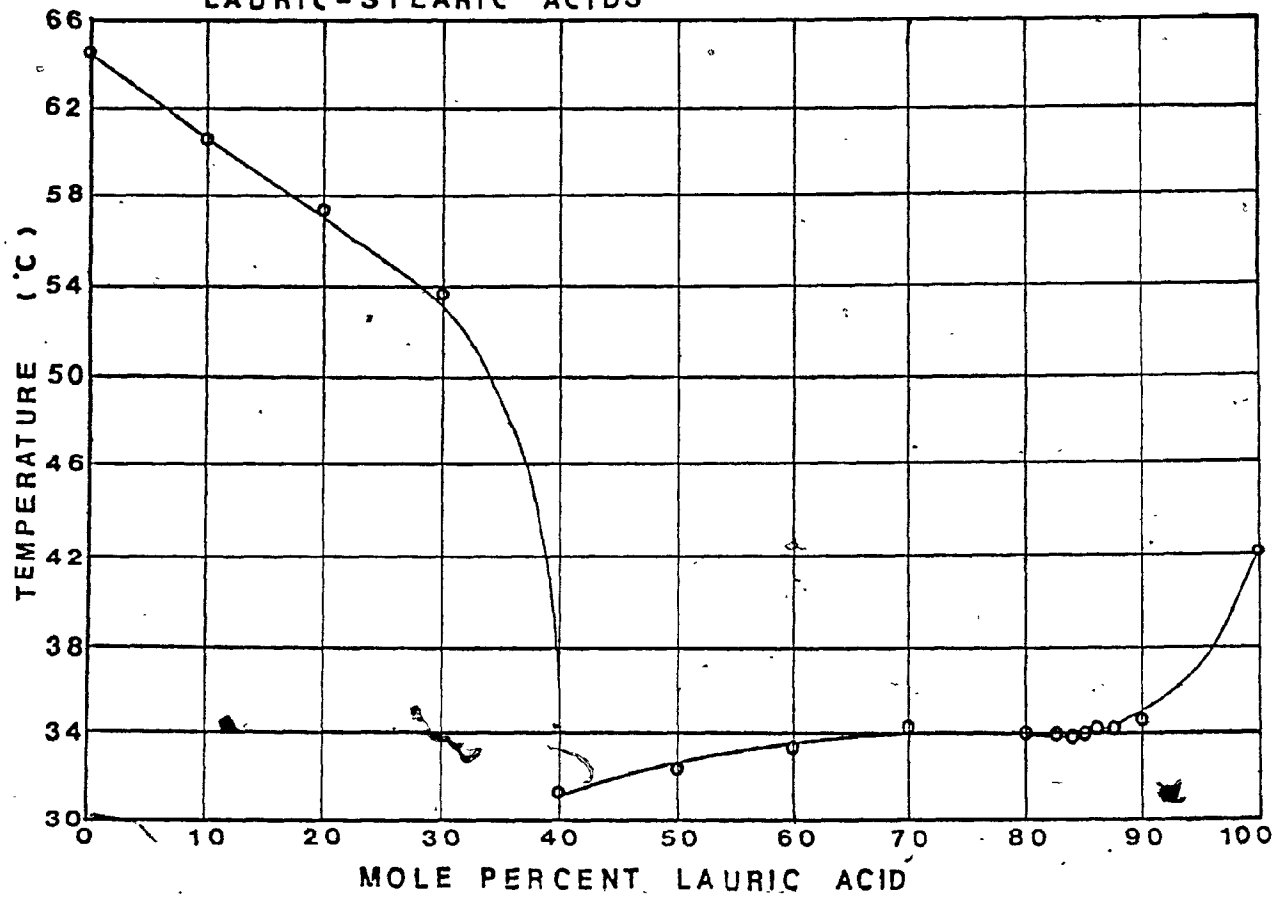

FIG.25 FREEZING POINTS OF BINARY SYSTEM
LAURIC-STEARIC ACIDS

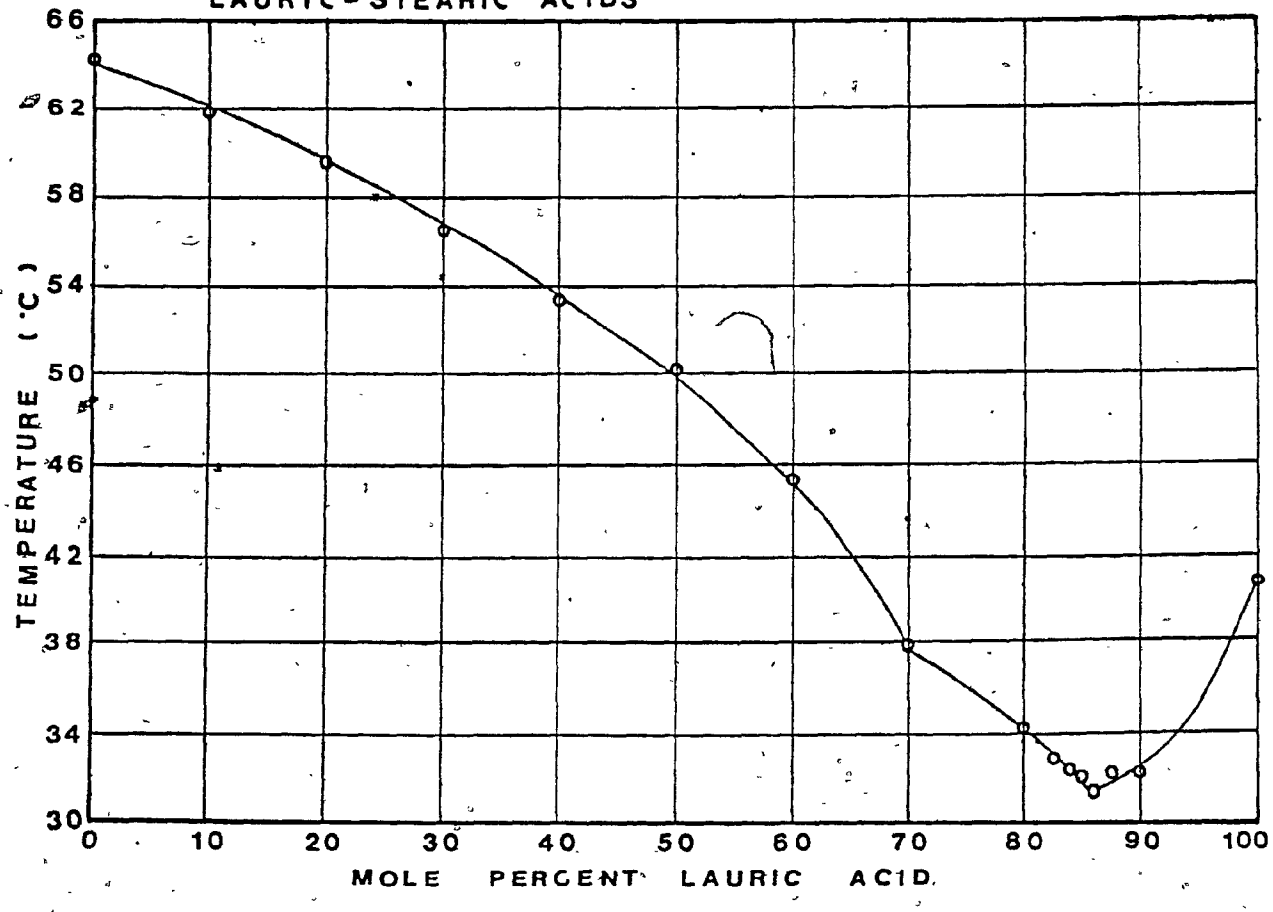

FIG.26 HEAT OF CRYSTALLIZATION OF BINARY SYSTEM LAURIC-STEARIC ACIDS

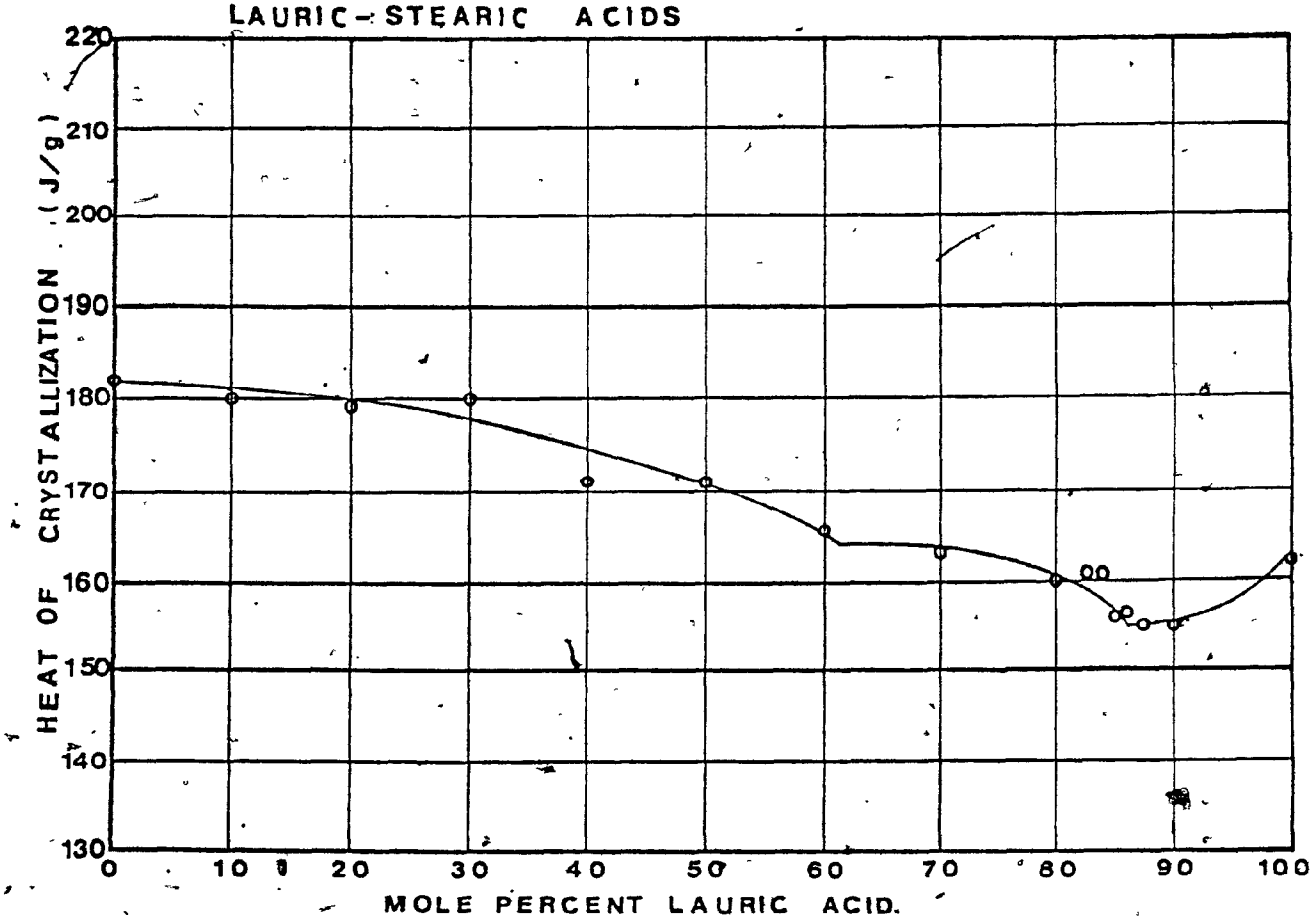

FIG.27 HEAT OF MELTING OF BINARY SYSTEM
LAURIC-STEARIC ACIDS

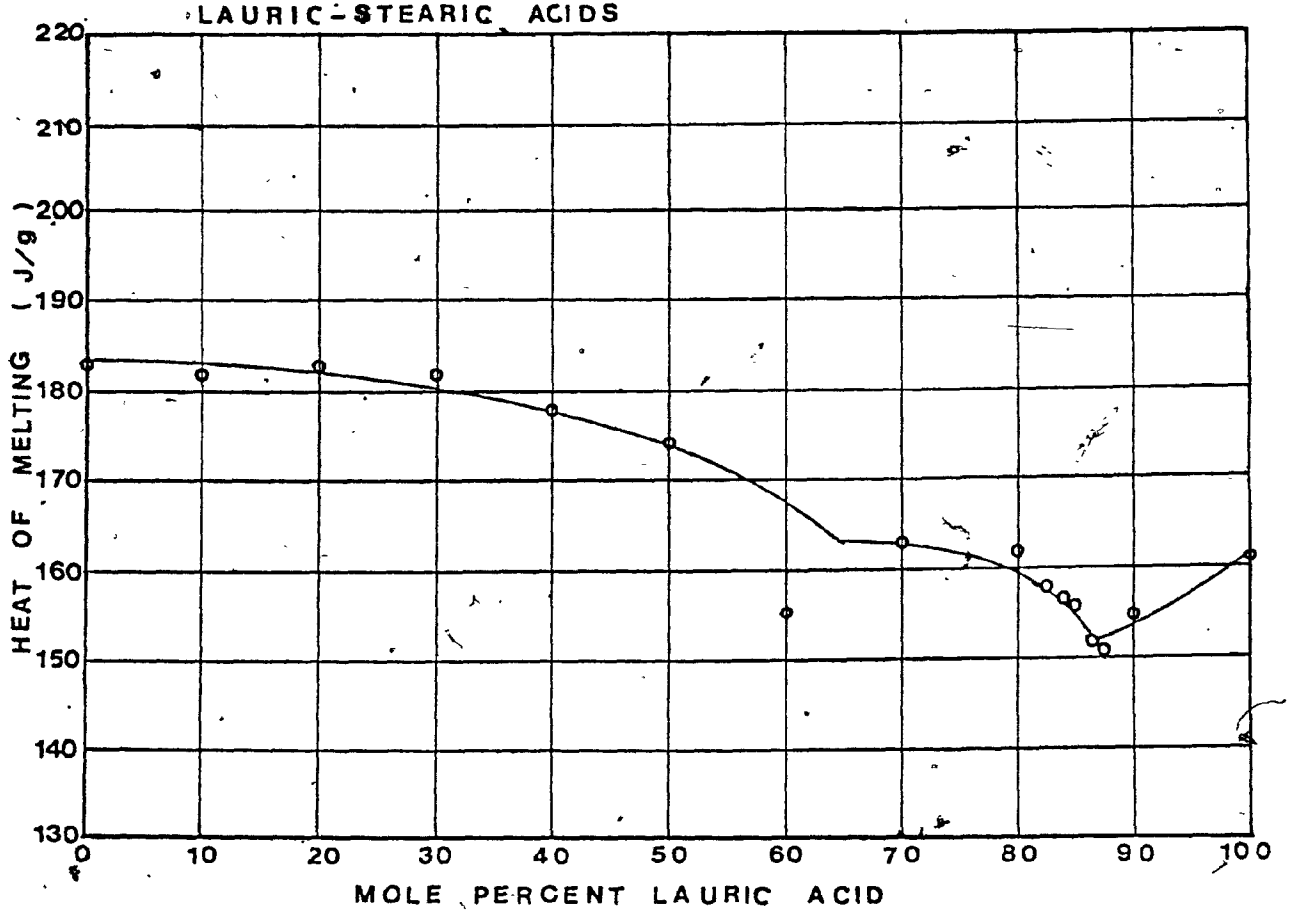

FIG.28 TEMPERATURE FOR MAXIMUM EXOTHERMIC HEAT FLOW OF BINARY SYSTEM LAURIC-STEARIC ACIDS

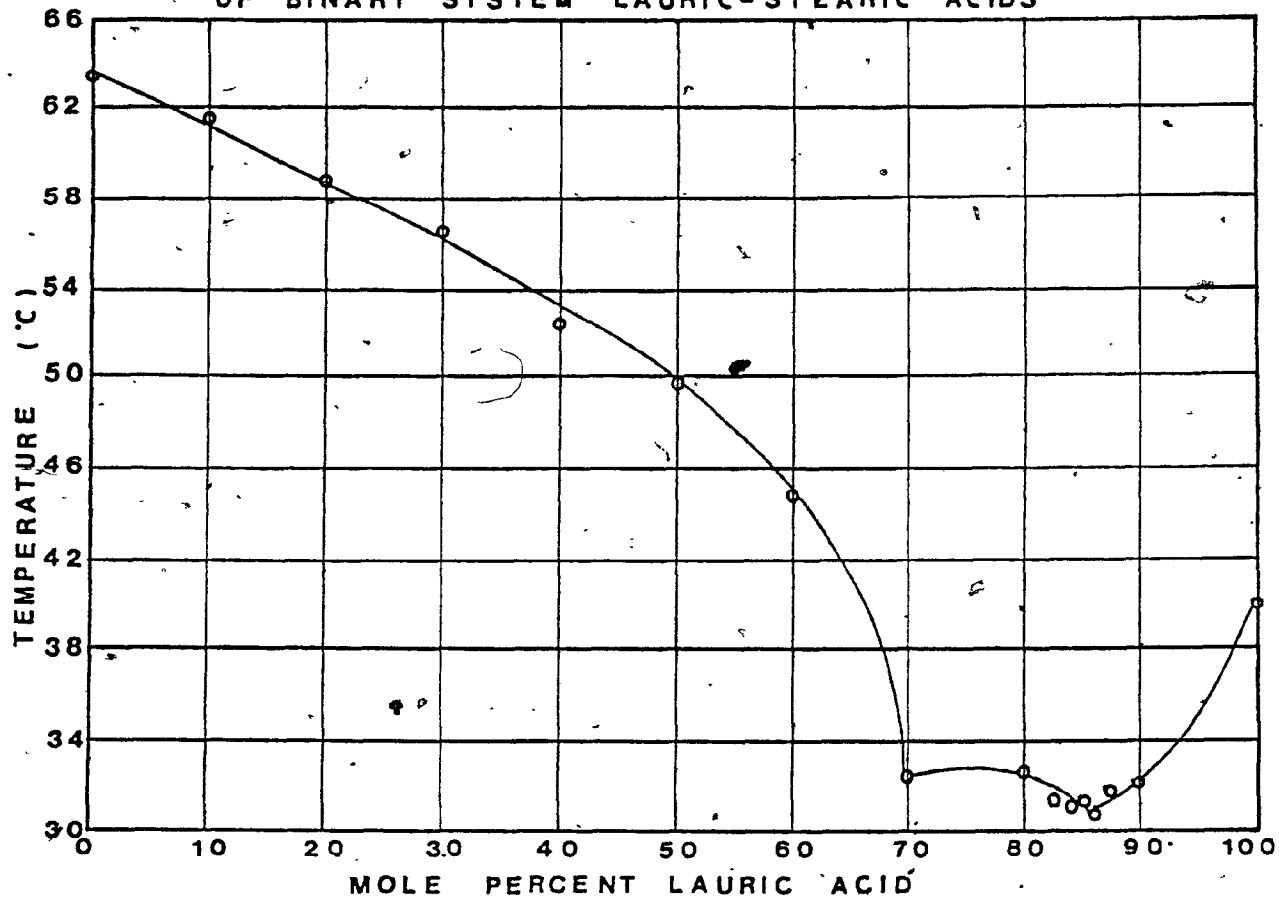

FIG.29 TEMPERATURE FOR MAXIMUM ENDOTHERMIC HEAT FLOW OF BINARY SYSTEM LAURIC - STEARIC ACIDS

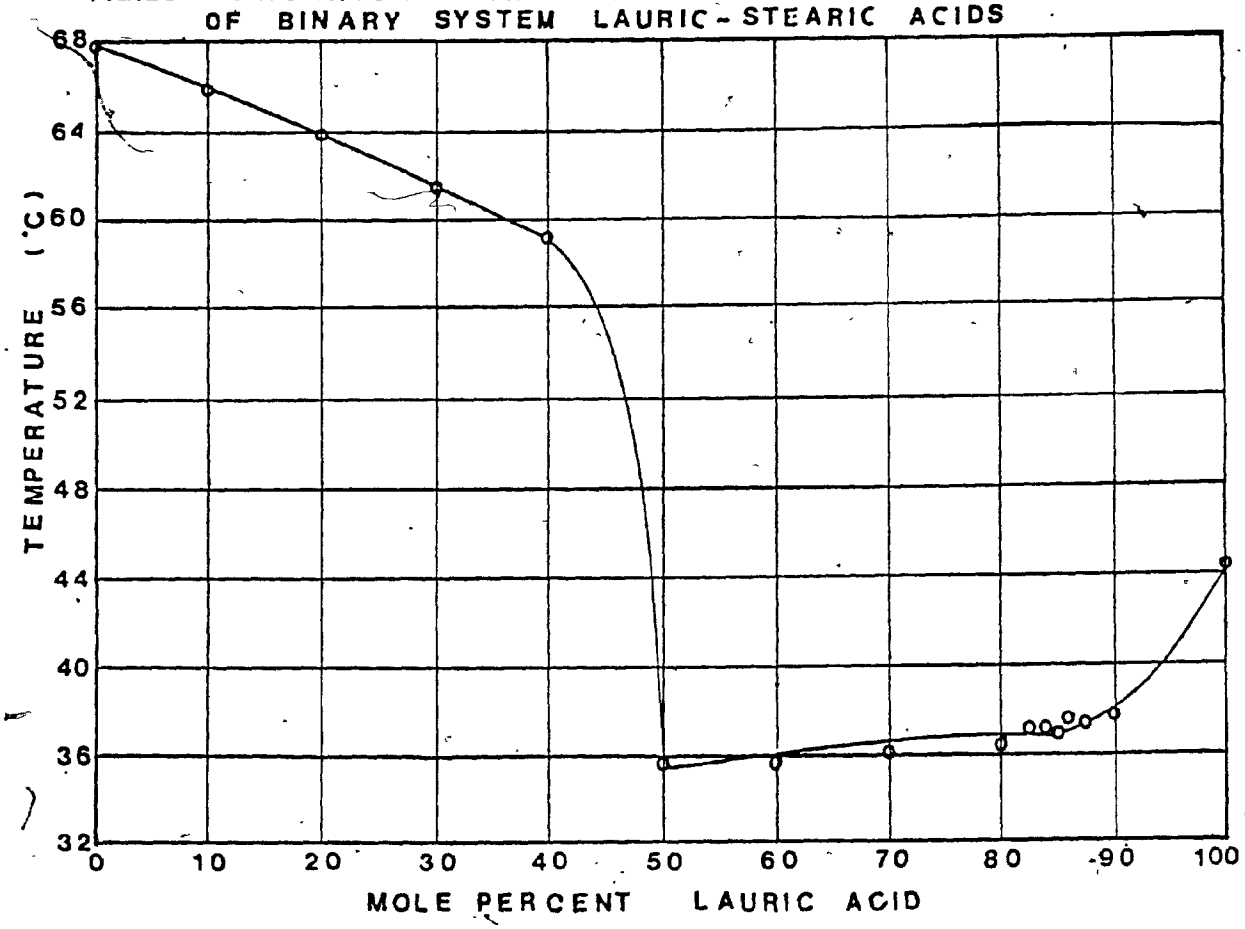

VII. THERMAL PROPERTIES OF FATTY ACIDS

Melting Points

The melting points of capric, lauric, palmitic and stearic acids were observed to be 30.0 ± 0.4°C, 42.2 ± 0.1°C, 59.0 ± 0.6°C and 65.6 ± 0.1°C respectively. The observed means and standard deviations of the melting points and other parameters are listed in Table VIII. The melting points of capric and lauric acids are about 1°C lower than the published values (Ref. 13) and those of palmitic and stearic acids are about 4°C lower. The generally accepted melting range of these acids is shown in Table VI. However, the observed melting points were close to the points found by Berchiesi (Ref. 14) which were 30.5°C, 42.8°C, 61.4°C and 66.2°C for capric, lauric, palmitic and stearic acids respectively. The discrepancy in the results appears to be due to the degree of impurities found in the reagent grade substances. Also, in the DSC calculations the melting point is taken at the inflection point of the curve which has the greatest rate of change of heat flow. The tangent drawn at the inflection point and projected to the base line can produce a value of the melting point which may differ from the value determined by other methods. In addition, in the DSC method the heating rate and mass of sample affect the melting point. The relationship between the melting point and the chain length (number of carbon atoms in the acid) is shown in Fig. 30. From the figure, it can be seen that the melting point increases directly with the chain length.

TABLE VIII. Observed Thermal Properties of Fatty Acids*

COMMON NAME	MELTING POINT (°C)	TEMPERATURE FOR MAX. ENDOTHERMIC HEAT FLOW (°C)	FREEZING POINT(°C)	TEMPERATURE FOR MAX. EXOTHERMIC HEAT FLOW (°C)	HEAT OF MELTING		HEAT OF CRYSTALLIZATION		ENTROPY OF MELTING J/g - °K
					J/g	Kcal/Mole	J/g	Kcal/Mole	
Capric	30.0 ± 0.4	31.8 ± 0.8	28.7 ± 0.3	28.6 ± 0.1	157 ± 6	6.5	153 ± 7	6.3	0.518
Lauric	42.2 ± 0.1	44.2 ± 0.4	40.7 ± 0.1	39.8 ± 0.1	164 ± 4	7.8	162 ± 7	7.8	0.520
Palmitic	59.0 ± 0.6	61.5 ± 0.1	58.1 ± 0.3	57.6 ± 0.7	175 ± 1	10.7	173 ± 3	10.6	0.527
Stearic	64.6 ± 0.1	67.9 ± 0.1	64.5 ± 0.2	63.4 ± 0.1	183 ± 3	12.4	182 ± 2	12.4	0.542

*. The results were obtained from 4 different runs on palmitic acid, 2 runs on capric acid, 2 runs on lauric acid and 2 runs on stearic acid. All determinations were done at a data scanning rate of 0.4 seconds per point and are listed in table A-1 of the appendix.

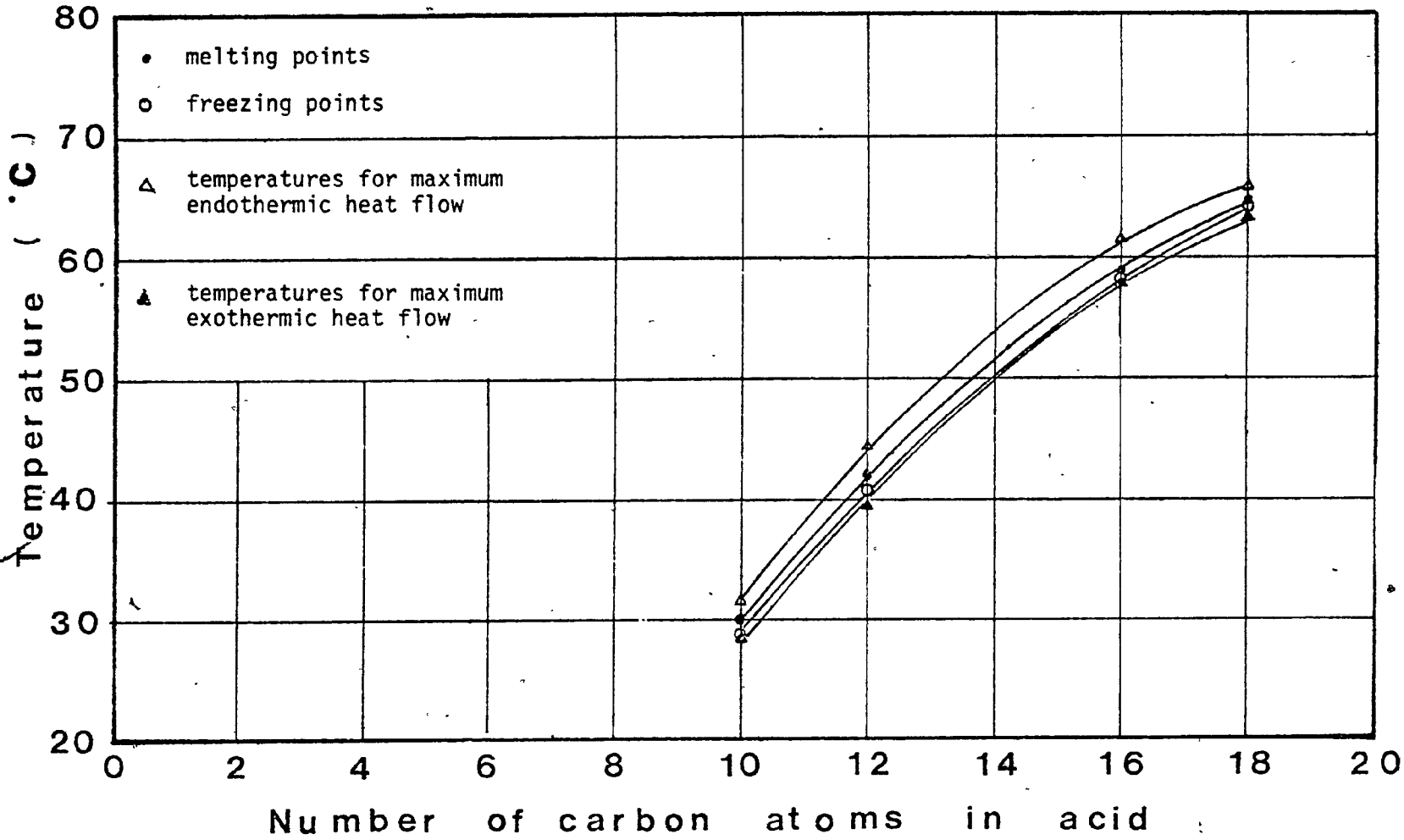

Fig. 30. Melting and freezing points and temperatures for maximum endothermic and exothermic heat flows of fatty acids.

Freezing Points

The freezing points of capric, lauric, palmitic and stearic acids were observed to be 28.7 ± 0.3°C, 40.7 ± 0.1°C, 58.1 ± 0.3°C and 64.5 ± 0.2°C respectively. The freezing points are slightly lower than the melting points. In contrast to the melting point, the freezing point is not an equilibrium measure and the supercooling effect is an important factor. Also, the cooling rate and mass of sample can affect the freezing point. Kulka et al (Ref. 10) found the freezing point of pure capric acid to be 31.2°C. Efremov et al (Ref. 13) observed freezing points of lauric, palmitic and stearic acids at 42.7°C, 59.2°C and 67.7°C respectively.

The discrepancy between the literature and experimental values is due to the presence of impurities in the reagents. Also, the literature values are based on the capillary tube method which has a lower error (max. 0.05°C) in reproduction of the freezing point (Ref. 10 and 12). In addition, the capillary tube method requires a larger sample weight than the DSC method and, therefore, the supercooling effect is smaller in the capillary tube method.

The freezing point dependence on the carbon chain length in the acid is illustrated in Fig. 30. The profile of the freezing curve is similar to the melting curve.

Temperatures for Maximum Endothermic and Exothermic Heat Flows

The temperatures for maximum endothermic and exothermic heat flows when plotted against the number of carbon atoms in the acid show a close resemblance to the melting and freezing curves.

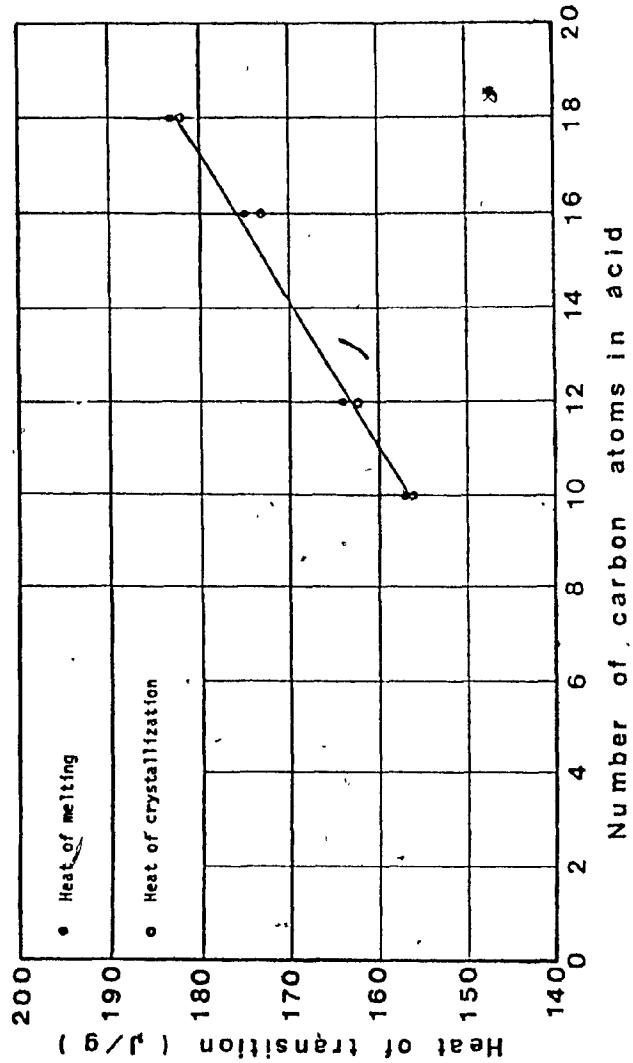

Fig. 31. Heats of melting and crystallization of fatty acids.

This is illustrated in Fig. 30. These points are highly dependent on the heating and cooling rates as shown in Fig. T-1 to T-5 of the appendix.

Heats of Melting and Crystallization

The observed heats of melting for capric, lauric, palmitic and stearic acids are 157 ± 6 J/g, 164 ± 4 J/g, 175 ± 1 J/g and 183 ± 3 J/g respectively. The corresponding heats of crystalli-

zation. 153 ± 7 J/g, 162 ± 7 J/g, 173.3 ± 3 J/g and 182 ± 2 J/g respectively. The heats of melting and crystallization appear to be essentially the same. These transition heats have been plotted versus the number of carbon atoms in the acid chain in Fig. 31. The resulting curve shows that the heats of melting and crystallization increase with an ascending number of carbon atoms.

The observed heats of melting of the pure acids are slightly lower than the published data (Ref. 13 and 15). However, Berchiesi et al (Ref. 14) found the heat of melting to be 8.2, 12.3, and 13.8 Kcal/mole for lauric, palmitic and stearic acids respectively. This compares to 7.8, 10.7 and 12.4 Kcal/mole for lauric, palmitic and stearic acids obtained in the DSC results after applying a conversion factor. The discrepancy in the observed values appears to be due to the degree of impurities found in the reagent substances and different measurement techniques.

Entropy of Melting

The entropy of melting of the pure fatty acids is shown in Table VIII. The relationship of the entropy with the number of carbon atoms in the acid chain is illustrated graphically in Fig. 32. The entropy of melting of the fatty acids has the same order of magnitude for this particular homologous series but tends to increase with an ascending number of carbon atoms in the acid chain.

The entropies of melting were calculated with the use of the following equation:

$$\Delta S = \frac{\Delta H_m}{T_{m.p.}}$$

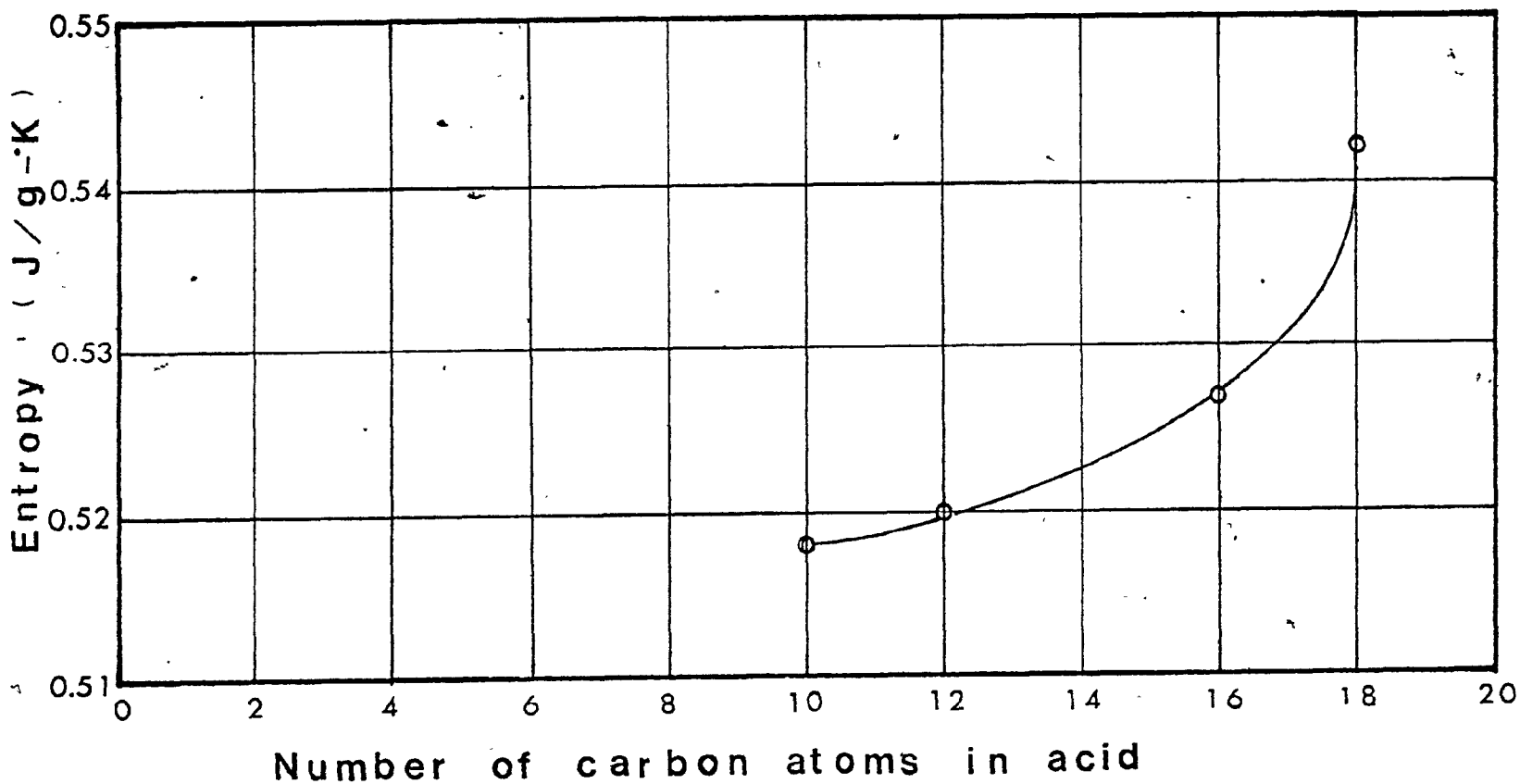

Fig. 32. Entropy of melting of fatty acids.

where: ΔS = entropy of melting in J/g - °K

ΔHm = heat of melting in J/g

Tm.p. = melting point temperature in °K (°C + 273.15)

Internal Energy Change of Melting

The change in internal energy during melting can be calculated using the enthalpy function at constant pressure.

$$\Delta H = \Delta E + P\Delta V$$

where: ΔH = heat absorbed by the system (heat of melting) in J/g

ΔE = change in internal energy of the system in J/g

P = pressure at which melting occurs in N/M^2

ΔV = molar volume change between the liquid and solid in cm^3/g-mole

Rearranging the above equation and introducing the terms for the molar volume of liquid and solid, the equation becomes

$$\Delta E = \Delta H - P (V_L - Vs)$$

where: V_L = molar volume of liquid in cm^3/g-mole

Vs = molar volume of solid in cm^3/g-mole

Using capric acid as an example with the following data:

V_L = 192.4 cm^3/g-mole (Ref. 16)

Vs = 170.2 cm^3/g-mole (Ref. 16)

P = 1 atmosphere

ΔH = 157 J/g

$$\Delta E = 157 \text{ J/g} - \left[1 \text{ ATM}\right]\left[\frac{1.0133 \times 10^5 \text{ N/m}^2}{1 \text{ ATM}}\right]\left[\frac{22.2 \text{ cm}^3}{\text{g-mole}}\right]\left[\frac{1 \text{ g-mole}}{172.27 \text{ g}}\right]\left[\frac{1 \text{ m}^3}{10^6 \text{ cm}^3}\right]\left[\frac{1 \text{ J}}{\text{N-m}}\right]$$

$$= 157 - 0.013 \text{ J/g} \qquad = 156.987 \text{ J/g}$$

The above calculation illustrates that very little work is expended when the fatty acid undergoes melting and the internal energy change is essentially the same as the heat of melting.

XIII. CRYSTAL STRUCTURE OF FATTY ACIDS AND THEIR BINARY SYSTEMS

Knowledge of the crystal structure of fatty acids and their solid solutions is essential in the understanding of the phase behaviour and polymorphism.

Extensive work has been done to determine the crystallographic structure of pure fatty acids and their binary systems using the X-ray powder and single crystal techniques (Ref. 17, 18, 19 and 20). As a result, a considerable amount of data has been obtained about the packing of the hydrocarbon chains, orientation of the carboxyl group and polymorphism.

The X-ray powder patterns of the compounds reveal the existence of two group spacings. These group spacings are illustrated in Fig. 33. The first group is referred to as a long spacing and the second group consists of two short spacings. The long spacing increases proportionally with the number of CH_2 groups in a given homologous series. The two short spacings have approximately the same value for a particular homologous series and are associated with the manner of packing of the hydrocarbon chains.

X-ray diffractometric results have shown the existence of three polymorphic forms for the even straight chain fatty acids (Ref. 35). These forms are known as A, B and C modifications with the long spacing diminishing in that order. The C form is the most stable modification (Ref. 35). When the A and B modifications are heated to 10-15°C below their melting point, the two modifications transform irreversibly to the C modification with little heat of transition (Ref. 22). Consequently, the C polymorph of the

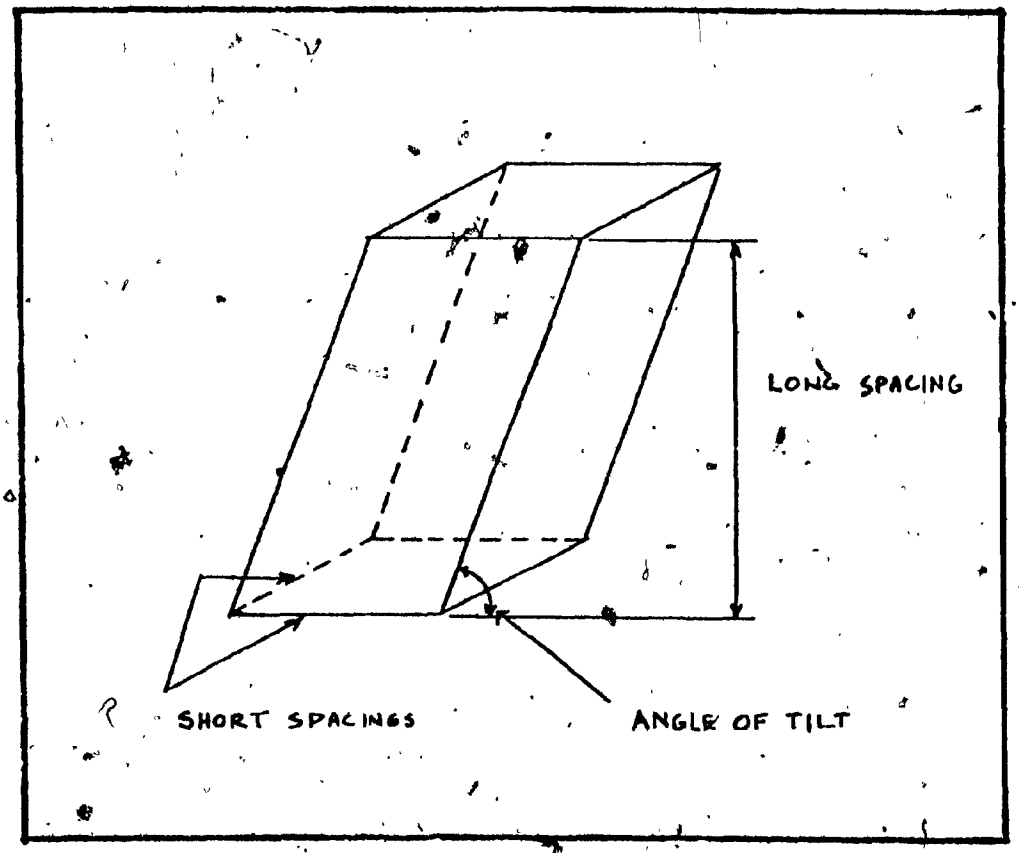

Fig. 33. Group spacings of unit crystal cell of fatty acids (Ref. 21).

acid is always obtained from a melt and the acids exhibit the property of monotropy.

The C-form has a monoclinic prismatic structure with four molecules to the unit cell. In this arrangement, the ends of the molecules are found at the corners and in the centre of the parallelopiped. Shearer (Ref. 23) found that the fatty acids crystallize with two molecules between successive layers. The active groups COOH of the molecules are located in the centre and the inactive groups CH_3 at the corners of the prism.

Müller (Ref. 29) showed that the carbon atoms in the chain are arranged in a zig-zag pattern and are joined to each other at a tetrahedral angle. Subsequent experimental work by Piper (Ref. 25) and other workers have found the angle to be 116°. The distance between the adjacent carbon atoms was found to be 2.6Å (Ref. 25).

The lattice dimensions of the C-form of the fatty acids are given in Table IX.

Name	Short Spacing a (Å)	Short Spacing b (Å)	Long Spacing c (Å)	Angle of Tilt β	Ref.
Capric			29.7		26
Lauric	9.524	4.965	35.39	129°13'	27
Palmitic	9.41	5.0	45.9	129'10'	27
Stearic	9.357	4.956	50.76	128'14'	27

TABLE IX. Crystal lattice dimensions of fatty acids

The unit cell dimensions vary slightly with chain length and, therefore, the series is not strictly homologous. The cross section of the unit cell decreases with a longer chain indicating that the molecules are packed closer together in the longer chain acid.

Fig 34 shows a diagrammatic representation of the unit cell of stearic acid.

The crystal structures of binary mixtures of fatty acids are well documented in the work of Frede et al (Ref. 28) and Baun (Ref. 26).

Frede et al examined different mixtures of the palmitic-stearic system by means of X-ray and electron diffraction and found that the crystal form occurring in all concentrations conforms to the C-form of the pure compounds. In the concentration range of 95-60 mole % of stearic acid, the shorter palmitic acid molecules are incorporated into the crystal lattice of stearic acid without affecting the long spacing, c, of the unit cell. In the concentration range of 50 to 20 mole % of stearic acid, the crystal structure is characterized by constancy of nearly all lattice parameters. The long spacing is approximately the arithmetic mean of the spacings of the pure components. Frede et al depict the mixed crystal form in terms of double molecules, which can be formed from two stearic acid molecules, two palmitic acid molecules and one stearic and one palmitic acid molecule. Within the concentration range of 0-10 mole % stearic acid, the longer stearic acid molecules can be incorporated into the crystal lattice of the palmitic acid. The unit cell of the palmitic acid is slightly affected by a decrease in the angle of tilt β, by 1-2° and an enlargement of the distance between the neighbouring atoms.

Saguchi and Asada (Ref. 18) determined unit crystal cell dimensions of binary systems of C_{12}-C_{16} and C_{16}-C_{18} by means of X-ray diffraction. The systems were classified into three groups:

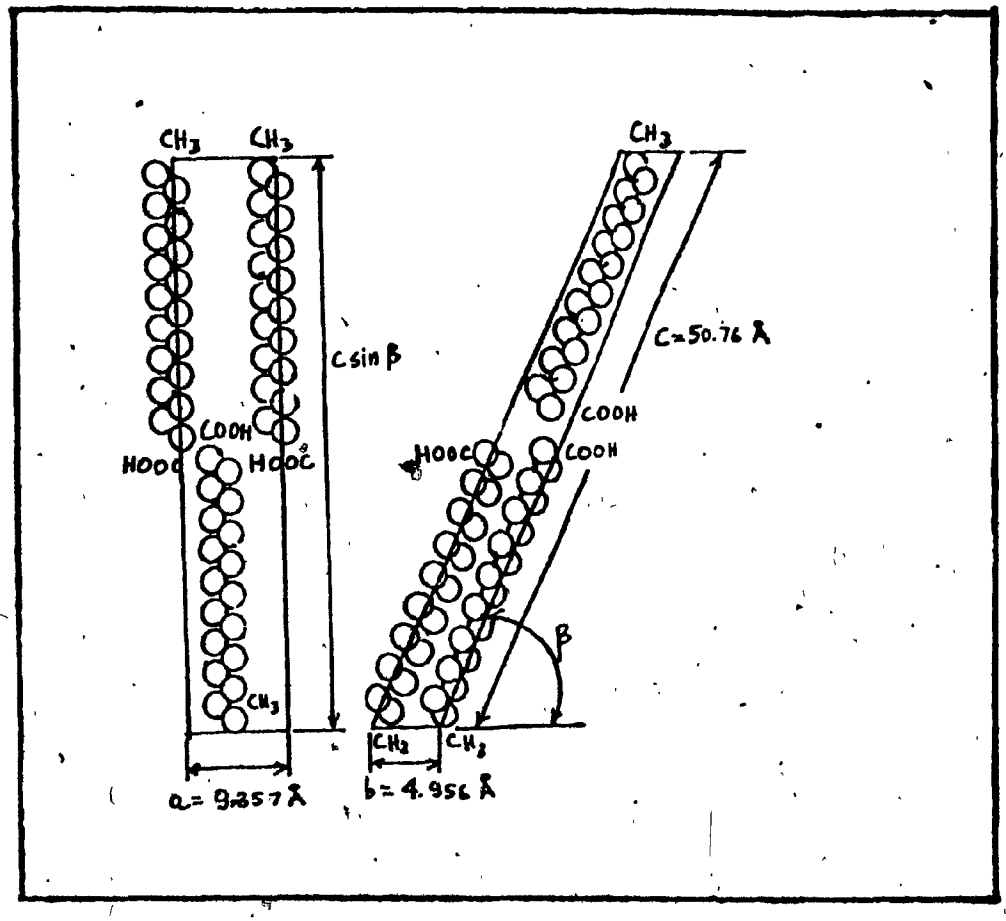

Fig. 34. Diagrammatic representation of the unit cell of a stearic acid crystal (Ref. 37).

1. A solid solution in which the lower-chain acid is dissolved by the higher-chain acid.
2. An equimolar compound composed from the two components containing one of the components in small excess.
3. A solid solution in which the higher-chain acid is dissolved by the lower-chain acid.

The stability of the crystal lattice is affected by the difference between the number of carbon atoms in the fatty acid molecules. As the difference rises, the stability of the lower acid in the higher acid increases, whereas the stability of the higher acid in the lower acid decreases (Ref. 18).

Baun (Ref. 26) has examined the binary system of C_{10}-C_{12} by X-ray diffraction. His results of mixed crystal formation are in general agreement with the other workers.

IX. ANALYSIS OF FATTY ACIDS AND THEIR EUTECTICS WITH AN X-RAY DIFFRACTOMETER

An X-ray diffractometer (manufactured by Picker) equipped with a Chromium tube (manufactured by Macklett) was used to obtain the X-ray patterns. Measurements were made of pure fatty acids and their eutectics (except for capric-lauric eutectic, which is liquid at ambient temperature). The samples were melted in an oven and later crystallized before being used on the instrument. Subsequently, the samples were ground on a watch glass with a pestle to obtain a fine homogeneous powder. The material was then pressed in a thin layer on a strip of glass to obtain sufficient adhesion. Due to the waxy nature of the compound, the samples easily adhered to the glass strip.

The X-ray patterns were recorded in an angular range of 6 to 50° at an angular velocity of 1°/min. A strip chart recorder was used to record the diffraction pattern.

All pure acids and their mixtures were found to be present in the C-form having a monoclinic crystal lattice. This form is characterized by short spacings at $2\theta=19.4°$, $2\theta=21.5°$ and $2\theta=24°$. This is in agreement with the results found by Frede et al (Ref. 28) except for the angle of $2\theta=19.4°$, which Frede et al found to be 20.2°.

The long spacings were found to be located at $2\theta=11.5°$ for capric acid, $2\theta=9.7°$ for lauric acid, $2\theta=7.4°$ for palmitic acid and $2\theta=6.6°$ for stearic acid. The values for palmitic and stearic acids are in agreement with the results of Frede et al.

The intensity of the long spacings essentially disappear in the binary mixtures of acids. The X-ray patterns conform to the results obtained by Frede et al, Van (Ref. 29) and Malta et al (Ref. 30).

The diffractometric results indicate that during crystallization of a binary mixture of fatty acids, the mixture does not decompose into the pure acid components (Ref. 28).

The scattering of X-rays depends on the concentration of electrons in a given area (Ref. 41). The terminal methyl groups in the fatty acids contain a low electron density due to the high concentration of hydrogen and, therefore, the methyl plane has a lower scattering power than the main body of the crystal. In contrast, the presence of a carboxyl group givesrise to planes of higher scatterin power than the main body of the crystal. With double molecules, the strongly diffracting and the weakly diffracting planes are separated by the same distance. This is illustrated in Fig. 35.

The results of the X-ray spectra are shown in Fig. S-1 to Fig. S-9 in the appendix. The vertical lines which appear on the spectra denote the location of the short and long spacings. These lines were drawn skewed rather than vertical as a result of a misaligned strip chart paper caused by a fault on the X-ray diffractometer recorder. The actual peak readings on the spectra were taken directly from the angle indicator on the diffractometer.

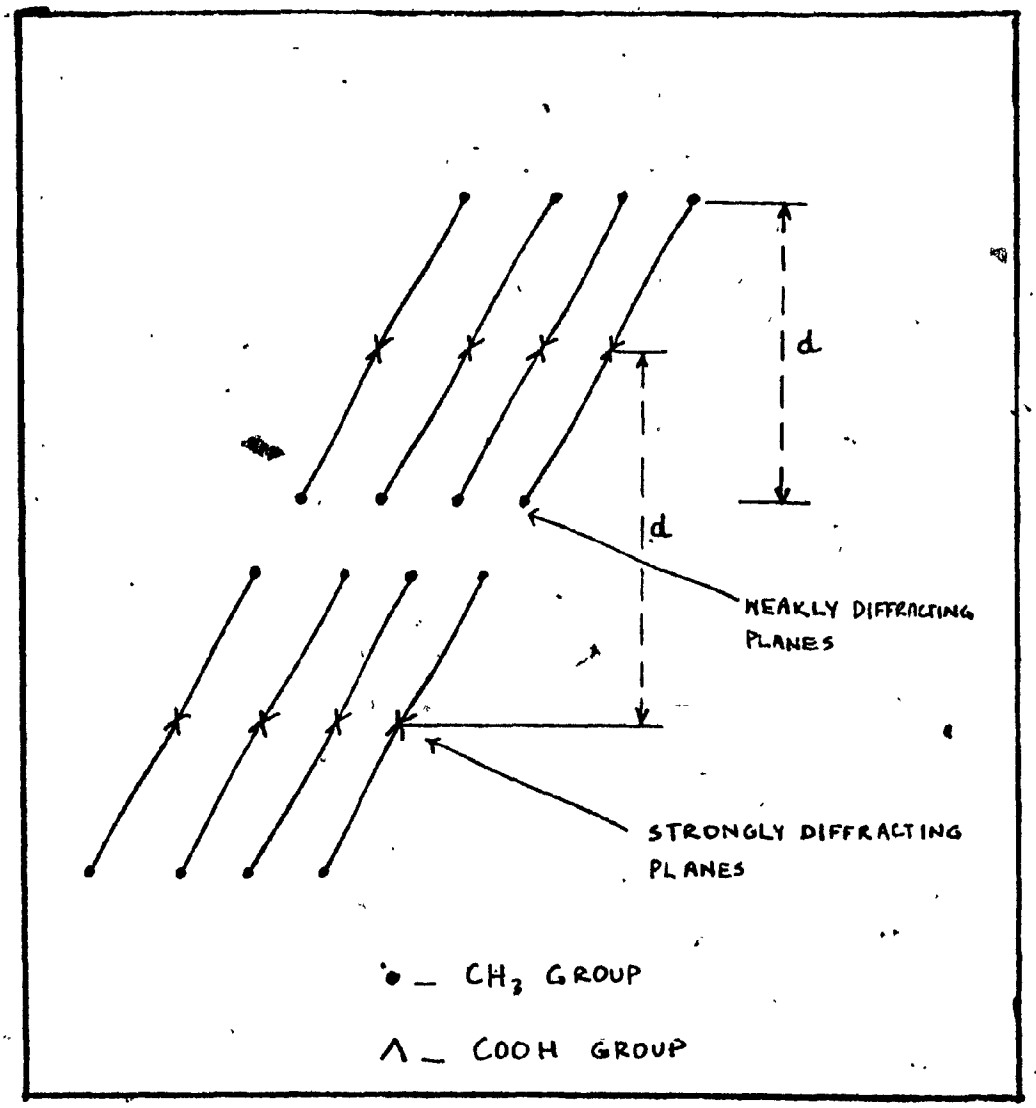

Fig. 35. X-ray diffracting planes of fatty acids (Ref. 41).

X. INFRARED SPECTRA OF FATTY ACIDS AND THEIR EUTECTICS

The fatty acids used for the experiments were obtained from commercial sources as given in Table VI. The samples were prepared by mixing about 10 mg of the compounds with about 1000 mg of potassium bromide in a mortar dish. Subsequently, the mixtures were ground with a pestle to a fine homogeneous powder. The powder was then placed in a die which was subjected to a force of 10 metric tons to produce a potassium bromide disk. The only sample which remained in a liquid form consisted of 74 mole % capric: 26 mole % lauric. Consequently, the IR analysis on this sample was performed by placing a capillary film of the sample between two potassium bromide disks. A Beckman spectrophotometer, Model IR 4240, was used to measure the IR spectra over a range of 4000 to 400 cm^{-1}.

The IR spectra of the pure fatty acids and their binary mixtures are shown in Fig. I-1 and I-2 in the appendix. Comparison of the spectra of the pure acids with standard published spectra (Ref. 31) show that the acids are present in the C-polymorphic form. This is particularly apparent at a wave number of about 930 cm^{-1}. where the O-H out-of-plane deformation occurs and no two crystal forms have the same absorption. This is consistent with the X-ray diffraction results.

The IR spectra of the even straight-chain fatty acids in crystalline form show a series of bands of uniform spacing in the region of 1300 to 1180 cm^{-1}. This is due to interaction of rocking and/or twisting vibrations of the CH_2 groups. The number of bands increases with the chain length of the molecule and the number of carbon

atoms can be calculated by multiplying the number of bands for a particular compound by a factor of 2. The spectra of the fatty acids in the 1300 to 1180 cm^{-1} region show 5 bands for capric acid, 6 bands for lauric acid, 8 bands for palmitic acid and 9 bands for stearic acid.

Table X shows the band positions for fatty acids and their binary mixtures. The bands were designated in a numerical order with decreasing wavelengths. The locations of the functional groups are in agreement with published data.

It is noteworthy that for the binary mixtures the region of 1300 to 1180 cm^{-1} is significantly altered from the one for pure fatty acids. The vibrations of the CH_2 groups are markedly different indicating a different order of molecular packing in the crystal lattice.

TABLE X. Infrared Spectra Band Positions for Fatty Acids and Their Binary Mixtures.

FUNCTIONAL GROUP	CAPRIC ACID		LAURIC ACID		PALMITIC ACID		STEARIC ACID		74% CAPRIC 26% LAURIC		85% LAURIC 15% STEARIC		72.5% PALMITIC 27.5% STEARIC		80% CAPRIC 20% PALMITIC	
	GRAPH ID	BAND	GRAPH ID	BAND	GRAPH ID	BAND	GRAPH ID	BAND	GRAPH ID	BAND	GRAPH ID	BAND	GRAPH ID	BAND	GRAPH ID	BAND
$C-H_3$ Assym. Stretching	1C	2955	1L	2940	1P	2940	1S	2955	1CL	2944	1LS	2940	1PS	2938	1LP	2940
$C-H_2$ Assym. Stretching	2C	2920	2L	2910	2P	2900	2S	2920	2CL	2910	2LS	2905	2PS	2900	2LP	2910
$C-H_3$ Sym. Stretching	3C	2870	3L	2860	3P	2855	3S	2870	3CL	2860	3LS	2860	3PS	2840	3LP	2860
$C-H_2$ Sym. Stretching	4C	2850	4L	2840	4P	2835	4S	2845	4CL	2845	4LS	2840	4PS	2830	4LP	2840
C=O Stretching	5C	1708	5L	1695	5P	1690	5S	1700	5CL	1698	5LS	1695	5PS	1690	5LP	1700
C-H Bending	6C	1410 1435 1462	6L	1404 1425 1460	6P	1400 1420 1455	6S	1410 1430 1465	6CL	1405 1430 1460	6LS	1402 1425 1458	6PS	1400 1420 1455	6LP	1402 1425 1455
C-H Wagging and/or Bending	7C	1235 to 1190	7L	1235 to 1185	7P	1285 to 1180	7S	1293 to 1182	7CL	1205 to 1270	7LS	1290 to 1180	7PS	1285 to 1175	7LP	1280 to 1170
O-H Vibration	8C	935	8L	925	8P	925	8S	930	8CL	925	8LS	925	8PS	925	8LP	925
$C-H_2$ Rocking	9C	718	9L	712	9P	718	9S	725	9CL	712	9LS	715	9PS	705	9LP	708

THEORY OF MELTING AND CRYSTALLIZATION OF FATTY ACIDS

The melting process is a function of the structure of the crystalline state and can be visualized as the structural breakdown of the crystal lattices. In the crystalline solid the molecules are arranged in a regular and symmetrical way. The process of melting causes the highly ordered arrangement to break down to a more random arrangement which normally characterizes a liquid.

The measure of the randomness of the molecular disorder of the system is expressed by a change of entropy which accompanies a phase change in a material. The change of entropy of fatty acids increases during melting as illustrated in Fig. 32.

The melting proceeds at a temperature level at which the thermal energy of the molecules is sufficiently high to overcome the crystalline forces holding the molecules together in the crystal lattice. First, the surface molecules acquire sufficient vibration energy to escape the lattice. Also, on a smaller scale, interior molecules can rupture the crystal lattice when sufficient vibrational energy is acquired. When the fatty acids undergo melting, the heat of melting is essentially converted to the internal energy of the molecules with little work done by the system during the phase-change process. This is illustrated by the calculation of internal energy change shown on pg. 61. The heat of melting depends on the molecular weight and tends to increase with an increase in the carbon chain length of the acid as shown in Fig. 31.

The intermolecular forces holding the molecules together in the crystal lattice can be viewed as composed of two types of forces; namely, the dipole-dipole interaction due to the presence of the polar OH group and the Van der Waals forces (Ref. 16). The latter forces are small, momentary polarizations of part of one molecule by part of another near-by molecule.

The monocarboxylic acid molecules are polar and are normally called associated liquids due to the presence of the hydrogen bond. These molecules are dimerized in a liquid phase and held together by two hydrogen bonds as shown below.

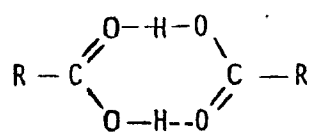

The hydrogen bond has a strength of about 5Kcal/mole (Ref. 40) and is the main factor for the higher than expected melting and boiling points of the fatty acids. The melting points of the acids depend on polarity and molecular weight. For a particular homologous series, the melting points increase with an increase in the molecular weight as illustrated in Fig. 30. The polarity of the acid molecules imposes on them an arrangement which gives the greatest attractive forces between molecules. This is counterbalanced by the kinetic energy of the molecules.

Crystallization is the reverse of melting and occurs when a number of molecules at a low energy level are grouped together to form a nucleus. Supercooling, a metastable state, can proceed in the absence of a nucleus on which the crystal growth is dependent. The acids are suseptible to the supercooling phonemenon as shown in Fig. T-6 and T-8 in the appendix.

XII. DISCUSSION OF THERMOGRAMS OF BINARY MIXTURES OF FATTY ACIDS

The analysis of multiple peaks on thermograms of binary mixtures of fatty acids can provide useful information about phase transitions and the possible structure of molecular crystals.

The nature of the peaks can be examined in terms of the solid solutions that can be formed by the two components. Analysis of the melting and freezing curves shows that an additional compound is formed at the hump in the curve. Therefore, the binary mixture of fatty acids can be considered to contain three types of solid solutions. These solutions have been reported by Saguchi and Asada (Ref. 18) and can be described as (1) solid solution of the shorter-chain fatty acid in the longer-chain fatty acid (2) equimolar compound of the two components containing one of them in small excess (3) solid solution with small amount of the longer-chain acid dissolved in the shorter-chain acid.

Binary mixtures of even straight-chain acids contain up to four discernible peaks on the thermograms depending on the concentration of the two components. The pure even straight-chain acids and their eutectic compounds are characterized by a single, sharp and well-defined peak. The number of peaks appearing on the thermograms for the binary systems of capric-lauric, lauric-palmitic, lauric-stearic and palmitic-stearic acids have been plotted in Fig. 36.

Fig. 36 shows that the region containing up to four peaks is rich in the high-molecular weight component. The X-ray diffractometric results clearly show that the crystal lattice in this concen-

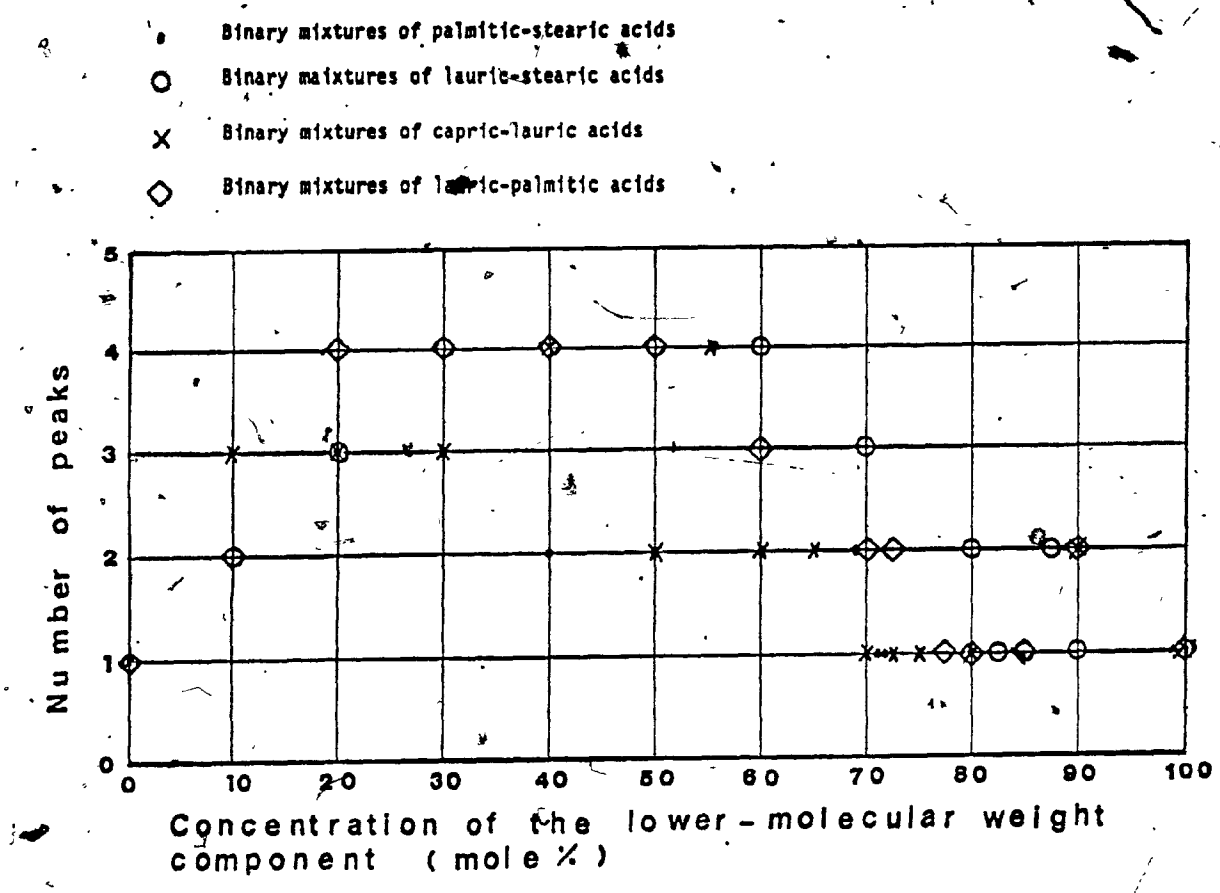

Fig. 36. Plot of number of peaks versus concentration for thermograms of binary mixtures of fatty acids.

tration region has the cell dimensions of the high-molecular weight component. Taking the example of the palmitic-stearic system for the purpose of discussion, it can be seen that in the region which is rich in the high-molecular weight component, stearic acid in this instance, the crystal lattice must conform to the stearic acid cell dimensions (Ref. 28).

The possible crystal lattice arrangements that can conform to the stearic acid cell dimensions are shown in Fig. 37 and consist of lattice structures Type 1, Type 2, Type 3 and Type 4. Fig. 37 shows that the acids crystllize in double-chain length molecules. The crystal lattices possess different stabilities (Ref. 18 and 28) which require different energy formation levels. When the crystal lattice absorbs sufficient thermal energy to disorder the molecular arrangement in the lattice, the crystal lattice is expected to rupture. This type of breakdown can be associated with the appearance of the peak on the thermogram. Therefore, the four peaks on the thermogram can be explained in terms of rupture of the four types of crystal lattices.

In the compound formation region, Fig. 36 shows that up to two peaks can appear on the thermograms. In this concentration range, all the crystal lattices must conform to a cell dimension corresponding to the arithmetic mean of the dimensions of the pure components (Ref. 28). Using again the example of palmitic-stearic system, the possible crystal lattice that can satisfy this constraint is crystal lattice type V. Since this compound is of the incongruent type, it transforms during melting to crystal type IV which is associated with the second peak.

In the region containing an excess of the lower-molecular weight

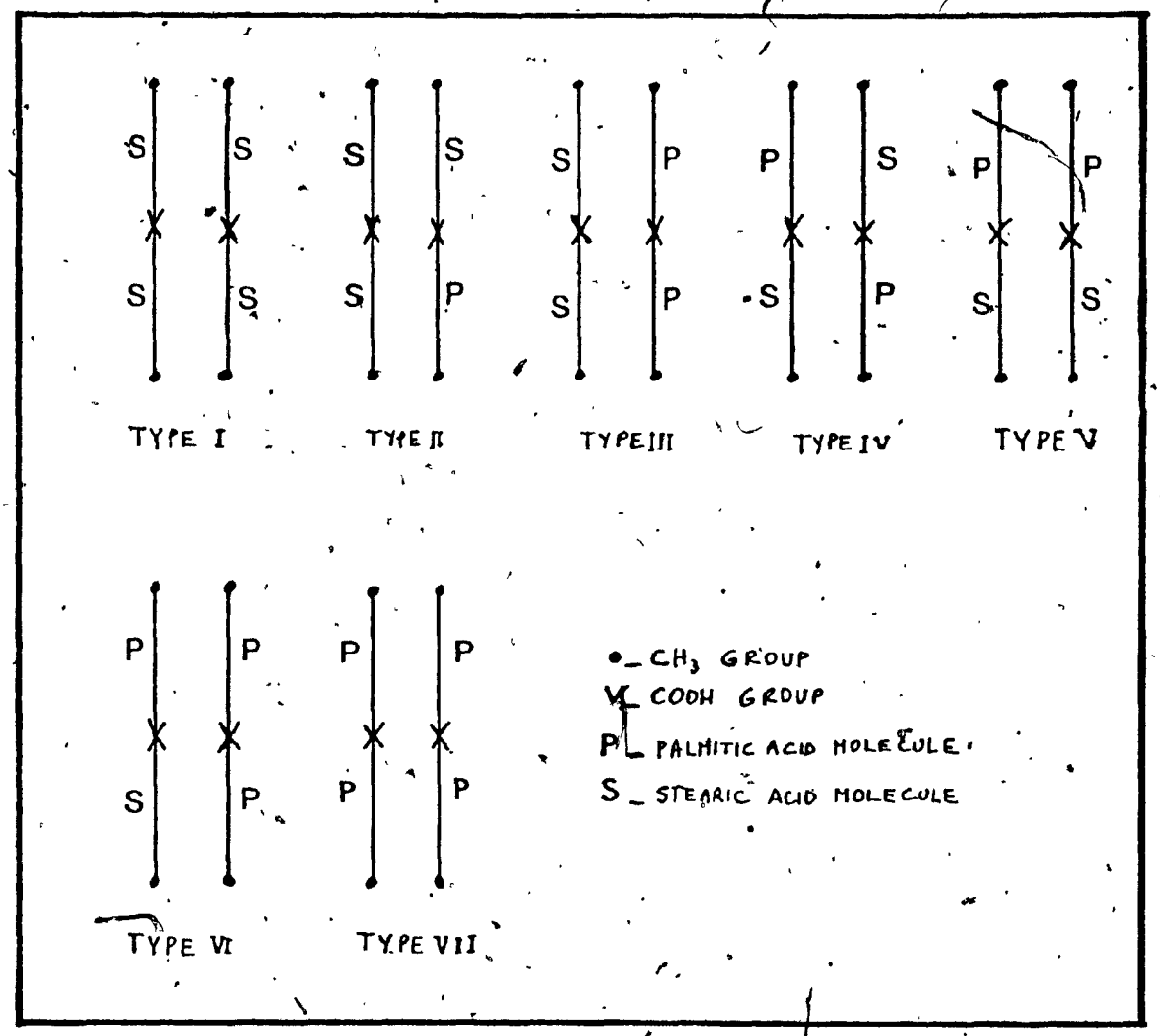

Fig. 37. Possible crystal lattice arrangements of binary mixtures of palmitic-stearic acids molecules.

component, i.e. between the eutectic point and 100% low-molecular weight component, Fig. 36 shows that up to two peaks are present on the thermograms. For the palmitic-stearic system Frede et al (Ref. 28) found that up to a concentration of 10 mole % palmitic: 90 mole % stearic, the longer stearic acid molecules can be incorporated in the crystal lattice of the palmitic acid molecule. In this concentration range, the two possible crystal lattices are types VI and VII in Fig. 37.

A similar analogy can be extended to the discussion of thermograms of other binary mixtures of fatty acids.

The analysis of the multiple peaks on the thermograms can also be considered from the standpoint of the possible influences of impurities present in the starting materials. However, due to the very low concentration of the impurities, it is possible that these effects are superimposed on the sharper peaks which are associated with the first-order transitions of materials.

XIII. CONCLUDING REMARKS

The melting point, freezing point, heat of melting and heat of crystallization of capric, lauric, palmitic and stearic acids and their binary mixtures have been determined by the Differential Scanning Calorimetry method. The melting points of capric, lauric, palmitic and stearic acids were observed to be 30.0 ± 0.4°C, 42.2 ± 0.1°C, 59.0 ± 0.6°C and 65.6 ± 0.1°C respectively. The corresponding freezing points of the fatty acids were found to be 28.7 ± 0.3°C, 40.7 ± 0.1°C, 58.1 ± 0.3°C and 64.5 ± 0.2°C respectively. The observed heats of melting of capric, lauric, palmitic and stearic acids were 157 ± 6 J/g, 164 ± 4 J/g, 175 ± 1 J/g and 183 ± 3 J/g. The corresponding heats of crystallization were 153 ± J/g, 162 ± 7 J/g, 173.3 ± 3 J/g and 182 ± 2 J/g respectively.

The eutectic points were determined for binary mixtures of capric-lauric acids, lauric-palmitic acids, lauric-stearic acids and palmitic-stearic acids. The eutectic mixtures were examined by Differential Scanning Calorimetry to ascertain the thermal properties of melting point, freezing point, heat of melting and heat of crystallization. The eutectic compositions of the binary systems were found to be 73 mole % capric: 27 mole % lauric, 80 mole % lauric: 20 mole % palmitic, 85 mole % lauric: 15 mole % stearic and 73 mole % palmitic: 27 mole % stearic. The corresponding melting points of the eutectics were observed to be 18.2°C, 32.7°C, 34.0°C and 51.1°C respectively. The corresponding freezing points were observed to be 16.6°C, 30.3°C, 31.3°C and 50.8°C respectively.

The heats of melting of the eutectic compositions of binary systems of capric-lauric acids, lauric-palmitic acids, lauric-stearic acids and palmitic-stearic acids, lauric-stearic acids and palmitic-stearic acids were found to be 120 J/g, 147 J/g, 152 J/g and 159 J/g respectively. The corresponding heast of crystallization of the eutectics were found to be 113 J/g, 149 J/g 155 J/g and 161 J/g respectively.

The pure fatty acids and their eutectic mixtures were examined with an X-ray diffractometer and an infrared spectrophotometer to establish the polymorphic form and crystal structure. The experimental results show that the acids are present in the stable C - polymorphic form and process a monoclinic crystal structure

The thermal properties of the fatty acids and their eutectics appear to be propitious for space heating applications. However, utilization of these materials for space heating and other applications depends on the development of an efficient and economic thermal energy storage system.

XIV. RECOMMENDATIONS FOR FURTHER WORK

Utilization of fatty acids for latent heat thermal storage applications will depend to a large extent on an efficient and economic design of the thermal storage system.

Saturated fatty acids possess a good chemical stability but, nonetheless, long-term stability ought to be verified by thermal-cycling (repeated melting and freezing of the material) to ensure the required longevity of the system.

The fatty acids possessing different grades of purity (such as research, reagent and technical grades) can be subjected to the thermal cycling technique and the constancy of the thermal parameters ought to be verified over a long period of time. If the chemical stability of the technical grade material is found comparable to the research grade material then the former should be selected due to a lower cost.

The supercooling effect is an important phenomenon and further work is required to characterize the liquid behavior at the freezing point. Several cooling rates can be used on samples having different purity levels and the relation between the cooling rate and supercooling be thus determined. For this purpose, the cooling accessory for the DSC cell should be fitted with a flow-meter to accurately measure the flow of the cooling gas.

The compatibility of fatty acids with conventional materials of construction is another area which requires further investigation. The evaluation of the material compatibility factor should have a

two-fold objective; namely, it should be considered from a corrosion point of view and the possible contamination of the fatty acid. Leached impurities from the container can combine with the fatty acids producing objectionable effects such as chemical decomposition. The decomposition, in turn, can affect the thermal properties of the acids as well as produce toxic or poisonous by-products. Some data has been published on the corrosion rates of fatty acids on conventional materials of construction (Ref. 1, 32, and 34). The materials which have a good corrosion resistance to fatty acids include aluminum, 304 stainless steel, fiberglass reinforced epoxy and polyester resin.

In the building construction industry, the flammability criterion is a crucial factor in the selection of materials. The widespread use of fatty acids will depend on how well these materials can meet the industry standards and municipal by-laws. The use of fire-retardant additives ought to be explored. To contain small fires, carbon dioxide gas, carbon tetrachloride and finely powdered sodium bicarbonate have been found effective. However, for large fires the use of foam is required.

The design and construction of heat exchangers requires further analysis. The geometry factor of the container must account for volume changes which occur during the phase transitions. Also, the factor of air-tightness should be examined to prevent water vapour and impurities from entering the system.

The experimental results on the binary mixtures of fatty acids indicate the formation of an incongruently melting compound.

Further work is required to determine the compound suitability for the thermal storage system.

Finally, the total package design of the thermal storage system must be cost-effective to favourably compete with alternate energy systems. Therefore, the economics and design of the system will depend on how well all the relevant parameters are optimized to meet the user criteria.

REFERENCES

1. E. Scott Pattison, Fatty Acids and their Industrial Applications, Marcel Dekker Inc., New York (1968).
2. Chemical Marketing Reporter (March 7, 1983).
3. F. Francis, F.T.E. Collins and S.H. Piper, Proc. Roy. Soc. (London), 158A, 691-718 (1937).
4. H.A. Schuette and H.A. Vogel, J. Am. Oil Chemists' Soc., 16, 209-121 (1939).
5. H.A. Schuette and H.A. Vogel, J. Am. Oil Chemists' Soc., 17, 155-157 (1940).
6. H.A. Schuette, R.M. Christenson and H.A. Vogel, J. Am. Oil Chemists' Soc., 20, 163-165 (1943).
7. H.A. Schuette, D.A. Roth and R.M. Christenson, J. Am. Oil Chemists' Soc., 22, 107-109 (1945).
8. H.A. Schuette and H.A. Vogel, J. Am. Oil Chemists' Soc., 22, 238-240 (1945).
9. J.C. Smith, J. Chem. Soc., 625-627 (1936).
10. M. Kulka and R.B. Sandin, J. Am. Chem. Soc., 59, 1347-1349 (1937).
11. B.T. Grondal and D.A. Rogers, J. Am. Oil Chemists' Soc., 21, 303-305 (1945).
12. R.L. Shriner, T.M. Foulton and D. Burks Jr., J. Am. Chem. Soc., 55, 1494-1499 (1933).
13. J. Timmermans, Physico-Chemical Constants of Pure Organic Compounds, Elsevier Publishing Co. Inc. (1950).

14. G. Berçhiesi et al, Gazzetta Chimica Italianna, 106, 549-556 (1976).

15. Klare S. Markley, Fatty Acids - Their Chemistry, Properties, Production and Uses, Part 4, Interscience Publishers (1967).

16. A.R. Ubbelohde, The Molten State of Matter, John Wiley & Sons (1978).

17. A. Müller, Proc. Roy. Soc., London, 114A, 542-561 (1927).

18. M. Saguchi and E. Asada, Nippon Kagaku Zusshi, 82, 958-962 (1961); Chem. Abst., 56, 8067 (1962).

19. G. Degerman and E. Von Sydow, Acta Chem. Scand., 12, 1176-1182 (1956).

20. S. Abrahamsson and E. Von Sydow, Arkiv Kemi, 14, 39-47 (1959).

21. F.P. Gunstone, An Introduction to the Chemistry and Bio-Chemistry of Fatty Acids and their Glycerides, Chapman and Hall Ltd. (1967).

22. E. Stanhagen and E. Von Sydow, Arkiv Kemi, 6, 305 (1953).

23. G. Shearer, Trans. Faraday Soc., 22, 465-468 (1926).

24. A. Müler, J. Chem. Soc., 2043 (1923).

25. S.H. Piper, J. Chem Soc., 234 (1929).

26. N.L. Baun, J. Phys. Chem., 65, 2122 (1961).

27. R.W.G. Wyckoff, Crystal Structures, Vol. 5, Interscience Pub. (1966).

28. E. Frede and D. Precht, J. Am. Oil Chemists' Soc., 53 (10), 668-70 (1976).

29. V. Vand, W.M. Morley, T.R. Lomer, Acta Crystallogr.,4:324 (1961).

30. Y. Malta, C. Giarcarlo, Z. Roberts, A.F. Martelli, J. Chem. Soc. (b), 548 (1971).

31. D.O. Hummel, Infrared Analysis of Polymers, Resins and Additives, An Atlas, Wiley-Interscience (1969).

32. A. Abbot, Low Temperature Latent Heat Thermal Energy Storage: Heat Storage Materials, Solar Energy, Vol. 30, No. 4, pp. 313-332 (1983).

33. D. Heine and A. Abbot, Investigation of Physical and Chemical Properties of Phase Change Materials for Space Heating/Cooling Applications. In Sun: Mankind's Future Source of Energy, (Edited by F. de Winter and M. Cox), Vol. 1, pp. 500-506, Pergamon Press, New York (1978).

34. D. Heine, The Chemical Compatibility of Construction Materials with Latent Heat Storage Materials. Proc. Int. Conf. on Energy Storage, pp. 185-192, Brighton (1981).

35. Klare S. Markley, Fatty Acids - Their Chemistry, Properties, Production and Uses, Part 1, Interscience Publishers (1967).

36. D. Chapman, The Structure of Lipids by Spectroscopic and X-ray Techniques, Methuen and Co. Ltd. (1956).

37. M.E. Jefferson, Fatty Acids (Survey) - Crystal Properties, Encyclodedia of Chemical Technology, R.E. Kirk and D.F. Othmer eds., Vol. 6, Interscience, New York (1951).

38. F. Reiter, Physical and Chemical Processes for Latent Heat Storage at Low Temperature, Proceedings of Second Miami International Conf. A.E.S., in Miami Beach, Florida, Dec. 10-13, 1979.

39. J.E. Ricci, The Phase Rule and Heterogeneous Equilibrium, pp. 186-197, D. Van Nostrand Company Inc., New York (1951).

40. R.T. Morrison and R.N. Boyd, Organic Chemistry, Allyn and Bacon Inc., Boston (1970).

41. T. Malkin, The Molecular Structure and Polymorphism of Fatty Acids and their Derivatives, Progress in Chemistry of Fats and other Lipids, Vol.1, Pergamon Press Ltd., London (1952).

APPENDIX

APPENDIX TABLES

TABLE A-1. Thermal Data of Pure Fatty Acids

SAMPLE	RUN NUMBER	DATA SCANNING RATE (SECONDS POINT)	MELTING			CRYSTALLIZATION			SAMPLE WEIGHT	FILE NUMBER
			MELTING POINT (°C)	TEMPERATURE FOR MAX. ENDOTHERMIC HEAT FLOW (°C)	HEAT OF MELTING (J/g)	FREEZING POINT (°C)	TEMPERATURE FOR MAX. EXOTHERMIC HEAT FLOW (°C)	HEAT OF CRYSTAL-LIZATION (J/g)		
Palmitic	1	0.2	59.6	61.4	177				2.113	Fuks 02/E3
Palmitic	2	0.2	59.6	61.4	178				2.113	Fuks 03/E3
Palmitic	3	0.4	59.6	61.4	176				2.113	Fuks 04/E3
Palmitic	4	0.4	59.6	61.4	175				2.113	Fuks 05/E3
Palmitic	5	0.6	59.7	61.4	176				2.113	Fuks 06/E3
Palmitic	6	0.6	59.7	61.4	176				2.113	Fuks 07/E3
Palmitic	7	0.4	59.1	61.5	175	58.3	58.2	171	4.14	Fuks 08/E3
Palmitic	8	0.4	58.8	61.5	175	58.0	57.7	173	5.618	Fuks 27/1
Palmitic	9	0.4	58.3	61.5	174	58.0	56.8	176	11.414	Fuks 02/3
Avg. for Palmitic	-	-	59.0	61.5	175	58.1	57.6	173	-	-
Stearic	1	0.4	64.5	67.8	185	64.3	63.4	180	7.465	Fuks 06/3
Stearic	2	0.4	64.6	67.9	181	64.6	63.3	183	7.465	Fuks 07/3
Avg. for Stearic	-	-	64.6	67.9	183	64.5	63.4	182	-	-
Lauric	1	0.4	42.3	44.7	167	40.7	39.8	157	9.24	Dor 08/8
Lauric	2	0.4	42.1	44.1	161	40.6	39.7	167	7.83	Fuks 03/3
Avg. for Lauric	-	-	42.2	44.4	164	40.7	39.8	162	-	-
Capric	1	0.4	30.2	32.4	152	28.9	28.5	151	11.54	Dor 10/8
Capric	2	0.4	29.7	31.2	161	28.5	28.6	161	3.114	Fuks 01/5
Avg. for Capric	-	-	30.0	31.8	157	28.7	28.6	156	-	-

TABLE A-2. Thermal Data of Binary Mixtures of Palmitic and Stearic Acids

SAMPLE	MELTING				CRYSTALLIZATION				SAMPLE WEIGHT (mg)	FILE - NUMBER
	MELTING POINT (°C)	TEMPERATURE FOR MAX. ENDOTHERMIC HEAT FLOW (°C)	HEAT OF MELTING (J/g)	NUMBER OF PEAKS ON THERMOGRAM	FREEZING POINT (°C)	TEMPERATURE FOR MAX. EXOTHERMIC HEAT FLOW (°C)	HEAT OF CRYSTAL-IZATION (J/g)	NUMBER OF PEAKS ON THERMOGRAM		
10P/90S	61.2	66.5	174	1	61.9	60.1	180	3	14.974	Fuks 16/4
20P/80S	57.4	63.8	174	3	59.7	58.7	176	3	8.552	Fuks 15/4
30P/70S	50.9	60.8	171	3	56.7	55.8	174	3	9.974	Fuks 14/4
40P/60S	52.7	55.5	163	1	54.2	52.4	168	2	7.239	Fuks 13/4
50P/50S	52.9	56.5	163	1	52.6	50.5	158	2	14.04	Fuks 12/4
60P/40S	51.9	55.5	163	2	51.9	50.5	166	1	11.503	Fuks 11/4
69P/31S	51.4	53.8	160	1	51.0	49.8	166	2	3.357	Fuks 17/4
70P/30S	51.1	54.3	160	1	51.0	49.4	165	1	12.461	Fuks 10/4
71P/29S	51.0	53.7	159	1	51.0	50.0	161	1	6.218	Fuks 18/4
72.55/27.5S	51.1	53.8	162	1	50.8	49.7	164	1	6.169	Fuks 19/4
74P/26S	51.3	54.1	161	1	51.1	50.1	162	1	6.457	Fuks 20/4
80P/20S	51.4	54.8	160	1	51.3	49.9	162	1	7.543	Fuks 09/4
90P/10S	53.8	58.6	170	2	54.3	52.8	162	1	4.496	Fuks 08/4

TABLE A-3. Thermal Data of Binary Mixtures of Capric and Lauric Acids

SAMPLE	MELTING				CRYSTALLIZATION				SAMPLE WEIGHT (mg)	FILE NUMBER
	MELTING POINT (°C)	TEMPERATURE FOR MAX. ENDOTHERMIC HEAT FLOW (°C)	HEAT OF MELTING (J/g)	NUMBER OF PEAKS ON THERMOGRAM	FREEZING POINT (°C)	TEMPERATURE FOR MAX. EXOTHERMIC HEAT FLOW (°C)	HEAT OF CRYSTAL-LIZATION (J/g)	NUMBER OF PEAKS ON THERMOGRAM		
10C/90L	35.7	40.1	199	2	36.5	36.3	158	3	5.081	Fuks 26/5
20C/80L	19.9	37.0	151	3	32.7	31.9	153	3	5.176	Fuks 23/5
30C/70L	20.4	22.3	141	3	29.3	28.3	143	2	4.479	Fuks 23/5
40C/60L	21.2	24.9	134	4	22.0	20.5	133	2	10.59	Dor 07/7
50C/50L	21.8	24.0	133	2	21.0	19.9	133	2	9.259	Fuks 05/1
55C/45L	21.7	24.0	128	2	20.0	18.8	131	3	6.145	Fuks 13/1
60C/40L	19.0	23.4	132	2	19.7	18.5	125	2	10.03	Dor 11/8 (C) Dor 12/8 (M)
65C/35L	19.3	22.3	127	1	19.0	18.1	129	2	11.706	Fuks 14/1
70C/30L	18.4	21.2	126	1	18.2	17.4	118	1	6.73	Dor 05/7
71C/29L	18.6	22.0	125	1	18.0	16.4	115	1	21.18	Dor 04/6
72C/28L	18.7	22.0	126	1	17.2	16.3	116	1	19.48	Dor 13/6
72.5S/27.5L	18.5	22.0	120	1	17.9	16.2	111	1	19.48	Dor 04/7
73C/27L	18.2	20.8	124	1	15.6	16.4	116	1	5.75	Dor 03/6
74C/26L	18.8	21.2	121	1	16.8	15.8	120	1	5.745	Fuks 29/4
75C/25L	18.5	21.6	122	1	17.5	16.3	114	1	9.79	Dor 08/6
80C/20L	19.6	21.7	122	1	17.8	16.7	120	1	5.908	Fuks 03/1
90C/10L	21.9	28.4	135	2	23.3	22.8	124	2	10.096	Fuks 06/1

TABLE A-4. Thermal Data of Binary Mixtures of Lauric and Palmitic Acids

SAMPLE	MELTING				CRYSTALLIZATION				SAMPLE WEIGHT (mg)	FILE NUMBER
	MELTING POINT (°C)	TEMPERATURE FOR MAX. ENDOTHERMIC HEAT FLOW (°C)	HEAT OF MELTING (J/g)	NUMBER OF PEAKS ON THERMOGRAM	FREEZING POINT (°C)	TEMPERATURE FOR MAX. EXOTHERMIC HEAT FLOW (°C)	HEAT OF CRYSTAL-LIZATION (J/g)	NUMBER OF PEAKS ON THERMOGRAM		
10L/90P	55.7	59.5	171	2	56.7	55.2	173	2	3.689	Fuks 40/3 (C)/Fuks 43/3 (M)
20L/80P	50.8	57.2	172	4	52.6	52.2	171	4	11.387	Fuks 01/2
30L/70P	35.0	54.6	170	4	49.1	48.2	169	4	16.166	Fuks 27/2 (M)/Fuks 01/3 (C)
40L/60P	36.3	38.8	166	4	45.6	45.3	166	4	8.816	Fuks 03/2
50L/50P	37.4	39.4	165	4	40.6	40.2	164	4	5.158	Fuks 04/2
60L/40P	33.7	40.6	161	3	36.0	34.2	158	2	8.867	Dor 11/9
70L/30P	33.9	36.5	156	2	33.0	30.2	157	2	12.377	Fuks 06/2
71L/29P	34.2	36.4	152	2	33.0	30.8	156	2	6.134	Fuks 07/2 (M)/Fuks 08/2 (C)
72.5L/27.5P	33.9	35.7	150	2	32.0	30.7	155	2	3.628	Fuks 13/2
75L/25P	33.8	36.3	154	2	31.4	30.2	154	1	6.573	Fuks 05/2
77.5L/22.5P	33.2	36.0	148	1	31.0	30.0	150	1	6.024	Fuks 12/2
79L/21P	32.8	35.6	151	1	30.6	29.3	149	1	6.939	Fuks 29/2 (C)/Fuks 30/2 (M)
80L/20P	32.7	35.6	150	1	30.3	29.1	151	1	8.550	Fuks 28/2
81L/19P	33.3	36.4	151	1	30.6	29.1	152	1	12.303	Fuks 21/2 (C)/Fuks 31/2 (M)
82.5L/17.5P	33.1	36.2	146	1	30.8	30.3	149	1	6.945	Fuks 23/2 (C)/Fuks 24/2 (M)
85L/15P	33.7	36.9	149	1	31.6	30.7	152	1	6.393	Fuks 11/2
90L/10P	34.2	37.1	153	2	34.0	33.7	153	2	4.575	Fuks 10/2

TABLE A-5. Thermal Data of Binary Mixtures of Lauric and Stearic Acids

SAMPLE	MELTING				CRYSTALLIZATION				SAMPLE WEIGHT (mg)	FILE NUMBER
	MELTING POINT (°C)	TEMPERATURE FOR MAX. ENDOTHERMIC HEAT FLOW (°C)	HEAT OF MELTING (J/g)	NUMBER OF PEAKS ON THERMOGRAM	FREEZING POINT (°C)	TEMPERATURE FOR MAX. EXOTHERMIC HEAT FLOW (°C)	HEAT OF CRYSTAL-LIZATION (J/g)	NUMBER OF PEAKS ON THERMOGRAM		
10L/90S	60.7	65.9	182	2	61.9	61.5	180	2	8.08	Fuks 08/3
20C/80S	57.4	63.9	183	3	59.6	58.8	179	3	7.307	Fuks 09/3
30L/70S	53.7	61.5	182	4	56.5	56.5	180	4	8.557	Fuks 10/3
40L/60S	31.2	59.2	178	4	53.4	52.4	171	3	10.623	Dor 19/9
50L/50S	32.5	35.7	174	4	50.2	49.7	171	4	7.676	Dor 20/9
60L/40S	33.4	35.7	155	4	45.3	44.8	165	3	4.974	Fuks 01/4
70L/30S	34.2	36.1	163	3	37.9	32.4	163	2	3.999	Fuks 02/4
80L/20S	34.0	36.4	162	2	34.3	32.6	160	2	3.4	Fuks 03/4
82.5L/17.5S	34.0	37.1	157	1	32.9	31.4	161	1	8.496	Fuks 22/4
84L/16S	33.9	37.1	157	1	32.3	31.1	161	2	7.999	Fuks 23/4
85L/15S	34.0	36.7	156	1	32.0	31.3	158	1	5.038	Fuks 06/4
86L/14S	34.2	37.5	152	1	31.3	30.8	157	1	3.973	Fuks 24/4
87.5L/12.5S	34.2	37.3	151	1	32.2	31.8	155	2	8.152	Fuks 25/4
90L/10S	34.5	37.7	155	1	33.3	32.1	155	1	8.404	Fuks 04/4

30 MOLE % CAPRIC: 70 MOLE % LAURIC

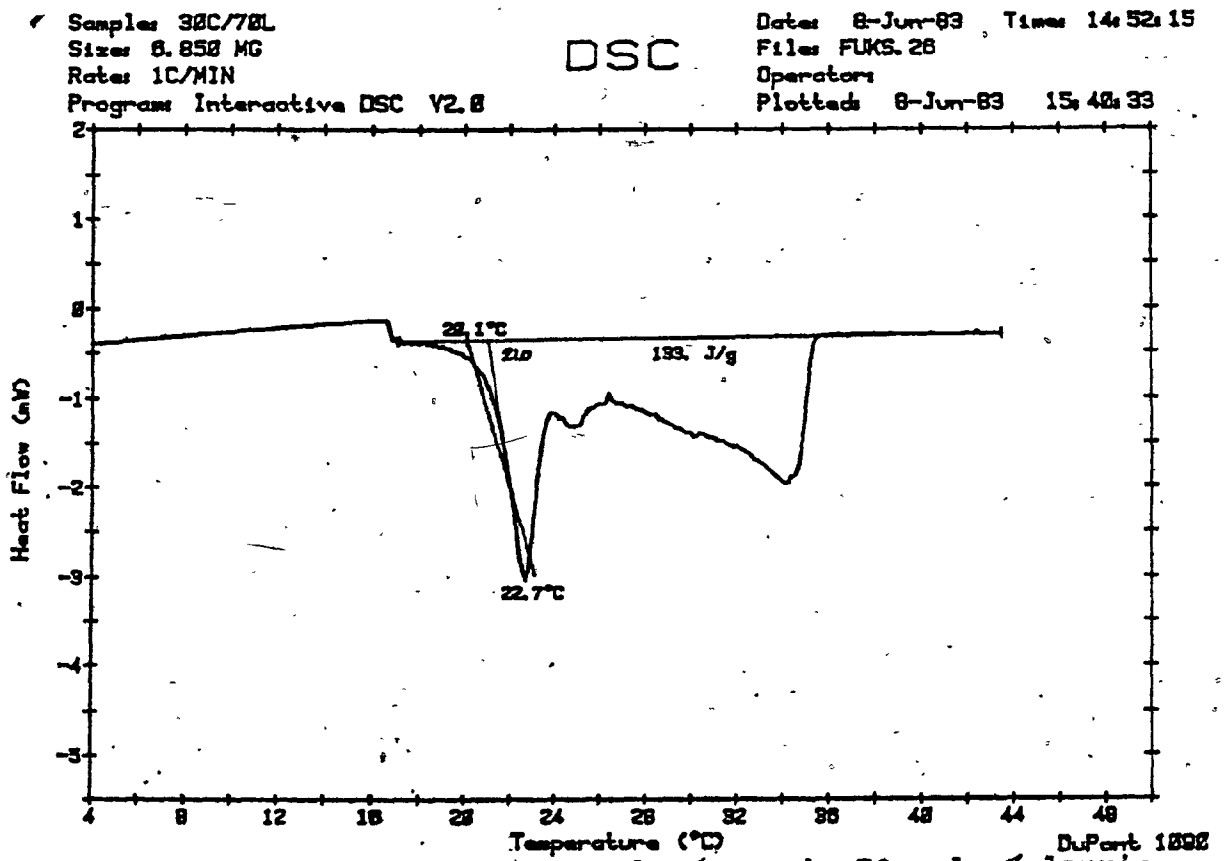

Fig. T-1. Thermogram of 30 mole % capric:70 mole % lauric

(1°C/min heating rate)

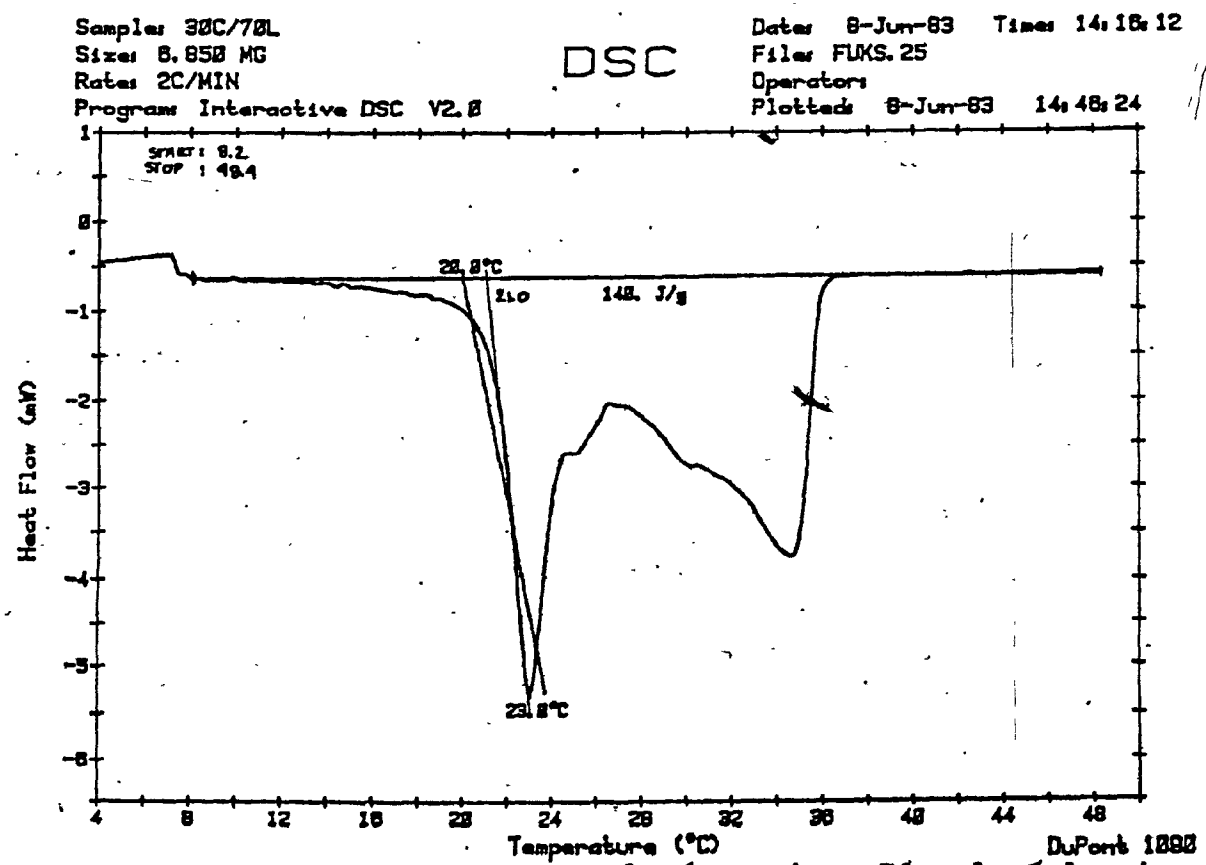

~~Fig. T-2.~~ Thermogram of 30 mole % capric : 70 mole % lauric

(2°C/min heating rate) .

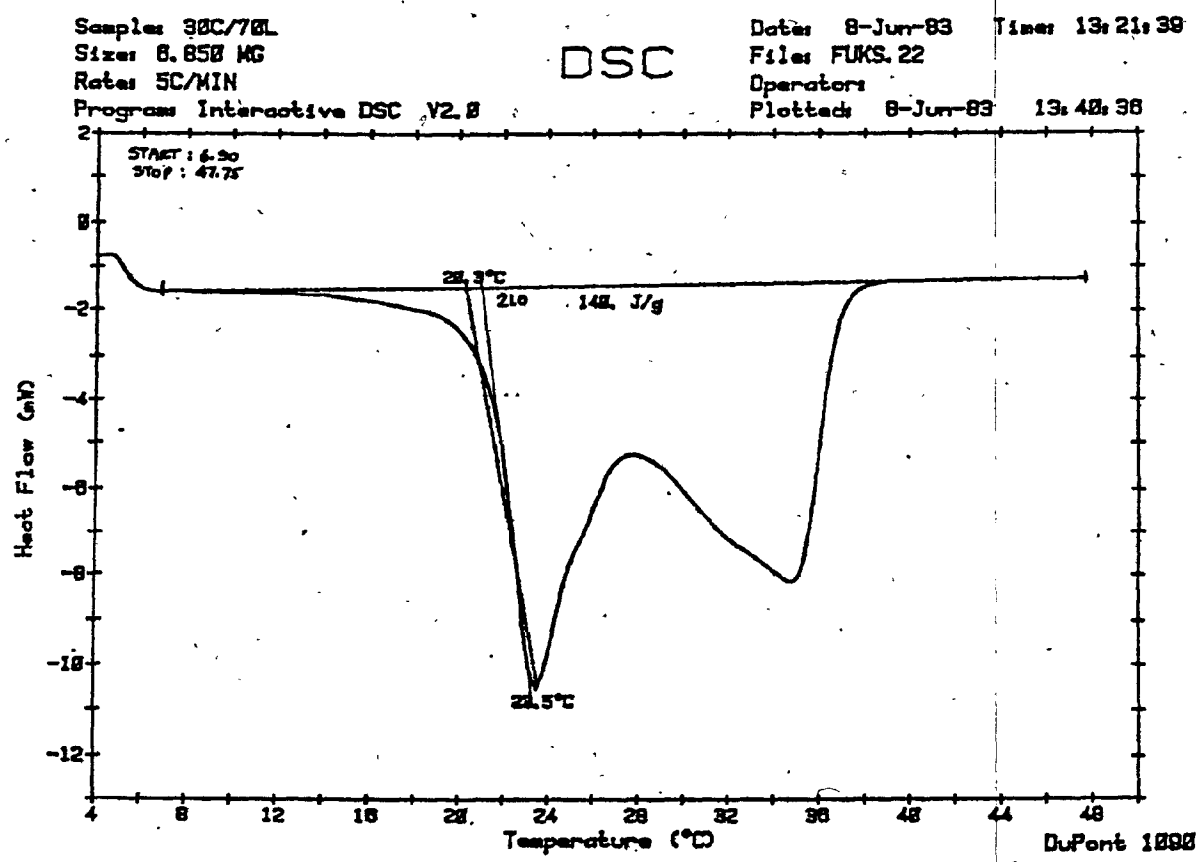

Fig. T-3. Thermogram of 30 mole % capric : 70 mole % lauric

(5 °C/min heating rate)

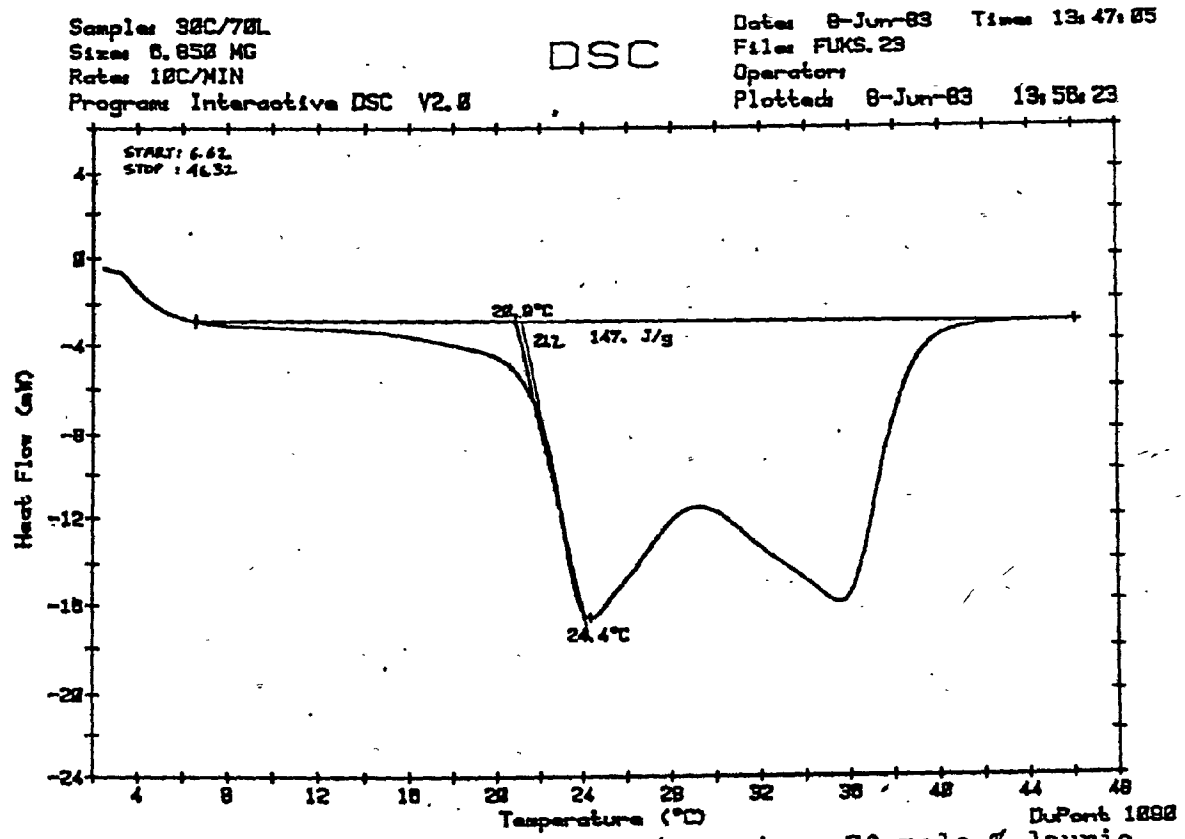

Fig. T-4. Thermogram of 30 mole % capric : 70 mole % lauric

(10°C/min heating rate)

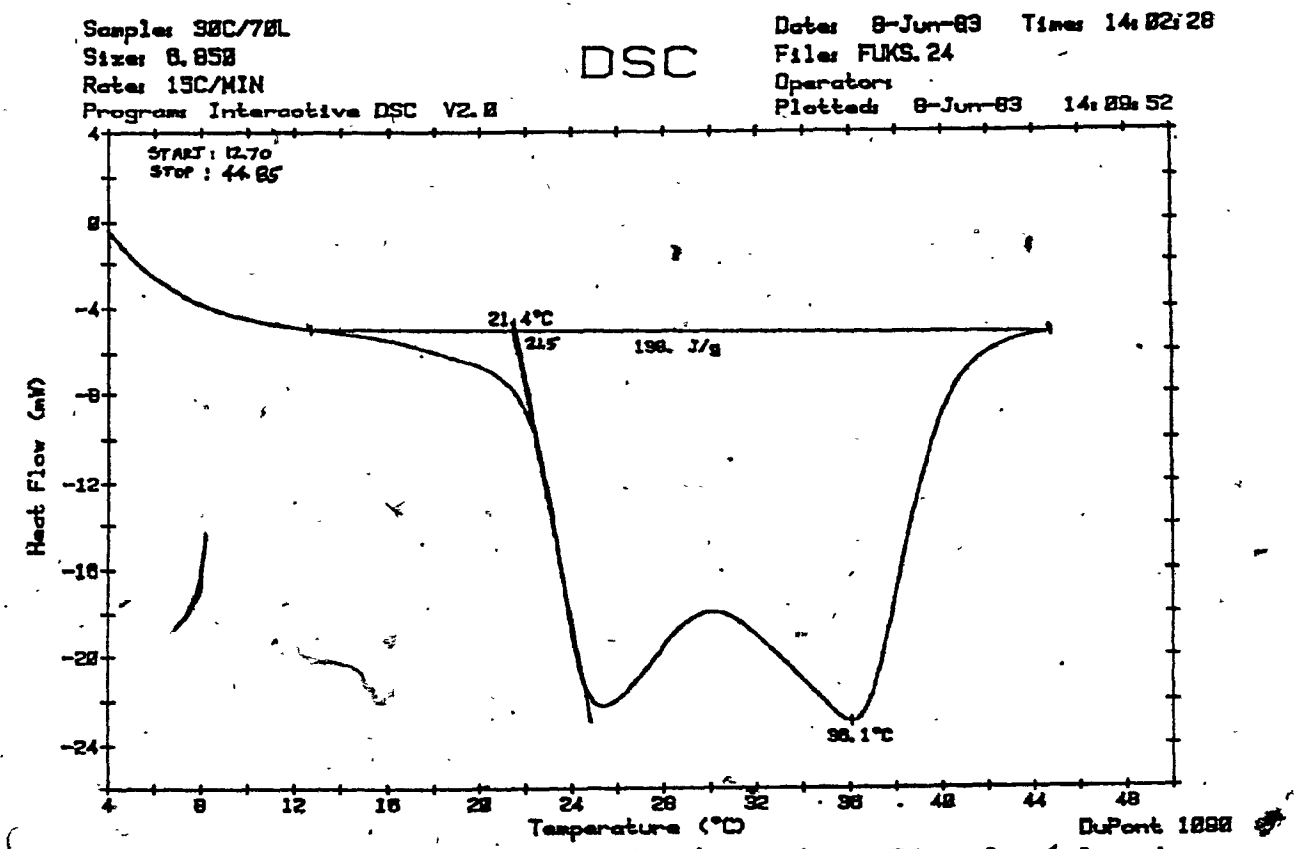

Fig. T-5. Thermogram of 30 mole % capric : 70 mole % lauric

(15°C/min heating rate)

PURE FATTY ACIDS

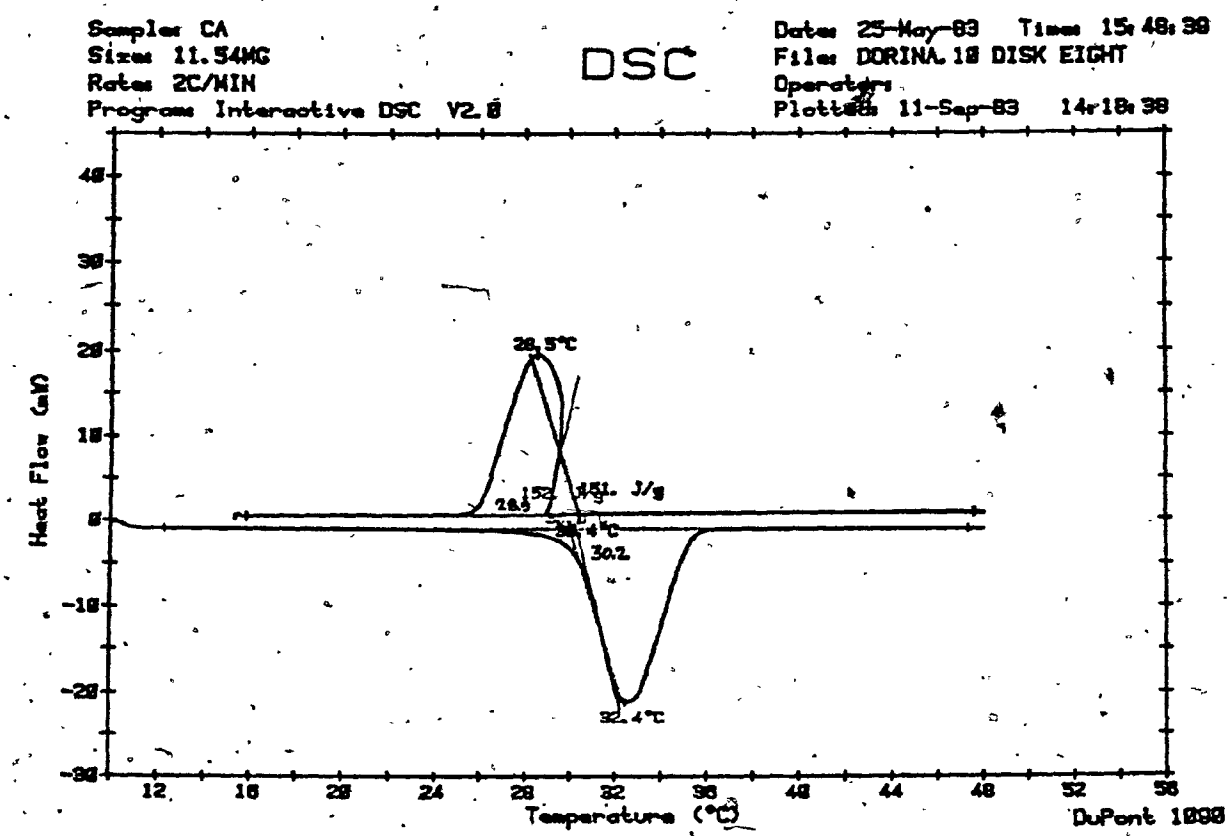

Fig. T-6. Thermogram of capric acid (11.54 mg)

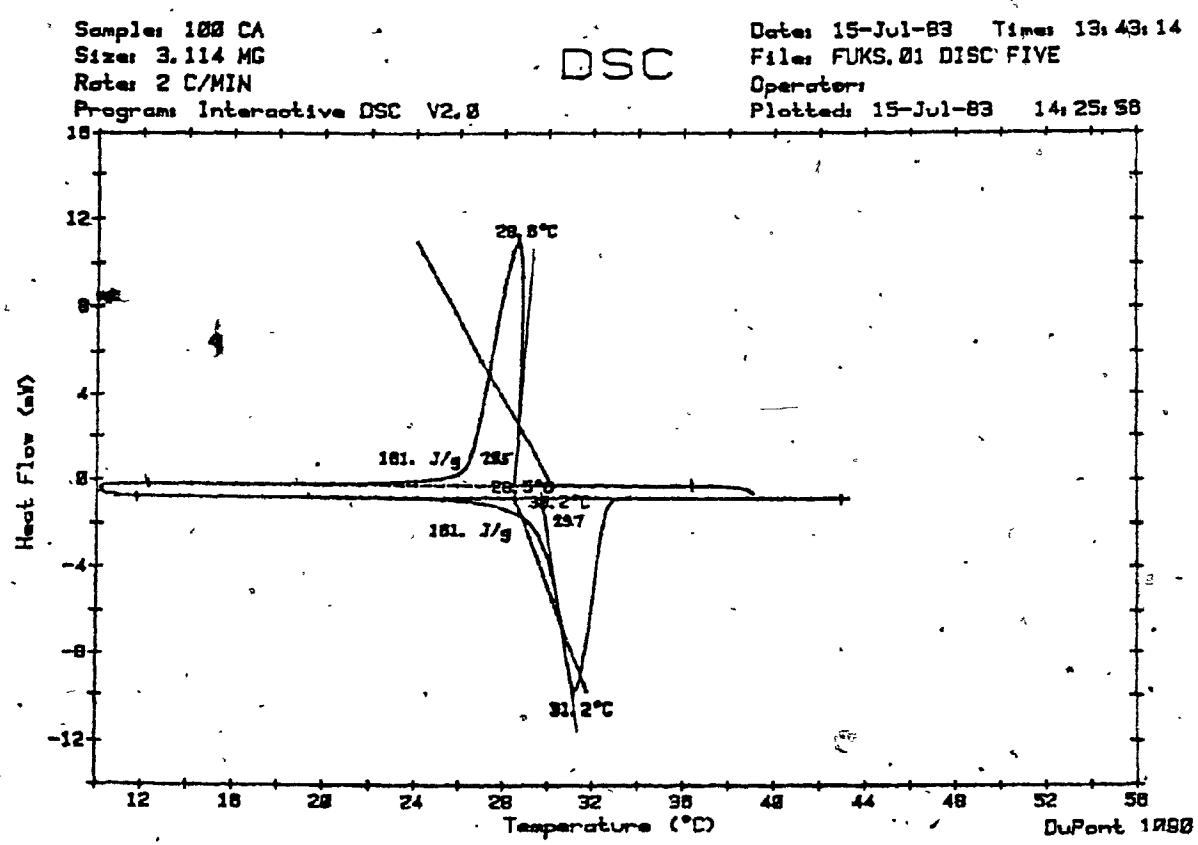

Fig. T-7. Thermogram of capric acid (3.114 mg)

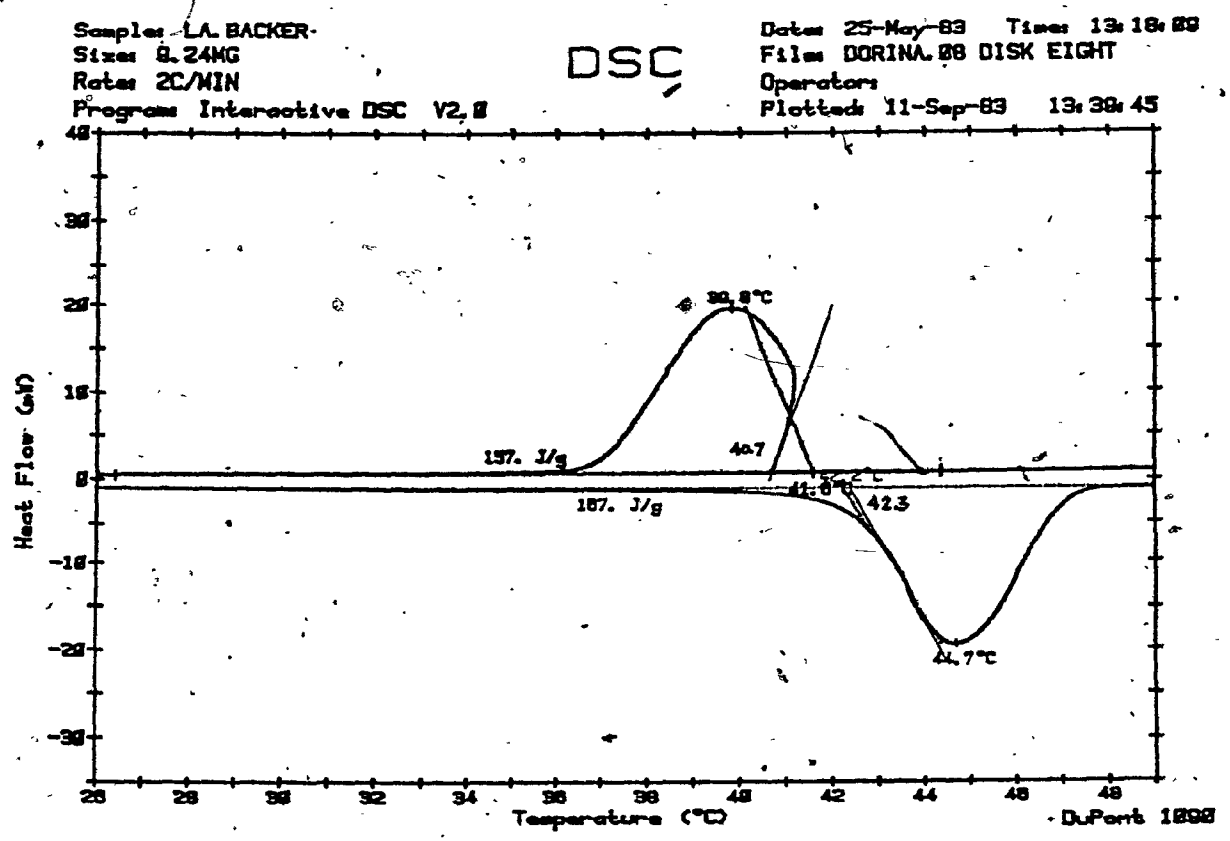

Fig. T-8. Thermogram of lauric acid (9.24 mg)

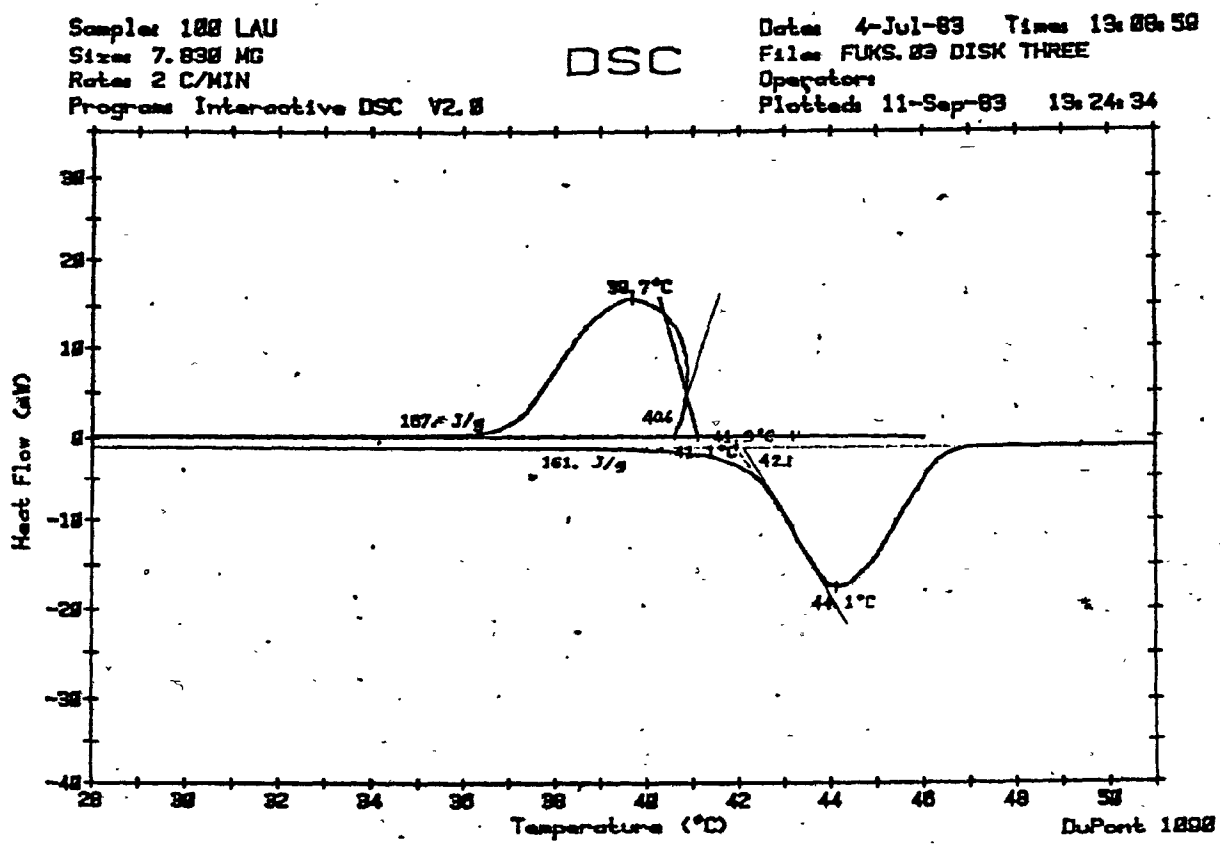

Fig. T-9. Thermogram of lauric acid (7.83 mg)

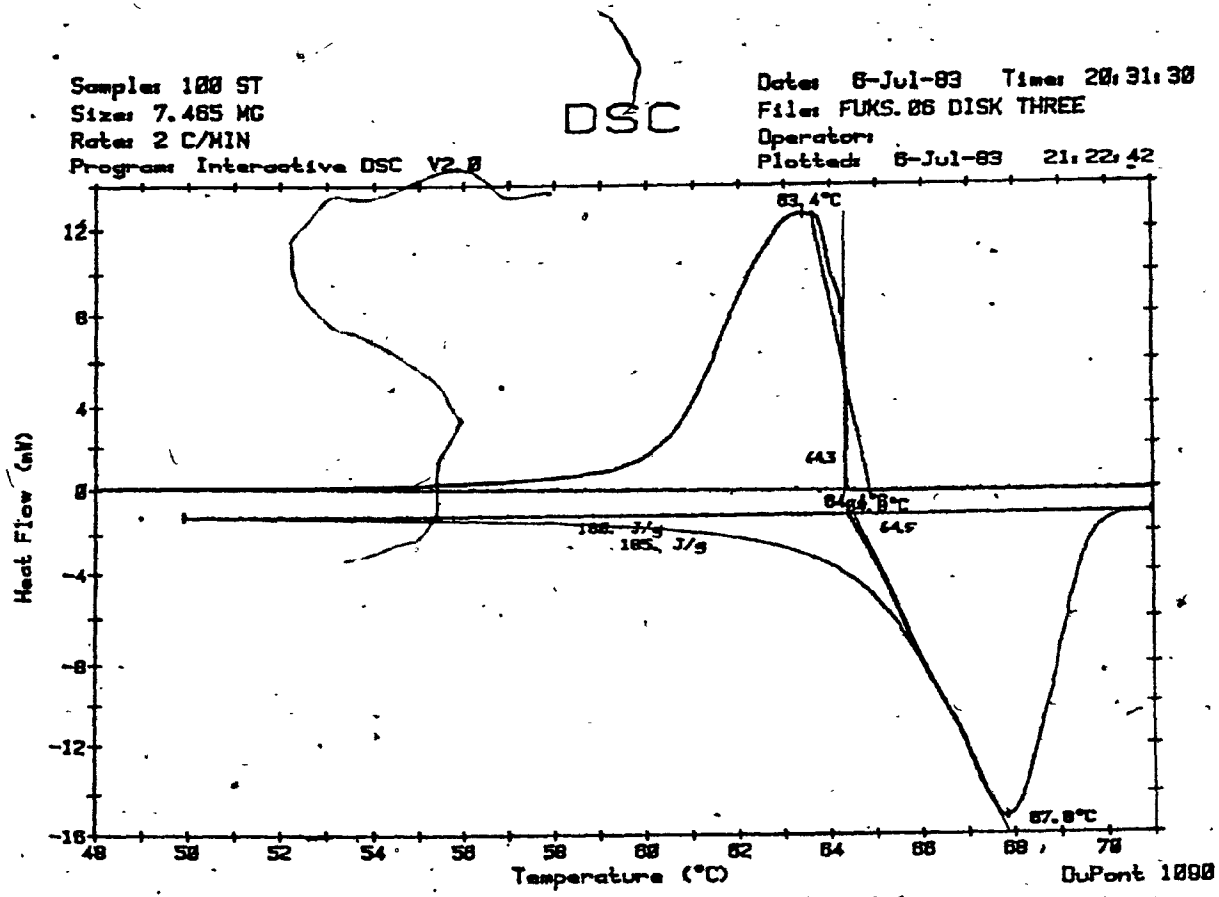

Fig. T-10. Thermogram of stearic acid (7.465 mg, run #1)

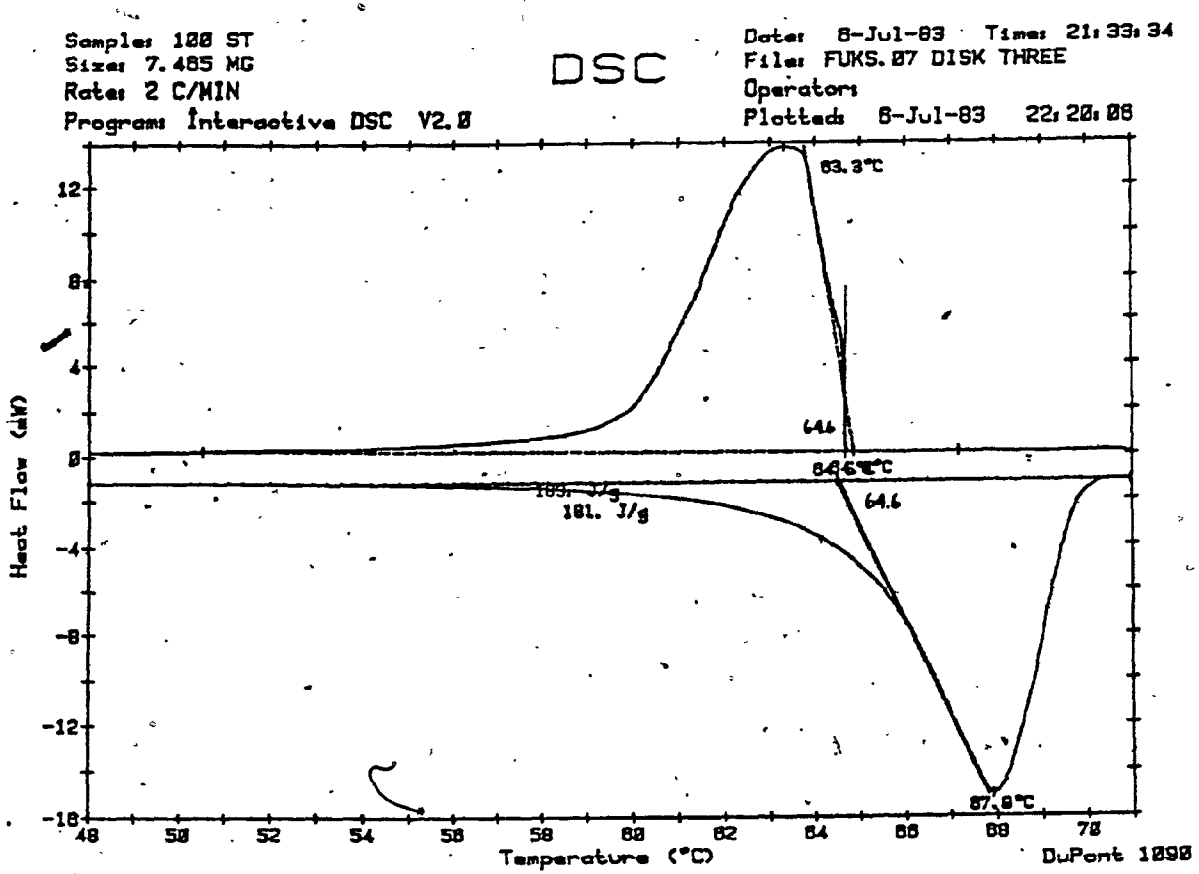

Fig. T-11. Thermogram of stearic acid (7.465 mg, run #2)

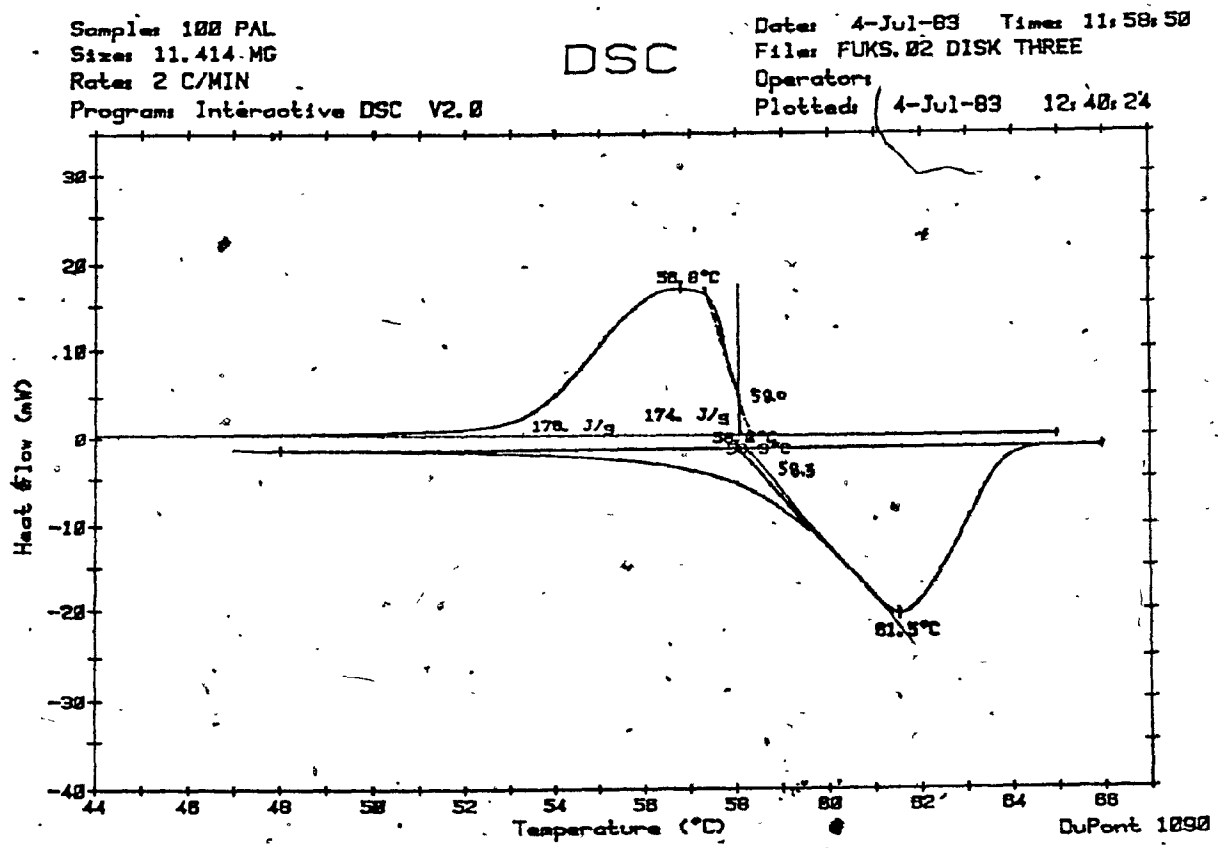

Fig. T-12. Thermogram of palmitic acid (11.414 mg)

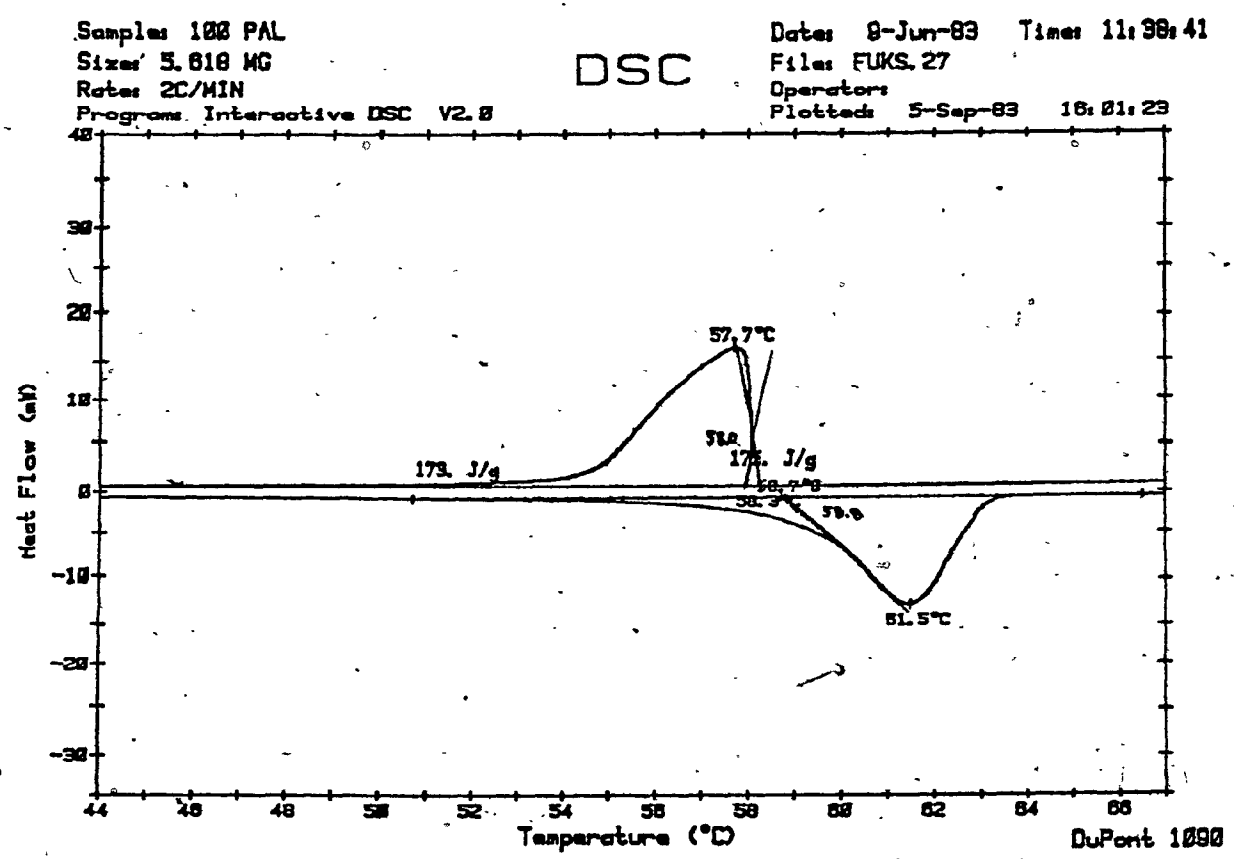

Fig. T-13. Thermogram of palmitic acid (5.618 mg)

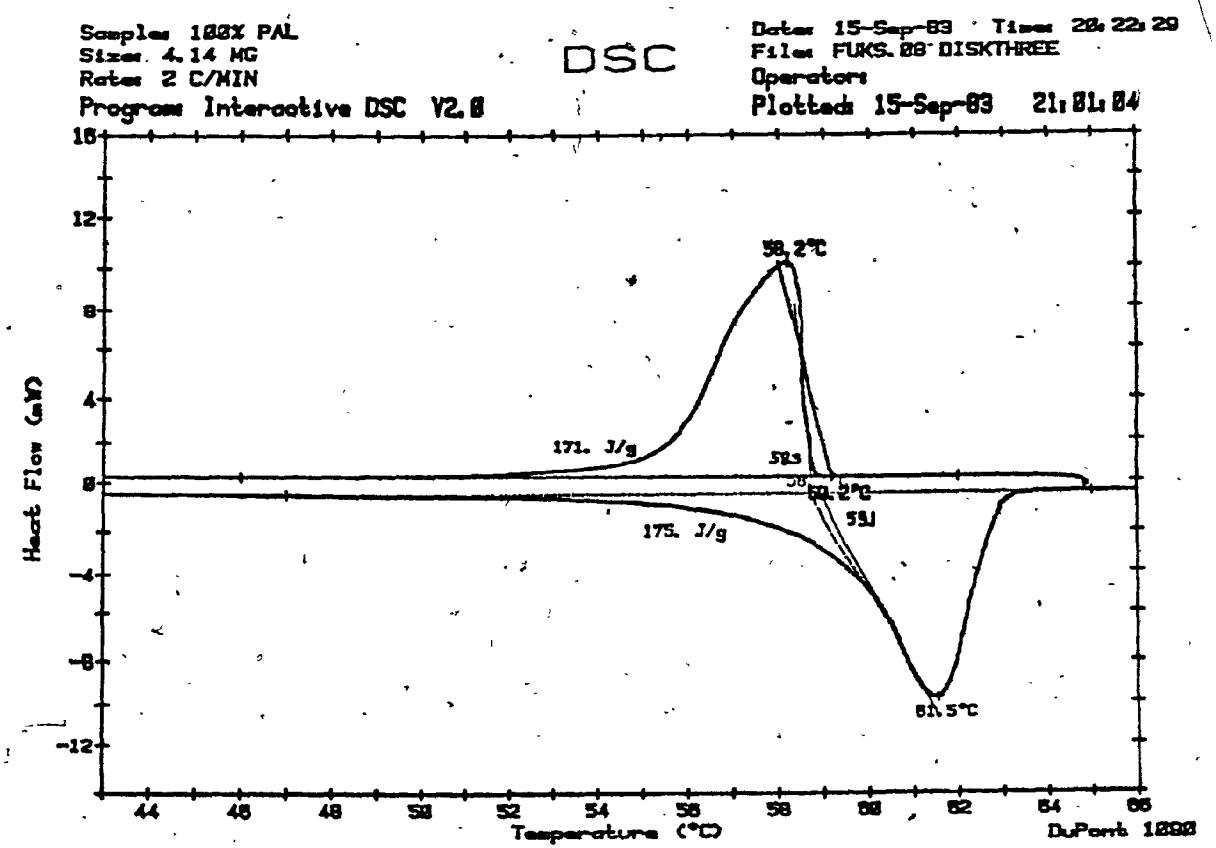

Fig. T-14. Thermogram of palmitic acid (4.14 mg)

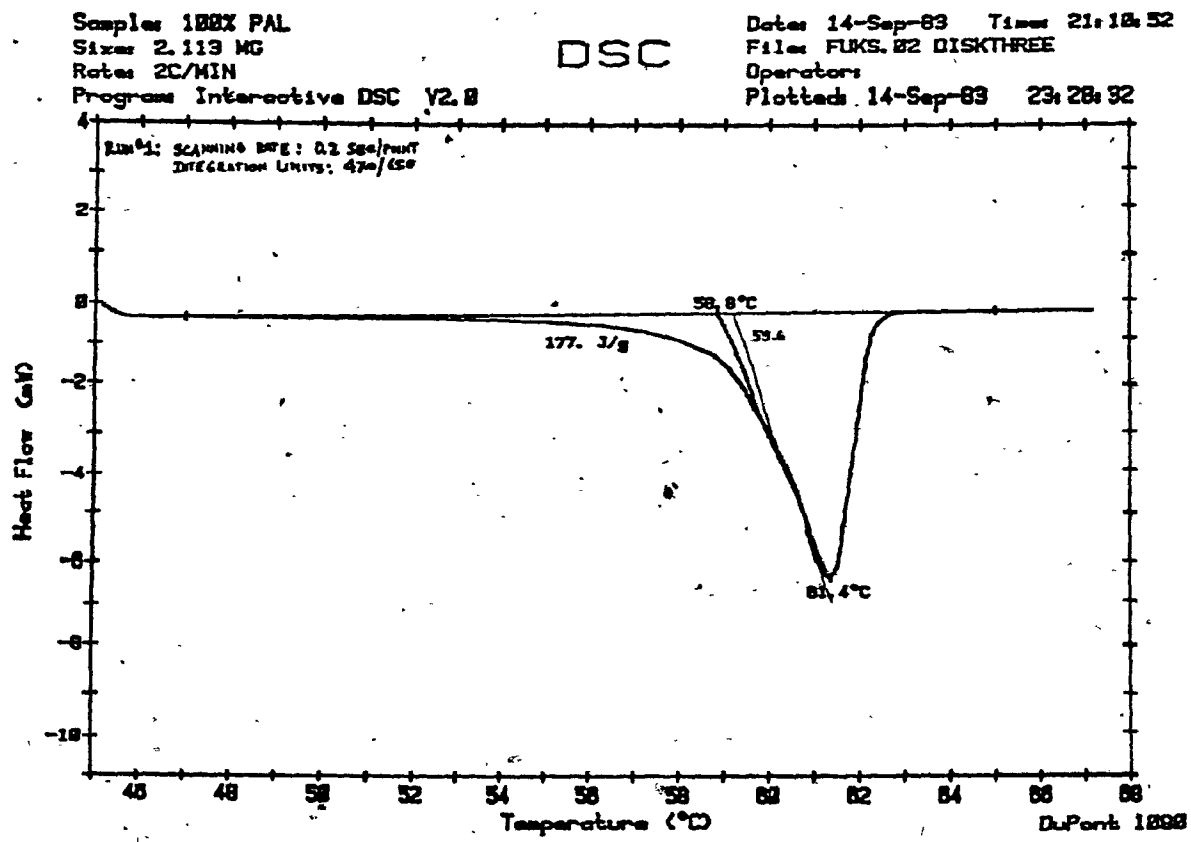

Fig. T-15. Thermogram of palmitic acid (run #1, scanning rate: 0.2 sec/point)

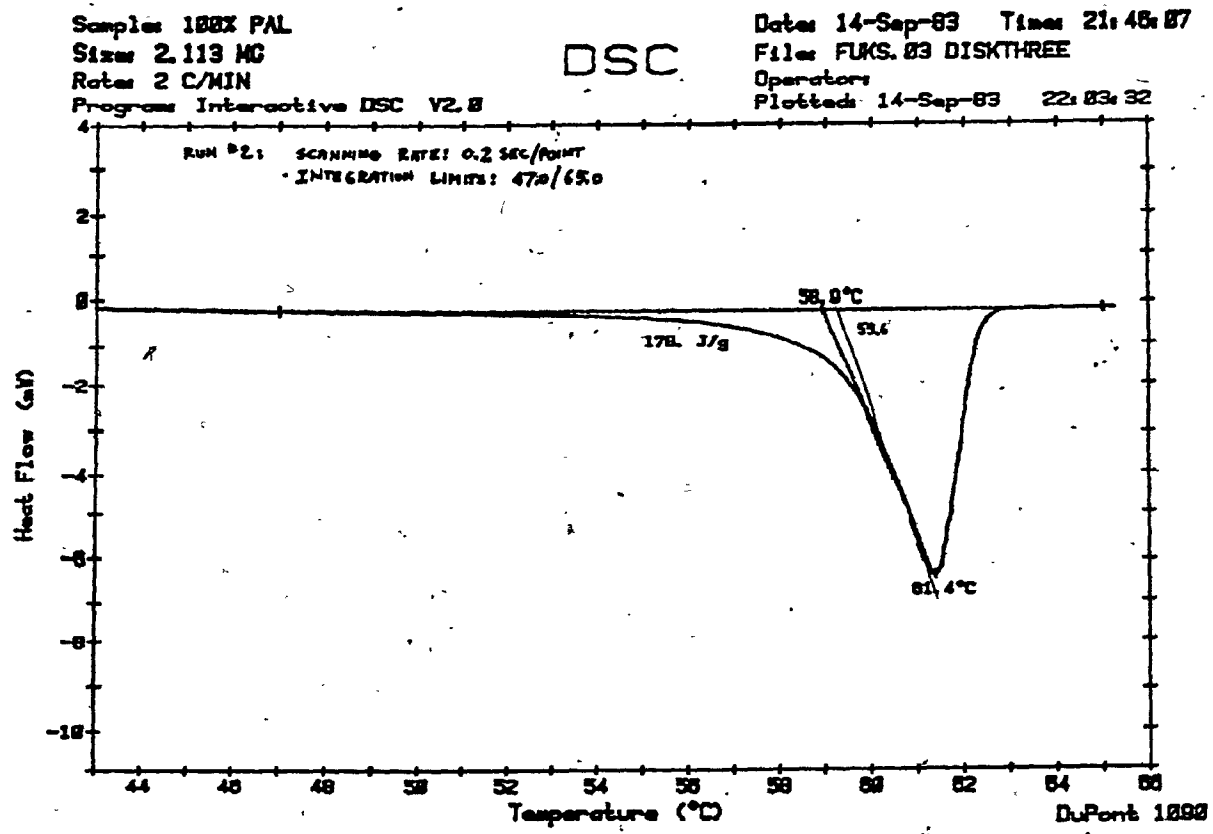

Fig. T-16. Thermogram of palmitic acid (run #2, scanning rate: 0.2 sec/point)

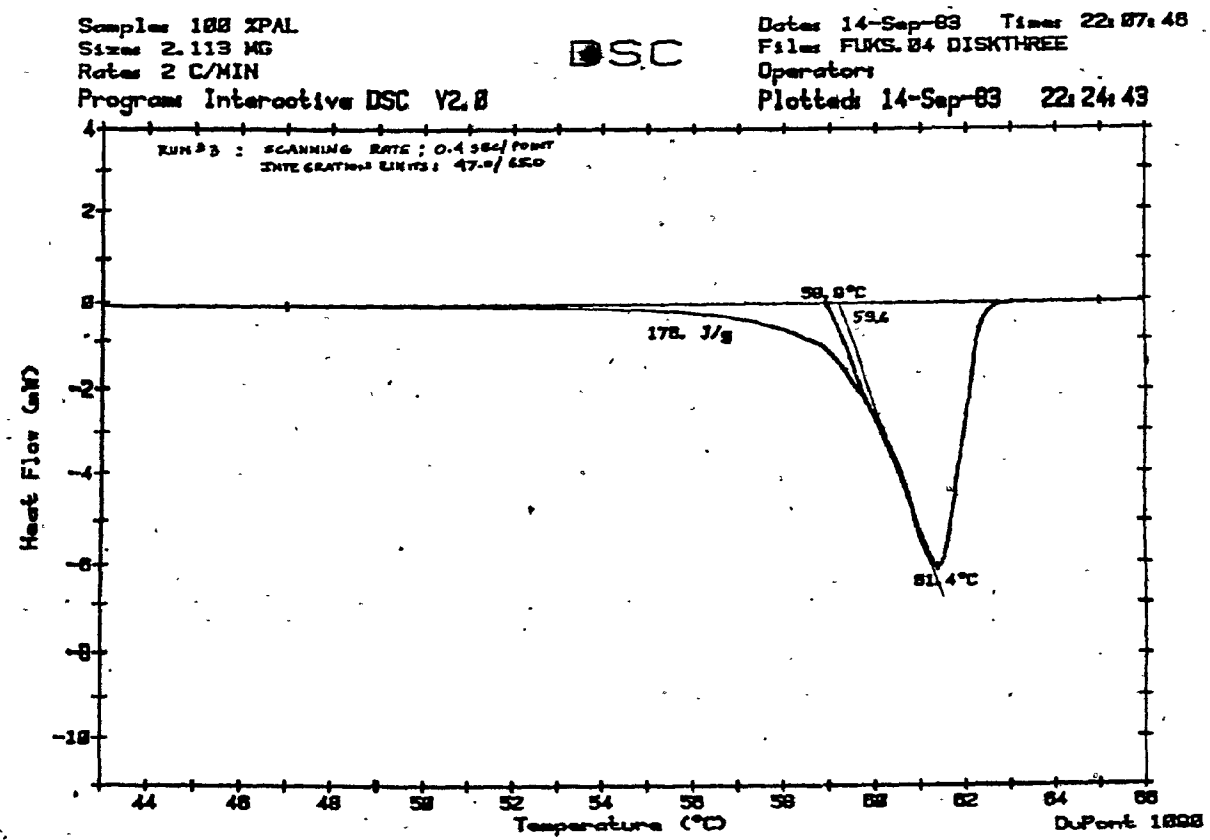

Fig. T-17. Thermogram of palmitic acid (run #3, scanning rate: 0.4 sec/point)

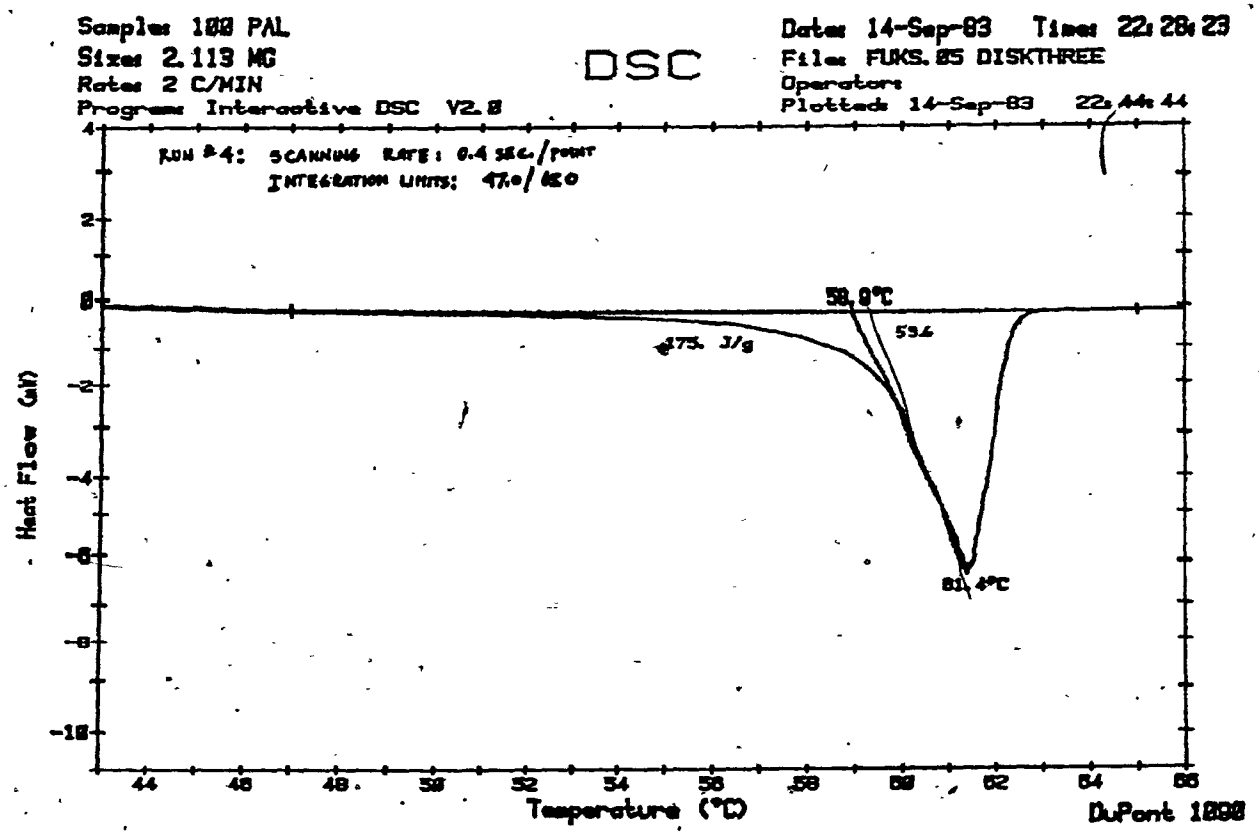

Fig. T-18. Thermogram of palmitic acid (run #4, scanning rate: 0.4 sec/point)

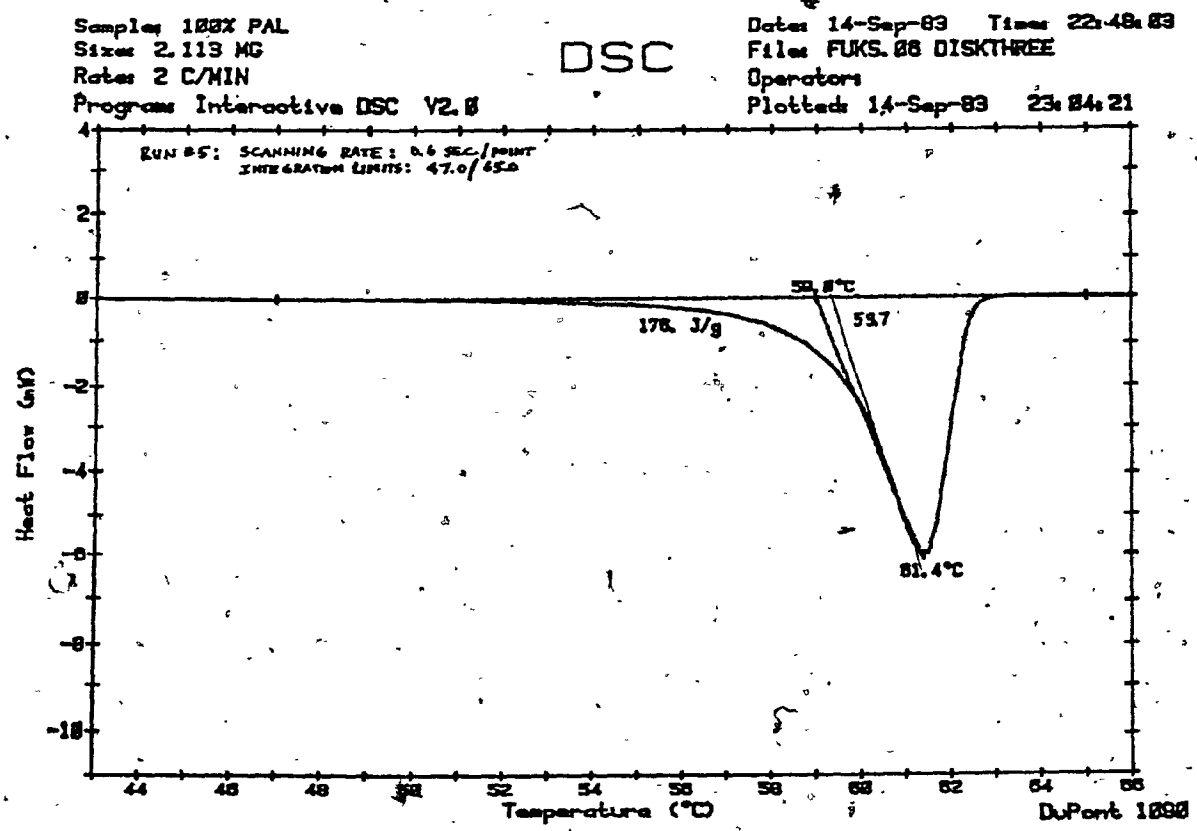

Fig. T-19. Thermogram of palmitic acid (run #5, scanning rate: 0.6 sec/point)

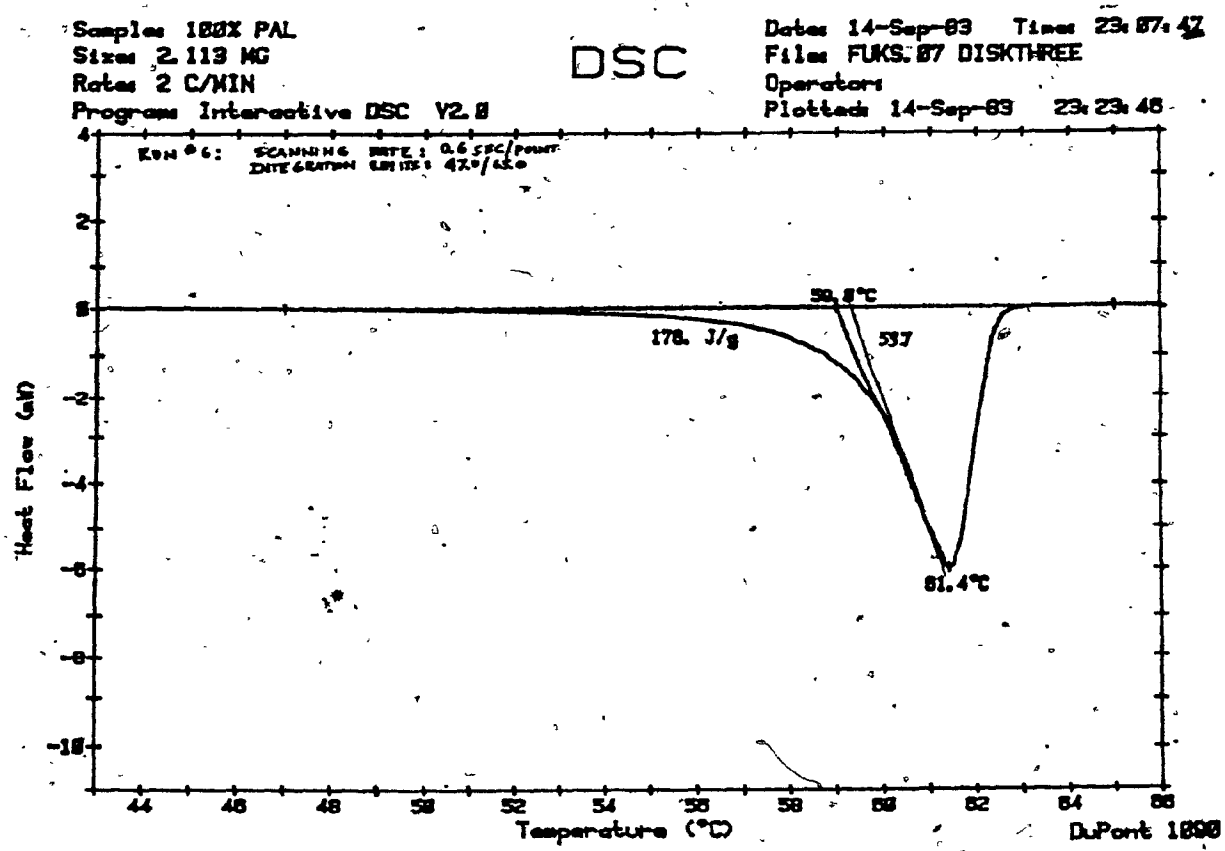

Fig. T-20. Thermogram of palmitic acid (run #6, scanning rate: 0.6 sec/point)

BINARY MIXTURES OF CAPRIC-LAURIC ACIDS

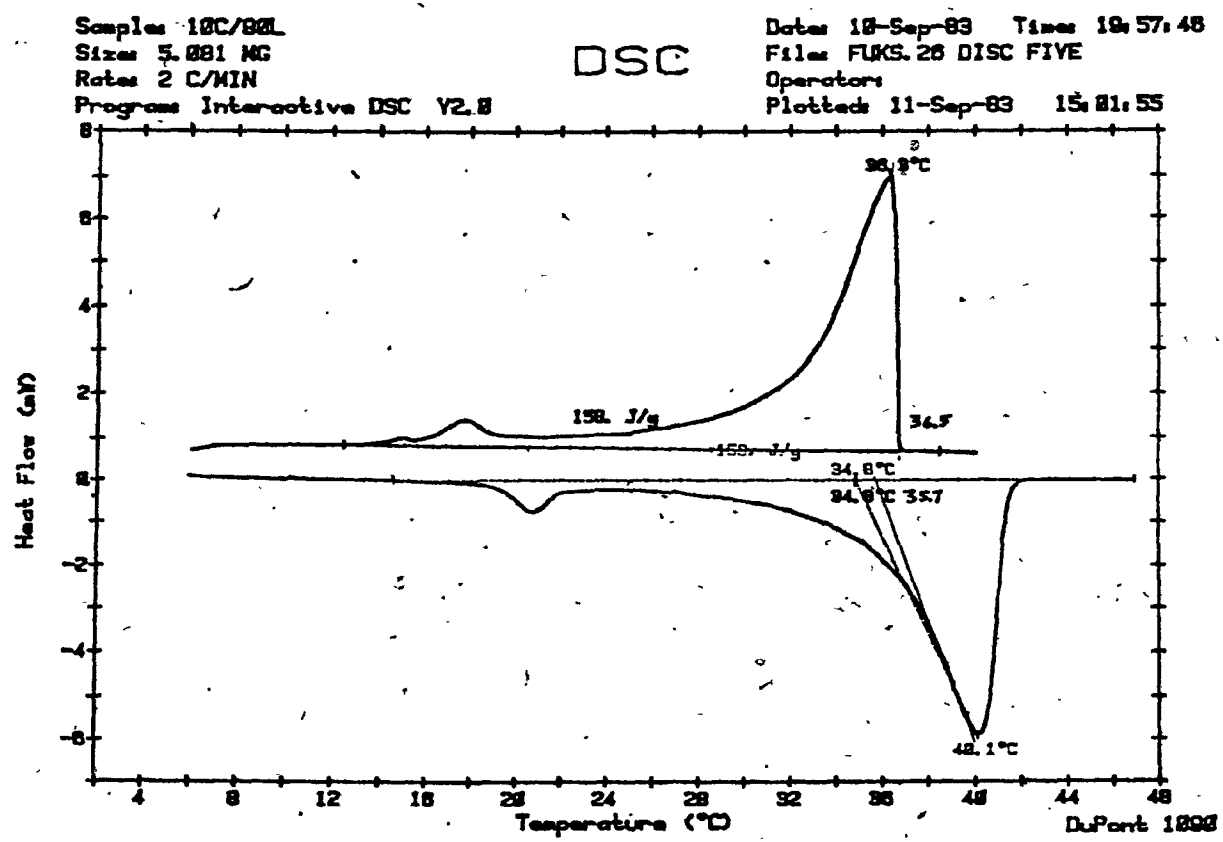

Fig. T-21. Thermogram of 10 mole % capric : 90 mole % lauric

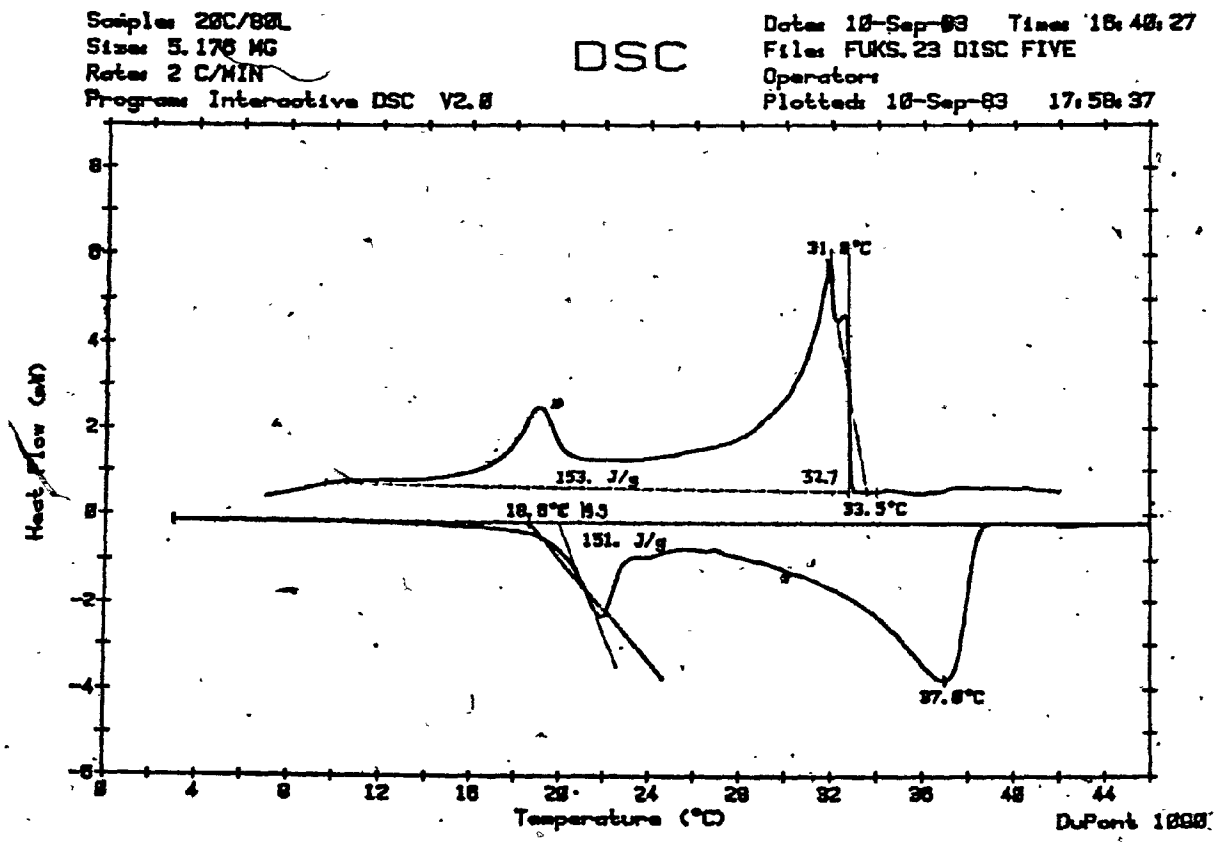

Fig. T-22. Thermogram of 20 mole % capric : 80 mole % lauric

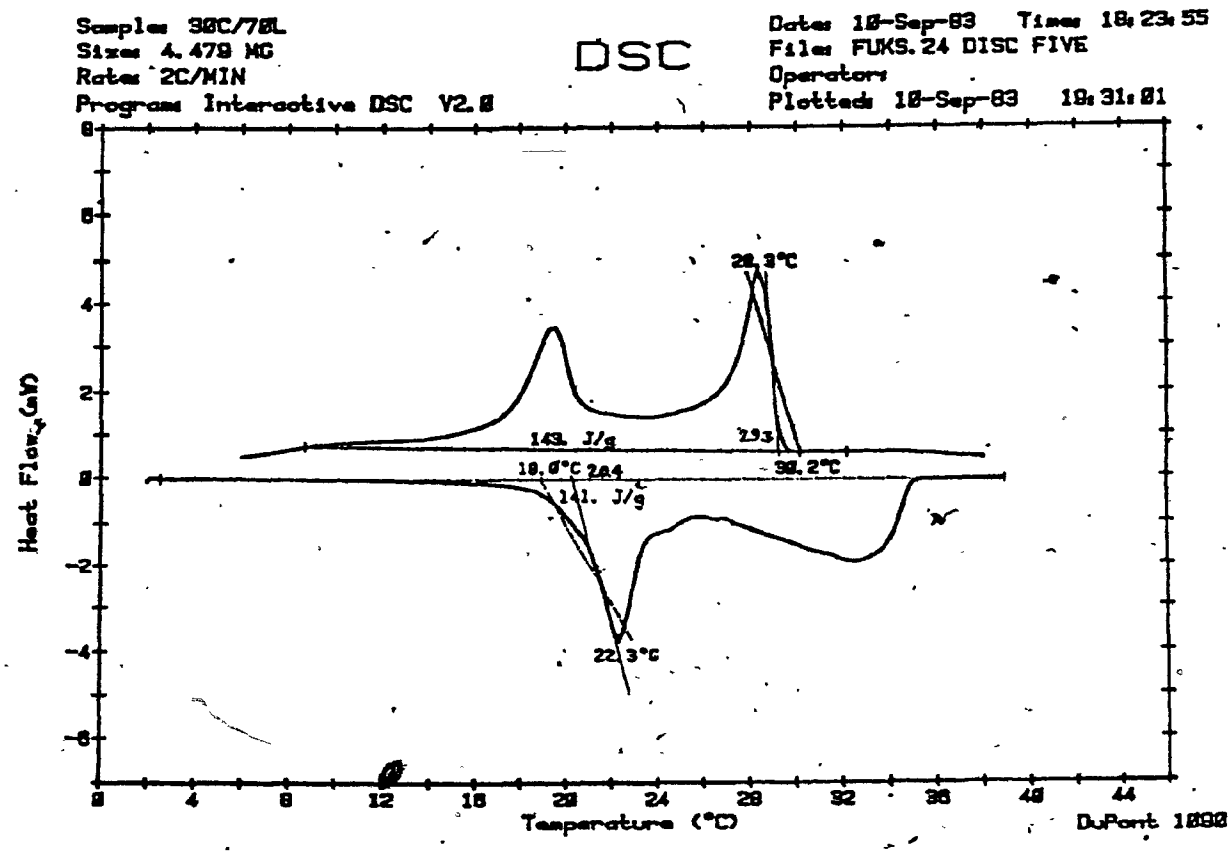

Fig. T-23. Thermogram of 30 mole % capric : 70 mole % lauric

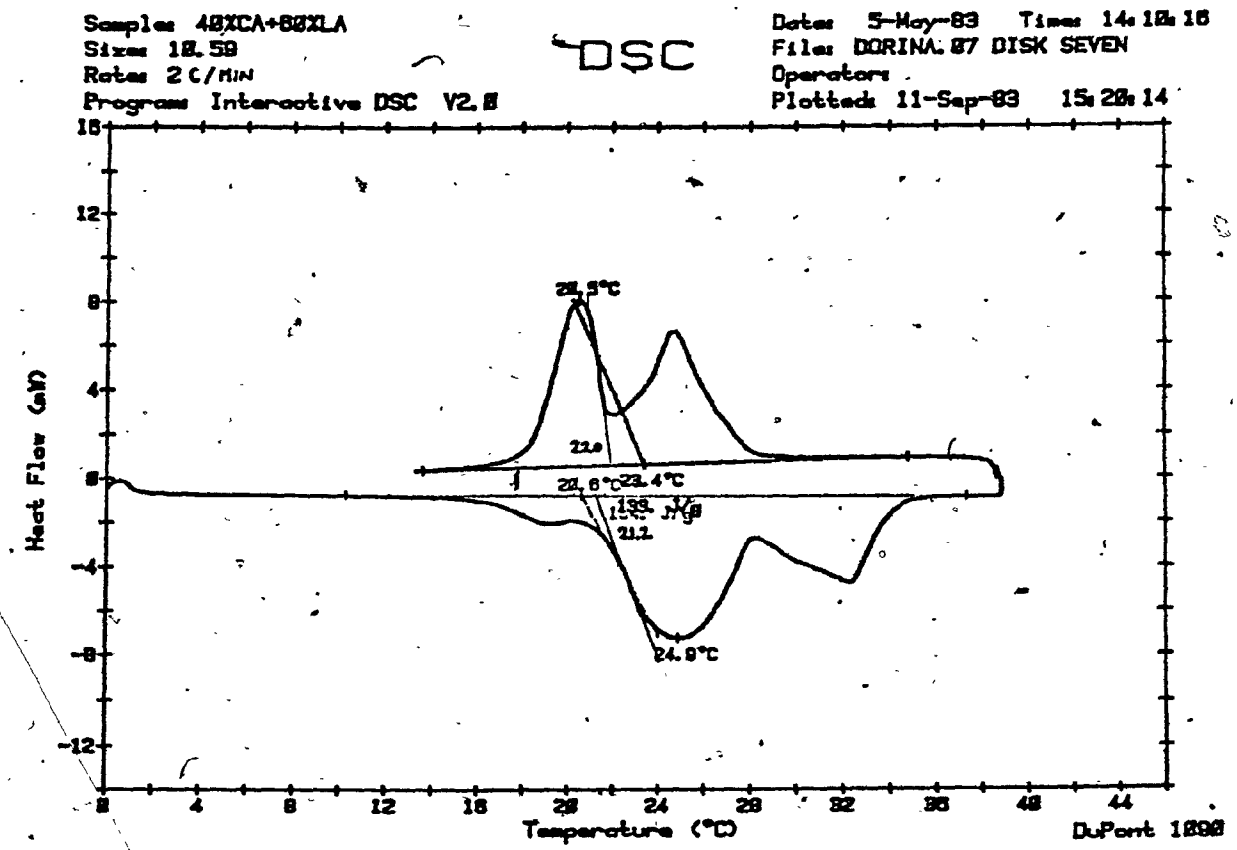

Fig. T-24. Thermogram of 40 mole % capric : 60 mole % lauric.

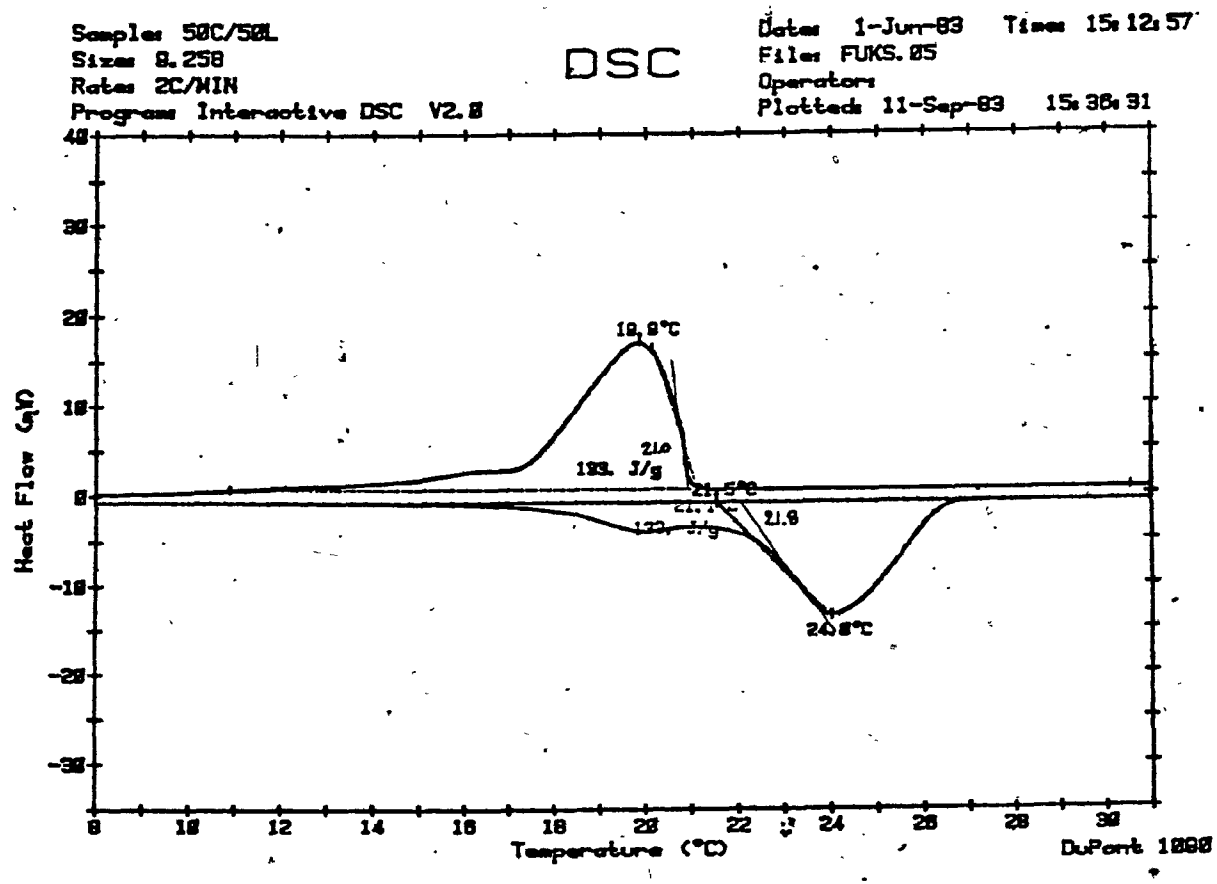

Fig. T-25. Thermogram of 50 mole % capric : 50 mole % lauric.

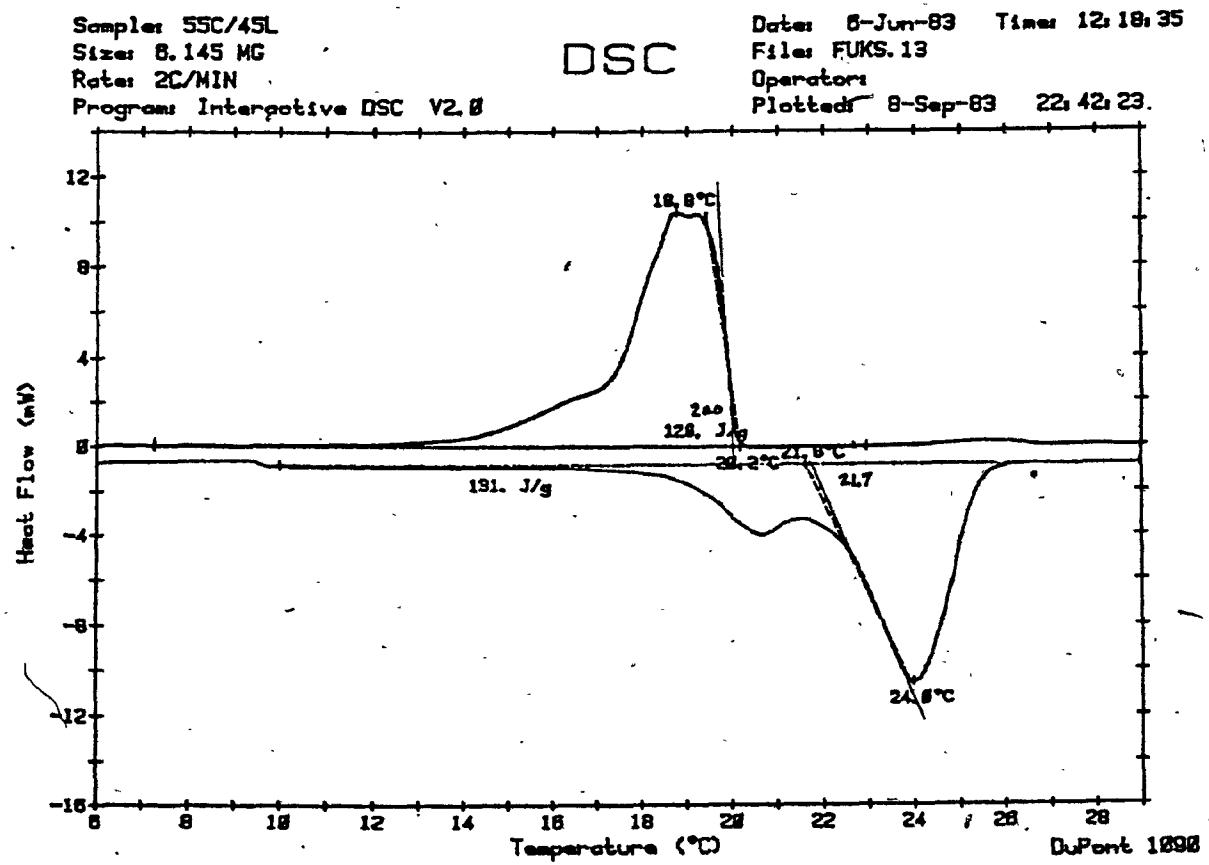

Fig. T-26. Thermogram of 55 mole % capric : 45 mole % lauric.

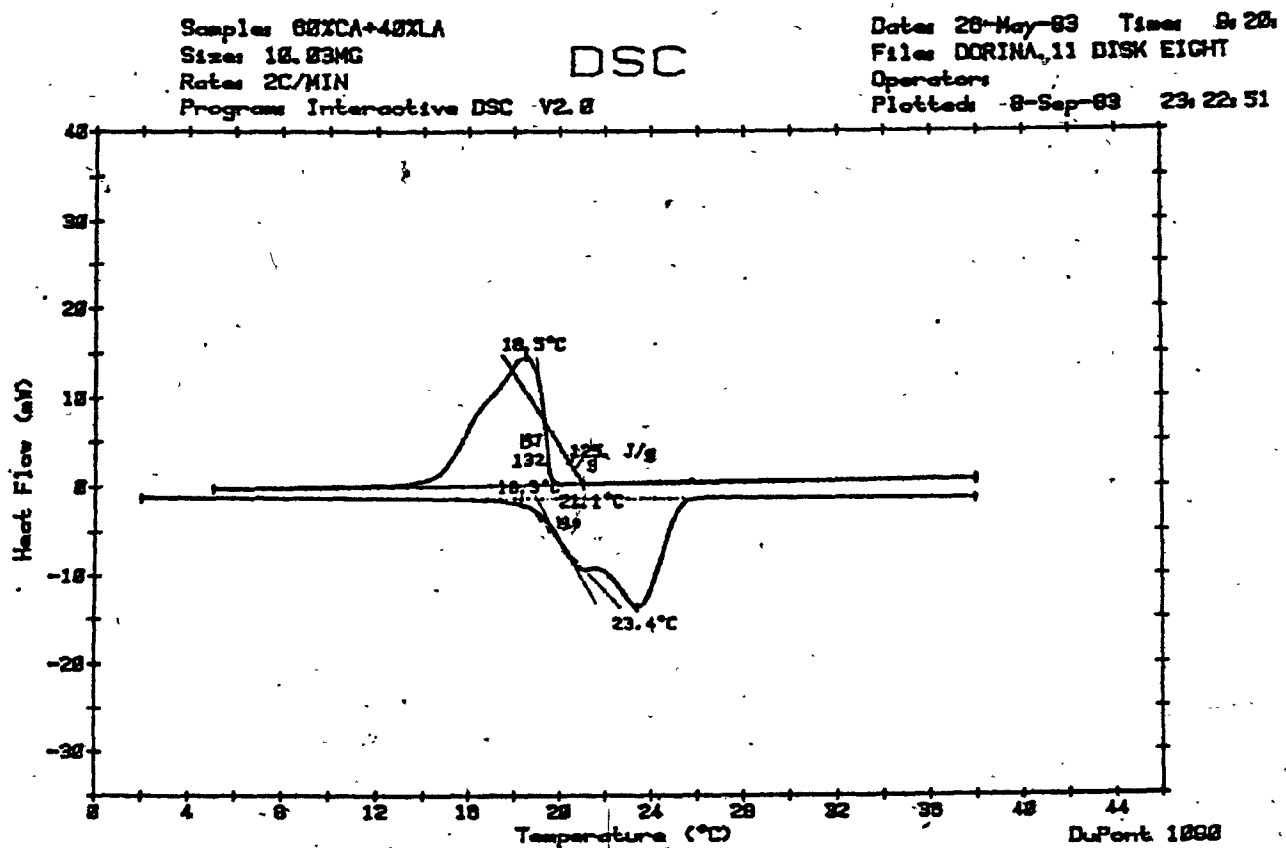

Fig. T-26. Thermogram of 60 mole % capric : 40 mole % lauric.

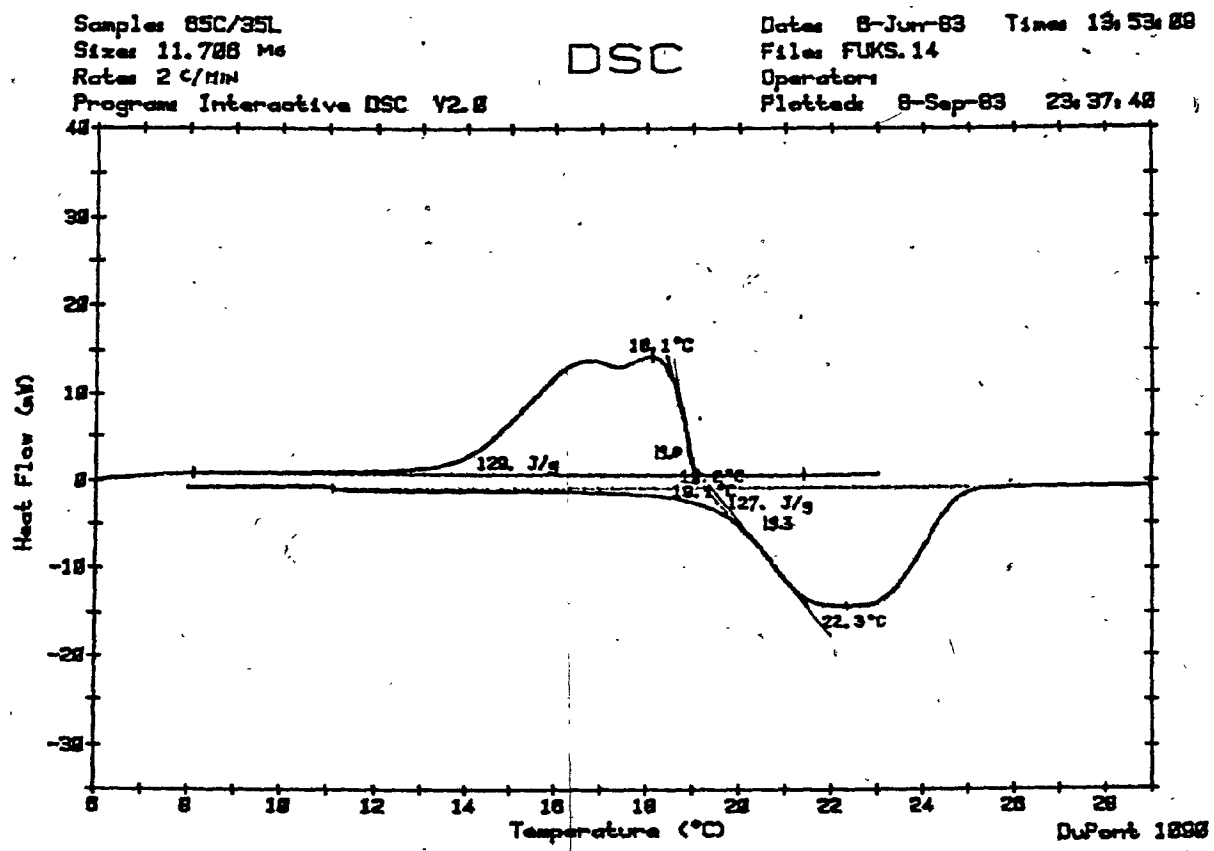

Fig. T-28. Thermogram of 65 mole % capric : 35 mole % lauric.

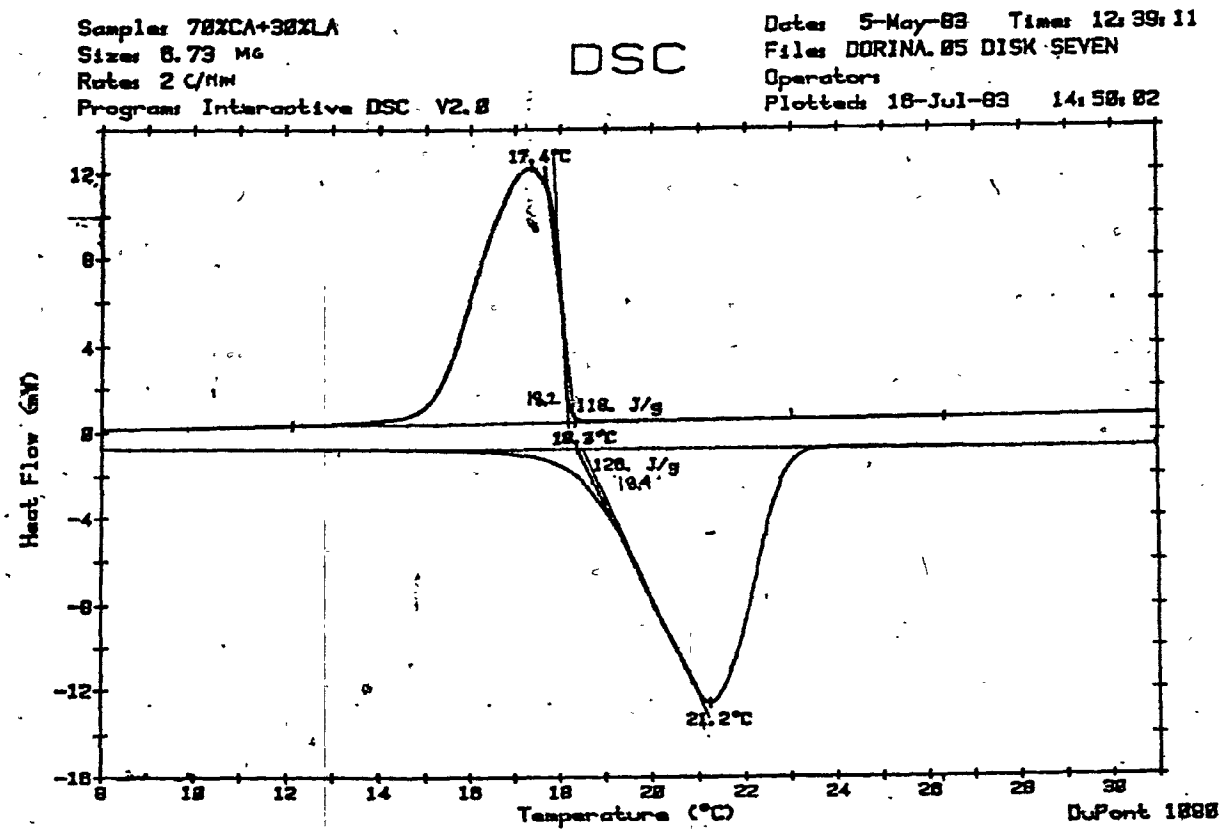

Fig. T-29. Thermogram of 70 mole % capric : 30 mole % lauric.

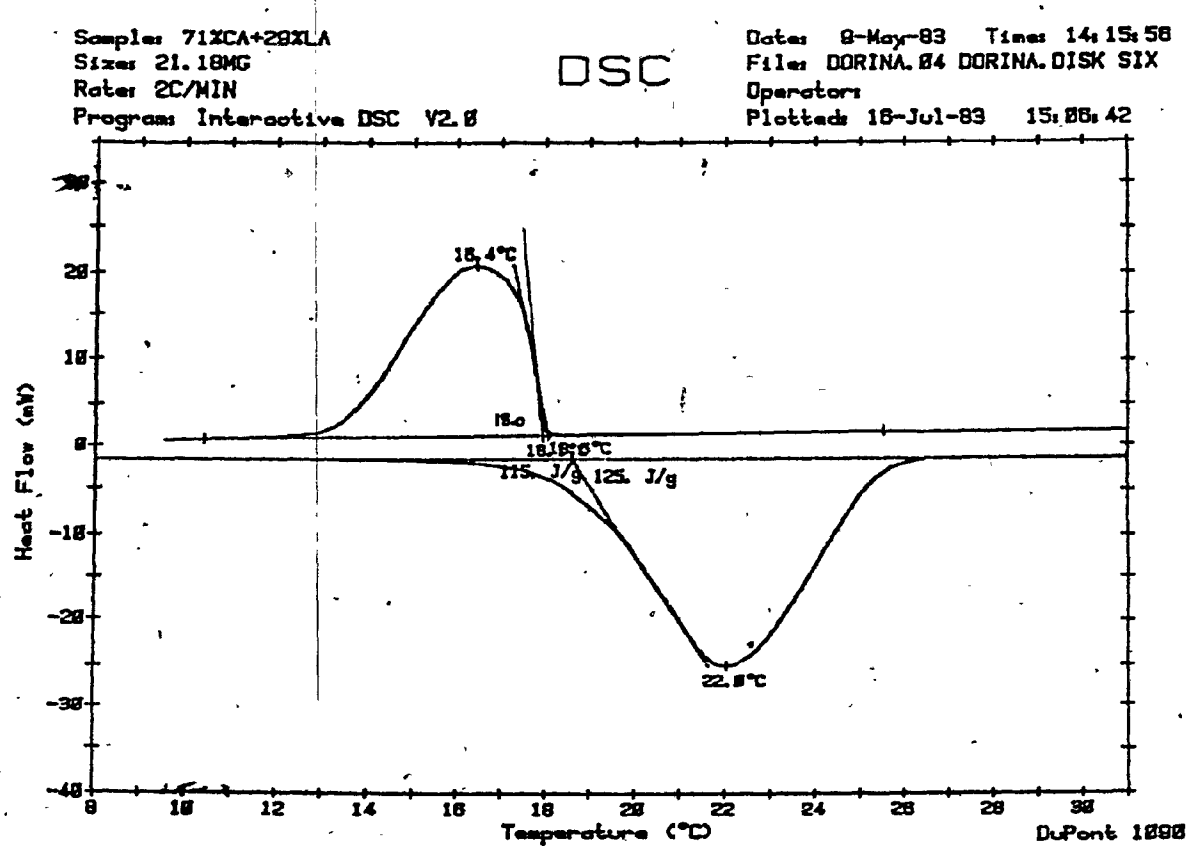

Fig. T-30. Thermogram of 71 mole % capric : 29 mole % lauric.

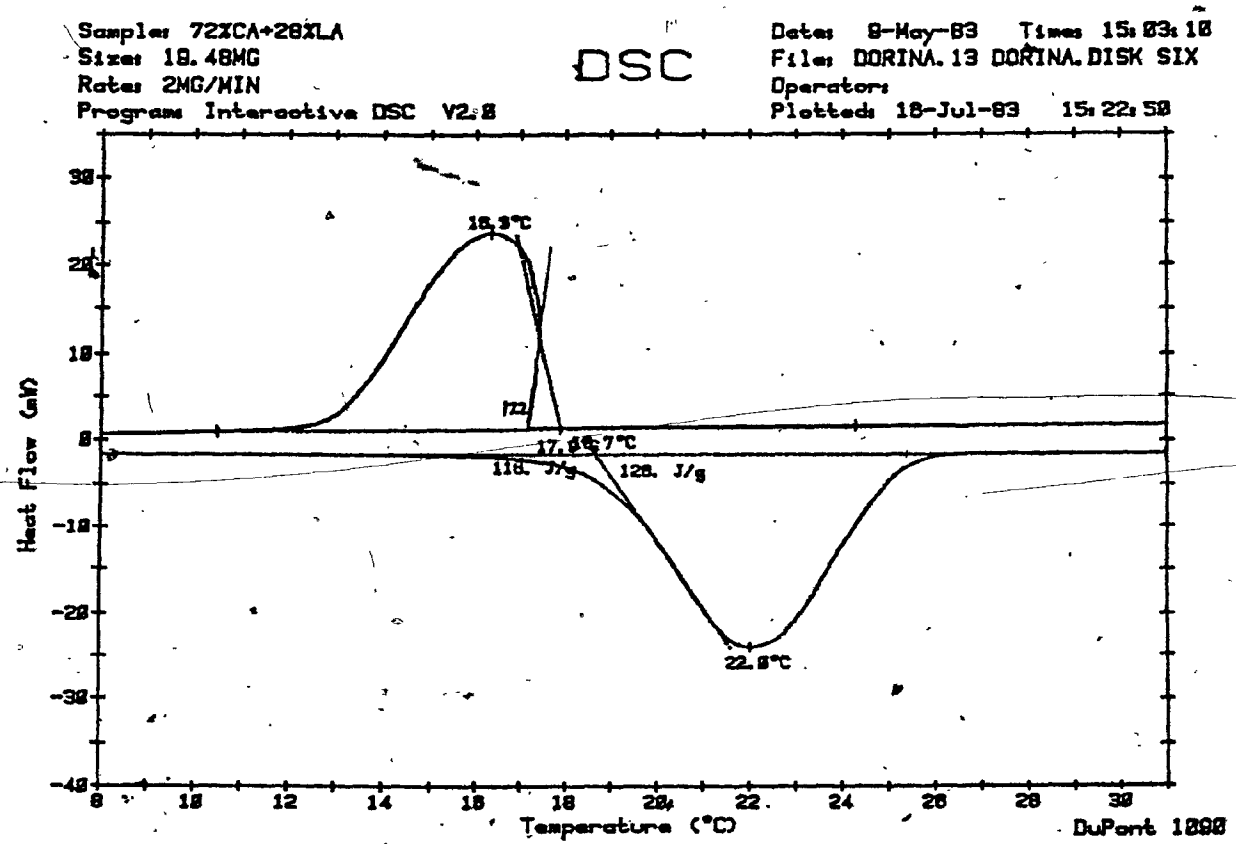

Fig. T-31. Thermogram of 72 mole % capric : 28 mole % lauric.

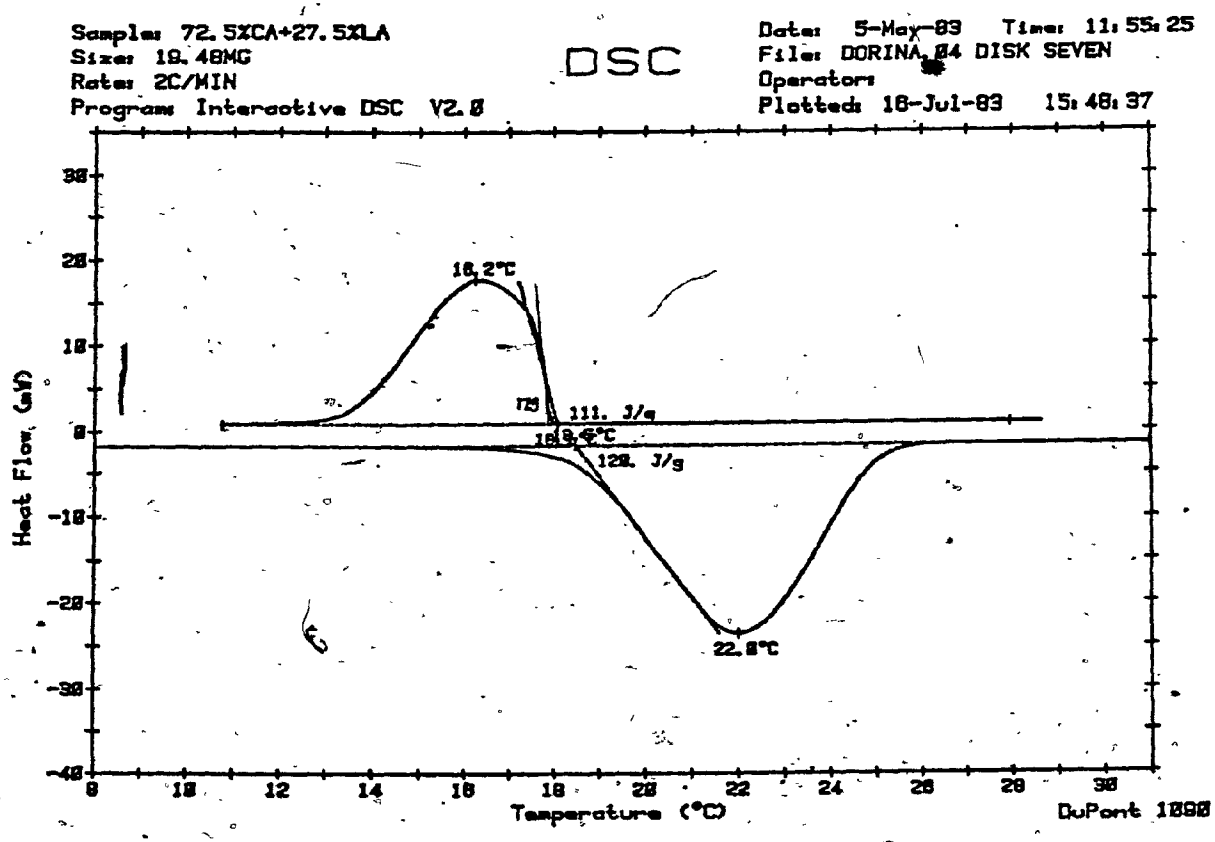

Fig. T-32. Thermogram of 72.5 mole % capric : 27.5 mole % lauric.

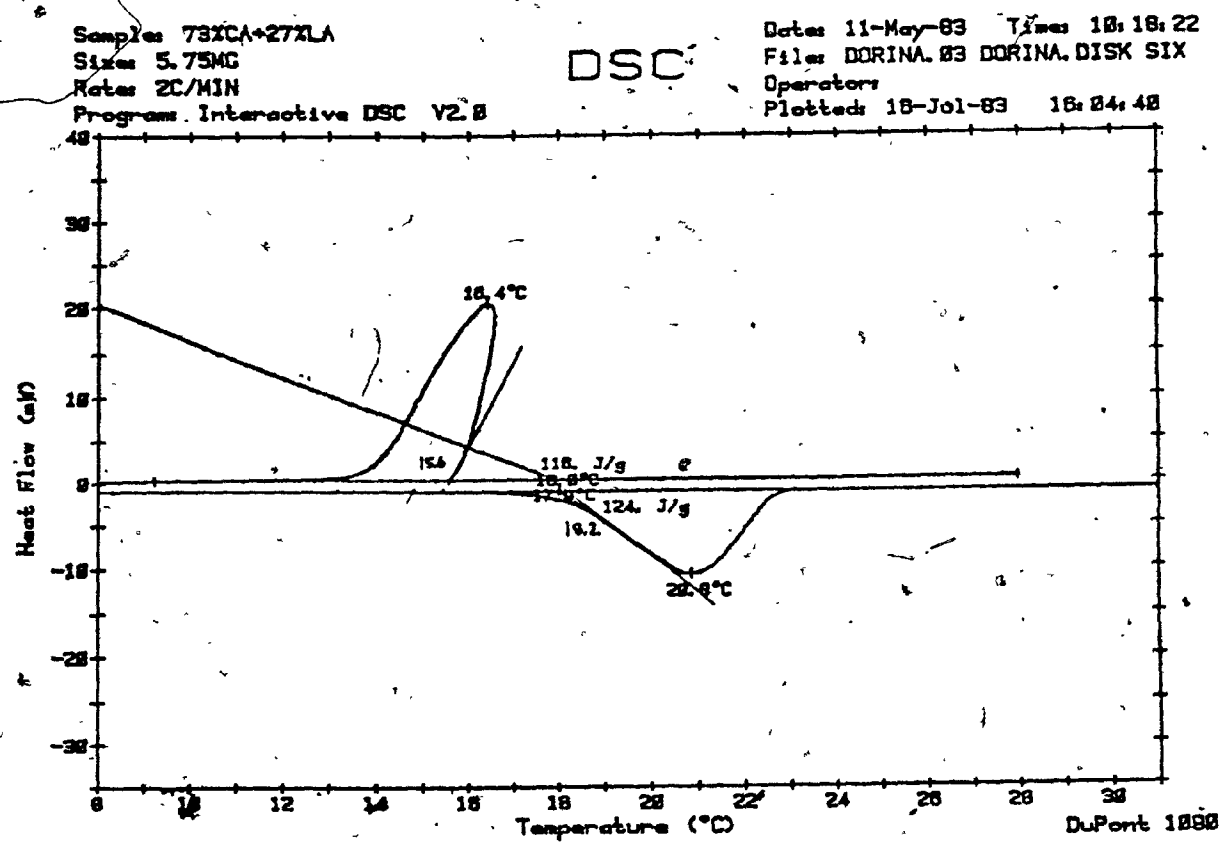

Fig. T-33. Thermogram of 73 mole % capric : 27 mole % lauric.

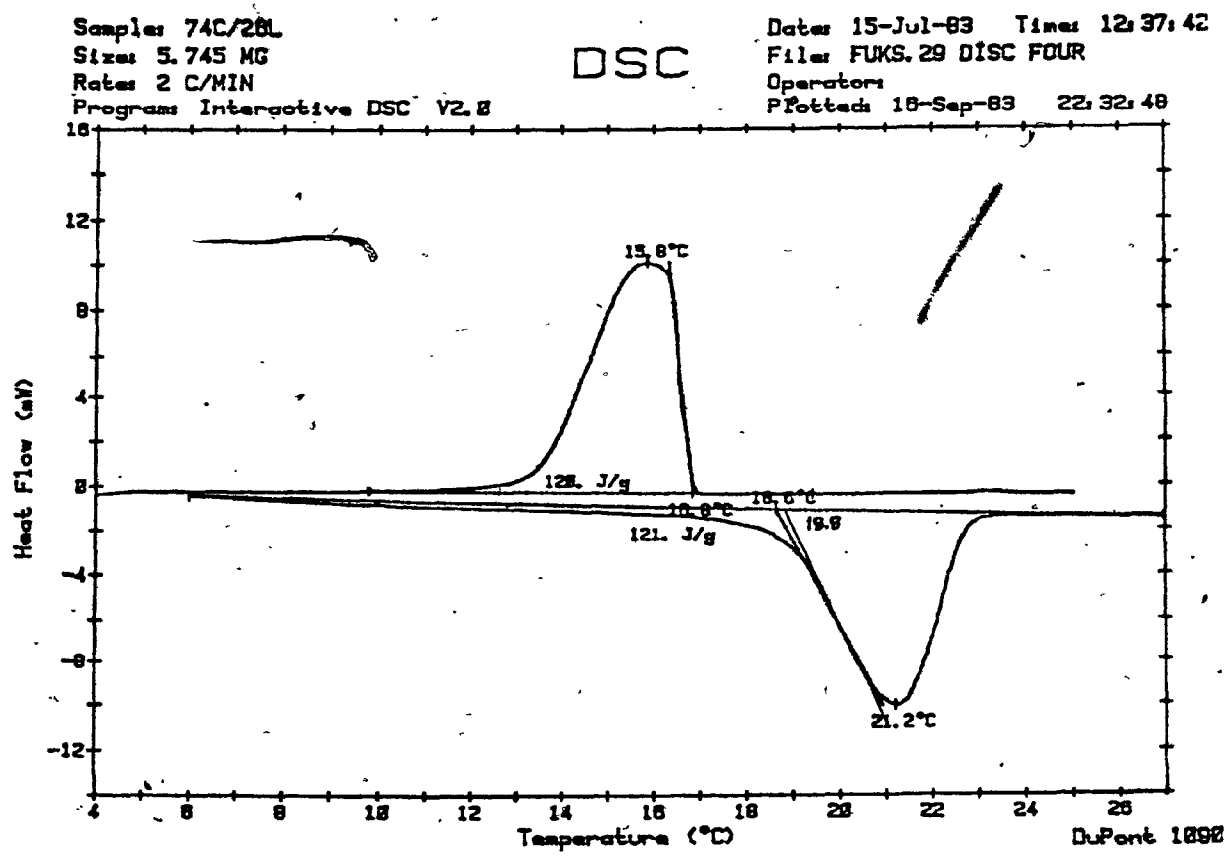

Fig. T-34. Thermogram of 74 mole % capric : 26 mole % lauric.

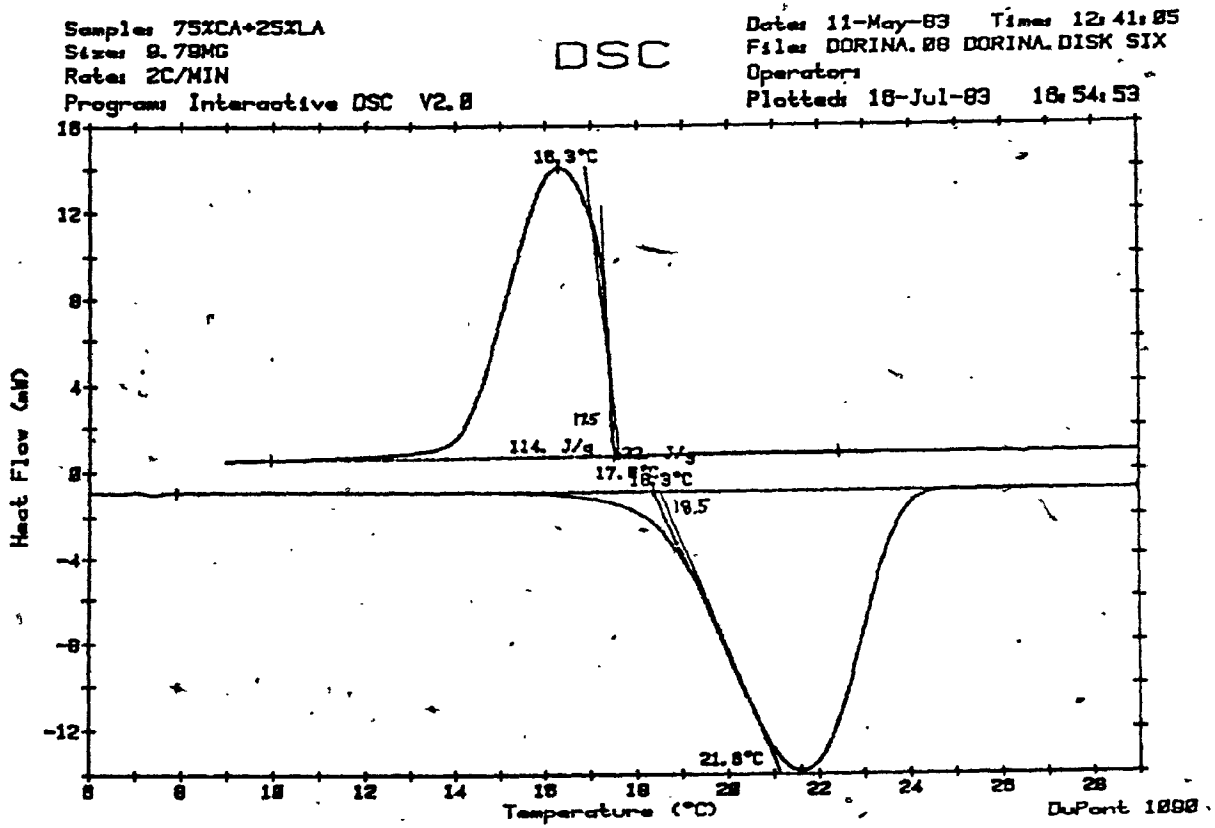

Fig. T-35. Thermogram of 75 mole % capric + 25 mole % lauric.

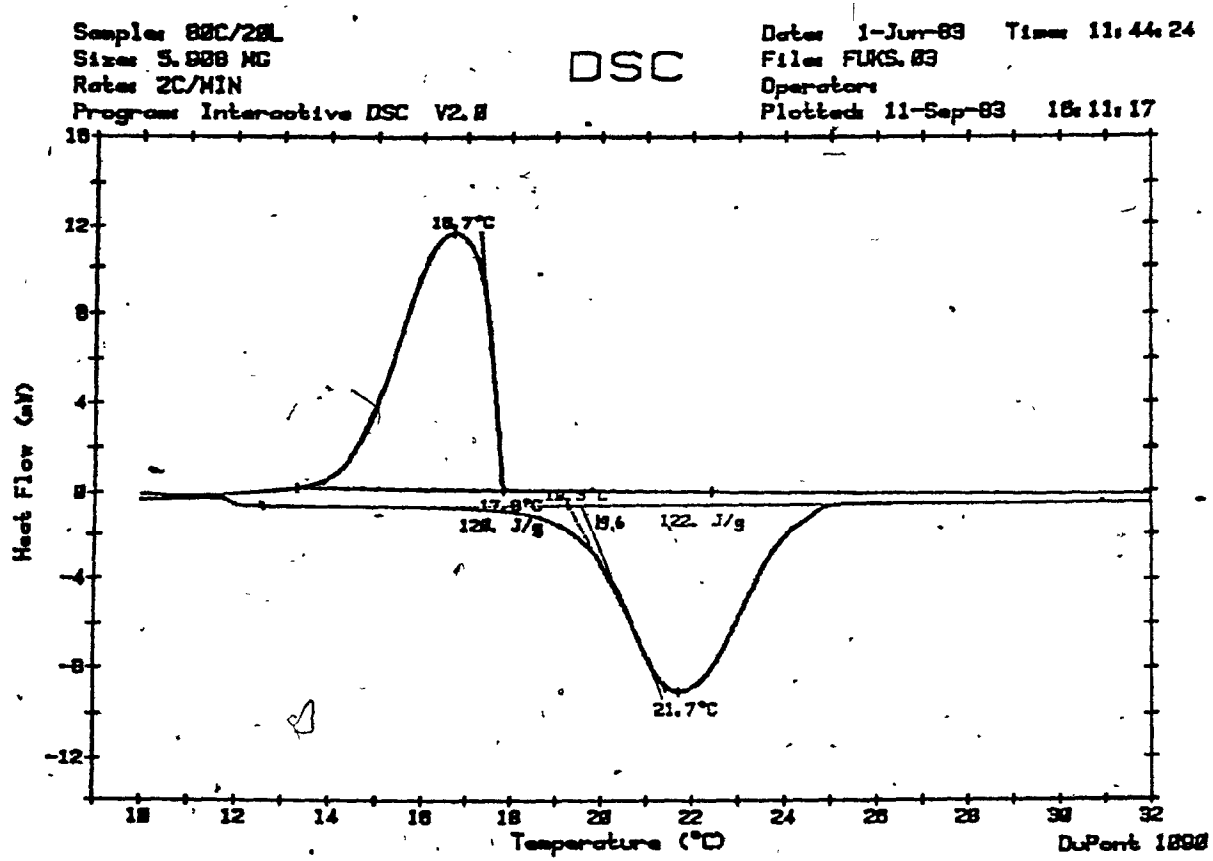

Fig. T-36. Thermogram of 80 mole % capric : 20 mole % lauric.

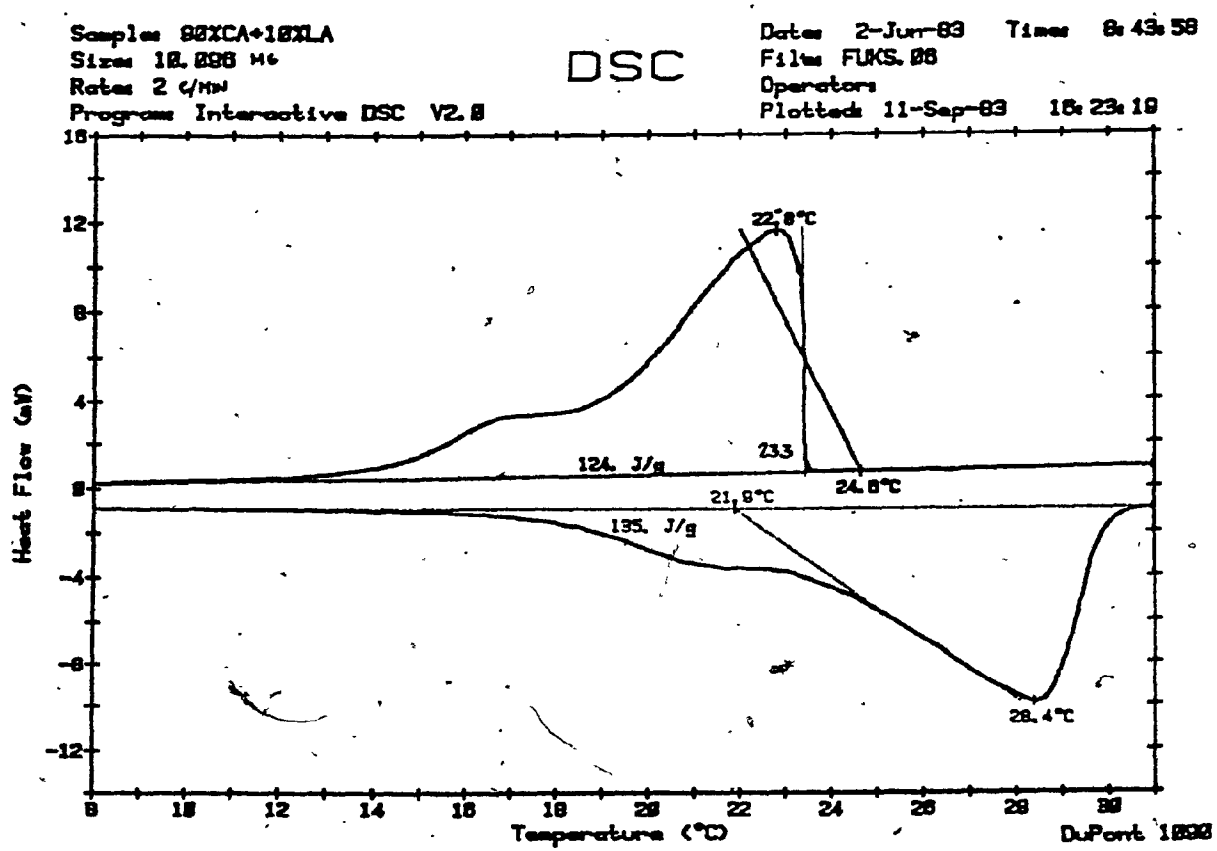

Fig. T-37. Thermogram of 90 mole % capric : 10 mole % lauric.

BINARY MIXTURES OF PALMITIC-STEARIC ACIDS

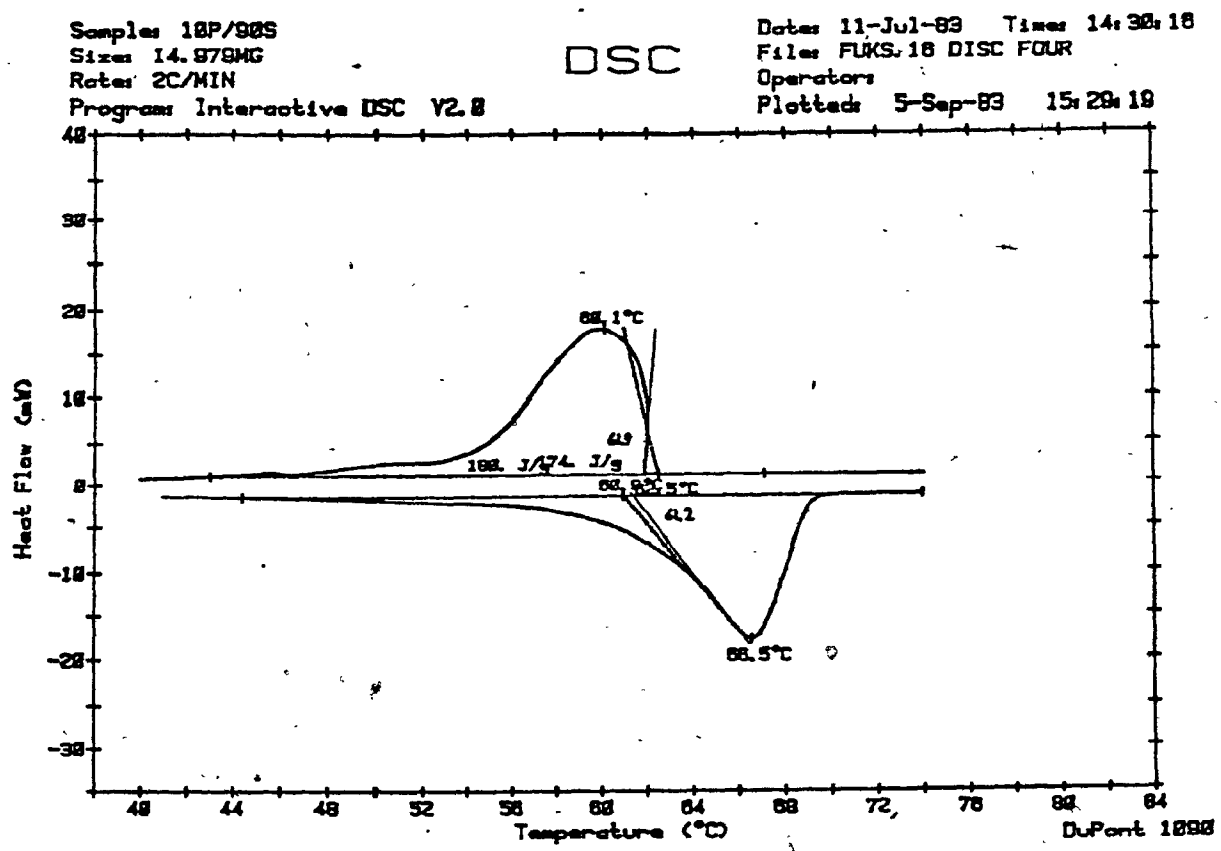

Fig. T-38. Thermogram of 10 mole % palmitic : 90 mole % stearic.

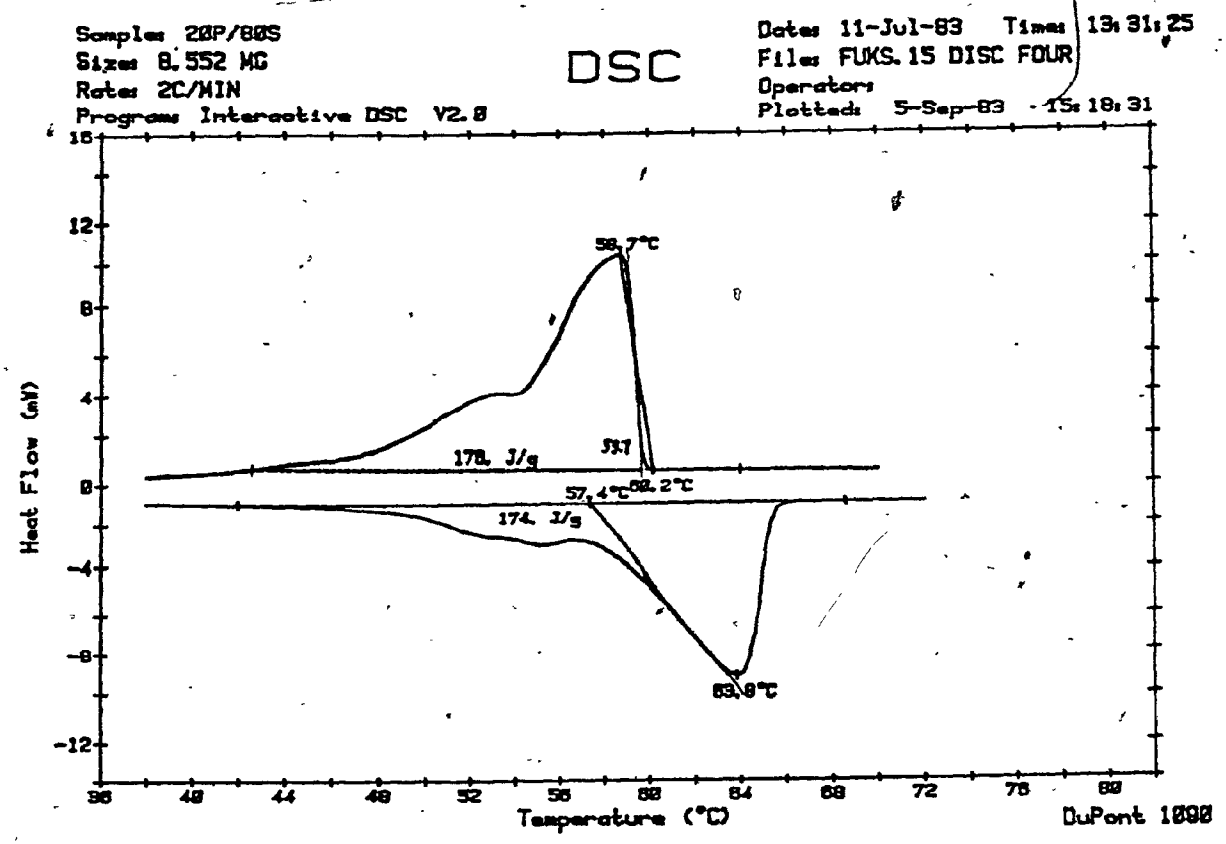

Fig. T-39. Thermogram of 20 mole % palmitic : 80 mole % stearic.

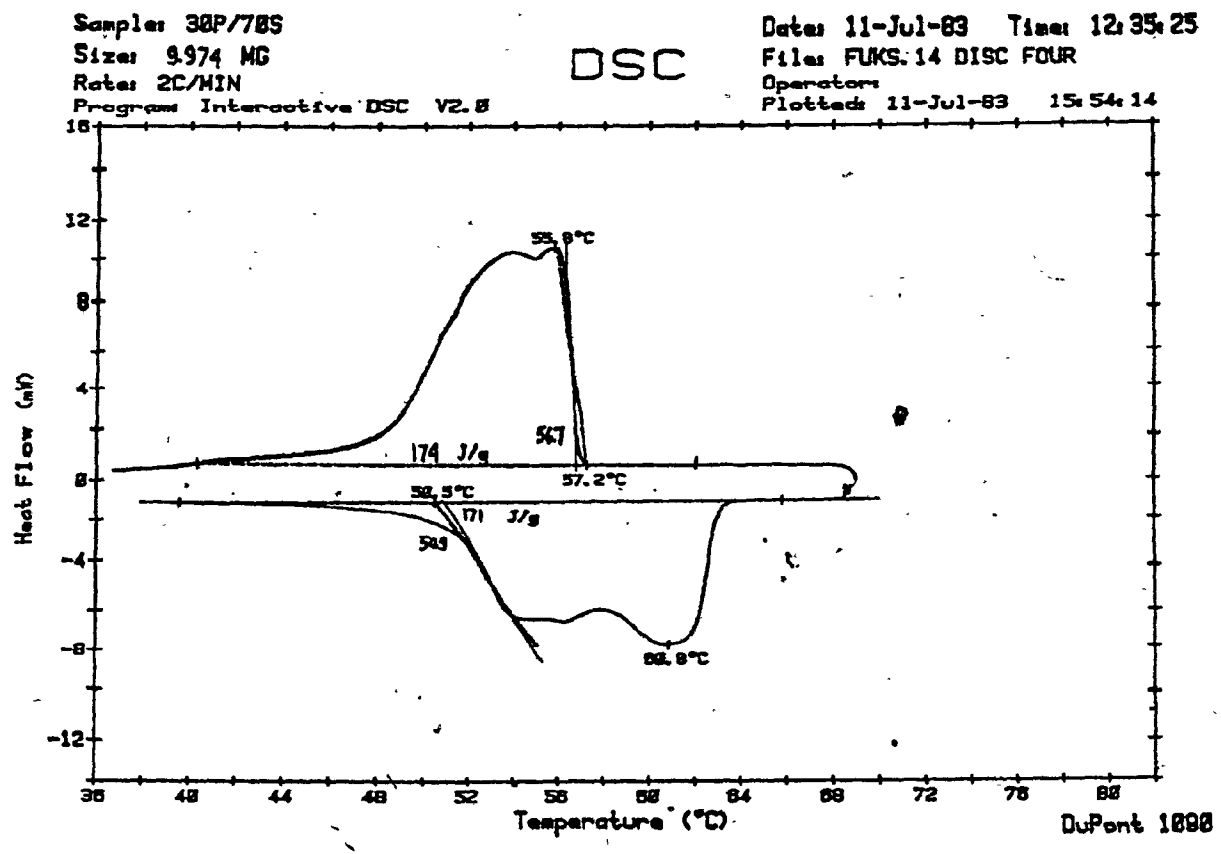

Fig. T-40. Thermogram of 30 mole % palmitic : 70 mole % stearic.

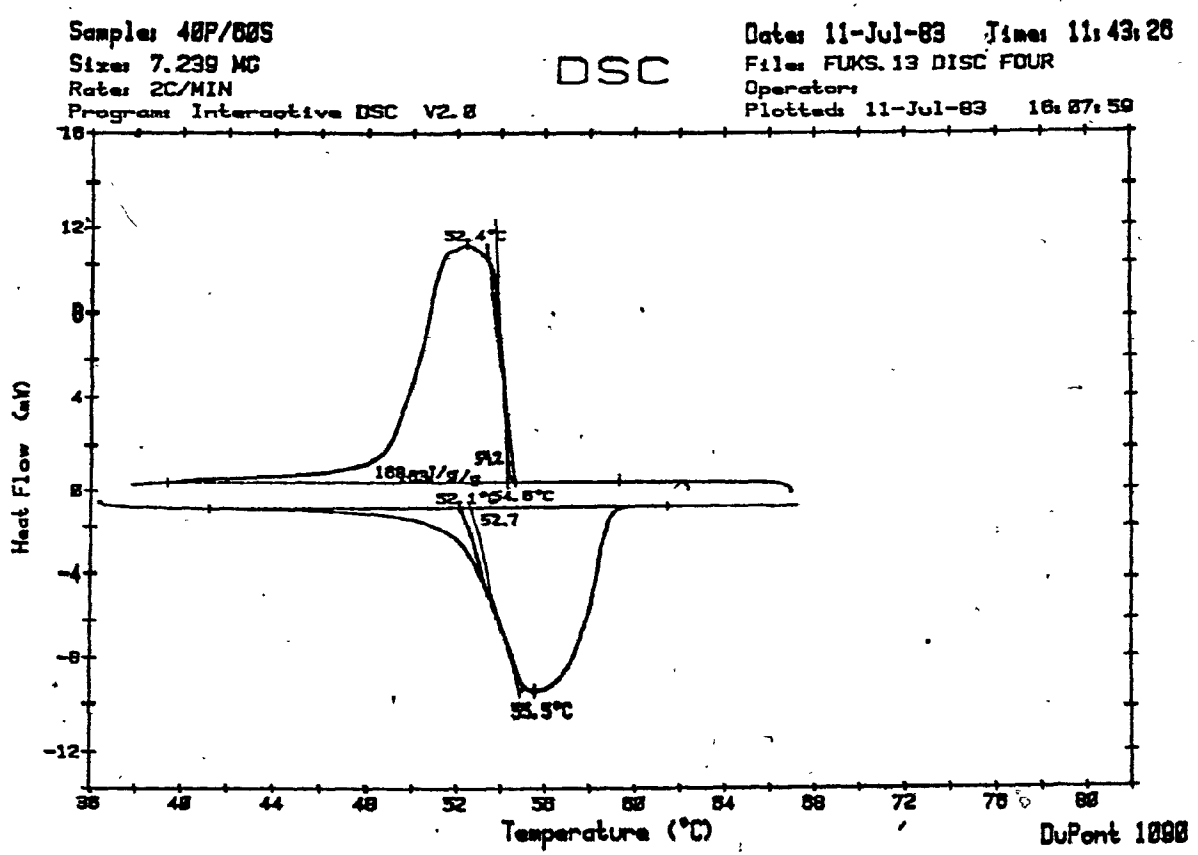

Fig. T-41. Thermogram of 40 mole % palmitic : 60 mole % stearic.

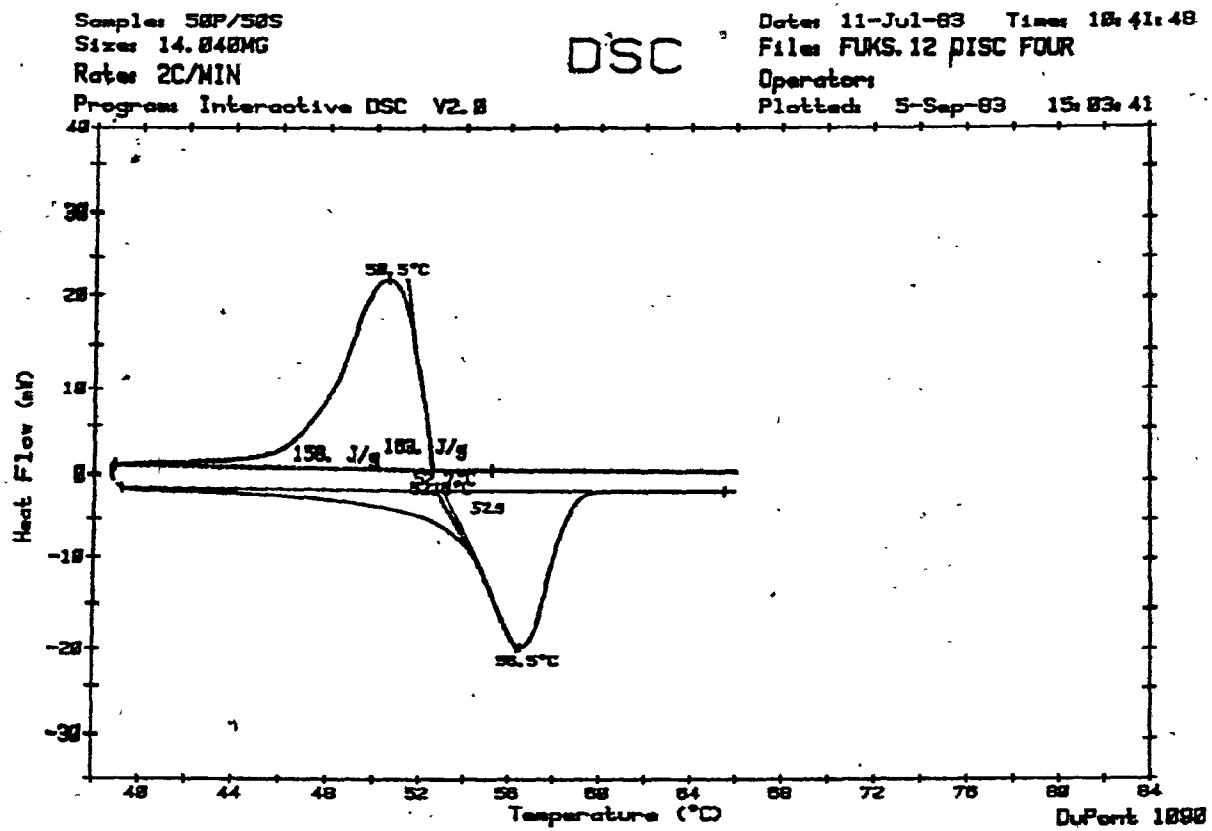

Fig. T-42. Thermogram of 50 mole % palmitic : 50 mole % stearic.

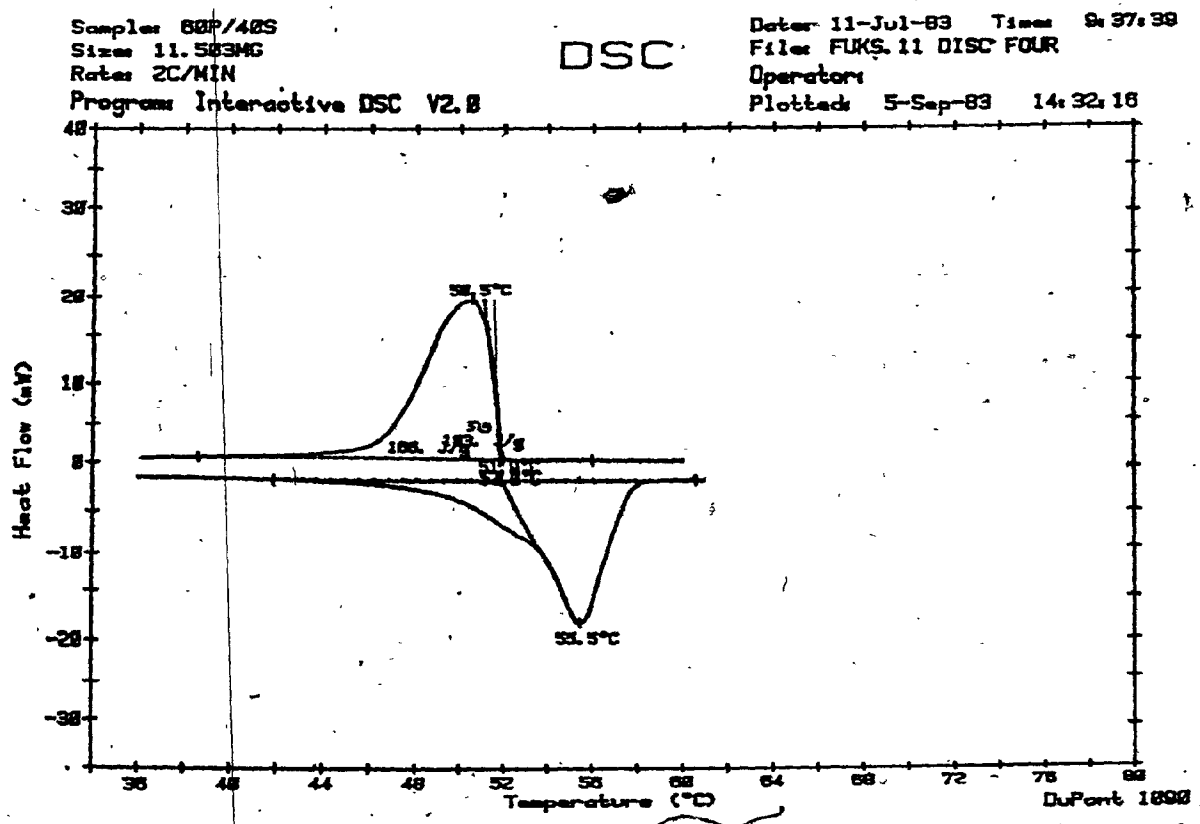

Fig. T-43. Thermogram of 60 mole % palmitic : 40 mole % stearic.

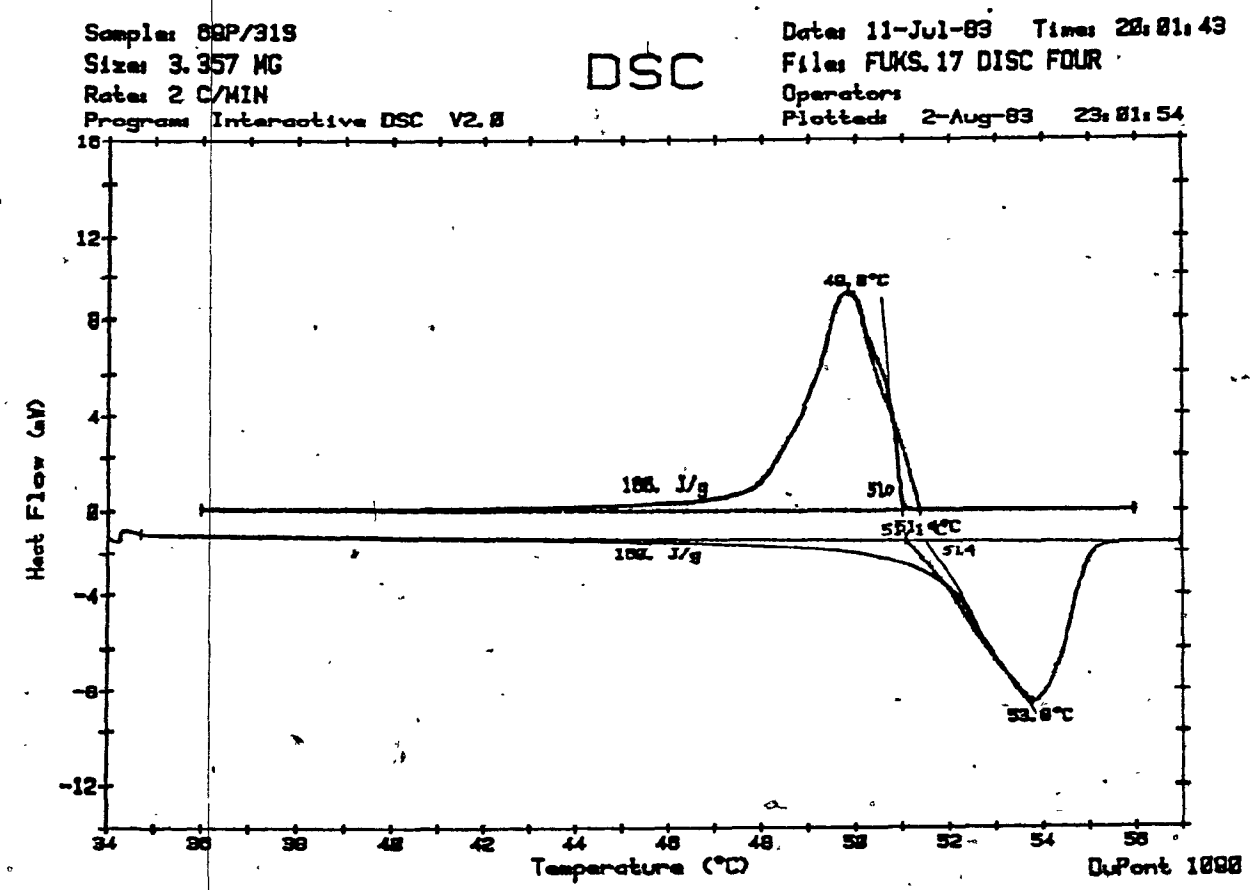

Fig. T-44. Thermogram of 69 mole % palmitic : 31 mole % stearic.

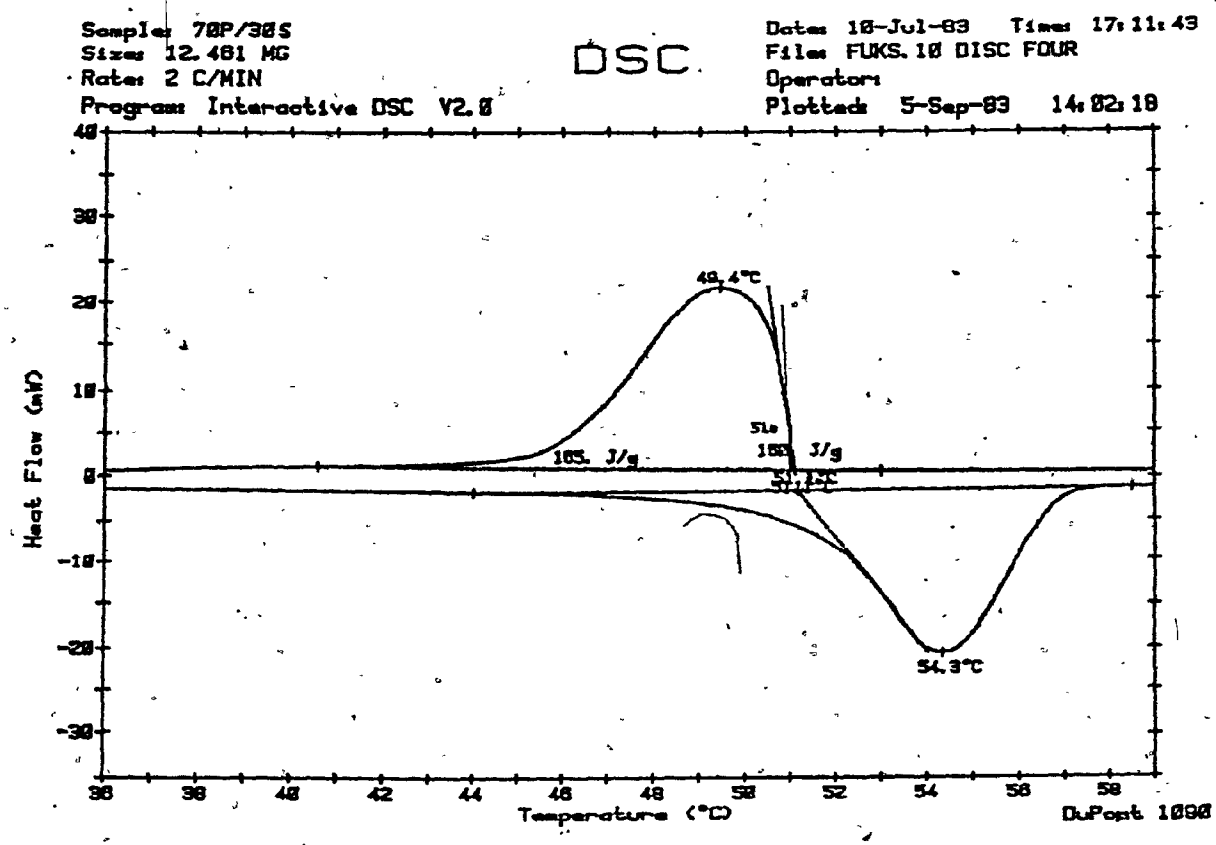

Fig. T-45. Thermogram of 70 mole % palmitic : 30 mole % stearic.

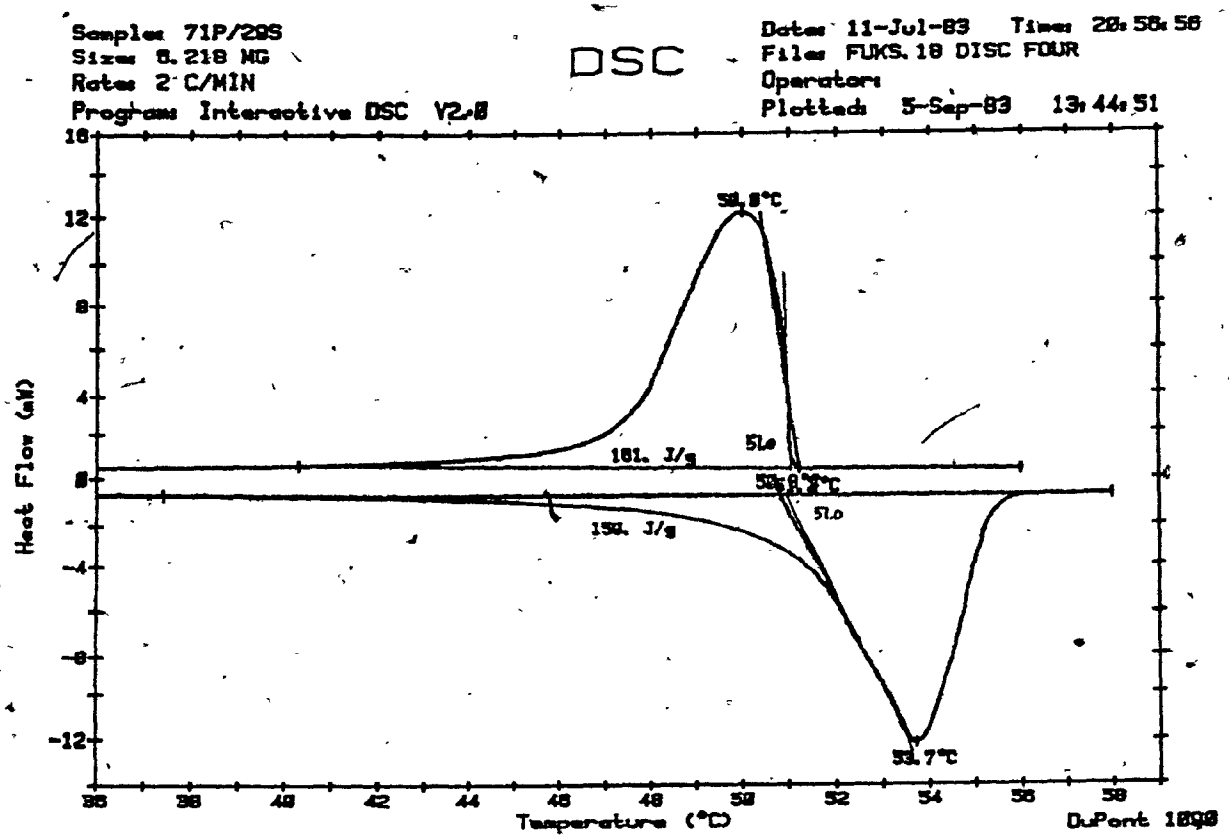

Fig. T-46. Thermogram of 71 mole % palmitic : 29 mole % stearic.

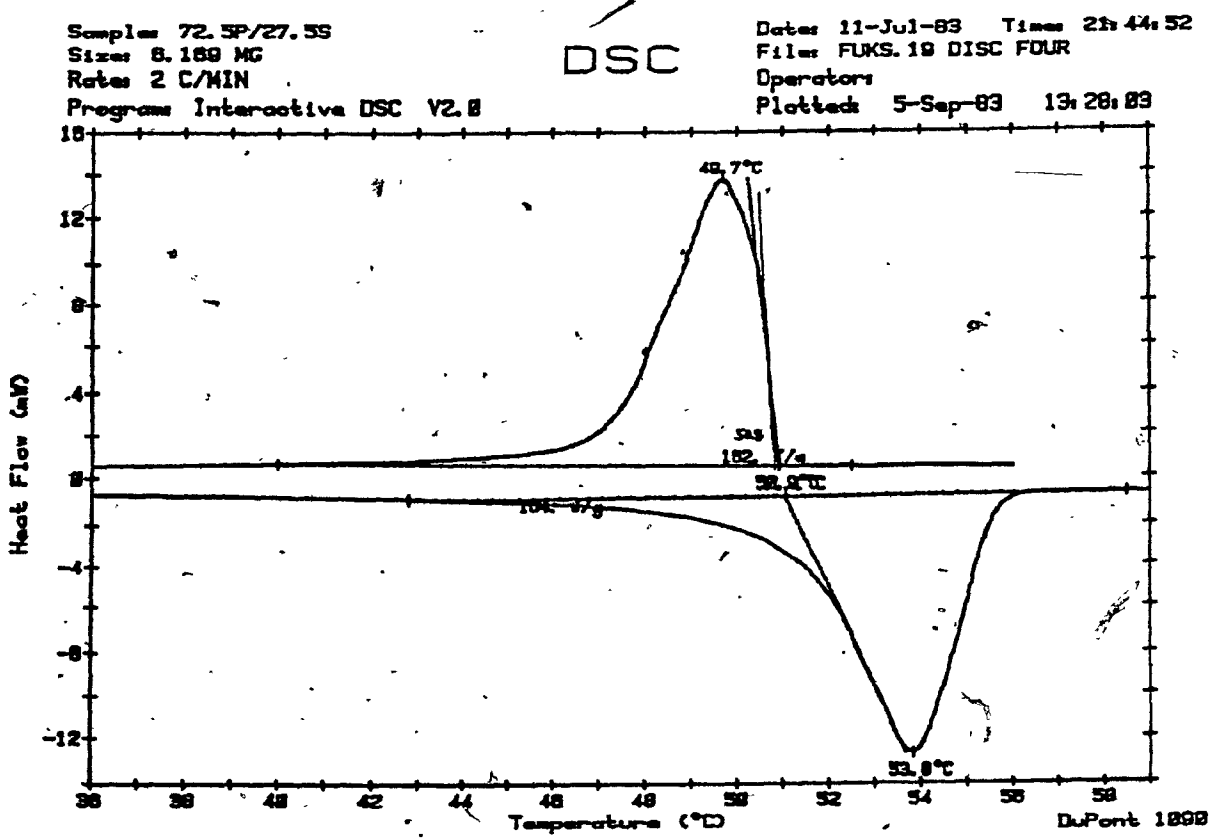

Fig. T-47. Thermogram of 72.5 mole % palmitic : 27.5 mole % stearic.

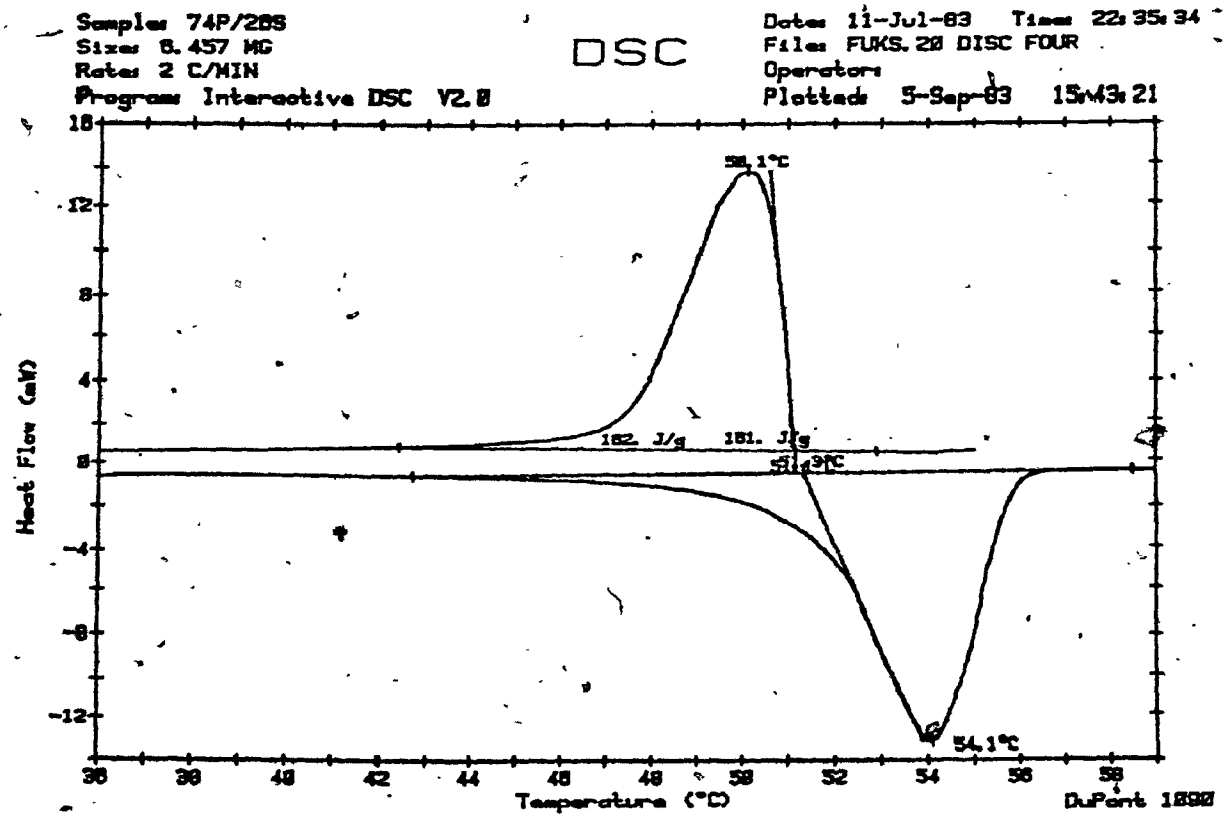

Fig. T-48. Thermogram of 74 mole % palmitic : 26 mole % stearic.

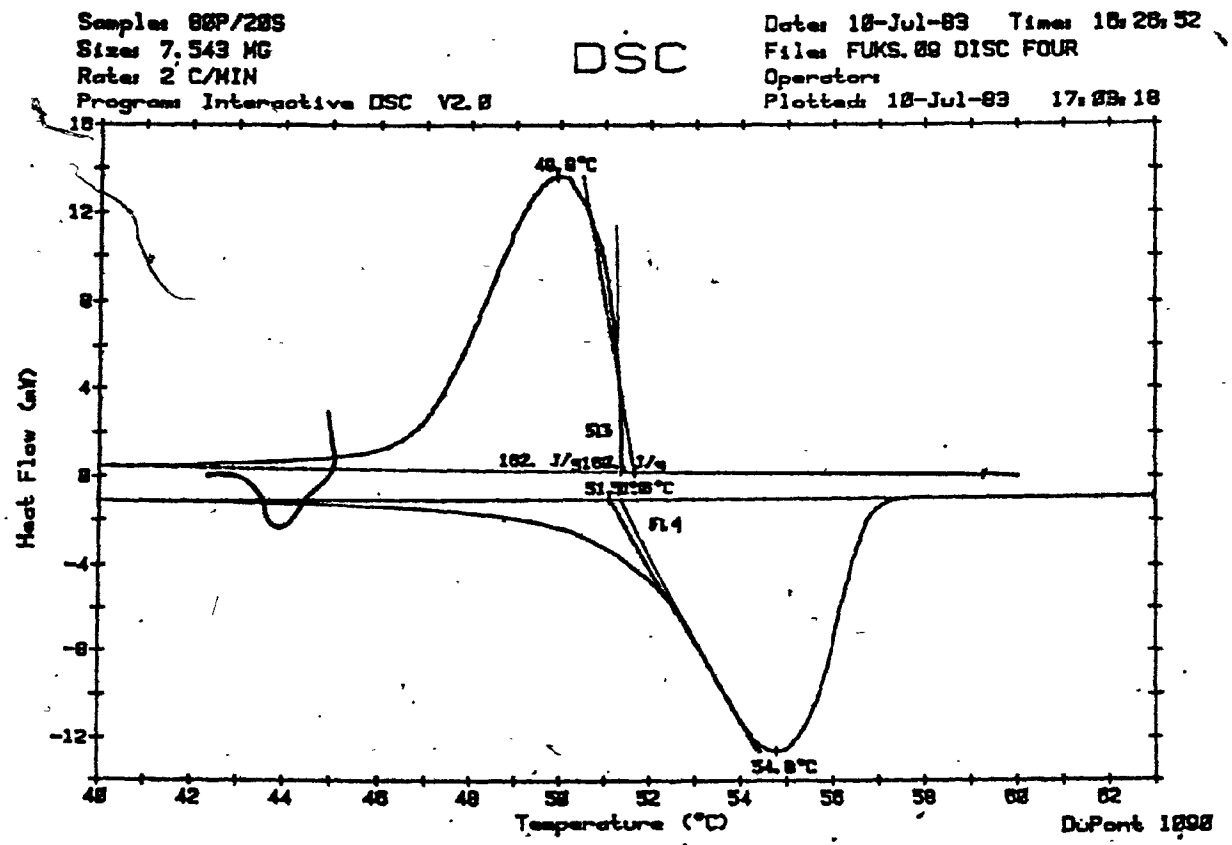

Fig. T-49. Thermogram of 80 mole % palmitic : 20 mole % stearic.

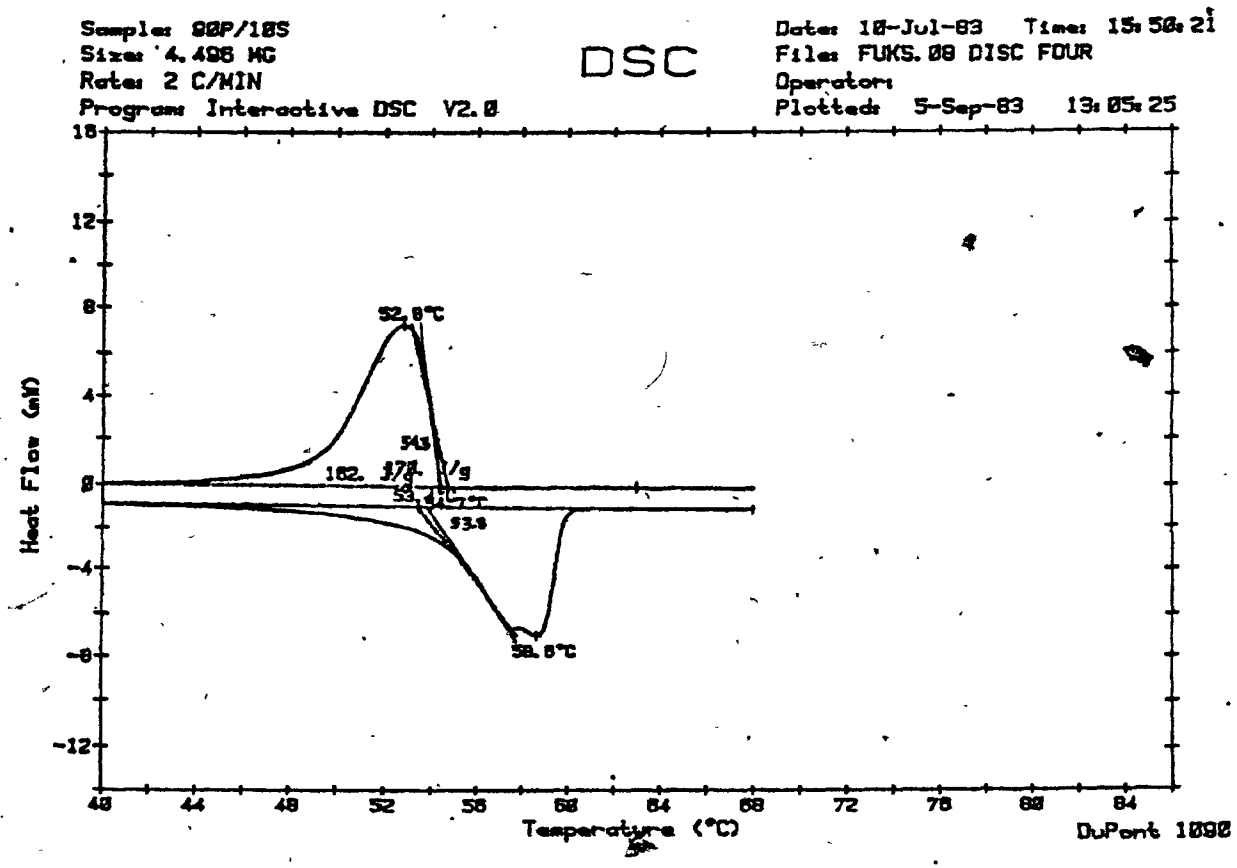

Fig. T-50. Thermogram of 90 mole % palmitic : 10 mole % stearic.

BINARY MIXTURES OF LAURIC-STEARIC ACIDS

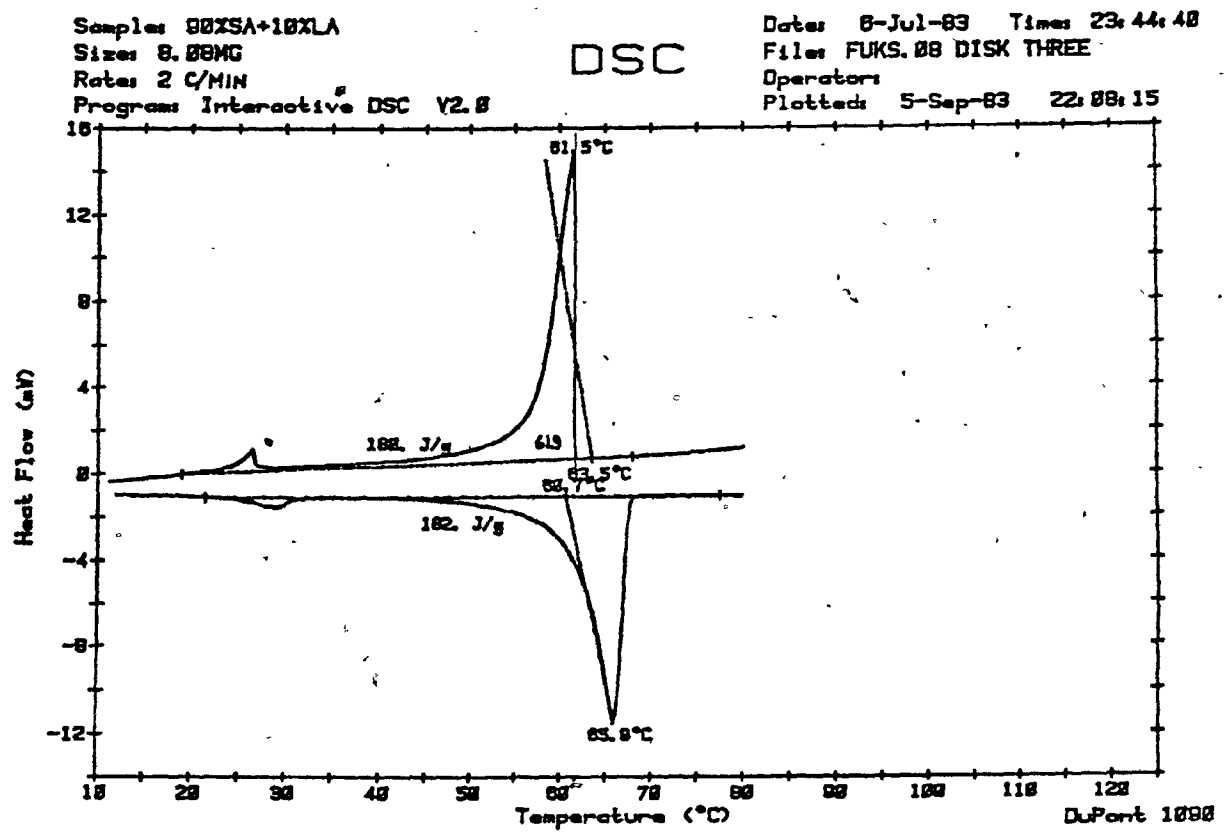

Fig. T-51. Thermogram of 10 mole % lauric : 90 mole % stearic.

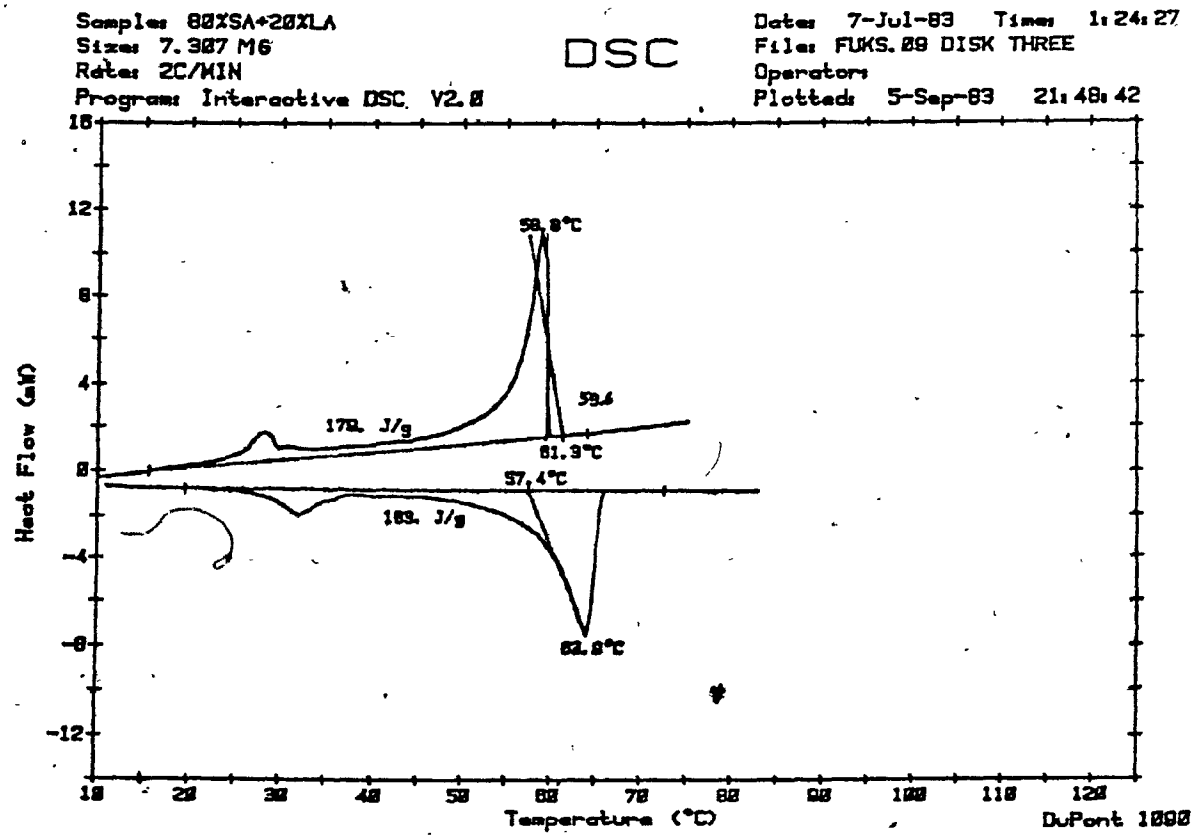

Fig. T-52. Thermogram of 20 mole % lauric : 80 mole % stearic.

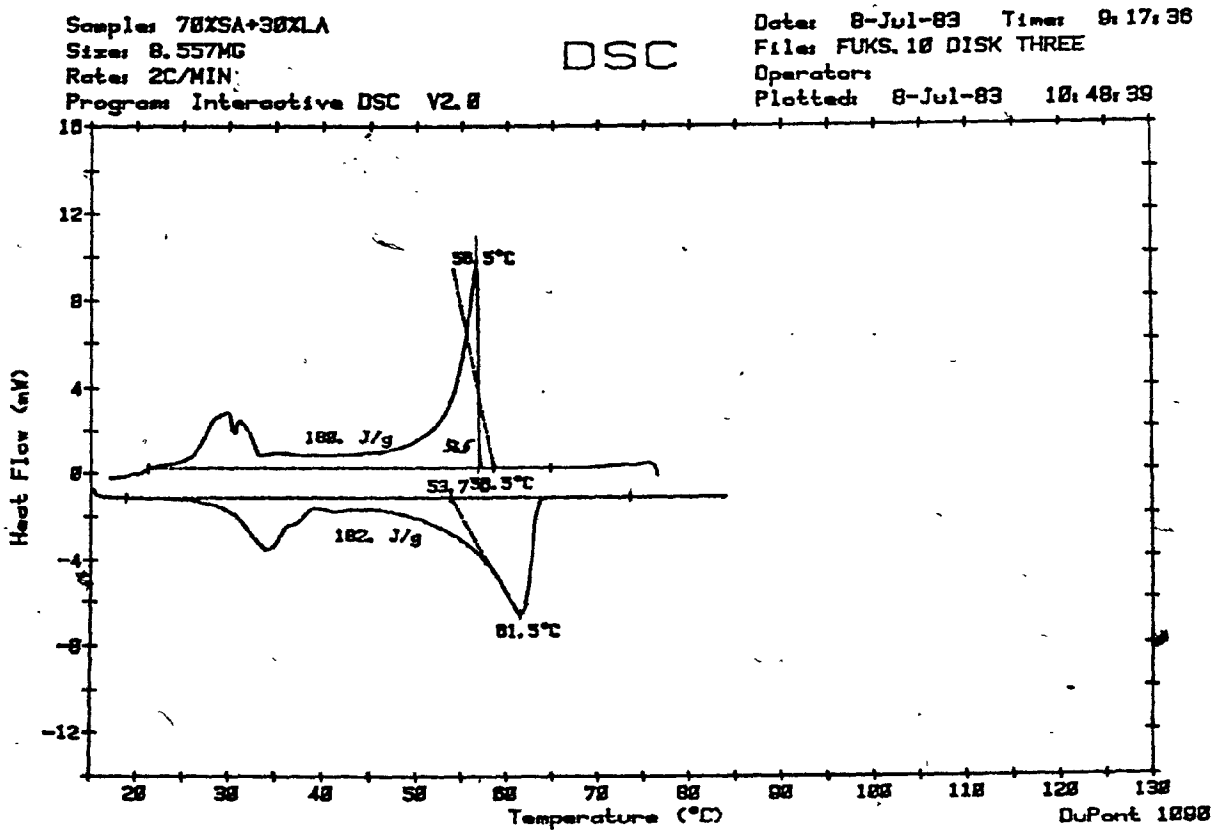

Fig. T-53. Thermogram of 30 mole % lauric : 70 mole % stearic.

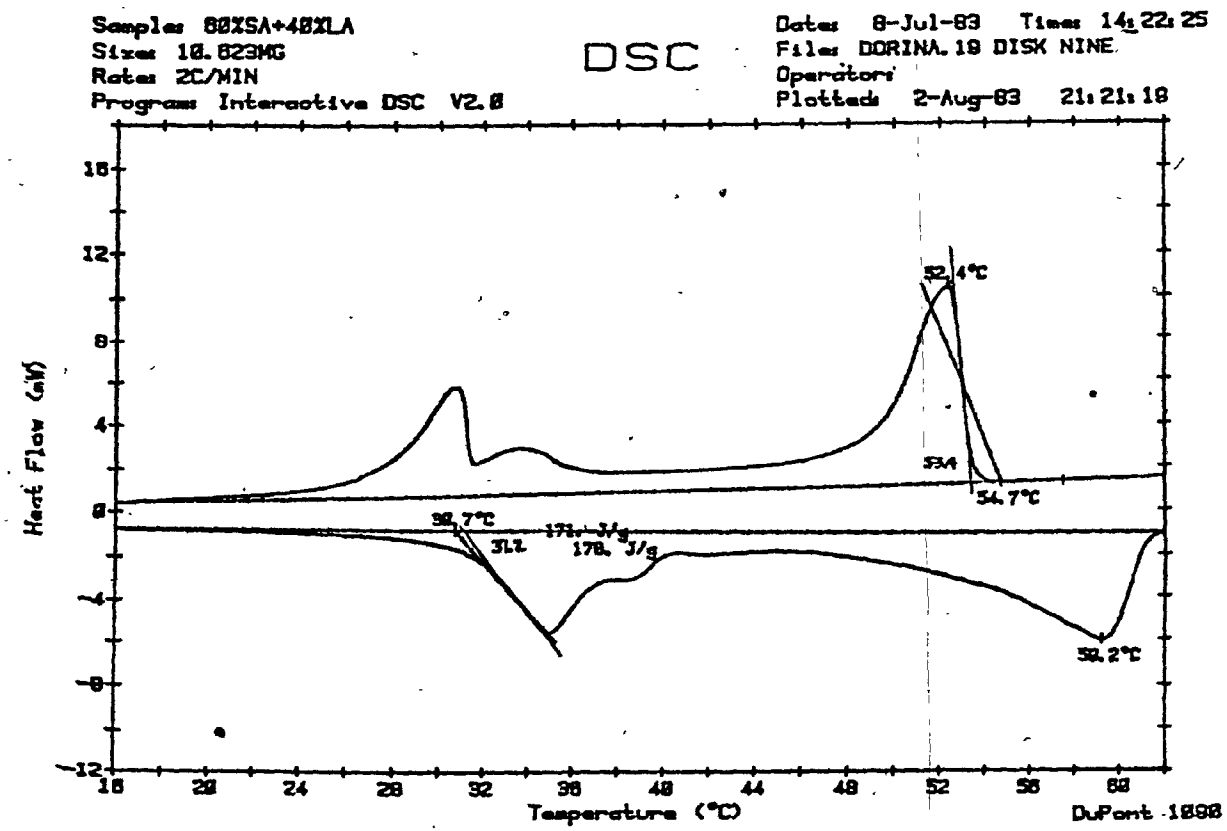

Fig. T-54. Thermogram of 40 mole % lauric : 60 mole % stearic.

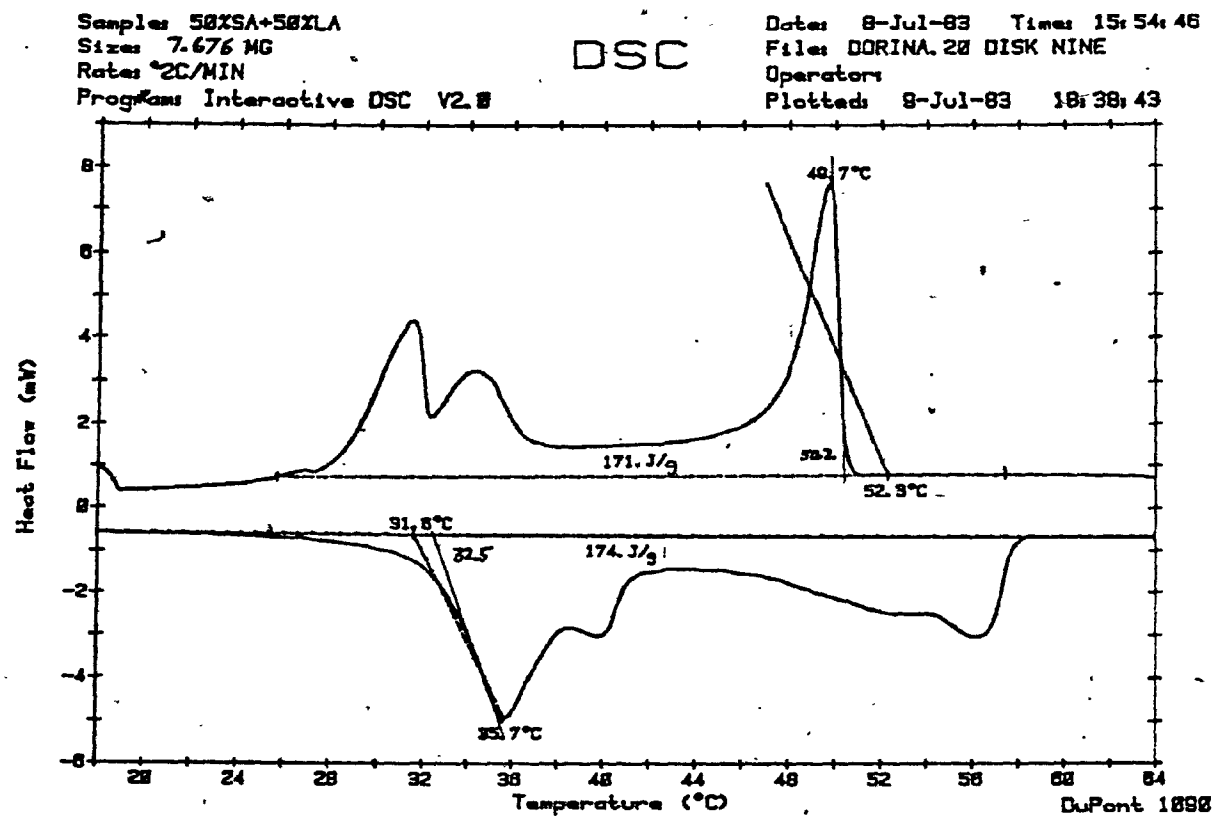

Fig. T-55. Thermogram of 50 mole % lauric : 50 mole % stearic.

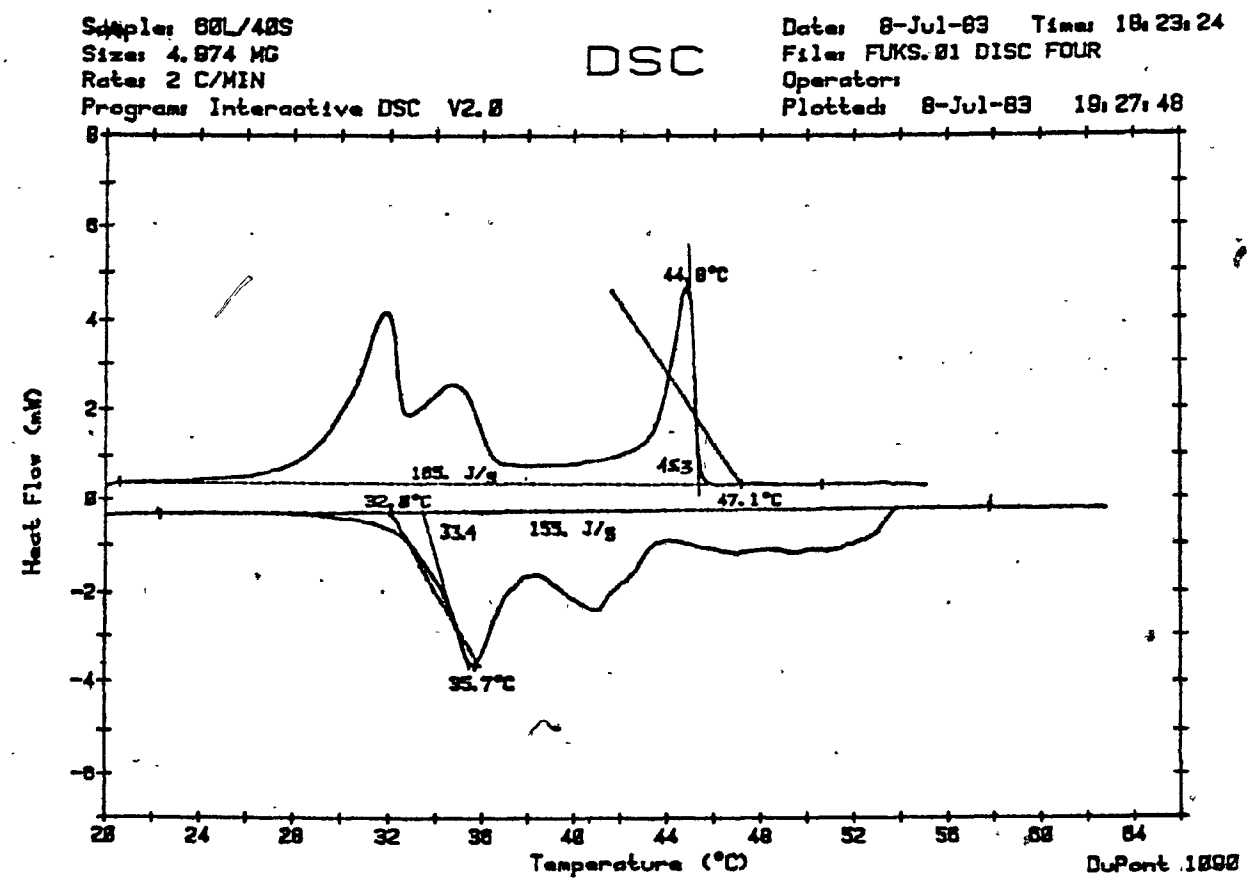

Fig. T-56. Thermogram of 60 mole % lauric : 40 mole % stearic.

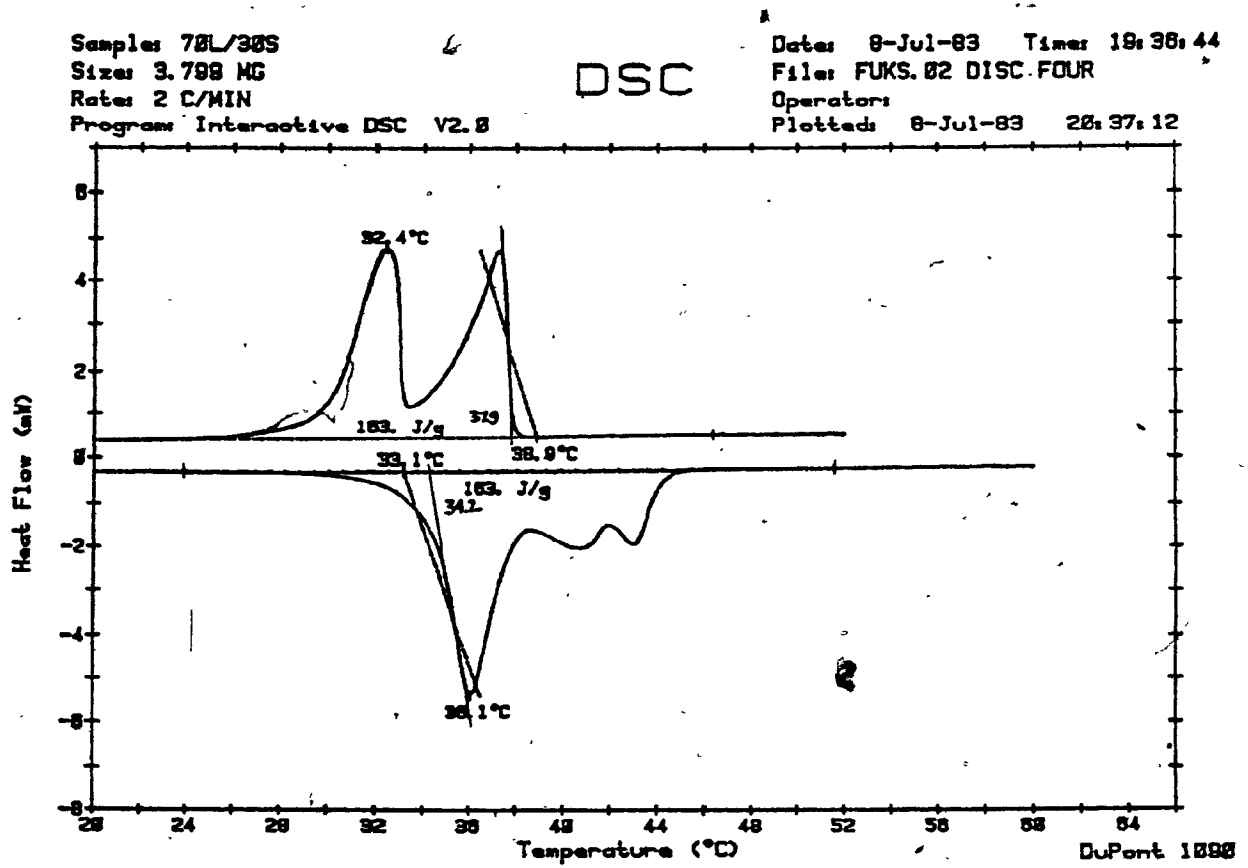

Fig. T-57. Thermogram of 70 mole % lauric : 30 mole % stearic.

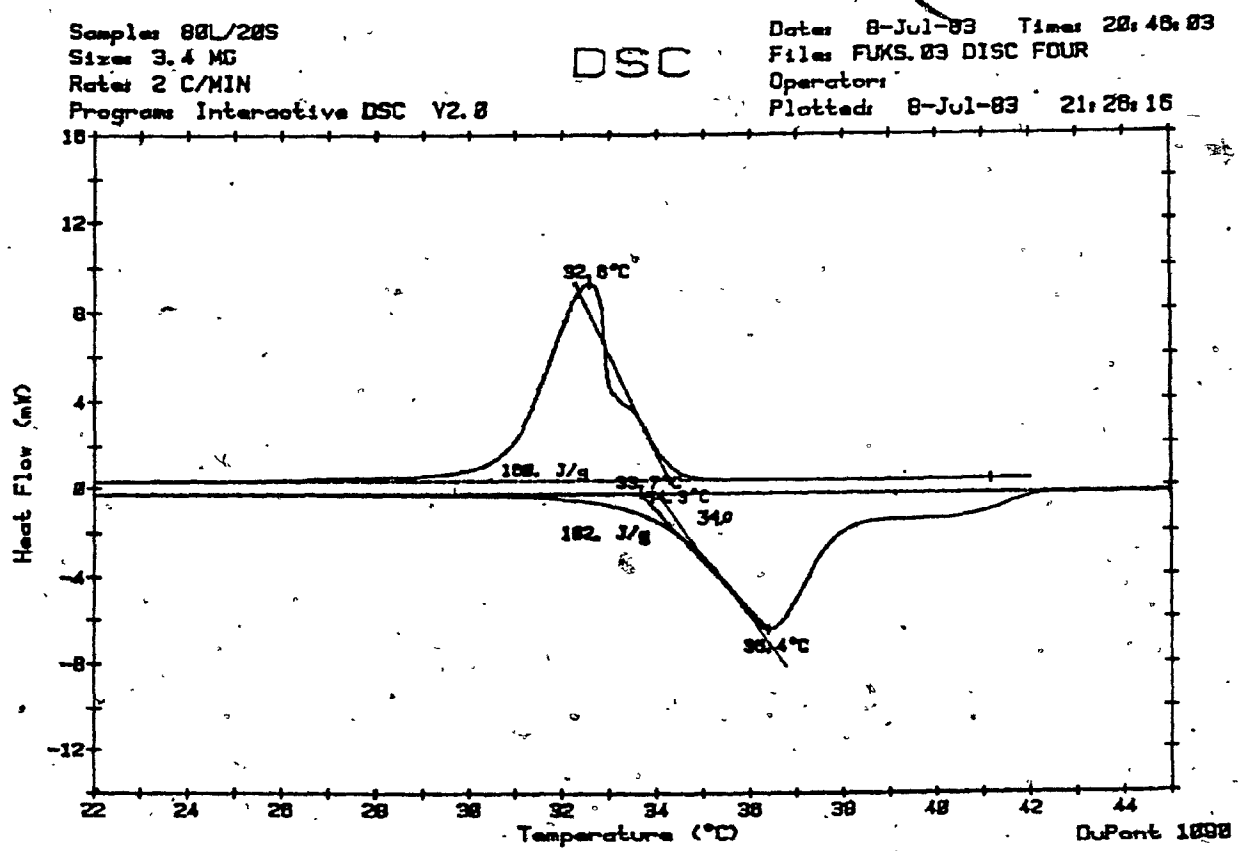

Fig. T-58. Thermogram of 80 mole % lauric : 20 mole % stearic.

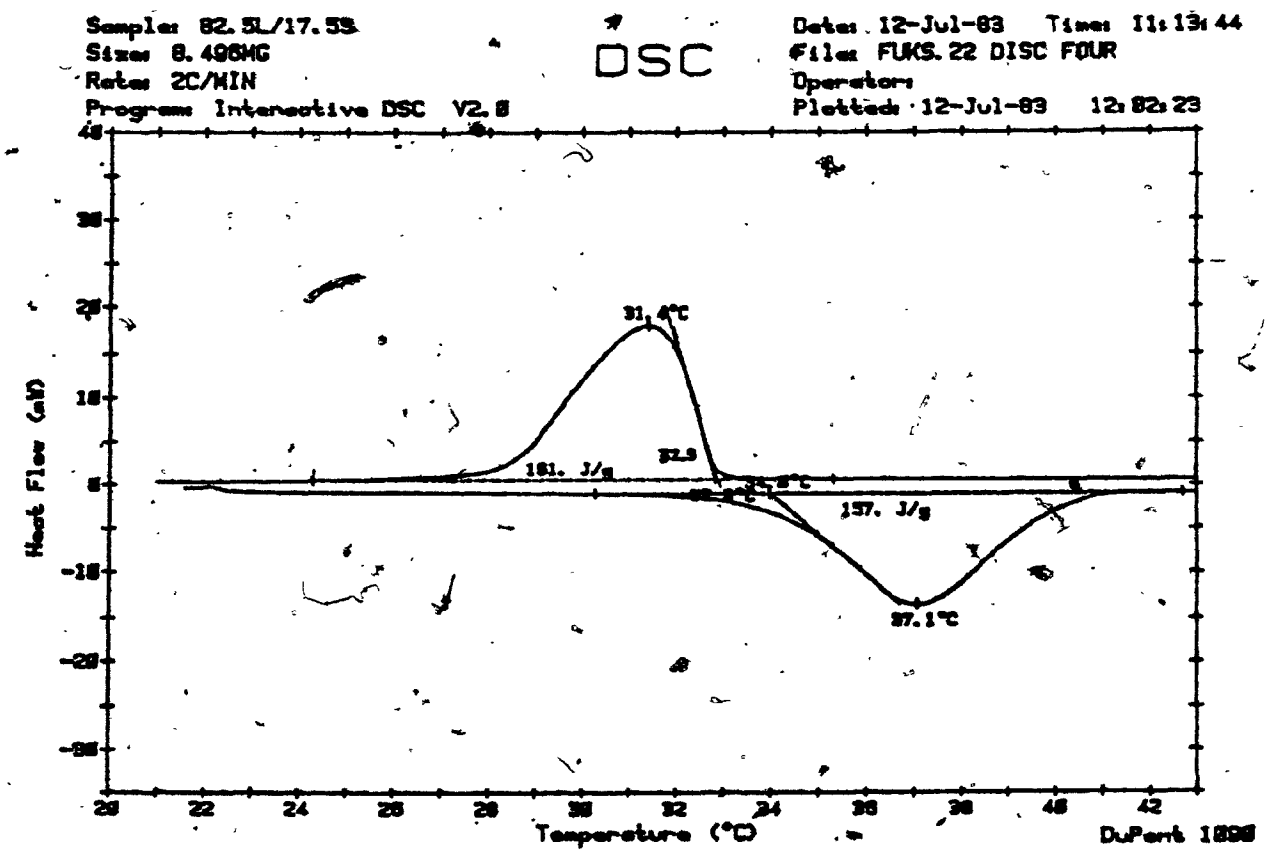

Fig.T-59. Thermogram of 82.5 mole % lauric : 17.5 mole % stearic.

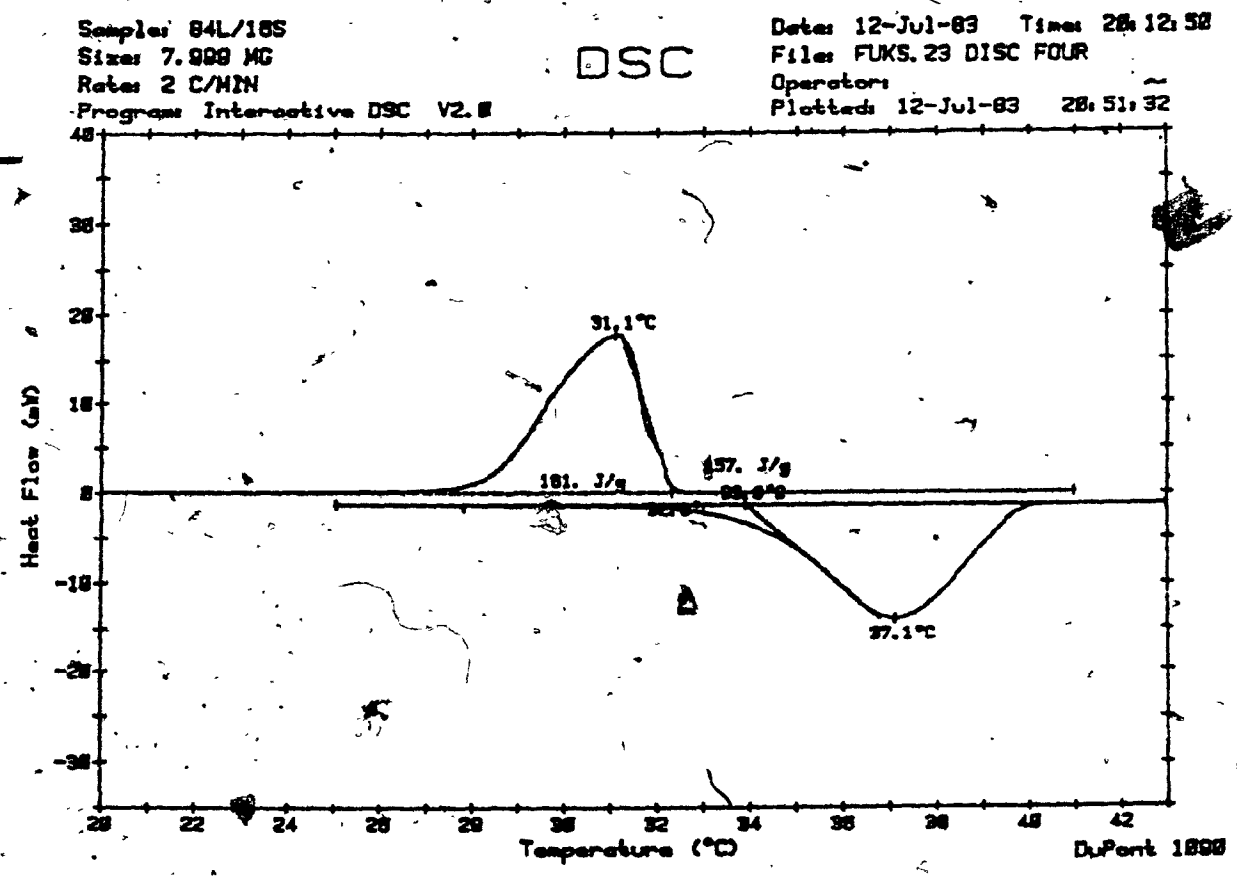

Fig. T-60. Thermogram of 84 mole % lauric, 16 mole % stearic.

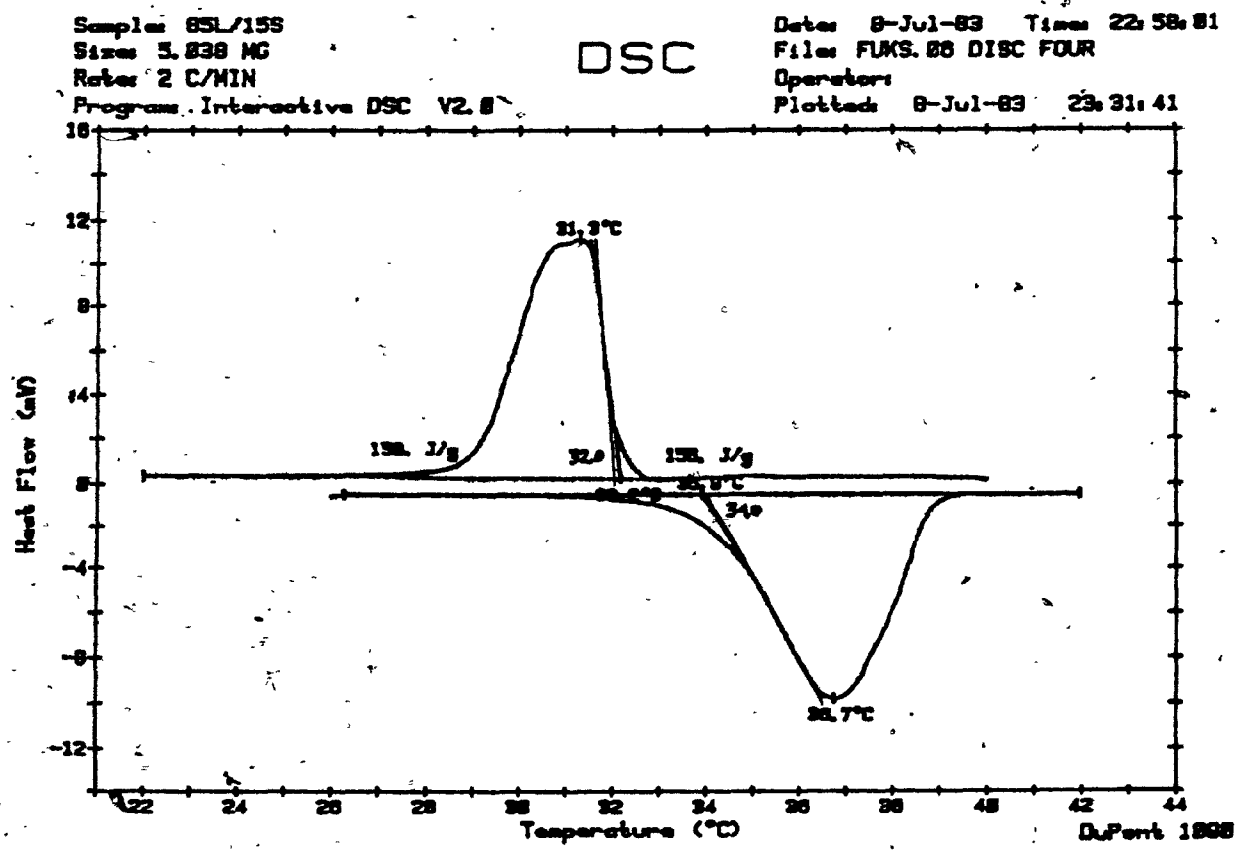

Fig. T-61. Thermogram of 85 mole % lauric : 15 mole % stearic.

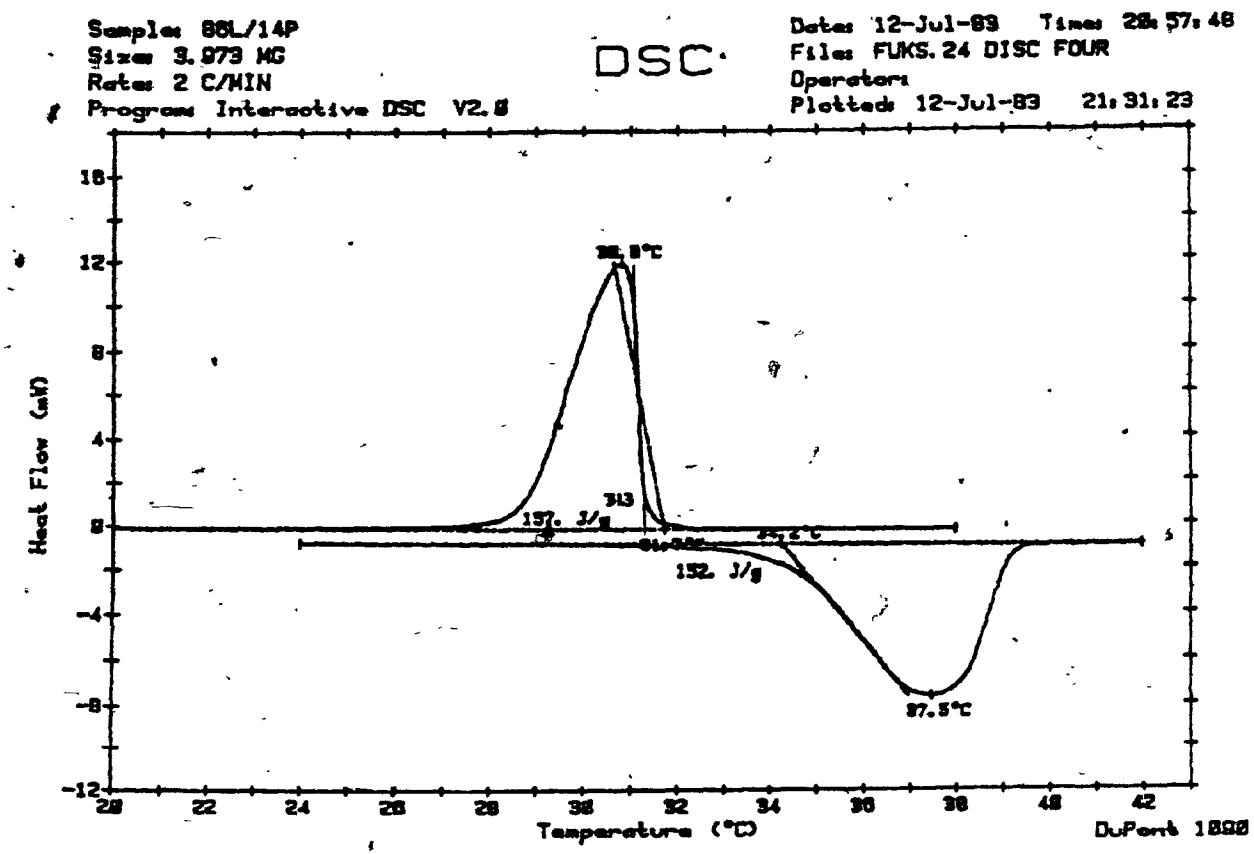

Fig. T-62. Thermogram of 86 mole % lauric : 14 mole % stearic.

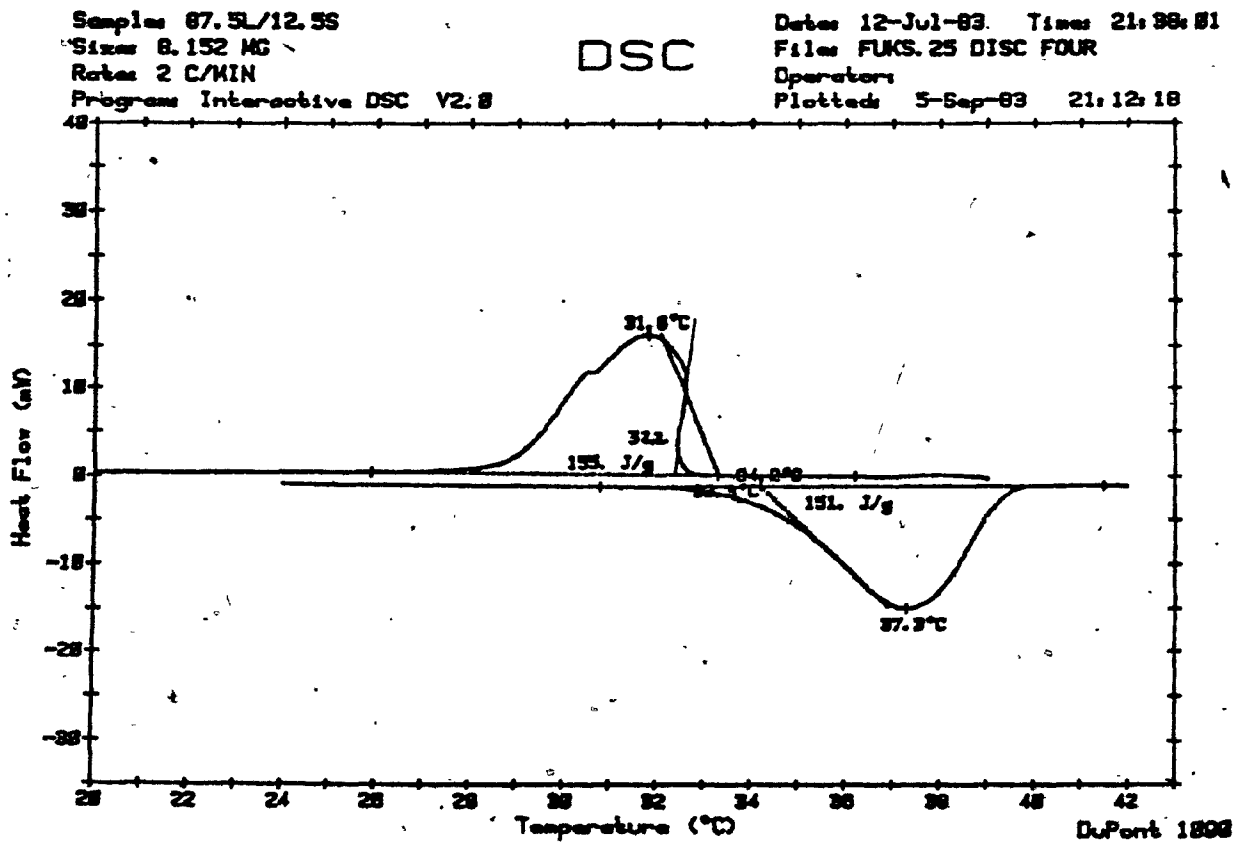

Fig. T-63. Thermogram of 87.5 mole % lauric : 12.5 mole % stearic.

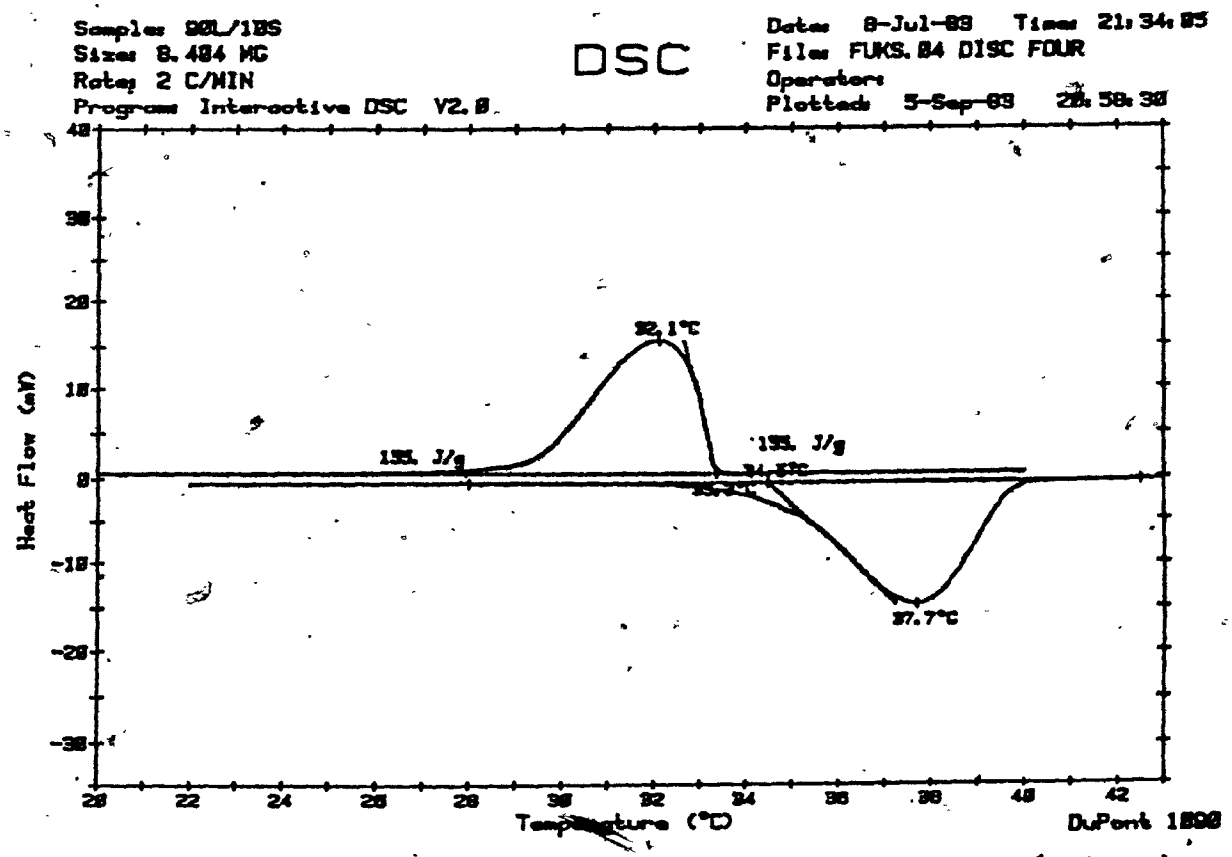

Fig. T-64. Thermogram of 90 mole % lauric : 10 mole % stearic.

BINARY MIXTURES OF LAURIC-PALMITIC ACIDS

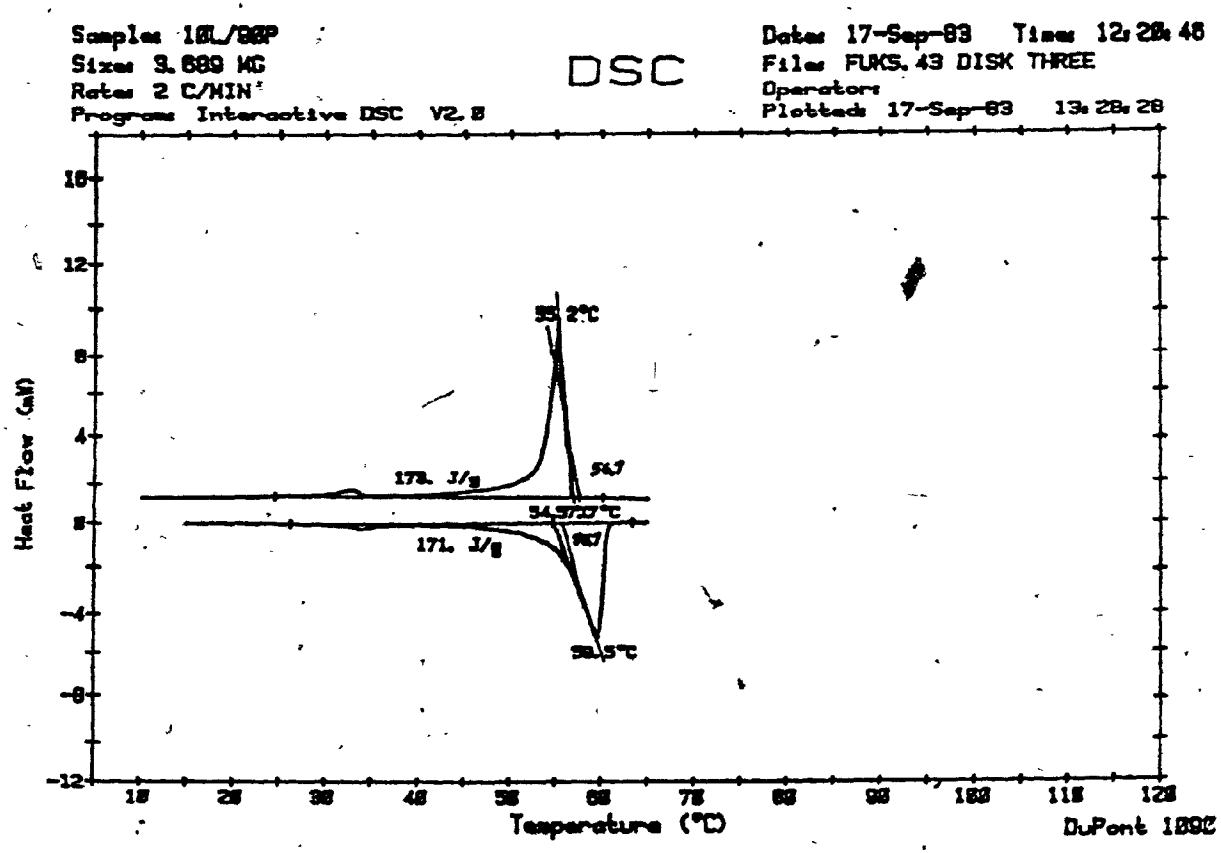

Fig. T-65. Thermogram of 10 mole % lauric : 90 mole % palmitic.

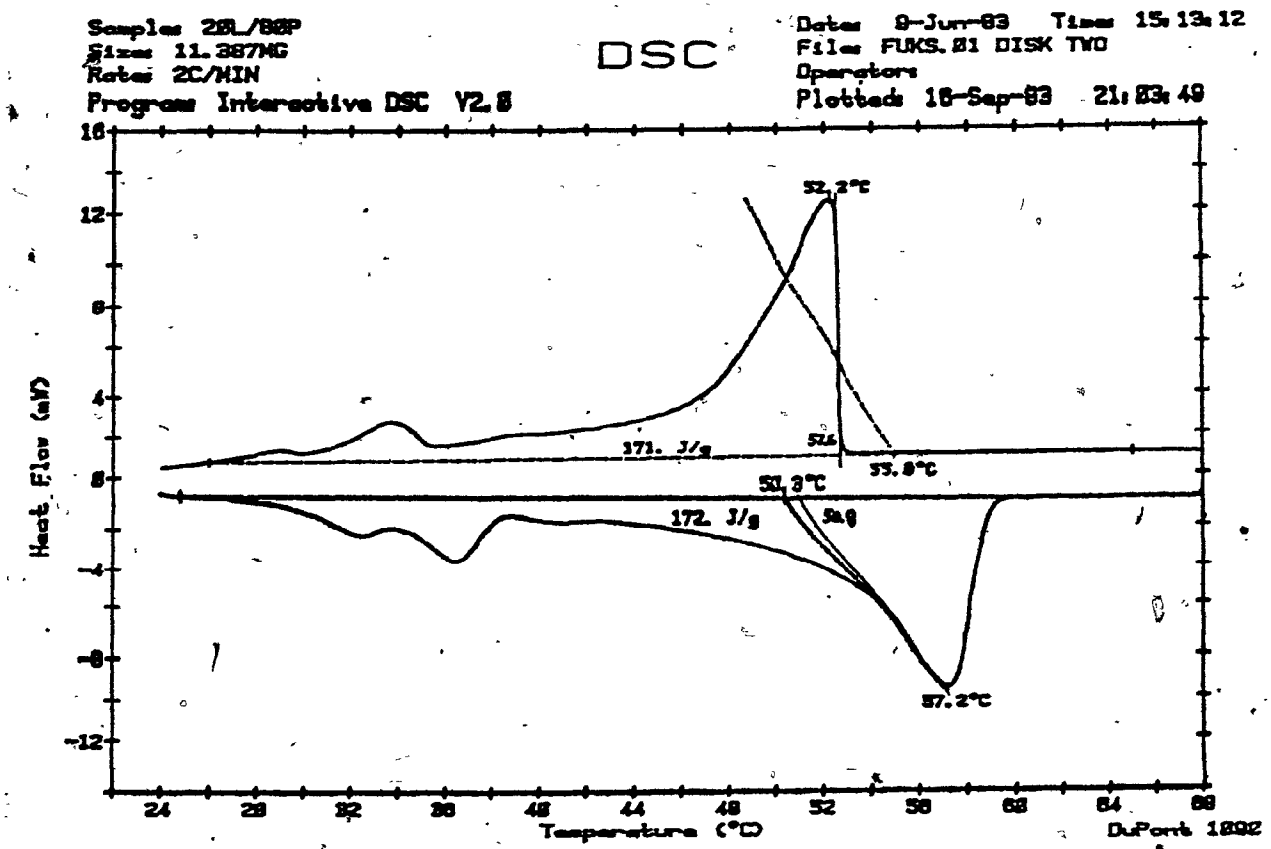

Fig. T-66. Thermogram of 20 mole % lauric : 80 mole % palmitic.

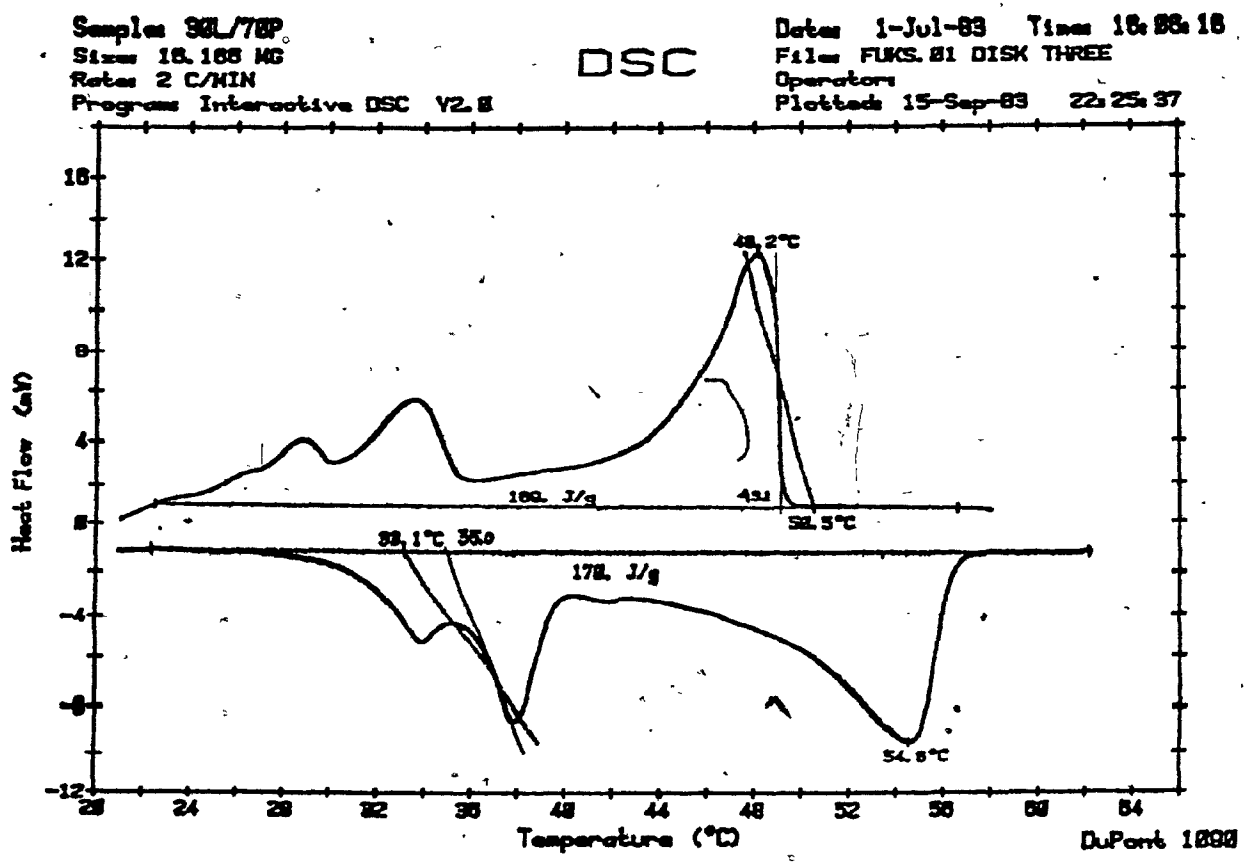

Fig. T-67. Thermogram of 30 mole % lauric : 70 mole % palmitic.

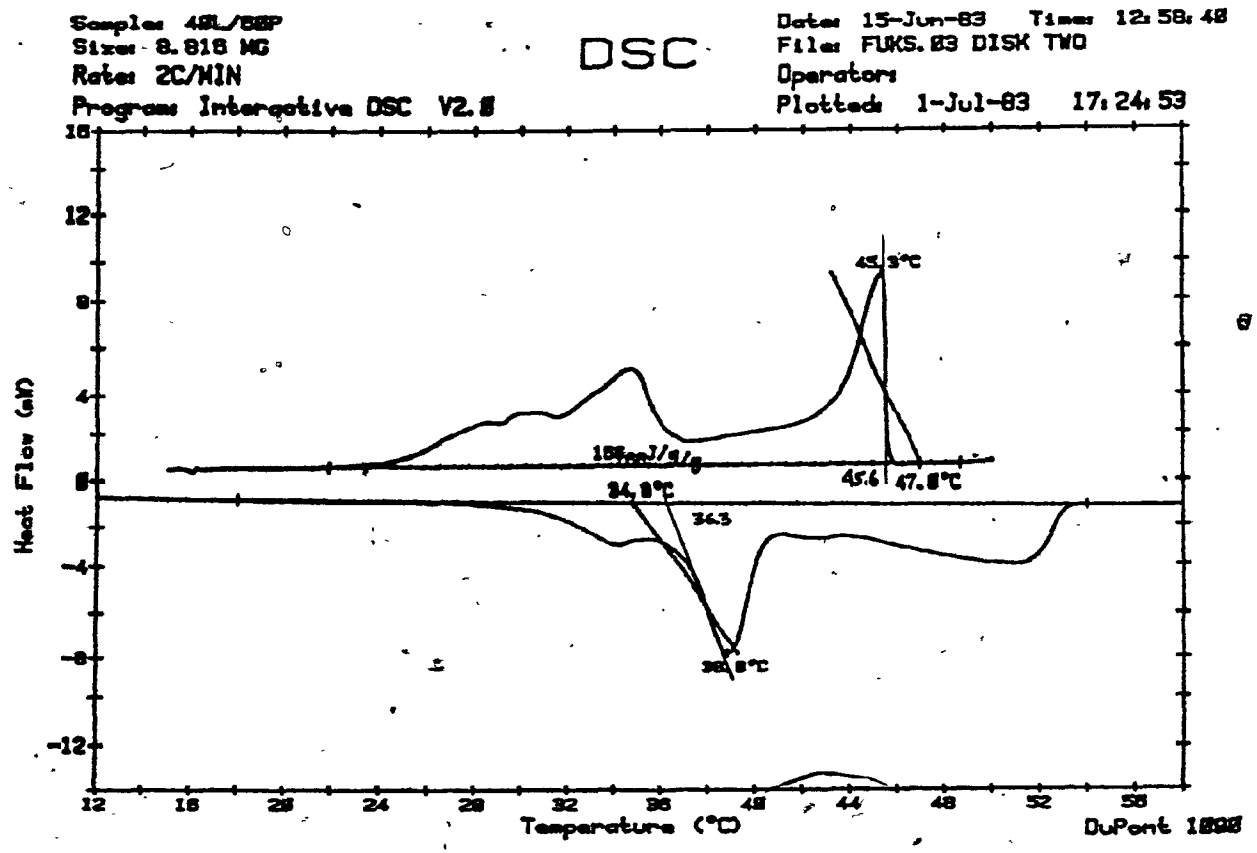

Fig. T-68. Thermogram of 40 mole % lauric : 60 mole % palmitic.

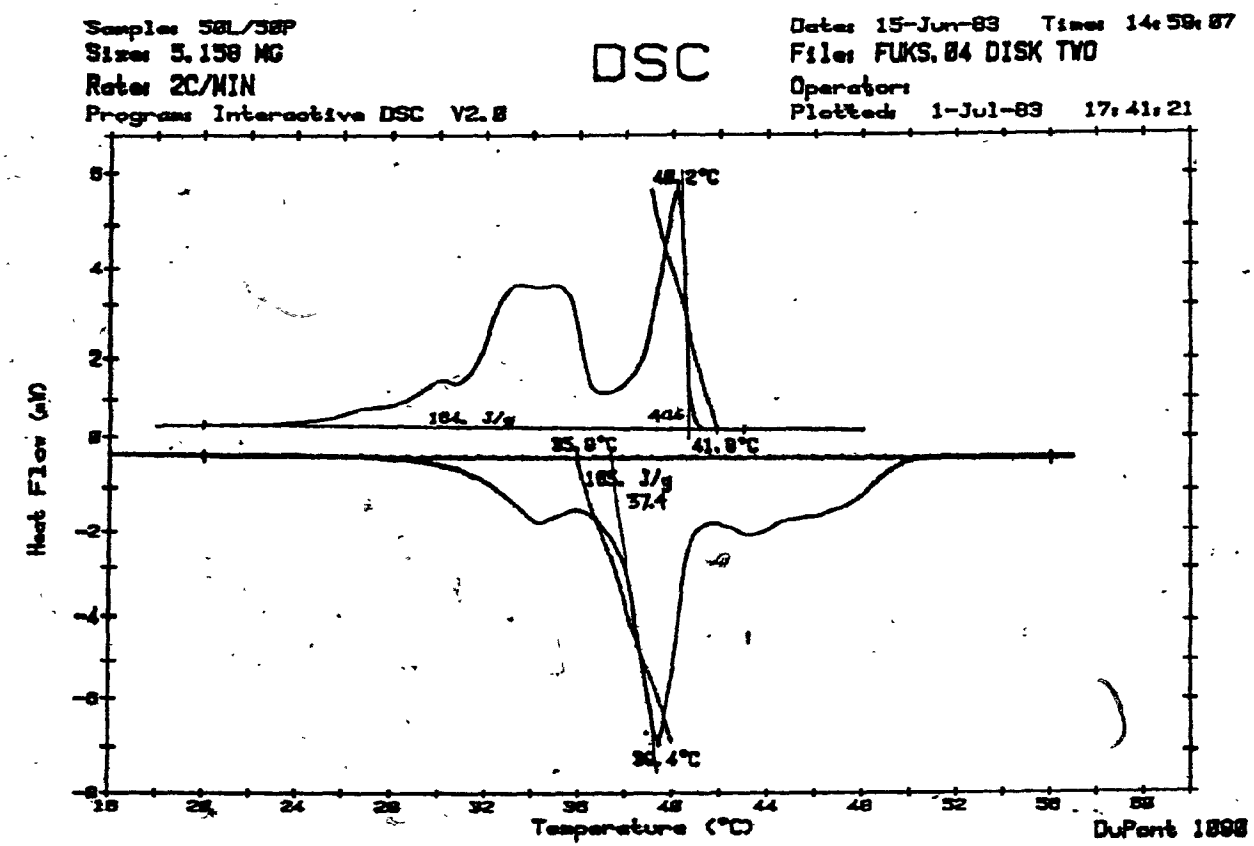

Fig. T-69. Thermogram of 50 mole % lauric : 50 mole % palmitic.

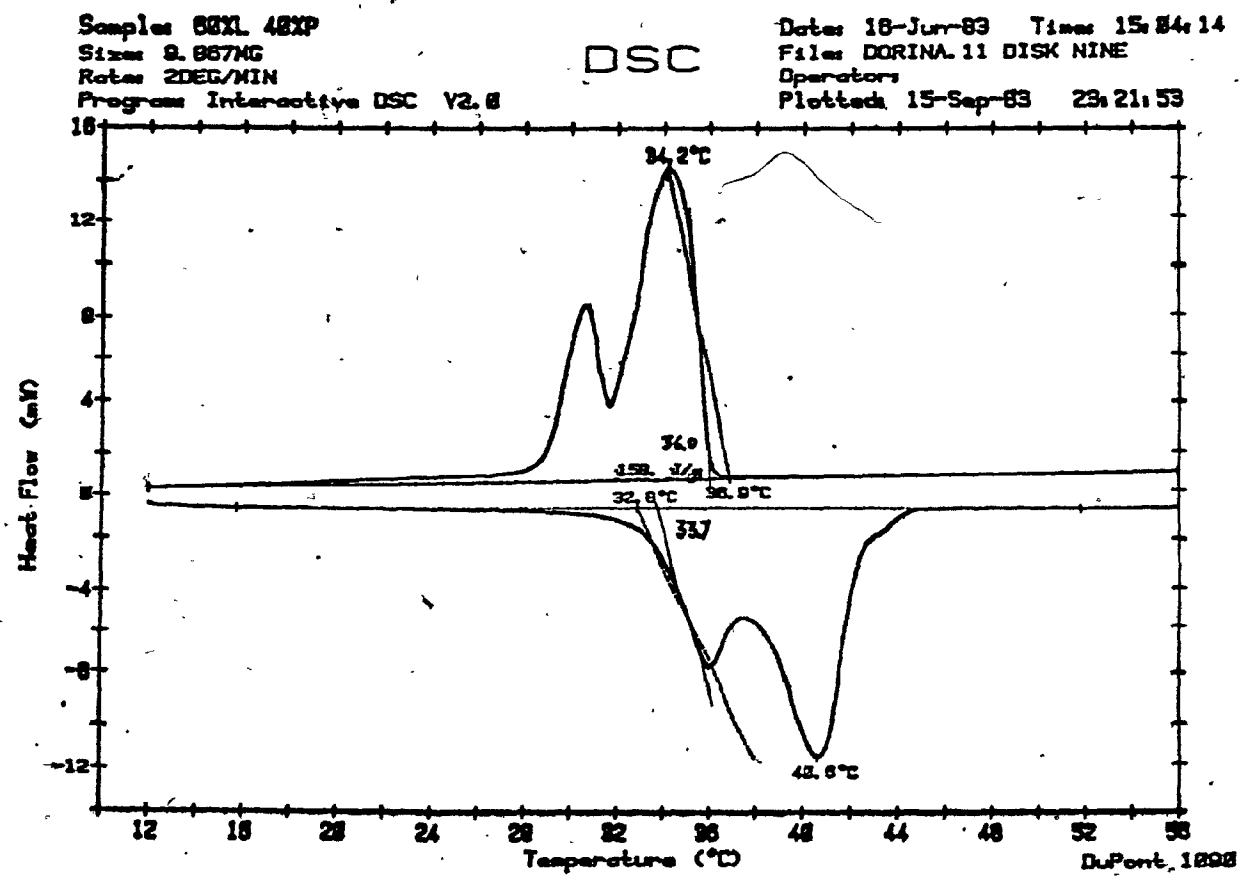

Fig. T-70. Thermogram of 60 mole % lauric : 40 mole % palmitic.

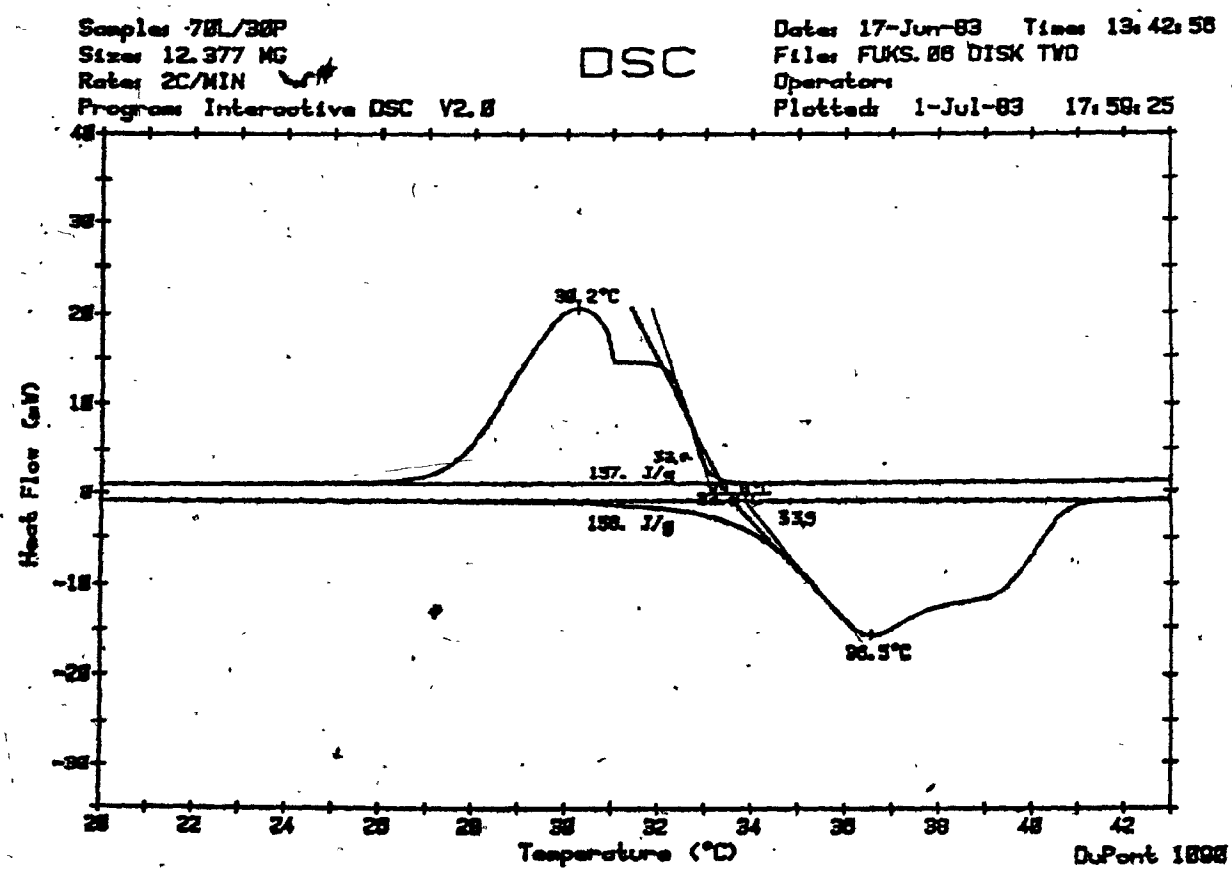

Fig. T-71. Thermogram of 70 mole % lauric : 30 mole % palmitic.

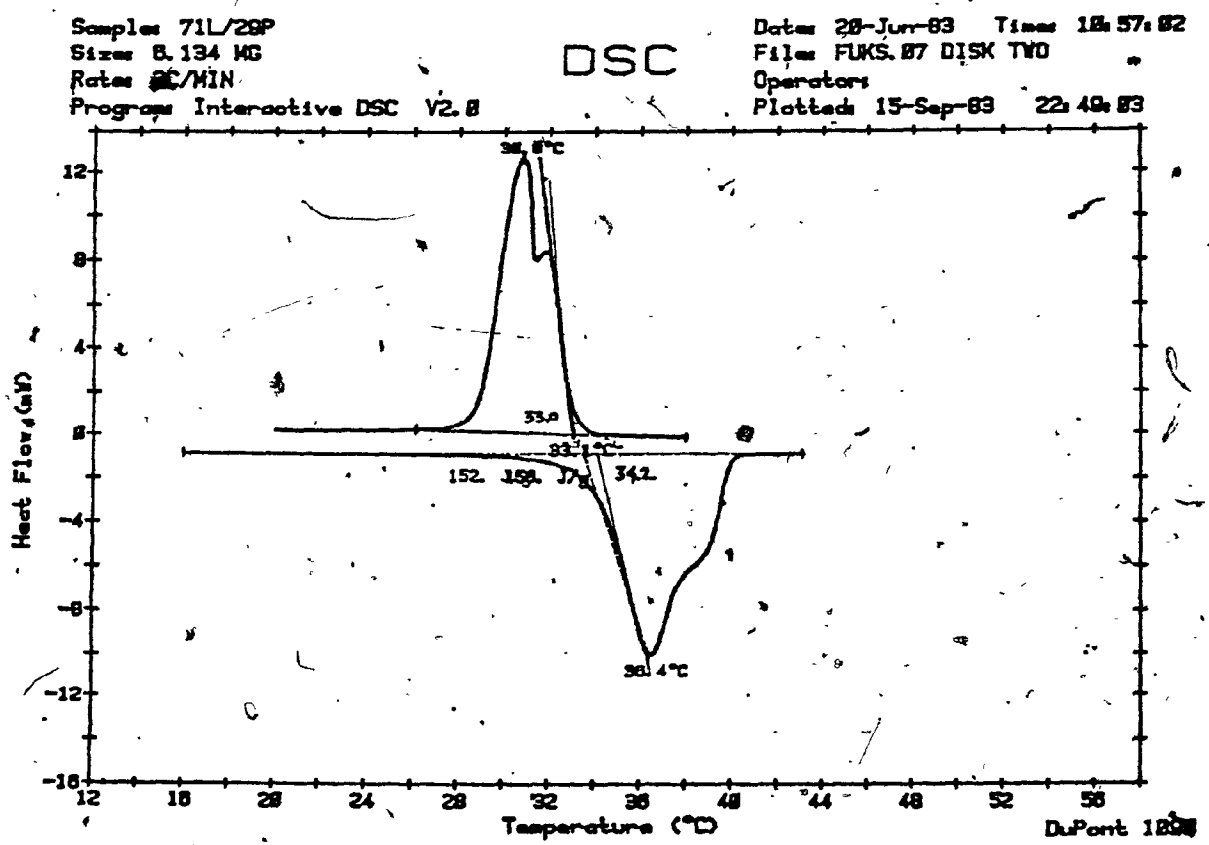

Fig. T-72. Thermogram of 71 mole % lauric : 29 mole % palmitic.

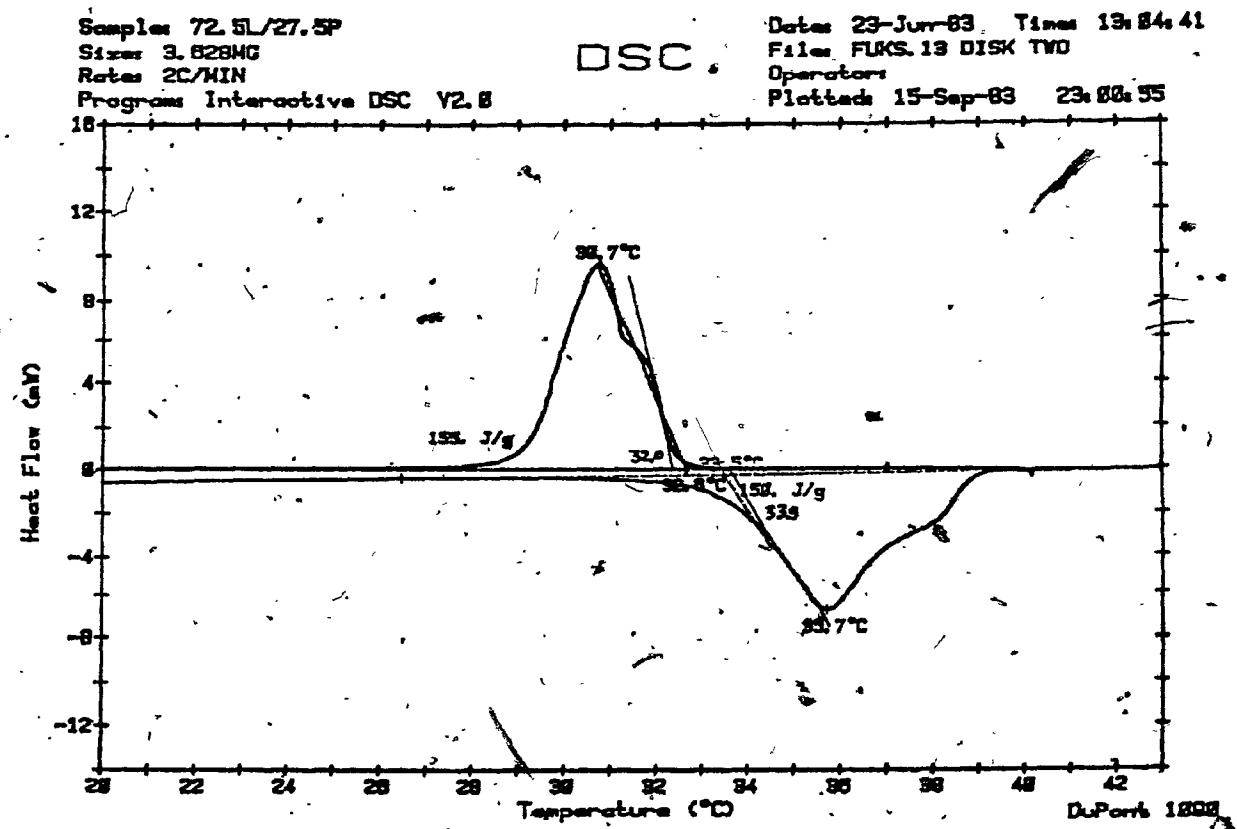

Fig. T-73. Thermogram of 72.5 mole % lauric : 27.5 mole % palmitic.

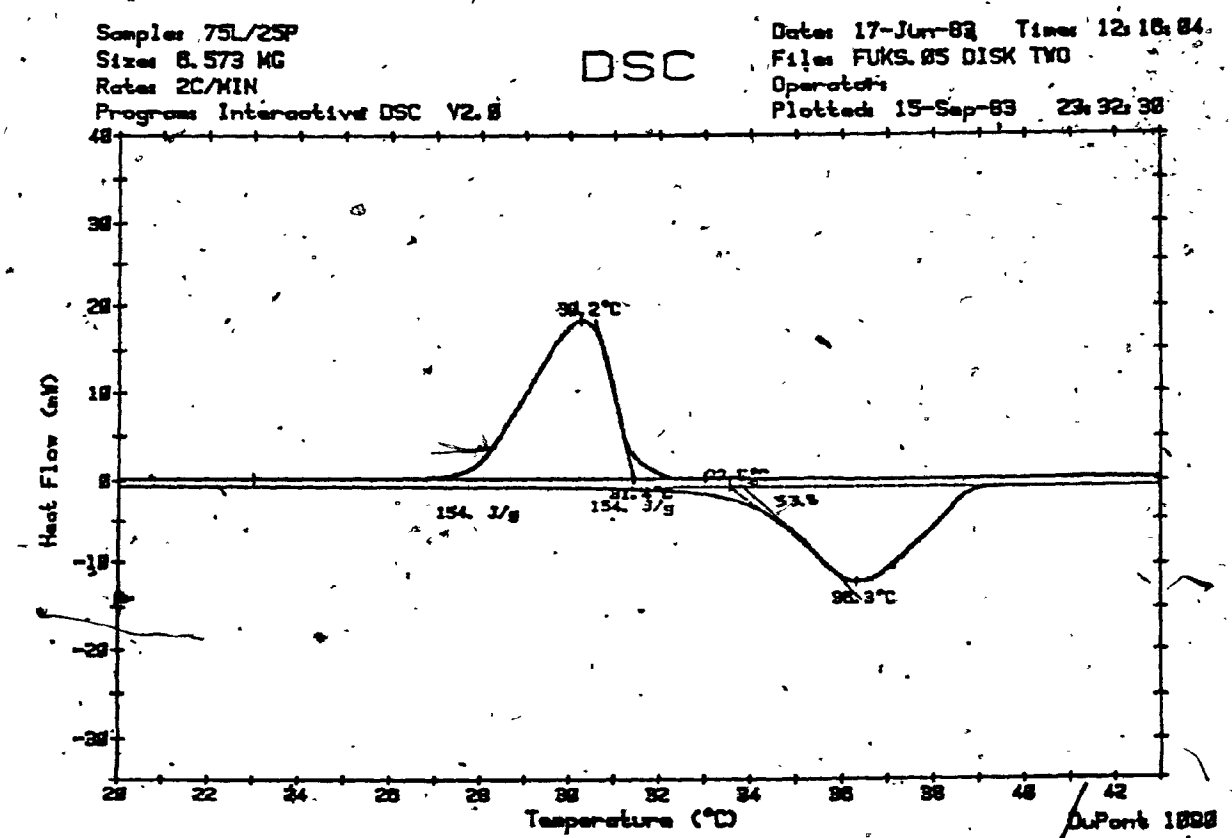

Fig. T-74. Thermogram of 75 mole % lauric : 25 mole % palmitic.

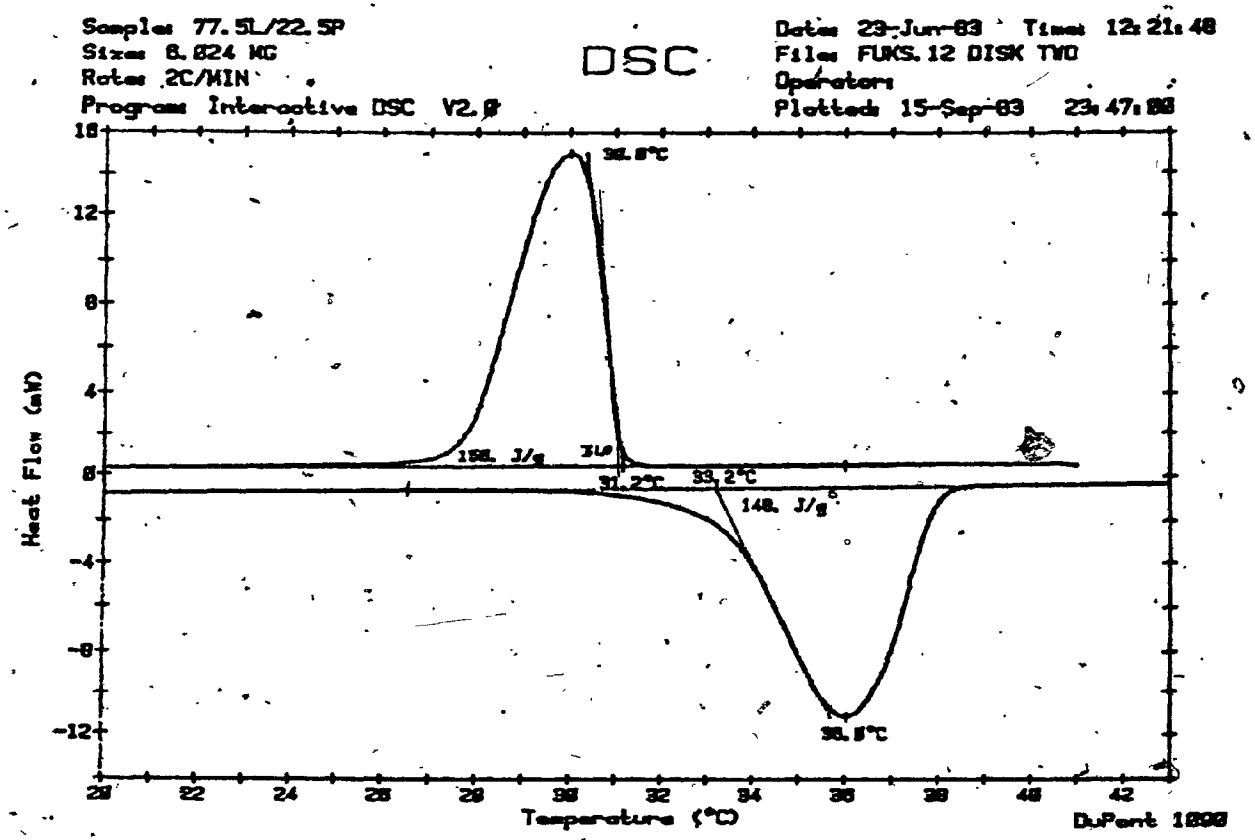

Fig. T-75. Thermogram of 77.5 mole % lauric : 22.5 mole % palmitic.

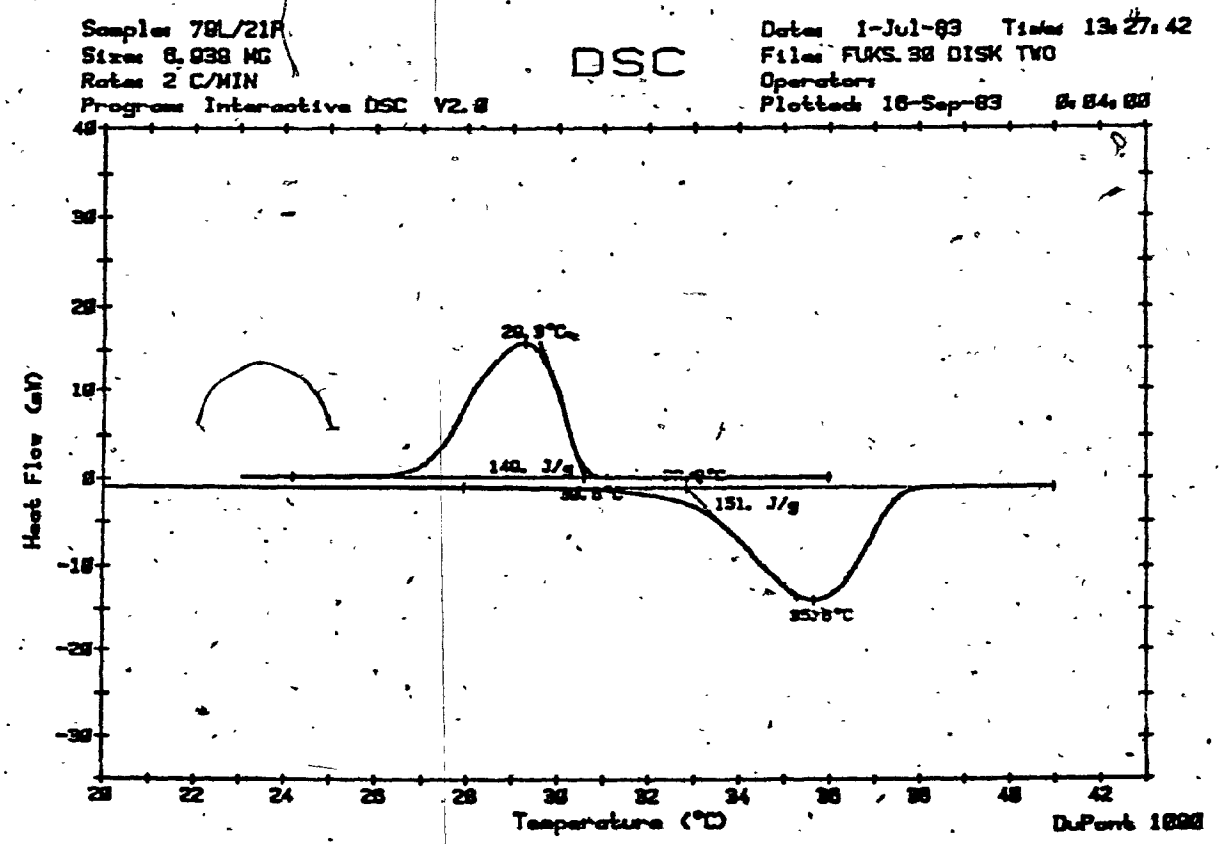

Fig. T-76. Thermogram of 79 mole % lauric : 21 mole % palmitic.

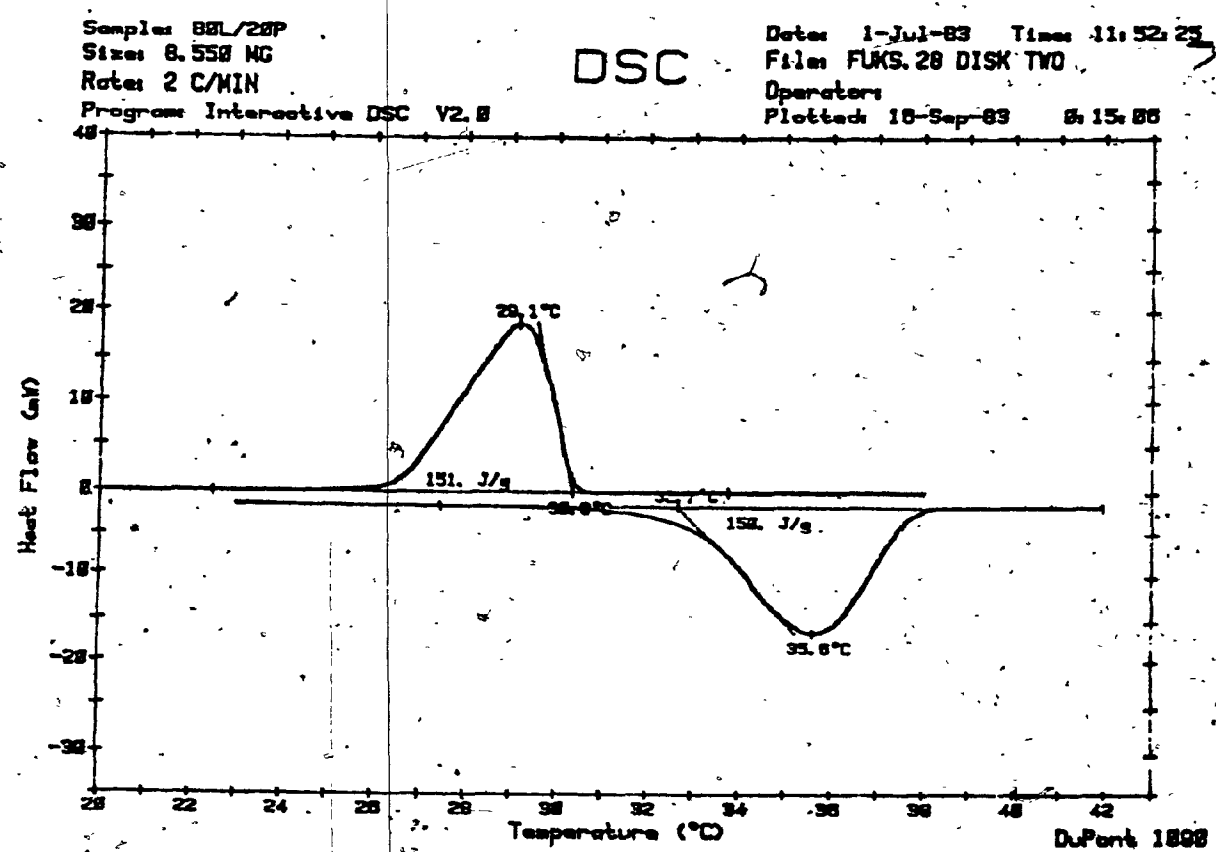

Fig. T-77. Thermogram of 80 mole % lauric : 20 mole % palmitic.

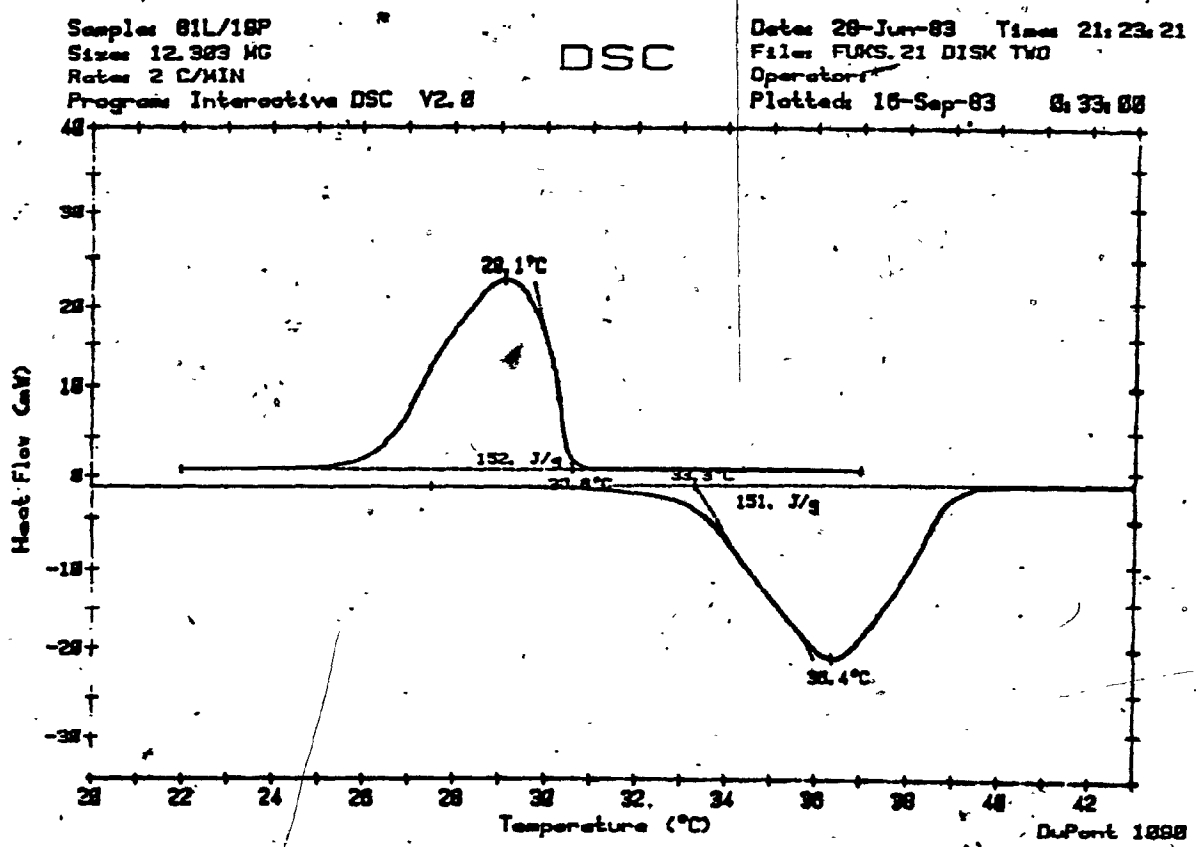

Fig. T-78. Thermogram of 81 mole % lauric : 19 mole % palmitic.

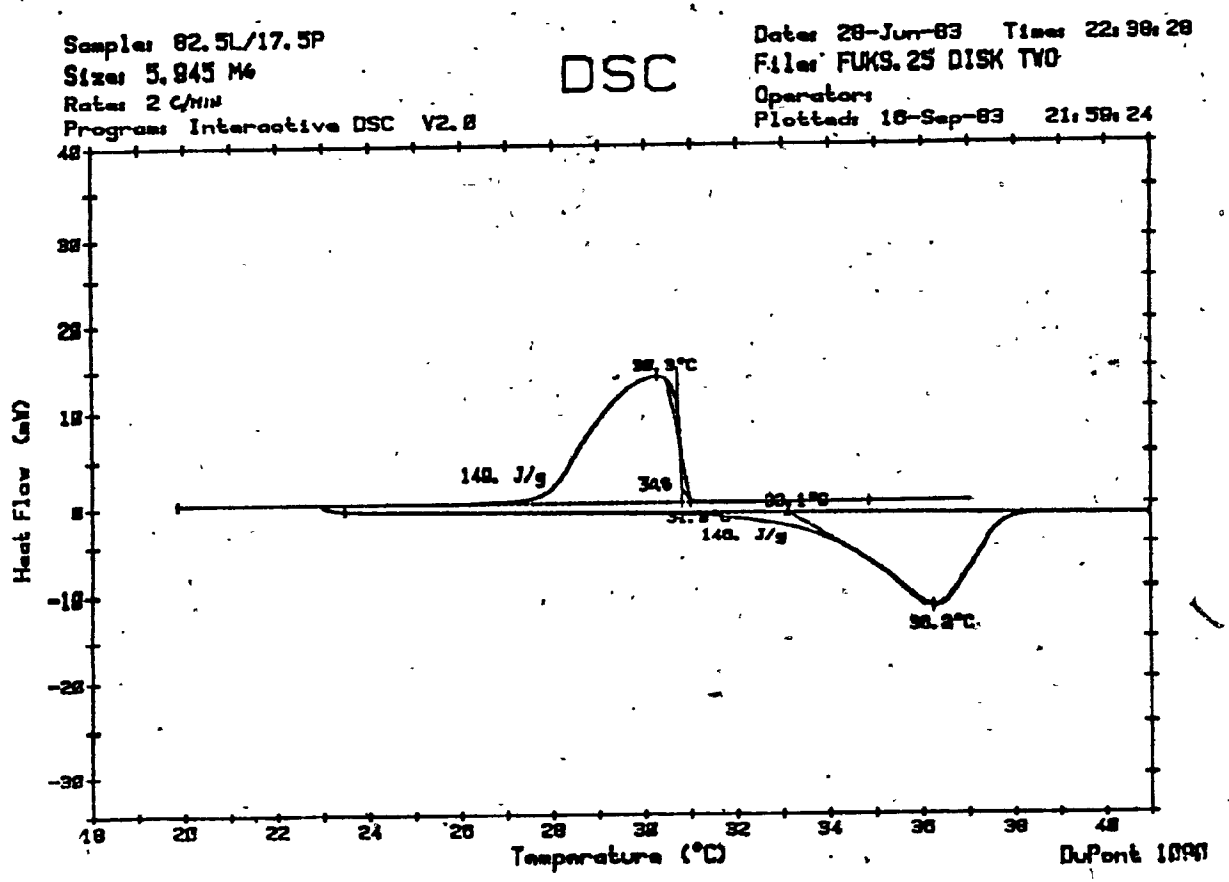

Fig. T-79. Thermogram of 82.5 mole % lauric : 17.5 mole % palmitic.

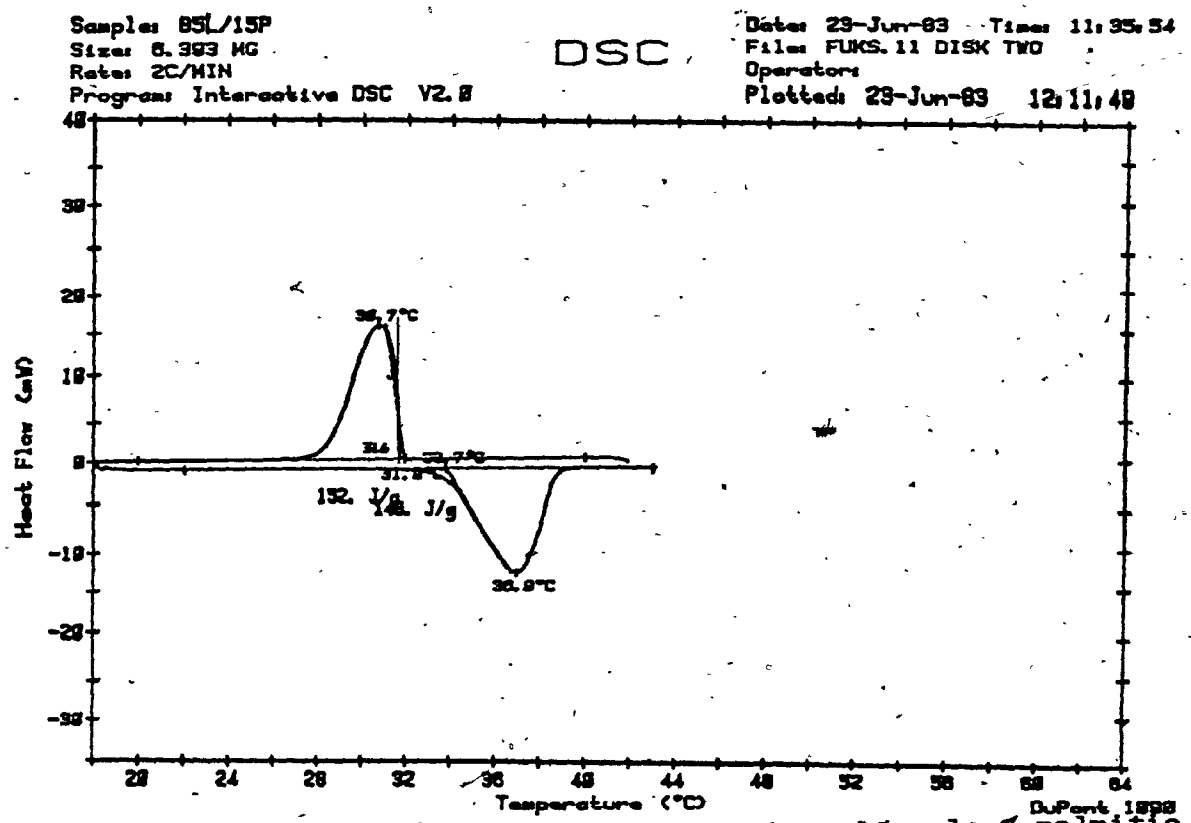

Fig. T-80. Thermogram of 85 mole % lauric : 15 mole % palmitic.

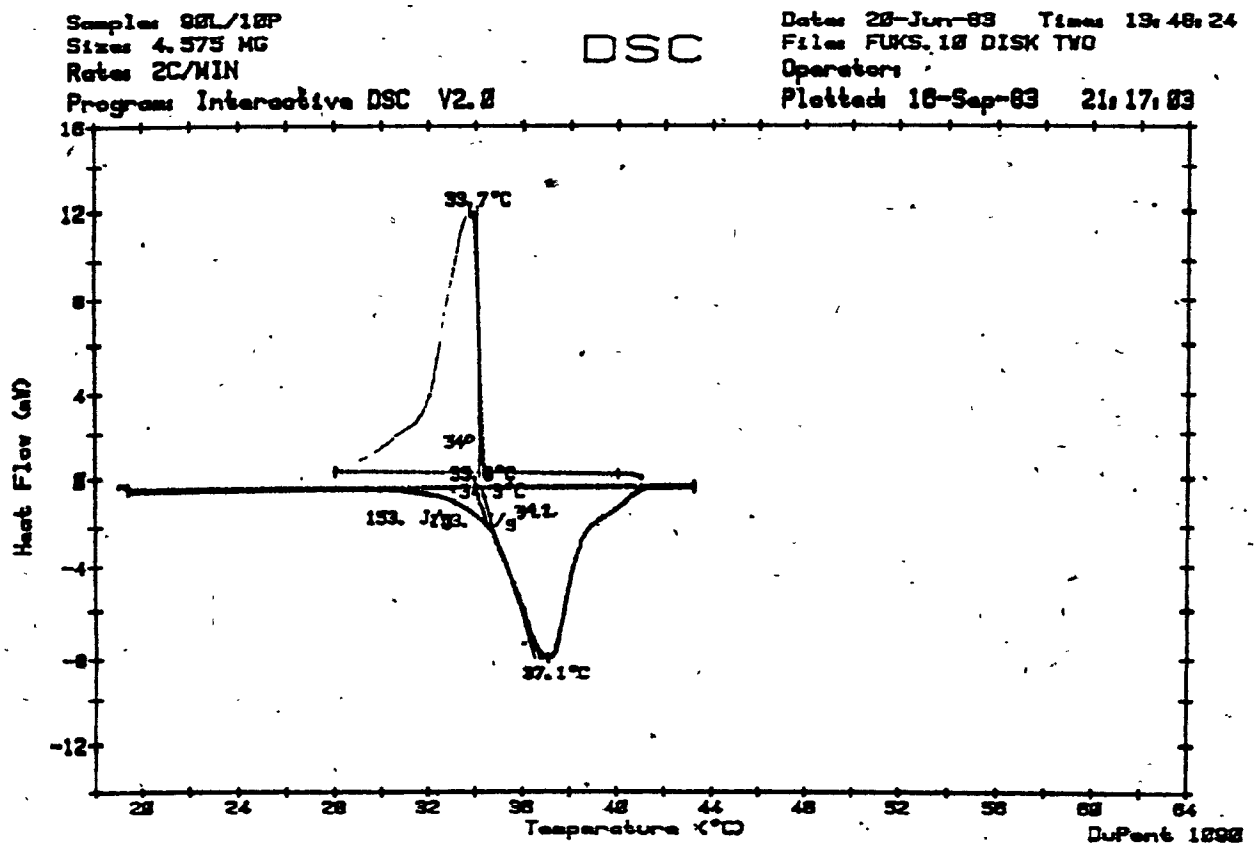

Fig. T-81. Thermogram of 90 mole % lauric : 10 mole % palmitic.

X-RAY DIFFRACTOMETRIC SPECTRA

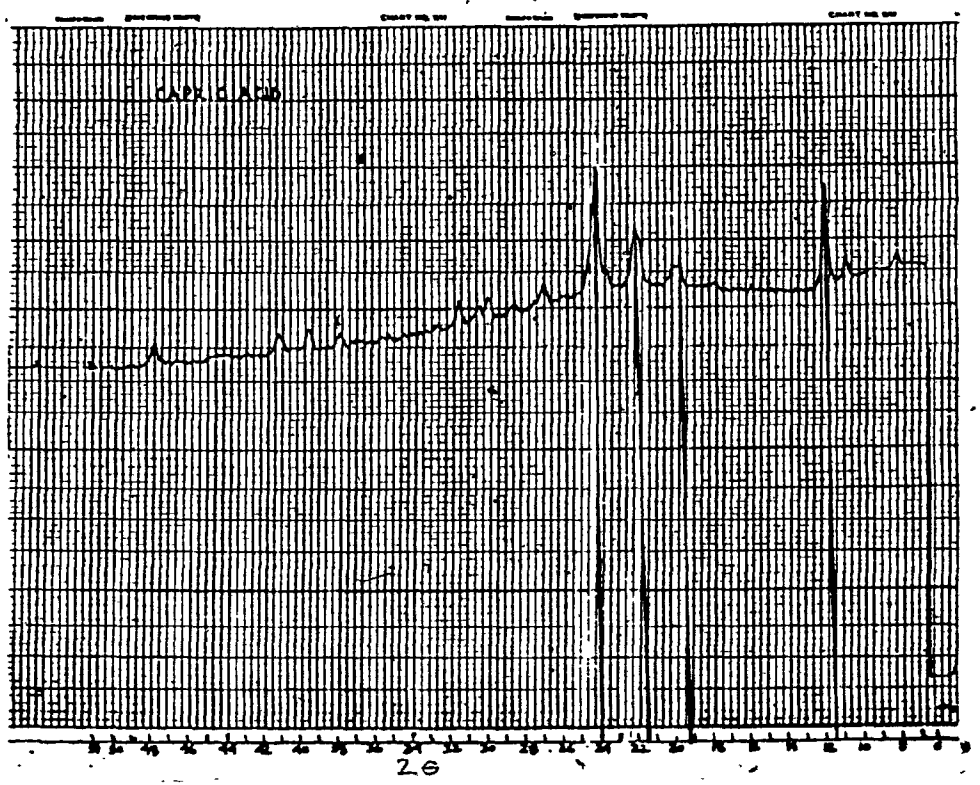

Fig. S-1. X-ray spectrum of capric acid.

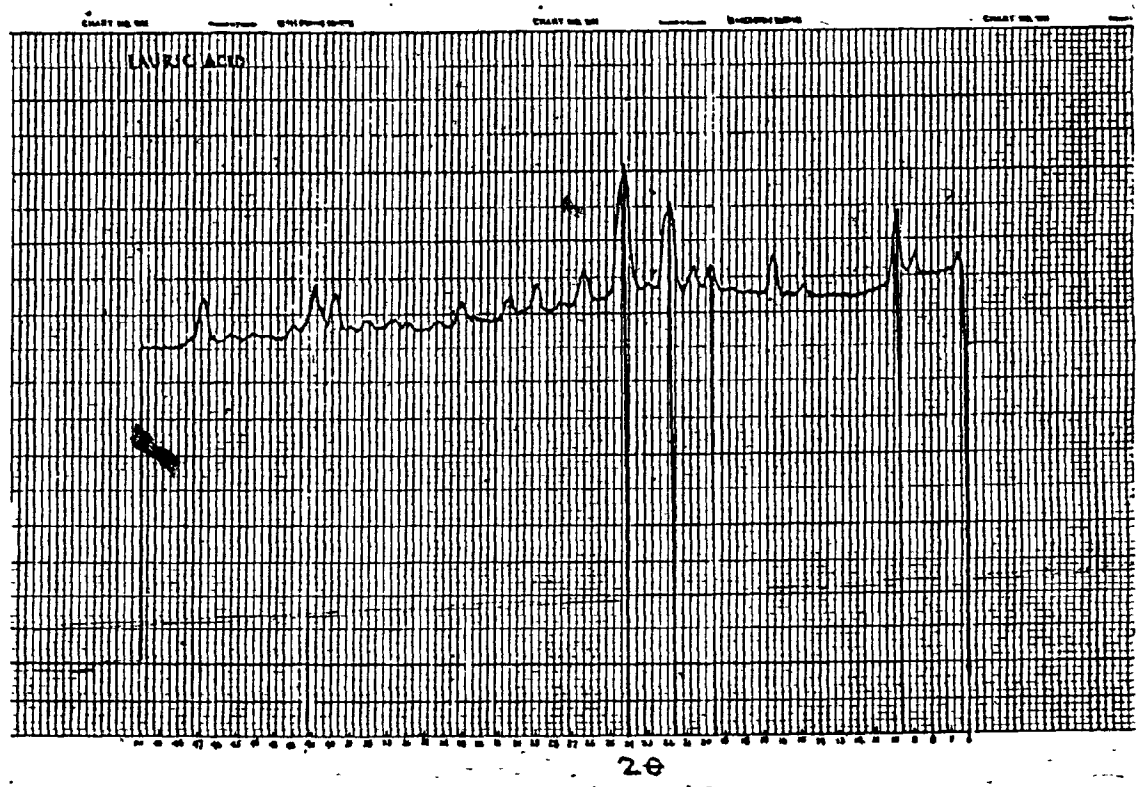

Fig. S-2. X-ray spectrum of lauric acid.

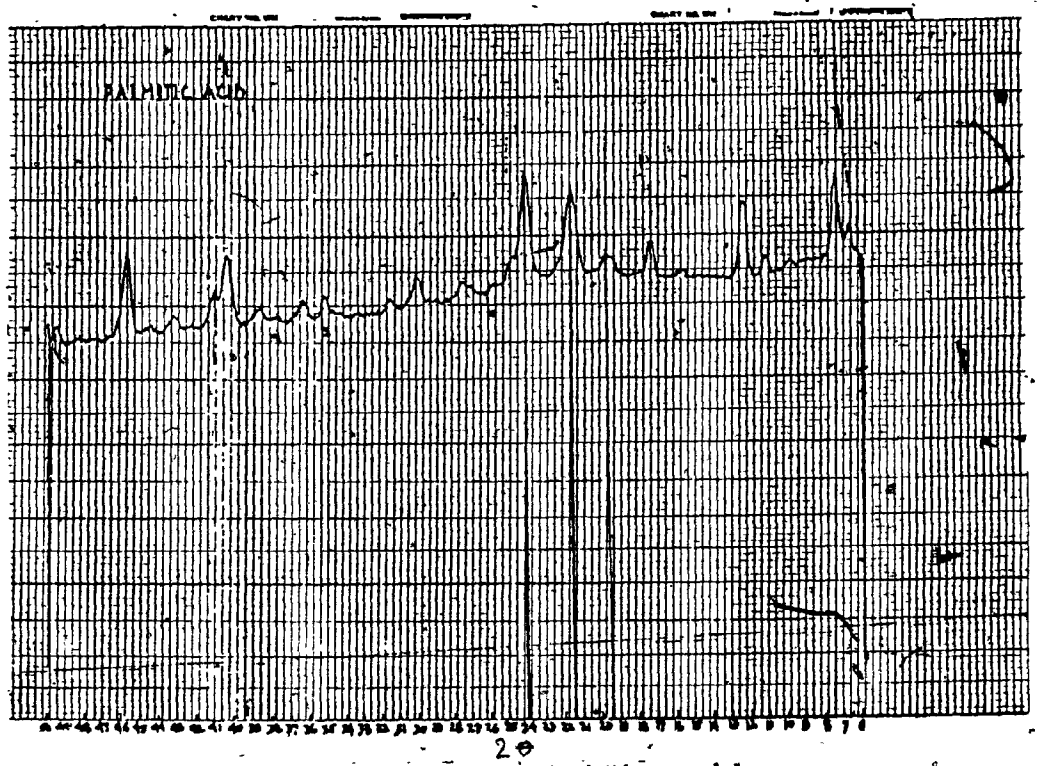

Fig. S-3. X-ray spectrum of palmitic acid.

Fig. S-4. X-ray spectrum of stearic acid.

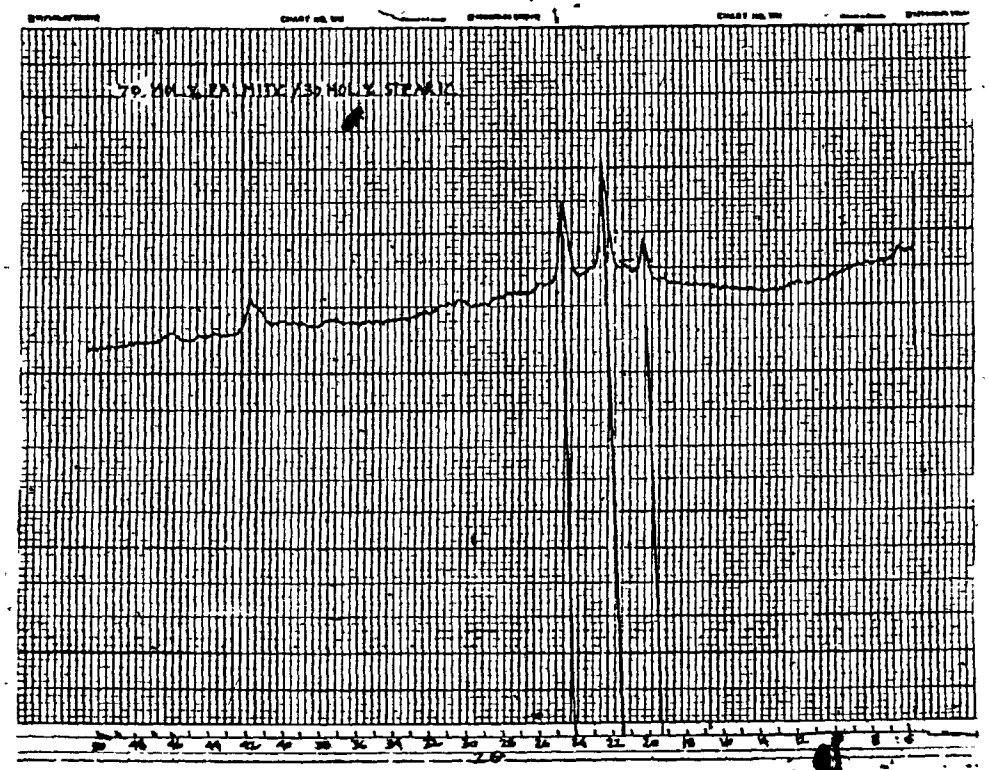

Fig. S-5. X-ray spectrum of 70 mole % palmitic : 2[illegible]5 mole % stearic.

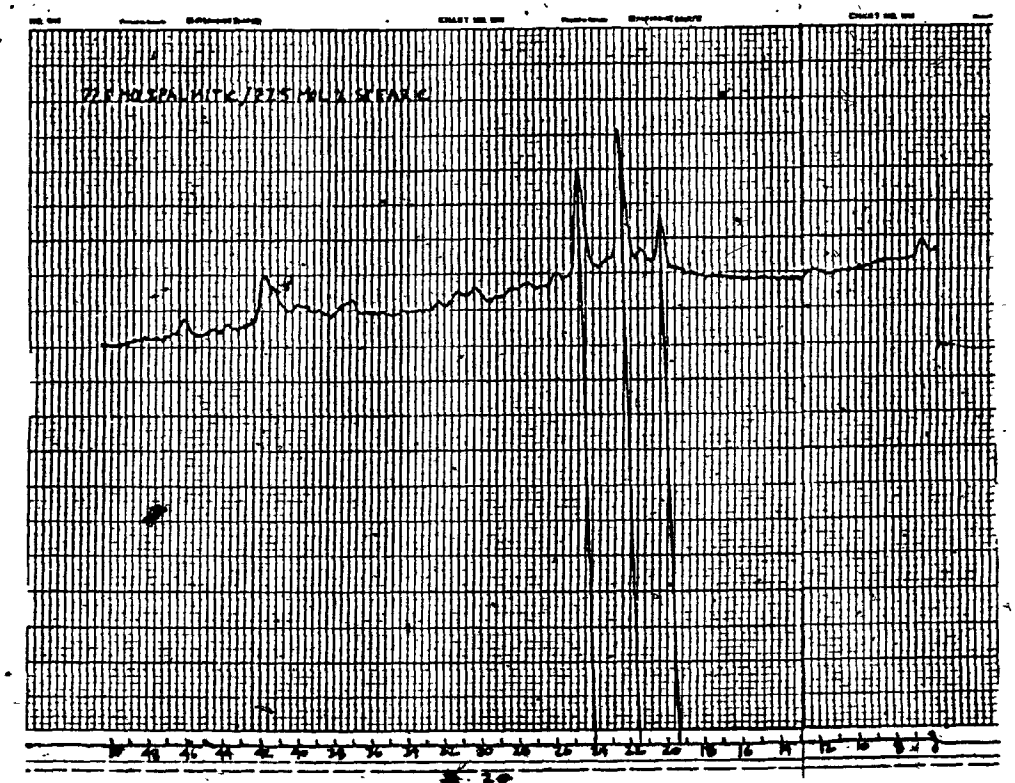

Fig. S-6. X-ray spectrum of 72.5 mole % palmitic : 27.5 mole % stearic.

Fig. S-7. X-ray spectrum of 84 mole % lauric : 16 mole % stearic.

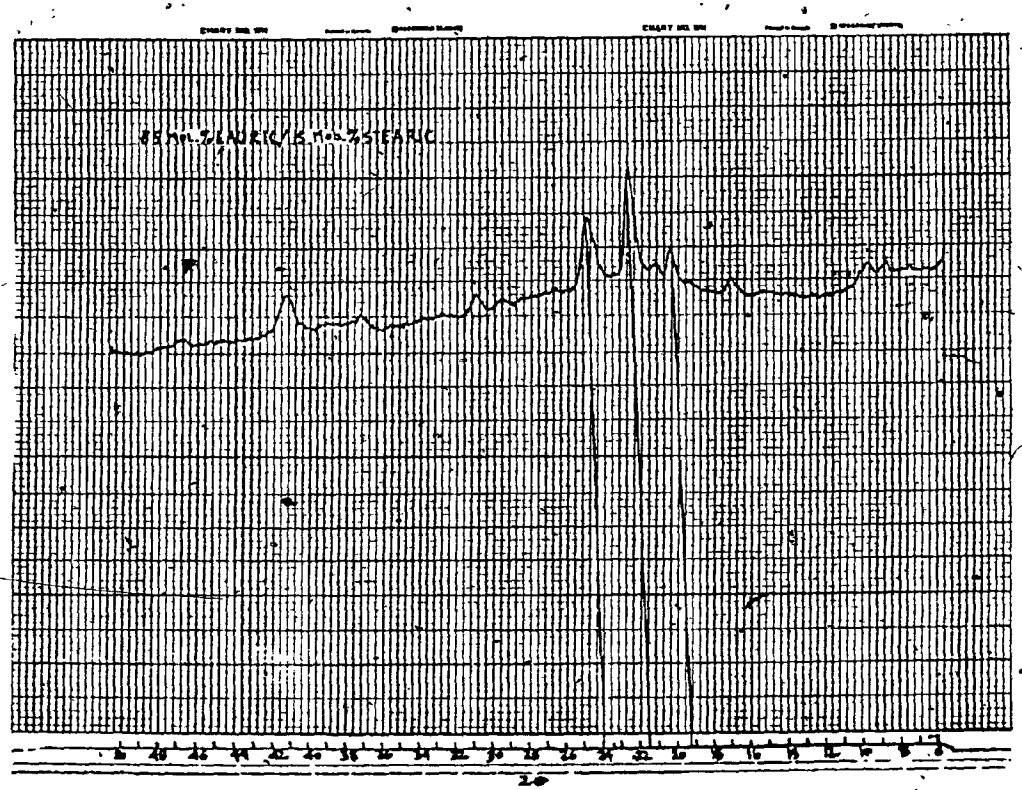

Fig. S-8. X-ray spectrum of 85 mole % lauric : 15 mole % stearic.

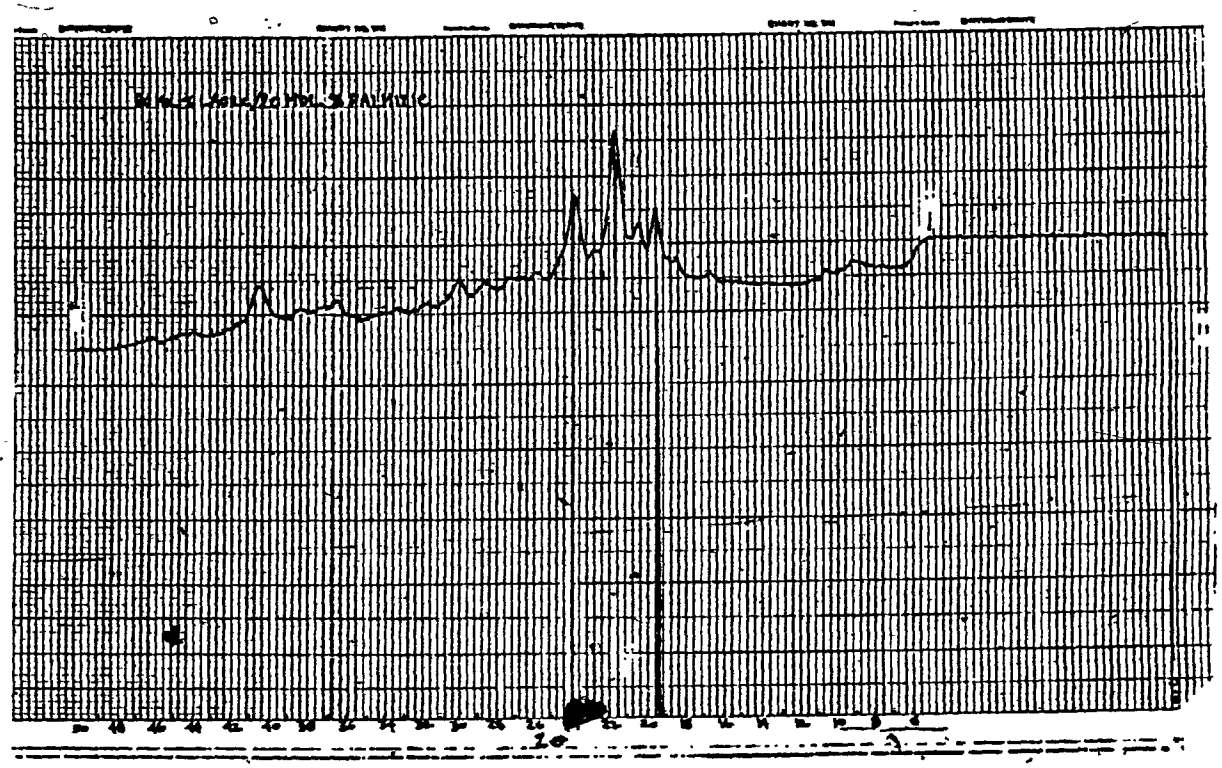

Fig. S-9. X-ray spectrum of 80 mole % lauric : 20 mole % palmitic.

INFRARED SPECTRA

SPECTRUM NO. 14

DATE

SAMPLE 1. 74% CA - 26% LA
2. 85% LA - 15% SA
3. 72.5% PA - 27.5% SA
4. 80% LA - 20% PA

SOURCE

STRUCTURE

PATH mm

SOLVENT

CONC.

PHASE

COMMENTS KBr disk
10mg/1000mg
74% CA - 26% LA
coppilary film betwen
KBr disks.

ANALYST

SPEED 600 cm^{-1}/min.

GAIN 2

PERIOD 1 SEC.

SLIT WIDTH 3 mm

@ 3000 cm^{-1}

BECKMAN
SPECTROPHOTOMETER

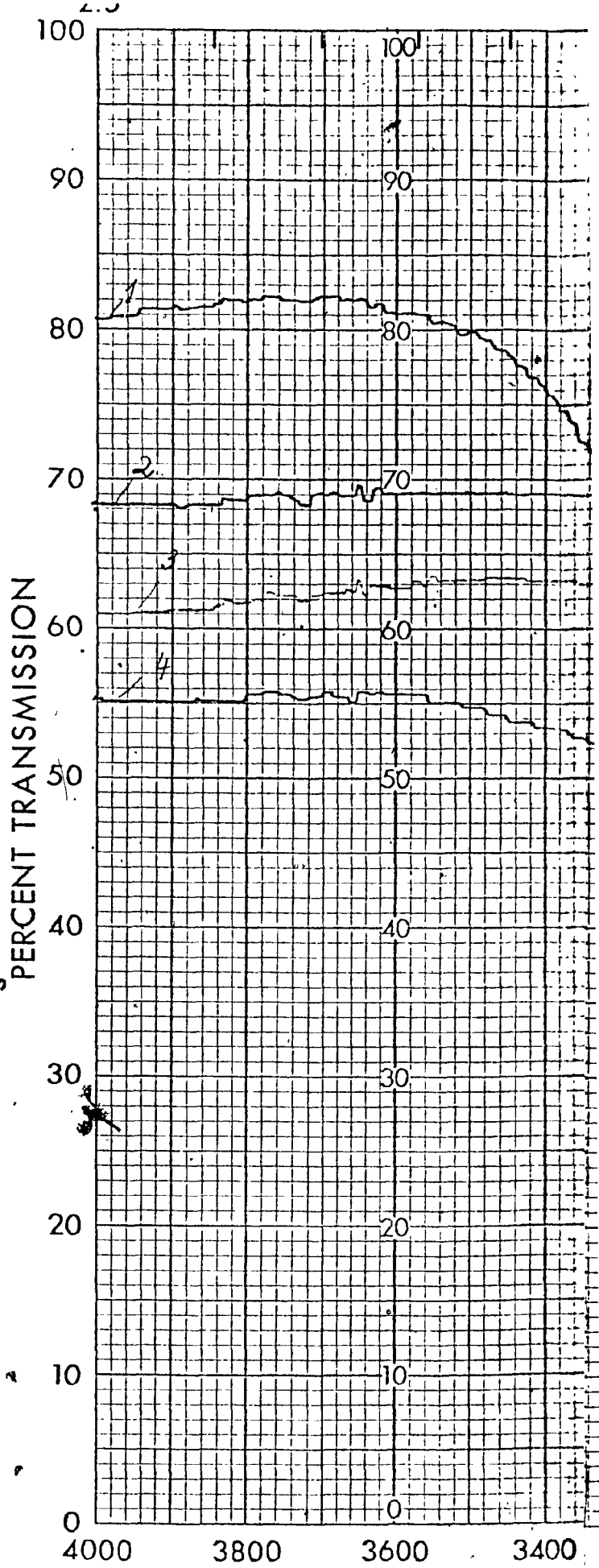

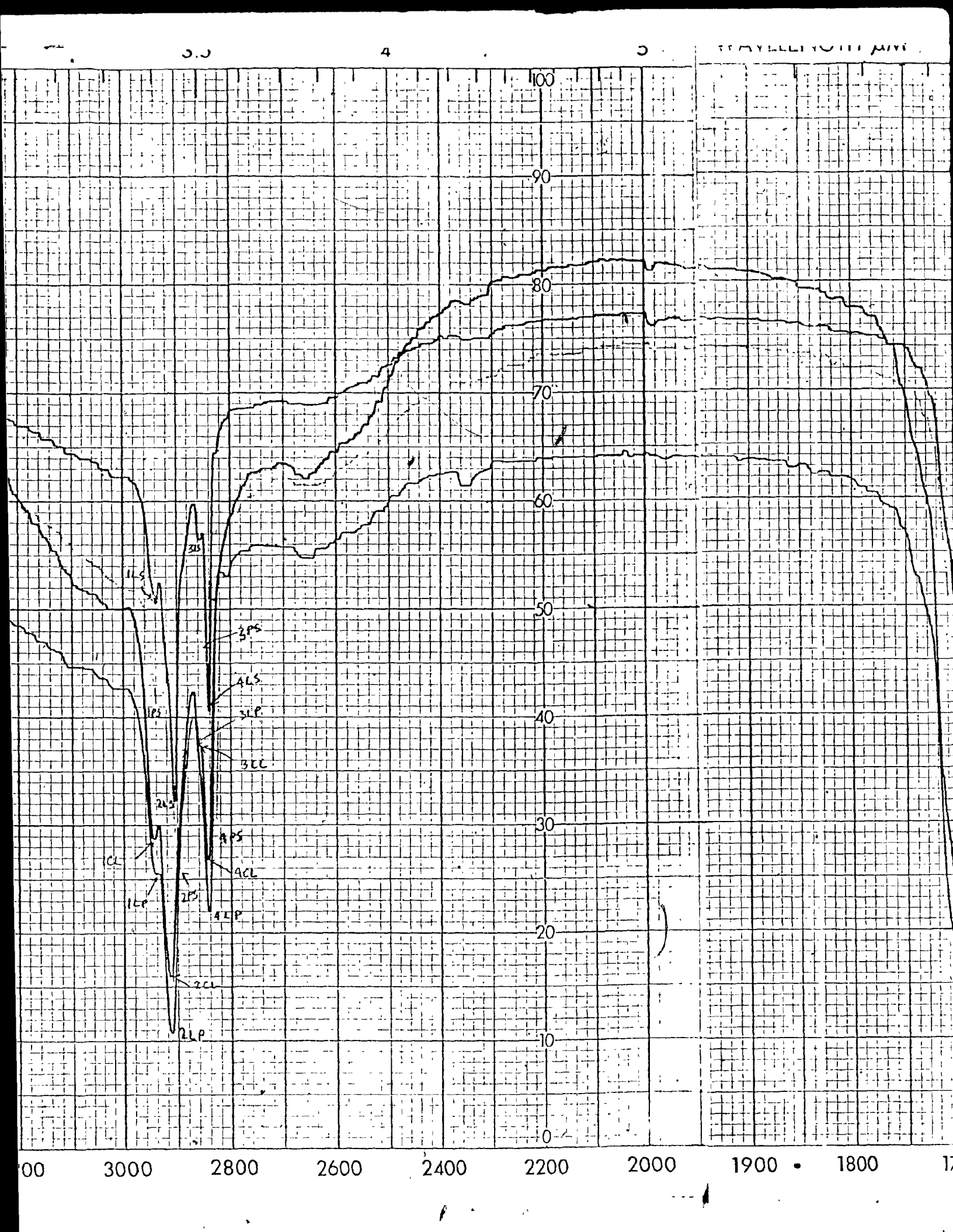
3.5
4
5
WAVELENGTH μm
100
90
80
70
60
50
40
30
20
10
0
3000
2800
2600
2400
2200
2000
1900
1800
1LS
3LS
3PS
4LS
3LP
3CL
2LS
4PS
1CL
4CL
1LP
2PS
4LP
2CL
2LP

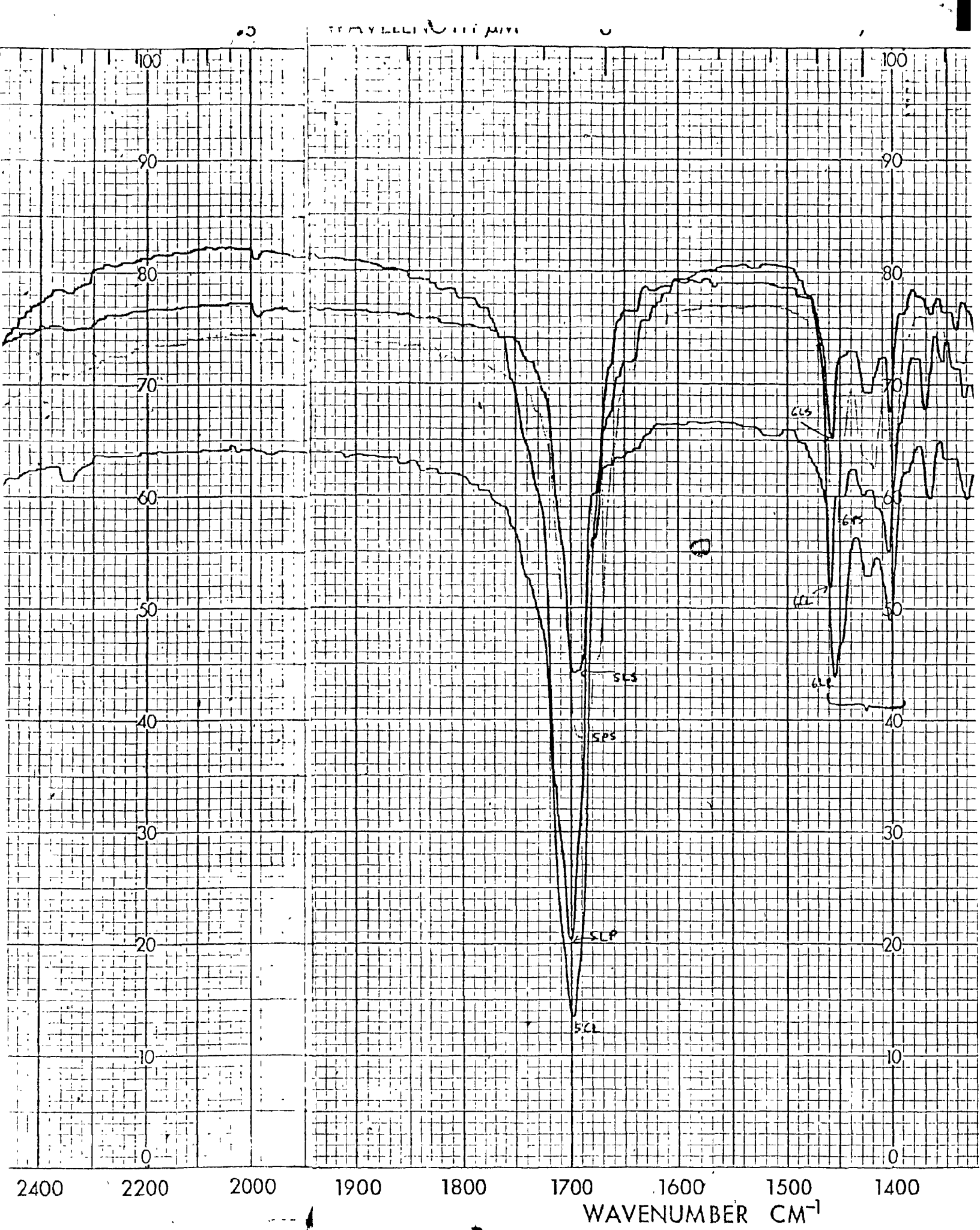
100
90
80
70
60
50
40
30
20
10
0
SCS
SPS
SCP
SCL
GCS
GPS
GCL
GCP
2400
2200
2000
1900
1800
1700
1600
1500
1400
WAVENUMBER CM⁻¹

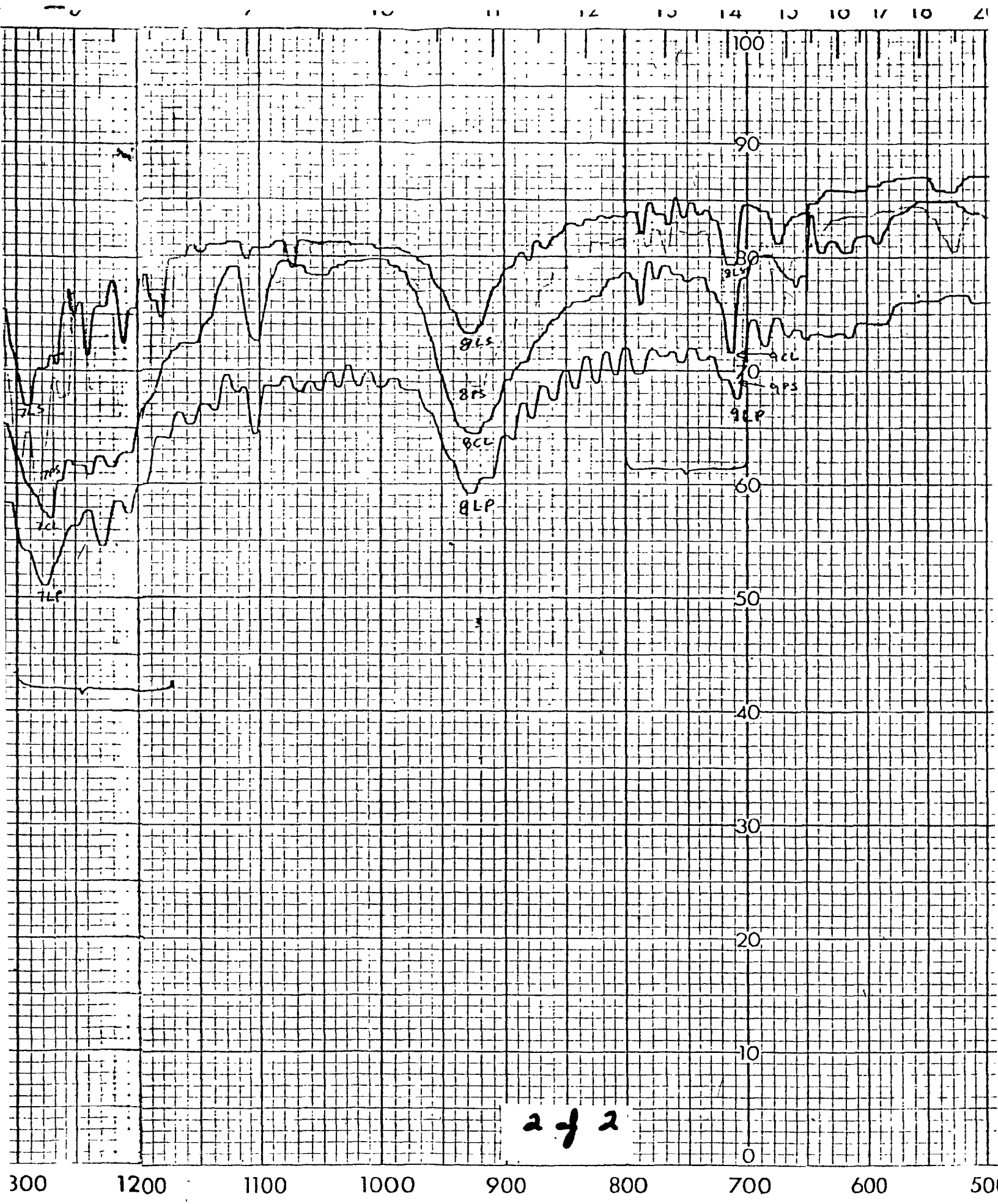
100
90
80
70
60
50
40
30
20
10
0
1200
1100
1000
900
800
700
600
7LS
7PS
7CL
7LP
8LS
8PS
8CL
8LP
9LS
9CL
9PS
9LP
2 of 2

SPECTRUM NO. 17

DATE

SAMPLE 1. Capric Ac.
2. Steoric Ac.
3. Palmitic Ac.
4. Lauric Ac.

SOURCE

STRUCTURE

PATH mm

SOLVENT

CONC.

PHASE

COMMENTS KBr disk
10mg / 1000mg

ANALYST

SPEED 600 cm^{-1} / min.

GAIN 2

PERIOD 1 SEC.

SLIT WIDTH 3 mm

@ 3000 cm^{-1}

BECKMAN
SPECTROPHOTOMETER

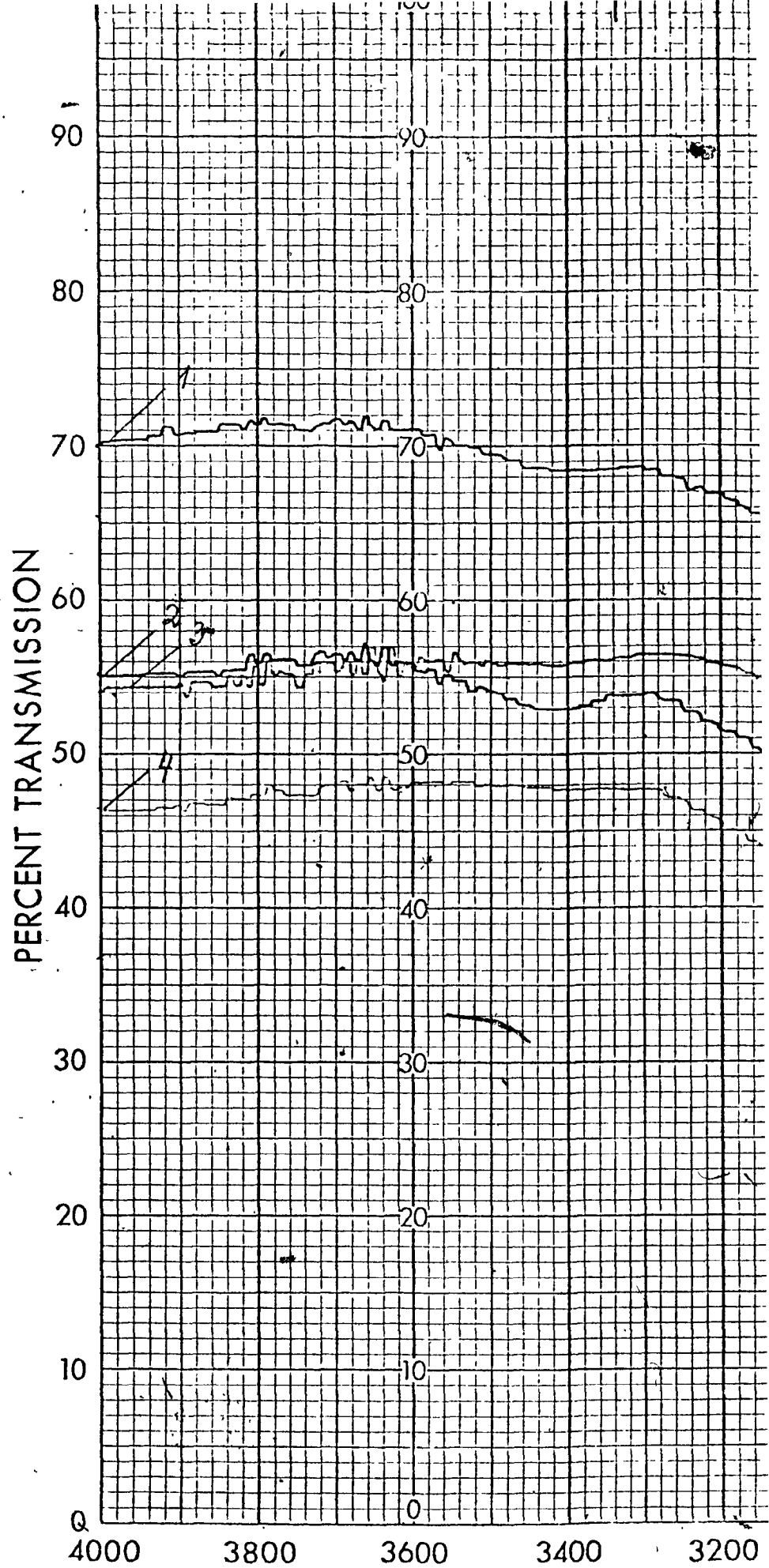

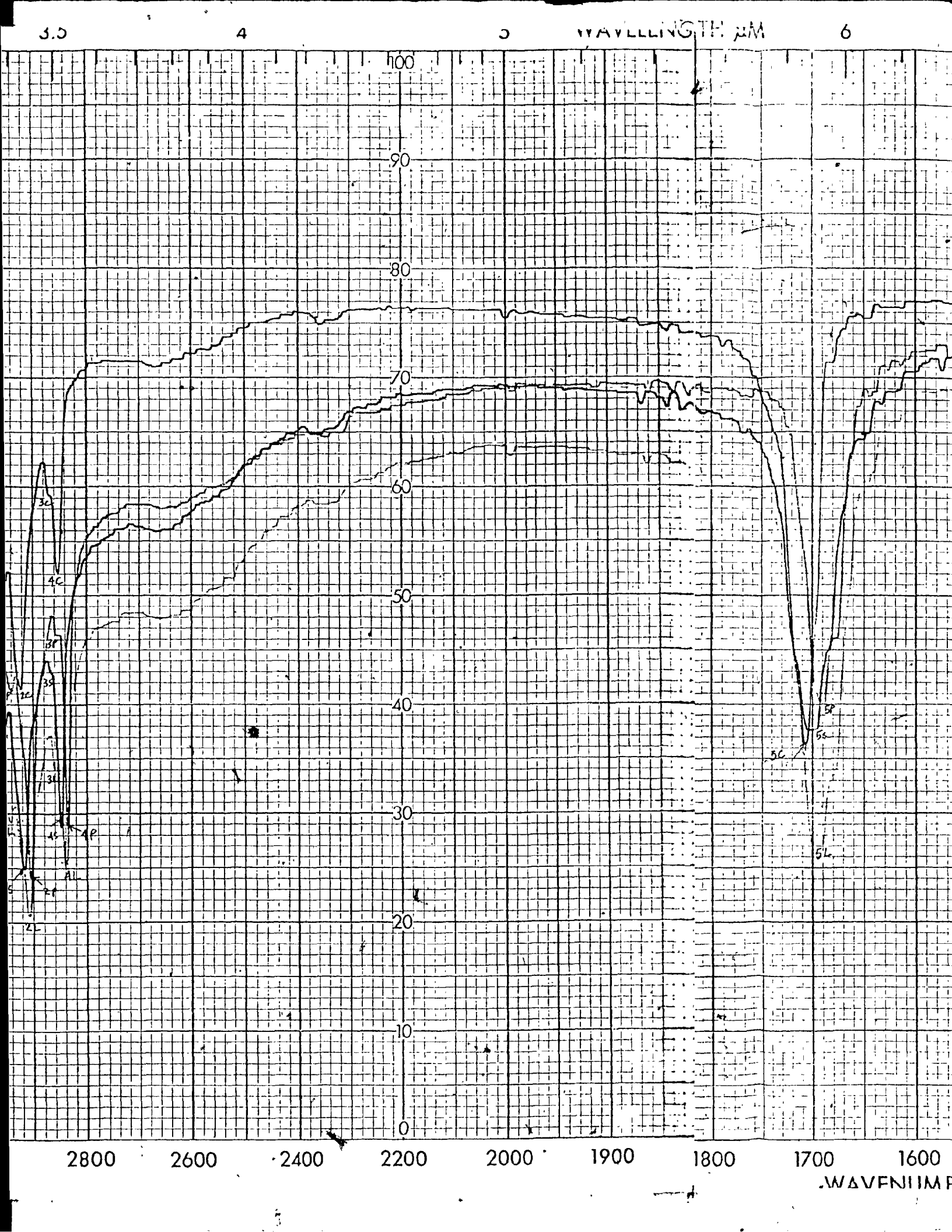
3.5
4
5
WAVELENGTH µM
6
100
90
80
70
60
50
40
30
20
10
0
2800
2600
2400
2200
2000
1900
1800
1700
1600
WAVENUMB
3C
4C
3P
3S
2C
3L
4S
4P
4L
2S
2P
2L
5P
5S
5C
5L

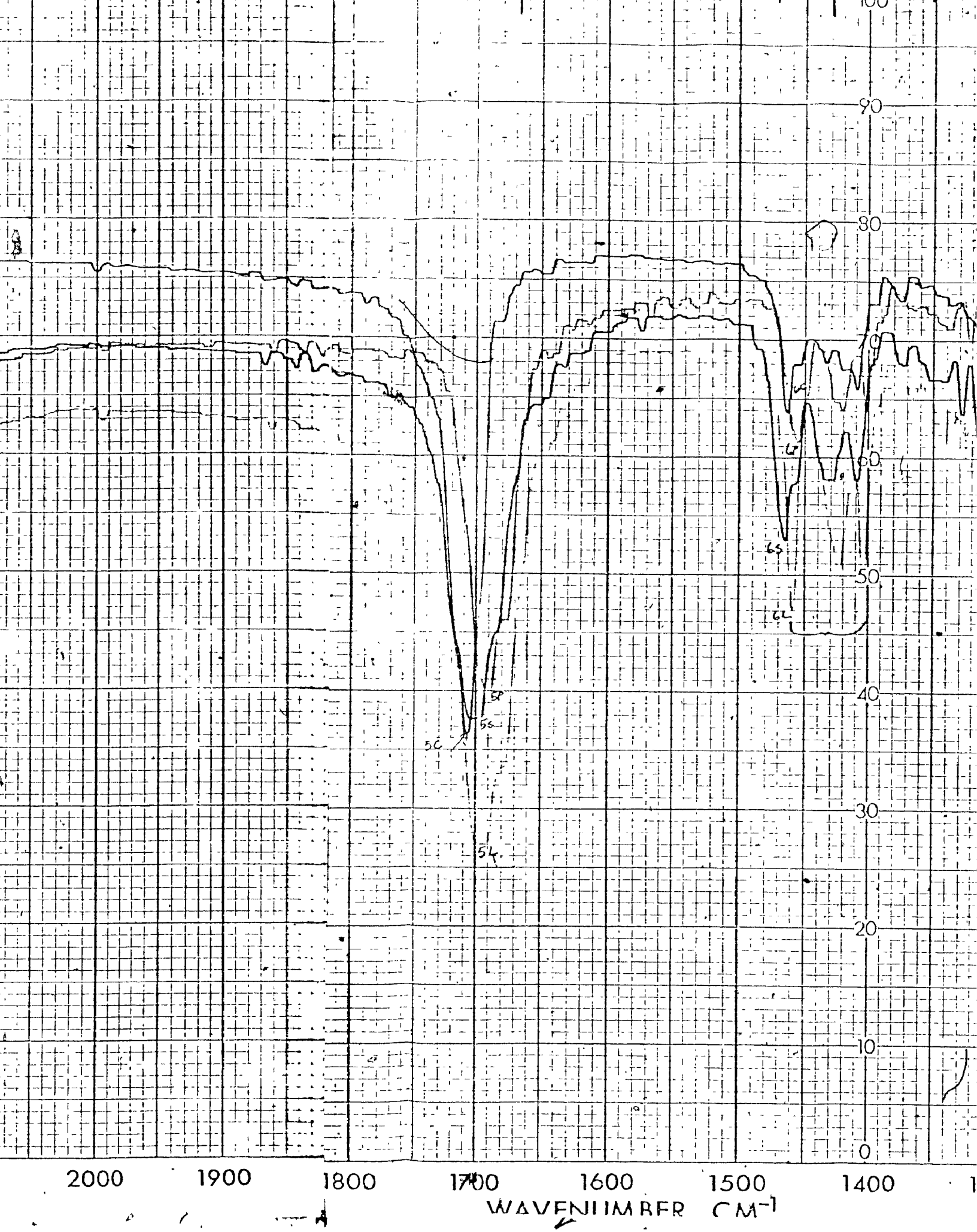
100
90
80
70
60
50
40
30
20
10
0
2000
1900
1800
1700
1600
1500
1400
WAVENUMBER CM⁻¹
5P
5S
5C
5L
6S
6L

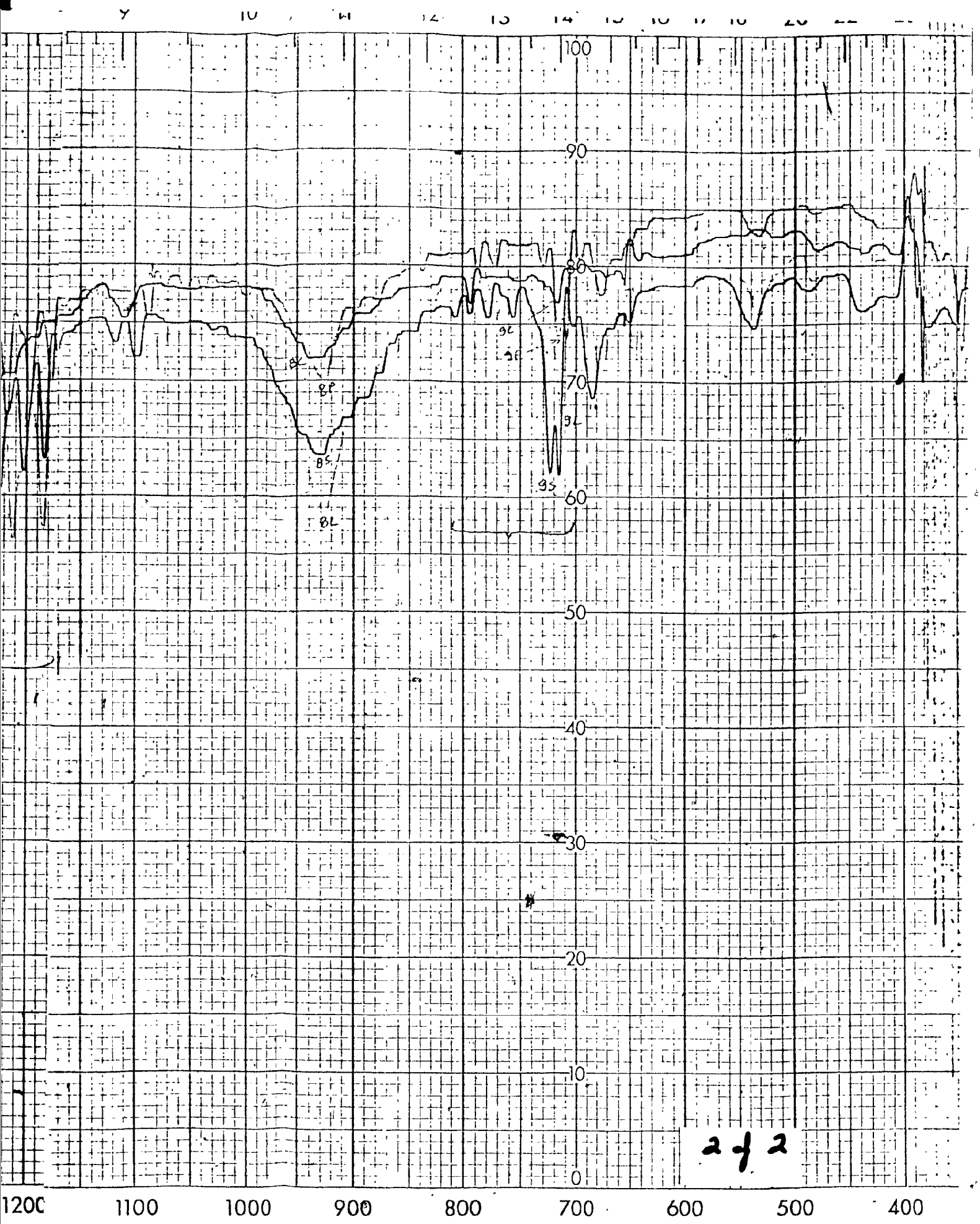
100
90
80
70
60
50
40
30
20
10
0
1200
1100
1000
900
800
700
600
500
400
2 of 2